

**THE STRUCTURE OF THE REPRODUCTIVE SYSTEM IN THE MALE
VERVET MONKEY, *CHLOROCEBUS AETHIOPS*, WITH SPECIAL
REFERENCE TO SPERMATOGENESIS**

Sogolo Lucky Lebelo

A thesis submitted in partial fulfilment of the requirements for the degree

Philosophiae Doctor

(Medical Biosciences)

**UNIVERSITY of the
WESTERN CAPE**

Faculty of Natural Sciences, Department of Medical BioSciences

University of the Western Cape

Supervisor: Prof G. van der Horst

NOVEMBER 2007

KEY WORDS

Vervet Monkey (*Chlorocebus aethiops*)

Male Reproductive Tract

Testis

Sertoli Cells

Leydig Cells

Epididymis

Microscopy

Spermiogenesis

Staging

Spermatogenesis



ABSTRACT:

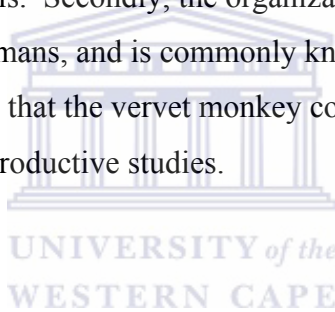
The vervet monkey, *Chlorocebus aethiops*, an Old World monkey, has been often used in biomedical research programs (toxicological studies and fertility) because of the inaccessibility of relevant human tissues. Data from nonhuman primates have been a vital component of advances in areas such as infertility, contraception, and other reproductive processes because of the phylogenetic closeness of the primates to humans. The aims and objectives of the study were 1) to describe the gross morphology, histology and ultrastructure of the male reproductive system, 2) to describe and compare the processes of spermatogenesis and spermiogenesis of the vervet monkey to humans and other nonhuman primates, and 3) to evaluate the vervet monkey as a possible experimental model for future human reproductive studies.

Twenty-nine adult male vervet monkeys, aged between 5 and 11 years, were used. Gross morphological features of different organs of the reproductive tract were recorded. Light and electron microscopic techniques, and methacrylate sections were used on selected tissues of the reproductive tract. The results showed that the vervet monkey has a male reproductive system similar to many non-human primates studied and man.

The epididymis was distinctively subdivided into the caput, corpus, and the caudal regions. No significant differences were observed on the epithelial height of these three regions. Four cell types, apical, principal, and basal cells, and the intraepithelial lymphocytes were observed. The basal cell distribution showed significant differences among three regions of the epididymis ($P \leq 0.01$). There were numerous phagocytic vesicles found in three regions of the epididymis.

The Sertoli cells showed perforated sleeve-like processes which encased elongated and mature spermatids ready for spermiation. The nuclei of the Sertoli cells were found to be multilobed (4 to 5) compared to the less lobular nuclei of the human Sertoli cells (2 to 3). The Leydig cells showed typical features of steroidogenic cells with abundant smooth endoplasmic reticulum, numerous large mitochondria, and few rough endoplasmic reticulum. The nuclei of the Leydig cells

showed both the euchromatin and heterochromatin regions which signified the activity of the cells. Three to four stages were recorded within individual cross-sections of the seminiferous tubules. Nine stages were found in the processes of spermatogenesis and 12 steps of spermatid development were recorded for the process of spermiogenesis. Diplotene spermatocytes and round spermatid distribution showed significant differences ($P \leq 0.01$) in the three sections of the testis (lateral, medial, and middle). Type A spermatogonia showed oval nuclei and one or two nucleoli near the nuclear membrane. Type B spermatogonia possessed spherical nuclei with several clumps of chromatin near the periphery associated with centrally positioned nucleoli. It was concluded that the gross morphology and structure of the reproductive tract of the vervet monkey has many similarities to humans and other mammals. Secondly, the organization of spermatogenesis is similar to that found in humans, and is commonly known as a helical arrangement. The results further suggest that the vervet monkey could be regarded as suitable model for human male reproductive studies.



DECLARATION

I declare that **THE STRUCTURE OF THE REPRODUCTIVE SYSTEM IN THE MALE VERVET MONKEY, *CHLOROCEBUS AETHIOPS*, WITH SPECIAL REFERENCE TO SPERMATOGENESIS**, is my own work, that it has not been submitted before for any degree or examination in any other university, and that all the sources I have used or quoted have been indicated and acknowledged as complete references.

Signed.....



ACKNOWLEDGEMENTS

I would like to express my sincere appreciation and gratitude to the following people, departments, institutions, without whose involvement this work would not been possible.

1. Prof G. van der Horst, my supervisor, who did not only advise and supported me throughout, but also instilled critical thinking in me.
2. MRC Primate Unit under the leadership of Dr J. Seier, for providing animals for this project and essential information on handling the vervet monkeys in captivity and the physiology of primates in general.
3. Dr Mdhluli, of the MRC Primate Unit for his assistance and support.
4. Department of Anatomical Pathology, University of Limpopo, Medunsa Campus, under the leadership of the late Prof MN Muthuphei for processing the light microscopic tissues.
5. Department of Electron Microscopy, University of Limpopo, Medunsa Campus under the leadership of Dr C. Baker, for processing both the TEM and SEM work.
6. Department of Physiology, University of Limpopo, Medunsa Campus, under the leadership of Prof L. Hay, for the time and support throughout the study.
7. National Research Foundation (NRF), for funding this research study.
8. My employer, University of Limpopo, Medunsa Campus for the time and financial assistance.

9. My family for their untiring encouragement, support and understanding throughout the challenges which I encountered during this study.

10. Last, but not the least I would like to thank the Almighty God, for life itself.



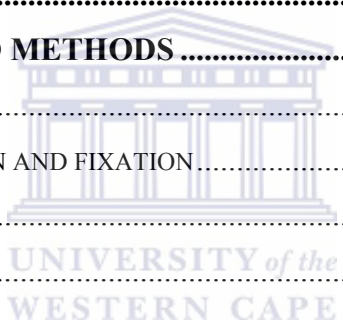
TABLE OF CONTENTS

CHAPTER 1: INTRODUCTION.....	1
1.1. GENERAL INTRODUCTION.....	1
1.2. TAXONOMY	2
1.3. DESCRIPTION.....	5
1.4. HABITAT	5
1.5. DISTRIBUTION	5
1.6. NUTRITION	5
1.7. REPRODUCTIVE BEHAVIOUR.....	6
1.8. BREEDING ASSESSMENT IN CAPTIVITY	7
1.9. REFERENCES.....	9
CHAPTER 2: MALE REPRODUCTIVE SYSTEM IN MAMMALS	12
2.1. OVERVIEW OF THE MALE REPRODUCTIVE SYSTEM IN MAMMALS.....	12
2.1.1. TESTES	13
2.1.2. SEMINIFEROUS TUBULES	13
2.1.3. SERTOLI AND LEYDIG CELLS	14
2.1.4. INTRATESTICULAR GENITAL DUCTS.....	14
2.1.4.1. Tubuli recti.....	15
2.1.4.2. Rete testis	15
2.1.4.3. Ductuli efferentes.....	16
2.1.5. DUCTUS EPIDIDYMIS.....	16
2.1.6. DUCTUS DEFERENS	17
2.1.7. AMPULLA	17
2.1.8. EJACULATORY DUCT	18
2.1.9. PROSTATIC URETHRA.....	18
2.1.10. PENIS.....	18

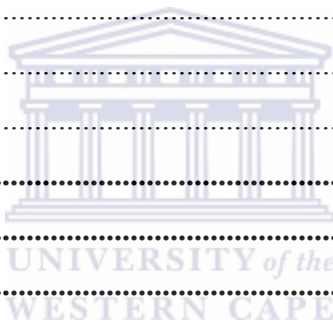
2.1.11. ACCESSORY SEX GLANDS	19
2.1.11.1. Seminal vesicles.....	19
2.1.11.2. Prostate gland.....	19
2.1.11.3. Bulbo-urethral glands.....	20
2.1.12. STRUCTURE OF THE SPERMATOZOON.....	20
2.2. REFERENCES.....	24

CHAPTER 3: GROSS MORPHOLOGY AND LIGHT MICROSCOPY OF THE MALE REPRODUCTIVE SYSTEM OF THE VERVET MONKEY 27

3.1. INTRODUCTION.....	27
3.1.1. OBJECTIVES	29
3.2. MATERIALS AND METHODS	29
3.2.1. STUDY ANIMALS.....	29
3.2.2. SAMPLE COLLECTION AND FIXATION.....	30
3.2.2.1. Testes	30
3.2.2.2. Epididymis	30
3.2.2.3. Vas deferens.....	30
3.2.2.4. Seminal vesicles.....	31
3.2.2.5. Prostate Gland.....	31
3.2.2.6. Penis	31
3.2.3. LIGHT MICROSCOPY.....	32
3.2.3.1. Tissue processing.....	32
3.2.4. FLEXIBLE IMAGE PROCESSING SYSTEM (FIPS).....	33
3.2.5. STATISTICAL ANALYSIS	33
3.3. RESULTS	34
3.3.1. GENERAL MACRO-ANATOMICAL DESCRIPTION OF THE MALE REPRODUCTIVE TRACT	34
3.3.2. HISTOLOGICAL DESCRIPTION OF THE MALE REPRODUCTIVE TRACT OF THE VERVET MONKEY.....	38



3.3.2.1. Testis	38
3.3.2.2. Seminiferous tubules.....	39
3.3.2.2.1. Sertoli Cells	40
3.3.2.2.2. Interstitial (Leydig) cells	42
3.3.2.2.3. Myoid cells	43
3.3.2.3. Ductus Epididymis.....	43
3.3.2.3.1. Caput epididymis (E1)	43
3.3.2.3.2. Corpus epididymis (E2)	44
3.3.2.3.3. Cauda epididymis (E3)	44
3.3.2.4. Vas deferens.....	52
3.3.2.10. Seminal vesicles.....	52
3.3.2.6. Prostate.....	54
3.3.2.7. Penis.....	57
3.3.2.8. Cavernous urethra	57
3.4. DISCUSSION	58
3.5. CONCLUSIONS	64
3.6. REFERENCES	66



CHAPTER 4: ULTRASTRUCTURE OF THE EPIDIDYMIS OF THE VERVET MONKEY	71
4.1. INTRODUCTION	71
4.1.1. ULTRASTRUCTURE OF THE EPIDIDYMIS	71
4.2. OBJECTIVES	73
4.2. MATERIALS AND METHODS	73
4.2.1. SCANNING ELECTRON MICROSCOPY (SEM)	73
4.2.2. TRANSMISSION ELECTRON MICROSCOPY (TEM).....	74
4.3. RESULTS	75
4.3.1. ULTRASTRUCTURE OF THE EPIDIDYMAL DUCT OF THE VERVET	75
4.3.1.1. Principal cells.....	83

4.3.1.2. Basal cells	86
4.3.1.3. Apical cells.....	87
4.3.1.4. Intraepithelial Lymphocytes	89
4. 4. DISCUSSION.....	90
4.5. CONCLUSIONS	95
4. 6. REFERENCES	96

CHAPTER 5: ULTRASTRUCTURE OF THE TESTES OF THE VERVET MONKEY, WITH SPECIAL REFERENCE TO THE NON-GERMINAL CELLS **101**

5.1. INTRODUCTION.....	101
5.1.1. ULTRASTRUCTURE OF THE TESTIS	101
5.1.2. ULTRASTRUCTURE OF THE SERTOLI CELL	102
5.1.3. ULTRASTRUCTURE OF THE LEYDIG CELL.....	105
5.2. OBJECTIVES	106
5.3. MATERIALS AND METHODS.....	107
5.3.1. SCANNING ELECTRON MICROSCOPY (SEM).....	107
5.3.2. TRANSMISSION ELECTRON MICROSCOPY (TEM).....	107
5.4. RESULTS	107
5.4.1. ULTRASTRUCTURE OF THE TESTIS OF THE VERVET MONKEY	107
5.4.2. ULTRASTRUCTURE OF THE SERTOLI CELL OF THE VERVET	118
5.4.3. ULTRASTRUCTURE OF THE LEYDIG CELL OF THE VERVET.....	122
5.4.4. ULTRASTRUCTURE OF OTHER CELLS OF THE INTERSTITIAL TISSUE (EXCLUDING LEYDIG CELLS).....	129
5.4.5. ULTRASTRUCTURE OF THE TISSUE IMMEDIATELY OUTSIDE THE TESTIS IN THE CONI VASCULOSI AREA.	133
5.5. DISCUSSION	135
5.5.1. HUMAN LEYDIG CELLS	138
5.6. CONCLUSIONS	139

5. 6. REFERENCES	141
CHAPTER 6: STAGING OF SPERMATOGENESIS IN THE VERVET MONKEY	148
6.1. INTRODUCTION.....	148
6.1.1. TYPE A SPERMATOGONIA	150
6.1.2. TYPE B SPERMATOGONIA.....	150
6.1.3. PRELEPTOTENE SPERMATOCYTES	151
6.1.4. PRIMARY SPERMATOCYTES.....	151
6.2. SPERMIOGENESIS AND ITS PHASES	153
6.2.1. GOLGI PHASE.....	153
6.2.2. CAP PHASE	154
6.2.3. ACROSOME PHASE.....	154
6.2.4. MATURATION PHASE	154
6.3. SERTOLI CELL ASSOCIATIONS AND ACTIVITY	155
6.4. OBJECTIVES	156
6.5. MATERIALS AND METHODS.....	156
6.6. STAGING OF SPERMATOGENESIS.....	157
6.7. STATISTICAL ANALYSIS	158
6.8. RESULTS.....	158
6.8.1. STAGING OF SPERMATOGENESIS.....	158
6.8.2. ELECTRON MICROSCOPY.....	159
6.8.3. SPERMIOGENESIS.....	159
6.9. DISCUSSION	198
6.9.1. SPERMATION	200
6. 10. CONCLUSIONS.....	203
6.11. REFERENCES.....	204

**CHAPTER 7: COMPARISON OF THE MALE REPRODUCTIVE SYSTEM
OF THE VERVET MONKEY AND HUMANS: A SUMMARY 211**

7.1. INTRODUCTION..... 211

7.2. CONCLUDING DISCUSSION..... 211

7.3. FUTURE INVESTIGATIONS 213

7.4. REFERENCES..... 215

CHAPTER 8: BIBLIOGRAPHY 216

LITERATURE CITED..... 216

CHAPTER 9: APPENDICES 240



LIST OF TABLES

TABLE 1. 1: THE TAXONOMY OF THE VERVET MONKEY, <i>CHLOROCEBUS AETHIOPS</i>	4
TABLE 2. 1. THE LENGTHS OF SPERMATOZOA IN DIFFERENT MAMMALIAN SPECIES ACCORDING TO GOULD (1980), SCHNOOR (1996), PESCH AND BERGMANN (2006), AND MODIFIED.....	22
TABLE 3. 1. AVERAGE MASS, SPERM DENSITY, pH, TESTICULAR MASS AND GONADOSOMATIC INDEX (TESTICULAR WEIGHT EXPRESSED AS A PERCENTAGE OF BODY MASS) OF VERVET MONKEY (THIS STUDY AND VAN DER HORST, 1995, PER PERMISSION).....	34
TABLE 3. 2. THE EPITHELIAL HEIGHT OF THE EPIDIDYMIS (FROM BASAL LAMINA TO THE STEREOCILIA), IN THREE DIFFERENT REGIONS OF THE EPIDIDYMIS IN THE VERVET MONKEY.....	51
TABLE 3. 3. THE NUMBER OF THREE DIFFERENT CELLS FOUND IN THREE DIFFERENT REGIONS OF THE EPIDIDYMIS OF THE VERVET MONKEY IN AN AREA OF $1000 \mu\text{m}^2$ (\pm SEM).	51
TABLE 3. 4. COMPARISON OF THE VERVET MONKEY, HUMANS AND OTHER MAMMALS ON SELECTED FEATURES OF THE REPRODUCTIVE TRACT.	64
TABLE 4. 1. COMPARISONS OF THE VERVET MONKEY, HUMANS, AND OTHER MAMMALS ON THE SELECTED FEATURES OF THE EPIDIDYMIS.	95
TABLE 5. 1. COMPARISONS OF VERVET MONKEY, HUMANS, AND OTHER MAMMALS ON SELECTED FEATURES OF THE TESTIS.	139
TABLE 6. 1. DESCRIPTION OF STAGES.....	173
TABLE 6. 2. THE CELLULAR ASSOCIATIONS OF THE NINE STAGES OF THE CYCLE OF THE SEMINIFEROUS EPITHELIUM IN THE VERVET MONKEY, <i>CHLOROCEBUS AETHIOPS</i> ..	196

TABLE 6. 3. GERM CELLS DISTRIBUTION PATTERN IN DIFFERENT REGIONS OF
TESTICULAR TISSUE OF THE VERVET MONKEY, *CHLOROCEBUS AETHIOPS* (MEAN ±
SEM). 197

TABLE 6. 4. DIFFERENT DEVELOPMENTAL STEPS IN EACH OF THE SIX STAGES OF HUMAN
SPERMATOGENIC CYCLE (HESS, *ET AL.*, 1990), UNMODIFIED..... 201

TABLE 6. 5. DIFFERENT ANIMAL MODELS AND THE NUMBER OF STAGES THAT HAVE
BEEN REPORTED IN THE SEMINIFEROUS TUBULES..... 202



LIST OF FIGURES

FIGURE 3. 1. PHOTOGRAPH SHOWING THE TESTIS, THE EPIDIDYMIS AND THE VAS DEFERENS OF THE VERVET MONKEY, <i>CHLOROCEBUS AETHIOPS</i> . SCALE IN MM.	35
FIGURE 3. 2. PHOTOGRAPH SHOWING THREE REGIONS OF THE EPIDIDYMIS WITH THE VAS DEFERENS OF THE VERVET MONKEY, (<i>CHLOROCEBUS AETHIOPS</i>), BEEN SPREAD OUT. SCALE IN MM.....	36
FIGURE 3. 3. PHOTOGRAPH SHOWING THE SEMINAL VESICLES OF THE VERVET MONKEY, <i>CHLOROCEBUS AETHIOPS</i> . SCALE IN MM.....	37
FIGURE 3. 4. PHOTOGRAPH SHOWING THE PENILE ORGAN AND ASSOCIATED STRUCTURES OF THE VERVET MONKEY, <i>CHLOROCEBUS AETHIOPS</i> . SCALE IN MM.	38
FIGURE 3. 5. THE LIGHT MICROGRAPH SHOWING THE GENERAL LAY-OUT OF THE SEMINIFEROUS TUBULES OF THE VERVET MONKEY, <i>CHLOROCEBUS AETHIOPS</i>	40
FIGURE 3. 6. THE LIGHT MICROGRAPH SHOWING THE SERTOLI CELLS AND ASSOCIATED SPERMATOGENIC CELLS IN THE SEMINIFEROUS TUBULES OF THE VERVET MONKEY, <i>CHLOROCEBUS AETHIOPS</i>	41
FIGURE 3. 7. THE LIGHT MICROGRAPH SHOWING THE SERTOLI CELLS IN THE SEMINIFEROUS TUBULES OF THE VERVET MONKEY, <i>CHLOROCEBUS AETHIOPS</i>	42
FIGURE 3. 8. LIGHT MICROGRAPH SHOWING INTERTUBULAR REGION WITH THE LEYDIG CELLS AND BLOOD VESSELS OF THE TESTIS OF THE VERVET MONKEY, <i>CHLOROCEBUS AETHIOPS</i>	43
FIGURE 3. 9. LIGHT MICROGRAPH SHOWING THE CAPUT EPIDIDYMIS OF THE VERVET MONKEY, <i>CHLOROCEBUS AETHIOPS</i>	46
FIGURE 3. 10. LIGHT MICROGRAPH SHOWING ZONE 2 OF THE CAPUT EPIDIDYMIS (E1) OF THE VERVET MONKEY, <i>CHLOROCEBUS AETHIOPS</i>	47
FIGURE 3. 11. LIGHT MICROGRAPH SHOWING THE CORPUS EPIDIDYMIS OF THE VERVET MONKEY, <i>CHLOROCEBUS AETHIOPS</i>	48
FIGURE 3. 12. LIGHT MICROGRAPH SHOWING THE CAUDA EPIDIDYMIS OF THE VERVET MONKEY, <i>CHLOROCEBUS AETHIOPS</i>	49
FIGURE 3. 13. LIGHT MICROGRAPH SHOWING ZONE 1 OF THE CAUDA EPIDIDYMIS (E3) OF THE VERVET MONKEY, <i>CHLOROCEBUS AETHIOPS</i>	50

FIGURE 3. 14. LIGHT MICROGRAPH SHOWING ZONE 2 OF THE CAUDA EPIDIDYMIS (E3) OF THE VERVET MONKEY, <i>CHLOROCEBUS AETHIOPS</i>	50
FIGURE 3. 15. LIGHT MICROGRAPH SHOWING ZONE 3 OF THE CAUDA EPIDIDYMIS (E3) EPIDIDYMIS OF THE VERVET MONKEY, <i>CHLOROCEBUS AETHIOPS</i>	51
FIGURE 3. 16. LIGHT MICROGRAPH SHOWING THE VAS DEFERENS OF THE VERVET MONKEY, <i>CHLOROCEBUS AETHIOPS</i>	52
FIGURE 3. 17. LIGHT MICROGRAPH SHOWING THE SEMINAL VESICLES OF THE VERVET MONKEY, <i>CHLOROCEBUS AETHIOPS</i>	53
FIGURE 3. 18. LIGHT MICROGRAPH SHOWING THE CELLS OF THE SEMINAL VESICLES OF THE VERVET MONKEY, <i>CHLOROCEBUS AETHIOPS</i>	54
FIGURE 3. 19. LIGHT MICROGRAPH SHOWING THE PROSTATE OF THE VERVET MONKEY <i>CHLOROCEBUS AETHIOPS</i>	55
FIGURE 3. 20. LIGHT MICROGRAPH SHOWING THE CELLS OF THE PROSTATE GLAND OF THE VERVET MONKEY, <i>CHLOROCEBUS AETHIOPS</i>	56
FIGURE 3. 21. LIGHT MICROGRAPH SHOWING THE CELLS OF THE PROSTATE GLAND OF THE VERVET MONKEY, <i>CHLOROCEBUS AETHIOPS</i>	56
FIGURE 3. 22. (A AND B). LIGHT MICROGRAPH SHOWING THE CORPUS SPONGIOSUM URETHRA WITH LAMINA PROPRIA, AND ERECTILE TISSUE OF THE VERVET MONKEY, <i>CHLOROCEBUS AETHIOPS</i>	57
FIGURE 3. 23. LIGHT MICROGRAPH SHOWING THE CORPUS CAVERNOSUM SHOWING THE ERECTILE TISSUE IN THE VERVET MONKEY, <i>CHLOROCEBUS AETHIOPS</i>	58
FIGURE 4. 1. SEM MICROGRAPH SHOWING THE GENERAL LAY-OUT OF THE CAPUT EPIDIDYMIS OF THE VERVET MONKEY, <i>CHLOROCEBUS AETHIOPS</i>	76
FIGURE 4. 2. SEM MICROGRAPH SHOWING THE MICROVILLI IN THE CAPUT REGION OF THE EPIDIDYMIS OF THE VERVET MONKEY, <i>CHLOROCEBUS AETHIOPS</i>	77
FIGURE 4. 3. TEM MICROGRAPH SHOWING THE BASAL CELLS OF THE CORPUS EPIDIDYMIS OF THE VERVET MONKEY, <i>CHLOROCEBUS AETHIOPS</i>	78
FIGURE 4. 4. TEM MICROGRAPH SHOWING THE BASAL CELL OF THE CORPUS EPIDIDYMIS OF THE VERVET MONKEY, <i>CHLOROCEBUS AETHIOPS</i>	79

FIGURE 4. 5. TEM MICROGRAPH SHOWING THE PRINCIPAL CELL OF THE CORPUS EPIDIDYMIS OF THE VERVET MONKEY, <i>CHLOROCEBUS AETHIOPS</i>	80
FIGURE 4. 6. TEM MICROGRAPH SHOWING THE MICROVILLI OF THE PRINCIPAL CELLS IN THE CORPUS REGION OF THE EPIDIDYMIS OF THE VERVET MONKEY, <i>CHLOROCEBUS AETHIOPS</i>	81
FIGURE 4. 7. SEM MICROGRAPH SHOWING THE CORPUS EPIDIDYMIS OF THE VERVET MOKEY, <i>CHOROCEBUS AETHIOPS</i>	82
FIGURE 4. 8. TEM MICROGRAPH SHOWING THE PRINCIPAL CELLS OF THE CAUDA EPIDIDYMIS OF THE VERVET MONKEY, <i>CHLOROCEBUS AETHIOPS</i>	85
FIGURE 4. 9. TEM MICROGRAPH SHOWING THE PRINCIPAL CELLS OF THE CAUDA EPIDIDYMIS OF THE VERVET MONKEY, <i>CHLOROCEBUS AETHIOPS</i>	86
FIGURE 4. 10. TEM MICROGRAPH SHOWING THE PRINCIPAL CELLS OF THE CAUDA EPIDIDYMIS OF THE VERVET MONKEY, <i>CHLOROCEBUS AETHIOPS</i>	88
FIGURE 4. 11. TEM MICROGRAPH SHOWING THE PRINCIPAL CELLS OF THE CAUDA EPIDIDYMIS OF THE VERVET MONKEY, <i>CHLOROCEBUS AETHIOPS</i>	89
FIGURE 5. 1. SEM MICROGRAPH SHOWING THE TUNICA ALBUGINEA OF THE TESTIS OF THE VERVET MONKEY, <i>CHLOROCEBUS AETHIOPS</i>	108
FIGURE 5. 2. SEM MICROGRAPH SHOWING THE INTERSTITIAL SEPTUM OF THE TESTIS OF THE VERVET MONKEY, <i>CHLOROCEBUS AETHIOPS</i>	109
FIGURE 5. 3. SEM MICROGRAPH SHOWING AT LOW MAGNIFICATION OF EXTERNAL APPEARANCE OF THE SEMINIFEROUS TUBULES IN THE TESTIS OF THE VERVET MONKEY, <i>CHLOROCEBUS AETHIOPS</i> . LINE SHOWS APPROXIMATE POSITION OF SEPTUM.	110
FIGURE 5. 4 . SEM MICROGRAPH SHOWING SEMINIFEROUS TUBULES IN TRANSVERSE SECTION FROM THE MEDIAL TESTIS OF THE VERVET MONKEY, <i>CHLOROCEBUS AETHIOPS</i>	111
FIGURE 5. 5. SEM MICROGRAPH SHOWING THE SEMINIFEROUS TUBULES OF THE MEDIAL TESTIS OF THE VERVET MONKEY, <i>CHLOROCEBUS AETHIOPS</i>	112

FIGURE 5. 6. SEM MICROGRAPH SHOWING THE SLEEVE –LIKE PROCESSES FOUND IN THE SERTOLI CELLS OF THE MIDDLE TESTIS, OF THE VERVET MONKEY, <i>CHLOROCEBUS AETHIOPS</i>	113
FIGURE 5. 7. SEM MICROGRAPH SHOWING THE SPERM TAIL AND SLEEVE LIKE PROCESSES IN THE TESTIS OF THE VERVET MONKEY, <i>CHLOROCEBUS AETHIOPS</i>	114
FIGURE 5. 8. SEM MICROGRAPH SHOWING THE SPERM TAIL AND SLEEVE LIKE PROCESSES IN THE TESTIS OF THE VERVET MONKEY, <i>CHLOROCEBUS AETHIOPS</i>	115
FIGURE 5. 9. TEM MICROGRAPH SHOWING THE INTERSTITIAL REGION OF THE TESTIS AND THE THREE LAYERS OF THE SEMINIFEROUS TUBULES OF THE VERVET MONKEY, <i>CHLOROCEBUS AETHIOPS</i>	116
FIGURE 5. 10. TEM MICROGRAPH SHOWING MYOID CELLS AND LIPID DROPLETS IN THE INTERSTITIAL TISSUE OF THE TESTIS OF THE VERVET MONKEY, <i>CHLOROCEBUS AETHIOPS</i>	117
FIGURE 5. 11. TEM MICROGRAPH SHOWING THE SERTOLI CELLS WITH PRIMARY SPERMATOCYTES (EARLY PACHYTENE) OF THE VERVET MONKEY, <i>CHLOROCEBUS AETHIOPS</i>	119
FIGURE 5. 12. TEM MICROGRAPH SHOWING THE SERTOLI CELL TIGHT JUNCTIONS, LIPID COMPLEX IN THE SEMINIFEROUS TUBULES OF THE VERVET MONKEY, <i>CHLOROCEBUS AETHIOPS</i>	120
FIGURE 5. 13. TEM MICROGRAPH OF THE SERTOLI CELLS, SHOWING MITOCHONDRIA AND TIGHT JUNCTION IN THE SEMINIFEROUS TUBULES OF THE VERVET MONKEY, <i>CHLOROCEBUS AETHIOPS</i> . PROMINENT IS THE DISPERSED CHROMATIN IN THE NUCLEUS INDICATING THE HIGH CELLULAR ACTIVITY.	121
FIGURE 5. 14. TEM MICROGRAPH SHOWING THE LEYDIG CELLS, SHOWING MITOCHONDRIA, LIPID DROPLETS, AND SER IN THE INTERSTITIAL REGION OF THE TESTIS OF THE VERVET MONKEY, <i>CHLOROCEBUS AETHIOPS</i>	123
FIGURE 5. 15. TEM MICROGRAPH OF THE LEYDIG CELLS, SHOWING MITOCHONDRIA WITH CHARACTERITICS AND EXTENSIVE CRISTAE, AND LIPID DROPLETS IN THE INTERSTITIAL REGION OF THE TESTIS OF THE VERVET MONKEY, <i>CHLOROCEBUS AETHIOPS</i>	124

FIGURE 5. 16. TEM MICROGRAPH SHOWING THE LEYDIG CELL NUCLEUS WITH ITS HETEROCHROMATIN AND EUCHROMATIN REGIONS, AND LIPID DROPLETS IN THE INTERSTITIAL REGION OF THE TESTIS OF THE VERVET MONKEY, <i>CHLOROCEBUS AETHIOPS</i> .	125
FIGURE 5. 17. TEM MICROGRAPH OF THE LEYDIG CELL, SHOWING MITOCHONDRIA, LIPID DROPLETS, AND SER IN THE INTERSTITIAL REGION OF THE TESTIS OF THE VERVET MONKEY, <i>CHLOROCEBUS AETHIOPS</i> .	126
FIGURE 5. 18. TEM MICROGRAPH SHOWING A CLUSTER OF LEYDIG CELLS, MITOCHONDRIA, AND LIPID DROPLETS IN THE INTERSTITIAL REGION OF THE TESTIS OF THE VERVET MONKEY, <i>CHLOROCEBUS AETHIOPS</i> . IN THIS INSTANCE THERE APPEARS TO BE LESS LIPID DROPLETS.	127
FIGURE 5. 19. TEM MICROGRAPH SHOWING THE LEYDIG CELL NUCLEUS WITH ITS HETEROCHROMATIN AND EUCHROMATIN REGIONS, AND LIPID DROPLETS IN THE INTERSTITIAL REGION OF THE TESTIS OF THE VERVET MONKEY, <i>CHLOROCEBUS AETHIOPS</i> .	128
FIGURE 5. 20. TEM MICROGRAPH SHOWING THE INTERSTITIAL AREA, LYMPHATICS AND SERTOLI CELL NUCLEUS, AND TWO SEMINIFEROUS TUBULES OF THE VERVET MONKEY, <i>CHLOROCEBUS AETHIOPS</i> .	129
FIGURE 5. 21. TEM MICROGRAPH SHOWING THE NUCLEUS OF THE MACROPHAGE IN THE INTERSTITIAL TUBULE OF THE VERVET MONKEY, <i>CHLOROCEBUS AETHIOPS</i> .	130
FIGURE 5. 22. TEM MICROGRAPH SHOWING THE MACROPHAGES AT DIFFERENT STAGES OF DEVELOPMENT IN THE INTERSTITIAL AREA OF THE TESTIS OF THE VERVET MONKEY, <i>CHLOROCEBUS AETHIOPS</i> .	131
FIGURE 5. 23. TEM MICROGRAPH SHOWING THE MACROPHAGE IN THE TESTIS OF THE VERVET MONKEY, <i>CHLOROCEBUS AETHIOPS</i> .	132
FIGURE 5. 24. TEM MICROGRAPH SHOWING THE ENDOTHELIAL CELL OF THE INTERSTITIAL TISSUE OF THE VERVET MONKEY, <i>CHLOROCEBUS AETHIOPS</i> .	133
FIGURE 5. 25. TEM MICROGRAPH SHOWING NERVES IMMEDIATELY OUTSIDE TESTIS IN THE CONI VASCULOSI AREA OF THE VERVET MONKEY, <i>CHLOROCEBUS AETHIOPS</i> .	134

FIGURE 6. 1 (A AND B). LIGHT MICROGRAPHS SHOWING TRANSVERSE SECTIONS THROUGH THE SEMINIFEROUS TUBULES OF THE VERVET MONKEY, <i>CHLOROCEBUS AETHIOPS</i>	160
FIGURE 6. 2. SCHEMATIC DIAGRAM SHOWING SPERMIOGENESIS IN THE HUMAN.....	161
FIGURE 6. 3. PHOTOGRAPHIC MONTAGE REPRESENTING THE PROGRESSIVE STEPS OF SPERMATID DEVELOPMENT (STEPS 1-12) IN THE SEMINIFEROUS TUBULES OF THE VERVET MONKEY, <i>CHLOROCEBUS AETHIOPS</i> . USING 1 μ M METHACRYLATE RESIN SECTIONS.	162
FIGURE 6. 4. TEM MICROGRAPH SHOWING DIFFERENT PHASES OF SPERMIOGENESIS AND PHAGOCYTOTIC EVENTS IN THE SEMINIFEROUS TUBULES OF THE VERVET MONKEY, <i>CHLOROCEBUS AETHIOPS</i>	163
FIGURE 6. 5. TEM MICROGRAPHS SHOWING THE DIFFERENT SPERMATIDS IN THEIR DEVELOPING STAGES IN THE SEMINIFEROUS TUBULES OF THE VERVET MONKEY, <i>CHLOROCEBUS AETHIOPS</i>	164
FIGURE 6. 6. TEM MICROGRAPH SHOWING THE DIFFERENT STAGES OF THE SPERMATIDS IN SEMINIFEROUS TUBULES OF THE VERVET MONKEY, <i>CHLOROCEBUS AETHIOPS</i> ..	165
FIGURE 6. 7. TEM MICROGRAPH SHOWING DIFFERENT STAGES OF SPERMATIDS IN A SEMINIFEROUS TUBULE OF THE VERVET MONKEY, <i>CHLOROCEBUS AETHIOPS</i>	166
FIGURE 6. 8. TEM MICROGRAPH SHOWING THE MANCHETTE OF THE DEVELOPING SPERMATID IN THE SEMINIFEROUS TUBULES OF THE VERVET MONKEY, <i>CHLOROCEBUS AETHIOPS</i>	167
FIGURE 6. 9. TEM MICROGRAPH SHOWING DIFFERENT PHASES OF SPERMIOGENESIS IN THE SEMINIFEROUS TUBULES OF THE VERVET MONKEY, <i>CHLOROCEBUS AETHIOPS</i>	168
FIGURE 6. 10. TEM MICROGRAPH SHOWING AN ELONGATED STAGE OF THE SPERMATID WITH HELICAL MITOCHONDRIAL ARRANGEMENT IN THE SEMINIFEROUS TUBULES OF THE VERVET MONKEY, <i>CHLOROCEBUS AETHIOPS</i>	169
FIGURE 6. 11. TEM MICROGRAPHS SHOWING THE DIFFERENT SPERMATIDS IN THEIR DEVELOPING STAGES IN THE SEMINIFEROUS TUBULES OF THE VERVET MONKEY, <i>CHLOROCEBUS AETHIOPS</i>	170

FIGURE 6. 12. TEM MICROGRAPH SHOWING THE ELONGATED SPERMATIDS DURING SPERMIOGENESIS IN THE VERVET MONKEY, <i>CHLOROCEBUS AETHIOPS</i>	171
FIGURE 6. 13. TEM MICROGRAPH SHOWING AN ELONGATED STAGE OF THE SPERMATID WITH SPHERICAL MITOCHONDRIAL ARRANGEMENT IN THE SEMINIFEROUS TUBULES OF THE VERVET MONKEY, <i>CHLOROCEBUS AETHIOPS</i>	172
FIGURE 6. 14. LIGHT MICROGRAPH OF THE LATERAL SECTION OF THE TESTICULAR TISSUE OF THE VERVET MONKEY, <i>CHLOROCEBUS AETHIOPS</i> , (SECTION 1 OF THE 4 SECTIONS).	175
FIGURE 6. 15. LIGHT MICROGRAPH OF THE LATERAL SECTION OF THE TESTICULAR TISSUE OF THE VERVET MONKEY, <i>CHLOROCEBUS AETHIOPS</i> , (SECTION 2 OF THE 4 SECTIONS).	176
FIGURE 6. 16. LIGHT MICROGRAPH OF THE LATERAL SECTION OF THE TESTICULAR TISSUE OF THE VERVET MONKEY, <i>CHLOROCEBUS AETHIOPS</i> , (SECTION 3 OF THE 4 SECTIONS).	177
FIGURE 6. 17. LIGHT MICROGRAPH OF THE LATERAL SECTION OF THE TESTICULAR TISSUE OF THE VERVET MONKEY, <i>CHLOROCEBUS AETHIOPS</i> , (SECTION 4 OF THE 4 SECTIONS).	178
FIGURE 6. 18. LIGHT MICROGRAPH OF THE LATERAL SECTION OF THE TESTICULAR TISSUE OF THE VERVET MONKEY, <i>CHLOROCEBUS AETHIOPS</i>	179
FIGURE 6. 19. LIGHT MICROGRAPH OF THE LATERAL SECTION OF THE TESTICULAR TISSUE OF THE VERVET MONKEY, <i>CHLOROCEBUS AETHIOPS</i>	180
FIGURE 6. 20. LIGHT MICROGRAPH OF THE LATERAL SECTION OF THE TESTICULAR TISSUE OF THE VERVET MONKEY, <i>CHLOROCEBUS AETHIOPS</i>	181
FIGURE 6. 21. LIGHT MICROGRAPH OF THE LATERAL SECTION OF THE TESTICULAR TISSUE OF THE VERVET MONKEY, <i>CHLOROCEBUS AETHIOPS</i>	182
FIGURE 6. 22. LIGHT MICROGRAPH OF THE LATERAL SECTION OF THE TESTICULAR TISSUE OF THE VERVET MONKEY, <i>CHLOROCEBUS AETHIOPS</i>	183
FIGURE 6. 23. LIGHT MICROGRAPH OF A METHACRYLATE RESIN SECTION SHOWING A SECTION OF THE TESTICULAR TISSUE (LATERAL) OF THE VERVET MONKEY, <i>CHLOROCEBUS AETHIOPS</i>	184

FIGURE 6. 24. LIGHT MICROGRAPH OF A METHACRYLATE RESIN SECTION SHOWING A SECTION OF THE TESTICULAR TISSUE (LATERAL) OF THE VERVET MONKEY, <i>CHLOROCEBUS AETHIOPS</i>	185
FIGURE 6. 25. LIGHT MICROGRAPH OF A METHACRYLATE RESIN SECTION SHOWING A SECTION OF THE TESTICULAR TISSUE (LATERAL) OF THE VERVET MONKEY, <i>CHLOROCEBUS AETHIOPS</i>	186
FIGURE 6. 26. LIGHT MICROGRAPH OF A METHACRYLATE RESIN SECTION SHOWING A SECTION OF THE TESTICULAR TISSUE (LATERAL) OF THE VERVET MONKEY, <i>CHLOROCEBUS AETHIOPS</i>	187
FIGURE 6. 27. LIGHT MICROGRAPH OF A METHACRYLATE RESIN SECTION SHOWING A SECTION OF THE TESTICULAR TISSUE (LATERAL) OF THE VERVET MONKEY, <i>CHLOROCEBUS AETHIOPS</i>	188
FIGURE 6. 28. LIGHT MICROGRAPH OF A METHACRYLATE RESIN SECTION SHOWING A SECTION OF THE TESTICULAR TISSUE (LATERAL) OF THE VERVET MONKEY, <i>CHLOROCEBUS AETHIOPS</i>	189
FIGURE 6. 29. LIGHT MICROGRAPH OF A METHACRYLATE RESIN SECTION SHOWING A SECTION OF THE TESTICULAR TISSUE (LATERAL) OF THE VERVET MONKEY, <i>CHLOROCEBUS AETHIOPS</i>	190
FIGURE 6. 30. LIGHT MICROGRAPH OF A METHACRYLATE RESIN SECTION SHOWING A SECTION OF THE TESTICULAR TISSUE (LATERAL) OF THE VERVET MONKEY, <i>CHLOROCEBUS AETHIOPS</i>	191
FIGURE 6. 31. LIGHT MICROGRAPH OF A METHACRYLATE RESIN SECTION SHOWING A SECTION OF THE TESTICULAR TISSUE (LATERAL) OF THE VERVET MONKEY, <i>CHLOROCEBUS AETHIOPS</i>	192
FIGURE 6. 32. LIGHT MICROGRAPH OF A METHACRYLATE RESIN SECTION SHOWING A SECTION OF THE TESTICULAR TISSUE (LATERAL) OF THE VERVET MONKEY, <i>CHLOROCEBUS AETHIOPS</i>	193
FIGURE 6. 33. TEM MICROGRAPH SHOWING GERM CELLULAR ASSOCIATIONS WITH SERTOLI CELLS IN THE SEMINIFEROUS TUBULES OF THE VERVET MONKEY, <i>CHLOROCEBUS AETHIOPS</i>	194

FIGURE 6. 34. TEM MICROGRAPH SHOWING LAYERS OF THE SEMINIFEROUS TUBULES,
TWO SERTOLI CELL NUCLEI, AND TWO SPERMATOGONIA, OF THE VERVET MONKEY,
CHLOROCEBUS AETHIOPS. 195



CHAPTER 1: INTRODUCTION

1.1. GENERAL INTRODUCTION

The close anatomical and physiological relationship of non-human primates to humans has led to an increased use of different primate species in biomedical research (Goodwin, 1970). Domestic production of non-human primates has become increasingly important with the decline of wild primate populations and source country export restrictions. The following non-human primates have been extensively used for different biomedical research activities: *Macaca mulatta*, (Plant, 1981), *Macaca fascicularis*, (Tarantal *et al.*, 1990), *Macaca arctoides*, (Zatuchin *et al.*, 1981), *Macaca radiata*, (Ramesh *et al.*, 1998), *Pan troglodytes*, (Gould *et al.*, 1993), and *Chlorocebus aethiops*, (Seier 1986; van der Horst *et al.*, 1999). The types of research undertaken involved a variety of biomedical research relevant to human health, including reproduction, contraceptive development, nutritional aspects, and toxicology. However, there are several other primate species that may prove to be preferable for many types of studies, based on a variety of reasons. The vervet monkey, *Chlorocebus aethiops*, for example, has on several occasions been preferred as a laboratory primate because of its numerous advantages. Its moderately small size makes it easier and less expensive to maintain than most Old World primates, and yet it is large enough for most biomedical requirements. In addition, it adapts quickly to a breeding group and has a significantly high reproductive potential once stable breeding groups have been established (Else, 1985).

Over the past three decades, the vervet monkey, *Chlorocebus aethiops*, has been constantly used in biomedical research as an animal model for human-related problems such as in virology, ophthalmology, and reproductive studies (Kushner *et al.*, 1982). There is considerable information on some aspects of the reproductive biology of this species, for example, a study on the sperm motility in the epididymis (van der Horst *et al.*, 1999), and again studies on breeding of vervets in a closed environment (Seier, 1986), and other studies on reproductive behaviour (Rowell, 1970). However, data on the anatomy of the reproductive system, physiology and endocrinology remain scanty (Skinner & Smithers, 1990; Eley, 1992). In addition,

there is a need to compare these physiological aspects with those found in humans and critically evaluate the vervet monkey for a possible experimental model in biomedical research. *Chlorocebus aethiops* belongs to the Old World monkey group and was evolutionarily separated from humans more than 50 million years ago. Their resemblance to man, however, in characteristics such as the nervous system, reproductive system, and susceptibility to certain parasites make them more relevant for biological studies (Harris, 1970). As a possible model for reproductive studies, information on taxonomy, its distribution, and reproductive behaviour in the wild is essential.

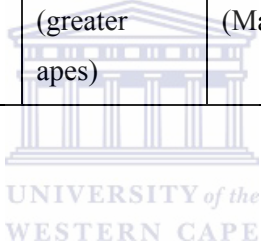
1.2. TAXONOMY

Chlorocebus aethiops, formerly known as *Cercopithecus aethiops*, is commonly referred to as the African green monkey, vervet, tantulus, savannah, or the grivet monkey. For the sake of clarity and consistency, from here onwards it will be referred to as the vervet monkey or simply as vervet. The taxonomic classification of the vervet monkey is outlined in Table 1.1. The order Primates consists of the two suborders, *viz.*, Prosimii and Anthropoidea. The prosimians are phylogenetically primitive and are the smaller of the two groups. They exhibit features that deviate from the primate pattern more often than any other primate group (Rosen, 1974). The prosimians are also often referred to as lower primates whereas the simians are regarded as the higher primates because of their similarities to human in terms of anatomy, biochemistry, and physiology. Anthropoids are divided into the Catarrhines (Old World monkeys found in Africa, Asia, and Europe) and the Platyrrhines (New World monkeys found in South and North America). The significance of these terms is related to the particular shape of the nose. In Catarrhines or Old World primates, the nostrils are separated by a narrow partition, whereas in the Platyrrhines or New World primates, the partition is broader, and the nostrils are positioned wider apart. The Old World monkeys are phylogenetically and biologically closer to humans than the New World primates. That could be the

reason why some of these species, especially the rhesus monkeys and the baboons, are common choice animals for biomedical research (Rosen, 1974).



Table 1. 1: The taxonomy of the vervet monkey, *Chlorocebus aethiops*.

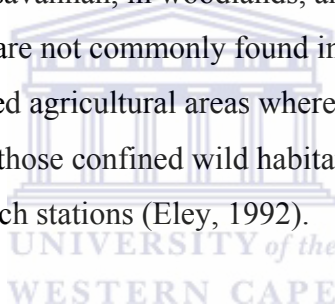
ORDER	PRIMATES				
SUBORDER	PROSIMII (Prosimians)	ANTHROPOIDEA (monkeys, apes, man)			
INFRAORDER		CATARRHINI (Old World)			PLATYRRHINI (New World)
SUPERFAMILY		HOMINOIDEA		CERCOPITHECOIDEA	
FAMILY		HYLOBATI DAE (lesser apes)	PONGIDAE (greater apes)	HOMINIDAE (Man)	CERCOPITHECIDAE
GENUS					<i>CHLOROCEBUS</i>
SPECIES					<i>AETHIOPS</i>
COMMON NAME					VERVET

1.3. DESCRIPTION

Vervet monkeys are grey-brown monkeys with greenish hue to the pelage on their backs, a white-fringed black face, long whitish cheek whiskers, white colour surrounding their eyes, black feet and a black tip to the tail. The male has a blue scrotum, red penis and red anus (Eley, 1992). The female has a red perineal region and the nipples have a blue hue. Adult males weigh between 4-7 kg, head and body length is between 40-60 cm and the tail is about 15cm longer than the body. The female is lighter and smaller with measurements about 60-80% of those of the male (Eley, 1992).

1.4. HABITAT

They are found in savannah, in woodlands, and in riverine, gallery lake shore and coastal forests. They are not commonly found in heavily forested areas or open grasslands or heavily settled agricultural areas where they have been displaced or exterminated. Despite all those confined wild habitats, they have been successfully propagated in many research stations (Eley, 1992).



1.5. DISTRIBUTION

They are regarded as the most widely distributed non-human primates in the world of all African monkeys (Eley, 1992). With the exception of the forests of the Congo basin and the deserts of southwestern Africa, the vervet monkeys are found throughout the African continent south of the Sahara. They occur from southern Ethiopia and Somalia to the Cape region (Skinner and Smithers, 1990). In addition, they are also found in the West Indies (Eley, 1992).

1.6. NUTRITION

Vervet monkeys are regarded as omnivores, feeding on both plant and animal materials. They feed on fruits, buds, seeds, roots, bark, small vertebrates, and eggs. Like baboons, they are regarded as opportunistic feeders and they are able to survive in a wide variety of conditions and eat a wide variety of food types (Eley, 1992). In

captivity, their basic diet consists of precooked maize meal with a protein-vitamin and mineral concentrate, which is mixed to a stiff porridge with water and fed in the mornings (Seier, 1986). Wholewheat brown bread is provided at noon, and apples and carrots, washed in chlorinated water, are given in the afternoon. Drinking water is supplied *ad libitum* via an automatic device (Seier, 1986). In the wild, products of *Acacia* trees provide a major source of food, and water can be found on the branches of other trees (Eley, 1989).

1.7. REPRODUCTIVE BEHAVIOUR

Vervet monkeys have shifted from an almost entirely arboreal existence to one where terrestrial activity is considerable. They appear equally at “home” in the trees or on the ground and this flexibility is reflected in their wide distribution (Eley, 1992). Vervets are found in multi male and multi female groups with a linear dominance hierarchy among the males and a matrilineal kin group relationship among the females (Eley, 1989). A vervet troop can vary between 6 and 60 individuals but most often consists of between 20-30 individuals. Typically one male is fully integrated into the group and the other males are peripheral. A vervet male will display a red penis, blue scrotum, and white rump hairs as a gesture of aggression (Eley, 1992).

In the wild, birth peaks are reported to be associated with the emergence of the flowers of the *Acacia tortulus*. It would appear that either the nutritive quality of the flowers or some other effects that are not yet elucidated, but presumably hormonal factors, will have an influence in the birth peaks of the vervet monkeys. The nutritive value of the flowers may alone be the major factor, for around the lodges or in captivity where food is more plentiful, breeding will probably occur throughout the year (Eley, 1989).

In captivity, births have been described as seasonal, fixed peak, non-fixed peak, and year-round (Booth, 1962; Conaway and Sade, 1969; Hess *et al.*, 1979). According to Fairbanks and McGuire (1984), vervet monkeys are capable of deviating from the seasonal breeding patterns when placed under favourable

conditions. Male rhesus monkeys, for example, are true seasonal breeders, they exhibit testicular atrophy during the off season and their female counterparts are acyclic. This trend has not been reported in captive vervet monkeys.

Conaway and Sade (1969) studied the testicular and epididymal tissue from 19 vervet monkeys, and they reported a degree of seasonality in testis size associated with reduction in spermatogenesis and seminiferous tubule diameter. They concluded that despite the small seasonal changes in testis volume, spermatogenesis, and seminiferous tubule diameter, the animals were probably fertile throughout the year. Kushner *et al.*, (1982), also observed the same trend and concluded that vervets mate throughout the year.

Eley *et al.*, (1986) studied testis size and testosterone concentration in adult male vervet monkeys over a one-year period. They found a rise and fall in testicular volume throughout the period. Testosterone concentration did not follow the pattern and the authors concluded that any rhythm was unlikely to have an effect on fertility. Histological appraisal of the testis revealed spermatogenesis to be ongoing at all times. They concluded that the male vervet in captivity exhibited a very marginal seasonal reproductive pattern, which did not prevent it from successfully breeding all year round. Breeding and birth peaks, which are seasonal, are overcome by nutrition as they disappear in captive animals and provisioned wild animals. Booth (1962), reported that the peaks in the wild were associated with food availability and varied widely among locations. In a recent review, Van der Horst (2005) suggested that the vervet monkey is more suitable for male and female reproductive research than most other Old World monkeys and primates.

1. 8. BREEDING ASSESSMENT IN CAPTIVITY

Breeding of vervet monkey in captivity has been studied by different authors and it has been noted to be very successful (Rowell, 1970; Johnson *et al.*, 1973; Hess *et al.*, 1979; Kushner *et al.*, 1982). Seier (1986; 2005), recorded 95 offspring from 115 pregnancies in five years from 26 females in an indoors captive breeding colony. Hess *et al.*, (1979), reported that mating for a six- day period improved conception to

45.8% from the 21.8 % for single day exposure to the male. Else (1985), recorded an annual live birth rate of over 85%. Fairbanks and McGuire (1984) noted that vervets had higher birth rates in captivity than other members of the genus. They reported over an 8-year period an average of one birth per female per year. The other advantage of breeding the vervets in captivity is the fact that under conducive conditions of accelerated growth and development, age of the first delivery can be brought forward by as much as one year compared to the wild (Eley, 1992). More importantly, is that all experimental animals born in captivity have a known history and are housed under almost identical conditions of temperature, humidity and balanced food intake.



1.9. REFERENCES

Booth, C. 1962. Some observations on behaviour of *Cercopithecus aethiops*. *Ann. N. Y. Acad. Sci.* **102**:477-487.

Conaway, C. H. and Sade, D. S. 1969. Annual testis cycle of the green monkey (*Cercopithecus aethiops*) on Kitts, West Indies. *J. Mammal.* **38**:217-219.

Eley, R. M. 1989. Know your monkeys: a guide to the primates of Kenya. National Museums of Kenya. pp 1-24.

Eley, R. M. 1992. Vervet reproduction. In: Occasional papers of the national museums of Kenya. (ed. L. A. Bennun). *Utafiti*, **4**: 1-33.

Eley, R. M., Else, J. G., Gulamhussein, N., and Lequin, R. M. 1986. Reproduction in the vervet monkey (*Cercopithecus aethiops*): Testicular volume and testosterone. *Am. J. Primatol.* **10**:229-235.

Else, J. M. 1985. Captive propagation of vervet monkeys (*Cercopithecus aethiops*) in harems. *Lab. Anim. Sci.* **35**:373-375.

Fairbanks, L. A. and McGuire, M. T. 1984. Determinants of fecundity and reproductive success in captive vervet monkeys. *Am. J. Primatol.* **7**: 27-38.

Goodwin, W. J. 1970. Current use of nonhuman primate in biomedical research. *Lab. Anim. Care.* **20**:329-332.

Gould, K. G., Young, L. G., Smithwick, E. B. and Python, S. R. 1993. Semen characteristics of the adult male chimpanzee (*Pan troglodytes*). *Am. J. Primatol.* **29**:221-232.

Harris, R. S. 1970. Feeding and Nutrition of Nonhuman Primates. Academic Press. New York.

Hess, D. L., Hendricks, A. G. and Stabenfeldt, G. H. 1979. Reproductive and hormonal patterns in the African green monkey (*Cercopithecus aethiops*) *J. Med. Primatol.* **8**:273-281.

Johnson, P. T., Valerio, D. A. and Thompson, G. E. 1973. Breeding the African green monkey, *Cercopithecus aethiops*, in a laboratory environment. *J. Anim. Sci.* **23**: 355-359.

Kushner, H., Kraft-Schreyer, N., Angelakos, E. T. and Wudarski, E. M. 1982. Analysis of reproductive data in a breeding colony of African green monkeys. *J. Med. Primatol.* **11**:77-84.

Plant, T. M. 1981. Time courses of concentrations of circulating gonadotropin, prolactin, testosterone and cortisol concentrations in adult male rhesus monkeys (*Macaca mulatta*) throughout the 24h light-dark cycle. *Biol. Reprod.* **25**:244-251.

Ramesh, V., Ramachandra, S. G., Krishnamurthy, H. N. and Rao, A. J. 1998. Electroejaculation and seminal parameters in bonnet monkeys (*Macaca radiata*). *Andrologia* **30**:97-100.

Rosen, S. I. 1974. Introduction to Primates – Living and Fossil. Prentice-Hall Inc. New Jersey.

Rowell, T. E. 1970. Reproductive cycles of *Cercopithecus* monkeys. *J. Reprod. Fert.* **22**:321-338.

- Seier, J. V. 1986. Breeding vervet monkeys in a closed environment. *J. Med Primatol.* **15**:339-349.
- Seier, J. V. 2005. Vervet monkey breeding. In: The Handbook of Experimental Animals. The Laboratory Primate. (ed. S. Wolfe-Coote). Chapter 12, Elsevier Academic Press. Amsterdam. pp 175-179.
- Skinner, J. D., and Smithers, R. H. N. 1990. The Mammals of the Southern African Subregion. University of Pretoria Press. Pretoria. pp 159-164.
- Tarantal, A. F., Vandevort, C. A. and Overstreet, J. W. 1990. Intrauterine insemination with ultrasound guidance in the long-tailed macaque (*Macaca fascicularis*). *J. Med Primatol.* **19**:447-453.
- Van der Horst, G., Seier, J. V., Spinks, A. C. and Hendricks, S. 1999. The maturation of sperm motility in the epididymis and vas deferens of the vervet monkey, *Cercopithecus aethiops*. *Int. J. Androl.* **22**:197-207.
- Van der Horst, G. 2005. Reproduction. In: The Handbook of Experimental Animals. The Laboratory Primate. (ed. S. Wolfe-Coote). Chapter 31, Elsevier Academic Press. Amsterdam. pp 527-536.
- Zatuchni, B., Hahn, D. W. and Zaneveld, L. J. 1981. Postcoital, vaginal, spermicidal potency of formulations: *Macaca arctoides* (stump-tailed macaque) as animal model. *Fertil Steril* **35**: 683-690.

CHAPTER 2: MALE REPRODUCTIVE SYSTEM IN MAMMALS

2.1. OVERVIEW OF THE MALE REPRODUCTIVE SYSTEM IN MAMMALS

The male reproductive system consists of a pair of testes, various extratesticular ducts, accessory glands (two seminal vesicles, prostate gland, and the bulbo-urethral glands, also known as Cowper's glands), and a penis. Gonadal differentiation is determined by the presence or absence of the Y chromosome. Gonadal specificity appears during the seventh week of intrauterine life when the indifferent gonadal tissue of a genetic male begins to differentiate into testes under the influence of the sex-determining region of the Y chromosome (SRY), the single gene that is responsible for sex determination. H-Y antigen, a specific plasma membrane protein found in males, directs differentiation of the gonads into testes (Sherwood, 2004). The male reproductive tract develops from the Wolffian ducts, and this process is enhanced by the activity of two hormones secreted by the fetal testes, testosterone and Müllerian-inhibiting factor (Sherwood, 2004). Testosterone is secreted by the Leydig cells and the Müllerian-inhibiting factor is released by the Sertoli cells. During the gestation period the testes descend from the abdominal cavity through the inguinal canal into the scrotum. Within the scrotal sac, the temperature of the testes is 2-3°C below body temperature. This lower temperature is essential for sperm production. During the descending process of the testes into the scrotal sac, they carry with them an extension of the peritoneum, called tunica vaginalis propria testis or simply the tunica vaginalis. This detaches itself from the peritoneal cavity and forms an independent serous cavity which covers the anterolateral surface of the testis to the point where the vessels and nerves enter the testis, on its posterior surface, and the visceral layer of the tunica vaginalis is continuous with its parietal layer (Bloom and Fawcett, 1994; Ross *et al.*, 1995).

2.1.1. Testes

The testis is surrounded by a thick capsule of collagenous connective tissue, the tunica albuginea (Junqueira *et al.*, 1983). The tunica albuginea is thickened on the posterior surface of the testis to form the mediastinum testis, from which fibrous septa penetrate into the gland, dividing it into about 250 pyramidal compartments called the testicular lobules. These septa are incomplete, and intercommunications frequently exist between the lobules. Each lobule is occupied by 1-4 highly convoluted seminiferous tubules enmeshed in a web of loose connective tissue rich in vessels, nerves and several types of cells, principally the specific interstitial cells (Leydig cells) and the sustentacular (Sertoli) cells. The Leydig cells were discovered by Franz Leydig (1850), and the Sertoli cells were named after Enrico Sertoli (1865). (Junqueira *et al.*, 1983; Leeson *et al.*, 1985).

2.1.2. Seminiferous tubules

Each seminiferous tubule is highly convoluted and is about 150 - 250 μ m in diameter and 30-70cm in length. The seminiferous tubule is lined by a complex germinal or seminiferous epithelium, which is a mixture of modified stratified cuboidal epithelium and columnar epithelial (Sertoli cells). This layer consists of both the proliferating spermatogenic cells and the nonproliferating or supporting cells, called the Sertoli cells or the sustentacular cells. These convoluted tubules form a network, wherein individual tubules are either blind-ended or branched. At the termination of each tubule, the lumen narrows and the epithelial lining abruptly changes into a simple cuboidal layer. These cells possess a single flagellum. There are also short segments known as straight tubules or *tubuli recti* which connect the seminiferous tubules to the anastomosing labyrinth of epithelium-lined channels, the rete testis (Junqueira *et al.*, 1983; Leeson *et al.*, 1985). The interstitial tissue between seminiferous tubules is occupied by a highly vascular loose connective tissue. Each seminiferous tubule is enclosed in a rich capillary network and the surrounding connective tissue contains perivascular mesenchymal cells, fibroblasts, and a few macrophages in a meshwork of fine reticular fibers. Within this loose stroma, there

are clusters of Leydig cells (interstitial cells) occupying the angular interstices between the seminiferous tubules.

2.1.3. Sertoli and Leydig cells

Sertoli cells are tall columnar cells evenly distributed in the seminiferous epithelium extending from the basement membrane to the tubule lumen. They are considered to be some of the largest cells in the body, with measurements of 70 -90 μm in length and about 30 μm in width. Their nuclei occupy a basal position and reveals extensive nuclear envelope infoldings (Dym, 1972). It has been reported that the Sertoli cells provide the microenvironment in which spermatogenesis occur. On the basis of their shape and strategic position in the seminiferous tubules, the functions of support for the germ cells and provision of blood-borne nutrients have been reported (Dym, 1972; Guyton and Hall, 1996). Dym (1972), reported that Sertoli cells could also be associated with the maintenance of the blood-testis barrier and the compartmentalization of the seminiferous tubules.

Besides the connective tissue elements, the stroma of the seminiferous tubules contains interstitial cells or Leydig cells. These cells are a major source of androgens (testosterone). Leydig cells are large and ovoid or polygonal in shape. They contain large nuclei which are often eccentrically situated. The interstitial cells appear in groups of various sizes in which small blood vessels are usually present, and they constitute about 20 percent of the mass of the adult testes (Camatini *et al.*, 1981; Guyton and Hall, 1996).

2.1.4. Intratesticular genital ducts

The intratesticular genital ducts are the *tubuli recti* (straight tubules), the rete testis, and the *ductuli efferentes*. These ducts carry spermatozoa and fluid from the seminiferous tubules to the ductus epididymis (Junqueira and Carneiro, 2003). From each of seminiferous tubule, there is an abrupt transition to the *tubuli recti* or straight tubules. The *tubuli recti* are lined with a simple cuboidal epithelium. The *tubuli recti* empty into the rete testis, a complex series of interconnecting channels within

the highly vascular connective tissue of the mediastinum. A simple cuboidal or low columnar epithelium lines the channels of the rete testis. These cells have a single apical cilium and few apical microvilli. The rete testis present in the connective tissue of the mediastinum, is connected to the cephalic or caput portion of the epididymis by 10-20 ductuli efferentes (Junqueira *et al.*, 1983; Leeson *et al.*, 1985; Ross *et al.*, 1995).

2.1.4.1. Tubuli recti

There is an abrupt structural change at the juncture of the seminiferous tubule and the straight tubule. Closer to the juncture, the developing germ cells of the seminiferous tubule decrease in number and finally disappear. The Sertoli cells undergo structural change, with their cytoplasm becoming more vacuolated and their nuclei becoming dense. These Sertoli cells will increase in number and finally form a continuous epithelial layer which protrudes into the enlarged initial portion of the straight tubule. The epithelial lining then changes abruptly into the columnar type characteristics of the straight tubules; subsequently turning into the cuboidal cells lining the rete testis (Kelly *et al.*, 1984; Ross *et al.*, 1995).

2.1.4.2. Rete testis

The rete testis is characterized by a simple cuboidal or low columnar epithelial lining. These cells have a single apical cilium and few apical microvilli that are connected to a basal body. The tubules of the rete testis have no definite lamina propria that is distinct from the connective tissue comprising the mediastinum (Kelly *et al.*, 1984). In guinea pigs, the cells of the *tubuli recti* and rete testis store a remarkable amount of glycogen which displaces the nucleus toward the lumen and all other organelles to the periphery (Ross *et al.*, 1995).

2.1.4.3. Ductuli efferentes

The efferent ductules connect the rete testis to the epididymis. As the efferent ductules exit the testis, they become highly coiled and form 6-10 conical masses, the *coni vasculosi*, whose bases form part of the head of the epididymis. The *coni vasculosi* contain highly convoluted ducts that measure 15-20 cm. At the base of the cones, the efferentes ductuli open into a single channel, the ductus epididymis. The efferent ductules are lined by pseudostratified ciliated columnar epithelium that contains clumps of tall and short cells, giving the luminal surface a saw tooth appearance (Ross *et al.*, 1995). In addition, the epithelium of the ductuli efferentes consists of nonciliated cuboidal cells. These nonciliated cells absorb much of the fluid secreted by the seminiferous tubules. The activity of the ciliated cells and fluid absorption create a fluid flow that sweeps spermatozoa toward the epididymis (Junqueira and Carneiro, 2003).

2.1.5. Ductus epididymis

The ductuli efferentes run into a single ductus epididymis. The epididymis is divided into three sections: the caput (head), the corpus (body), and the cauda (tail). The upper expanded portion, the caput, projects above the upper pole of the testis. This is followed by a narrower portion, the corpus and a thickened lower portion, the cauda (Kelly *et al.*, 1984). It is a long storage duct through which spermatozoa pass slowly. In their passage through this structure, they acquire motility and ability to fertilize the oocyte (Leeson *et al.*, 1985). The epithelium is pseudostratified, composed of basal cells, principal cells and apical cells. Principal cells are the most numerous and are very tall (80 μm) in the proximal segment of the epididymis but gradually decrease in height distally (40 μm), near the junction with the ductus deferens. Long, nonmotile microvilli called stereocilia extend from the apical surface of the principal cells (Krause and Cutts, 1986).

Basal cells are small, round cells that lie on the basal lamina interposed between the bases of the principal cells. The epididymal epithelium lies on a basal lamina and surrounded by a thin lamina propria and a thin layer of circularly arranged

smooth muscle cells. Near the ductus deferens, the muscle layer thickens and becomes three layered (inner longitudinal, middle circular layer, and outer longitudinal) continuous with that of the ductus deferens (Krause and Cutts, 1986). In addition, intraepithelial lymphocytes also called the halo cells, are found in the epithelium (Ross *et al.*, 1995). Throughout the length of the ductus epididymis, proteins and ions, are secreted, modified, and reabsorbed sequentially, and thus they contribute to the unique and region- specific character of the luminal fluid of mammalian epididymis (Smithwick and Young, 2001).

2.1.6. Ductus deferens

The ductus deferens unites the epididymis with the prostatic urethra. It is characterized by a thick wall consisting of a mucosa, muscularis, and adventitia. The mucosa is thrown into longitudinal folds that project into the lumen and consists of a pseudostratified columnar epithelium resting on a thin basal lamina. Similar to the epididymis the epithelium exhibits microvilli (stereocilia) on its luminal surface (Krause and Cutts, 1986). The mucosa rises into longitudinal folds, which are responsible for the stellate outline of the lumen one sees in cross sections. Beneath the lamina propria there is an ill-defined submucosa, containing numerous blood vessels, which separates the mucosa from the muscular coat. This coat is thick and consists of three distinct layers of smooth muscle. A fibrous adventitia surrounds the muscular coat and blends with that of adjoining tissues (Leeson *et al.*, 1985).

2.1.7. Ampulla

A pocket-like structure is formed at the terminal end of the ductus deferens. The ampulla differs from the ductus deferens mainly in the structure of its mucosa. The lumen is wider and the mucosa much more folded than in the main portion of the duct and forms crypts, many of which extend in tubular form into the underlying connective tissue. The epithelium which lines the lumen and the crypts is simple columnar or cuboidal and is secretory in nature and these cells occasionally contain yellow pigment granules (Eroschenko, 1996; Kelly *et al.*, 1984; Leeson *et al.*, 1985).

2.1.8. Ejaculatory duct

This is a short, narrow region of the ductus deferens extending beyond the ampulla and joins the duct of the seminal vesicle. This combined duct forms the ejaculatory duct, which empties into the prostatic urethra. It measures about 1 cm in length and is lined by a pseudostratified or simple columnar epithelium. The mucosa forms outpocketings similar to but less well developed than those in the ampulla. The remainder of the wall of the ejaculatory duct consists only of fibrous connective tissue (Krause and Cutts, 1986).

2.1.9. Prostatic urethra

The ejaculatory duct penetrates the substance of the prostate gland and opens into the prostatic portion of the urethra. The prostatic urethra is lined by a thin, transitional epithelium and bears a dome-shaped elevation called the colliculus seminalis on its posterior wall. A small blind invagination, the prostatic utricle, lies on the summit of the colliculus and represents a remnant of the Müllerian duct in the male (Krause and Cutts, 1986).

2.1.10. Penis

The penis serves as the common outlet for urine and seminal secretions and as a copulatory organ. It is formed by the three cylinders of erectile tissue: the paired corpora cavernosa penis dorsally and the single corpus cavernosum urethra ventrally (Leeson *et al.*, 1985). The glans penis is formed as the corpus cavernosum of the urethral ends. The corpora cavernosa are covered by a resistant membrane of dense connective tissue, the tunica albuginea, which is composed of the collagenous fibers. The elastic fibers are also predominant in this tissue (Junqueira *et al.*, 1983; Kelly *et al.*, 1984).

2.1.11. Accessory sex glands

The accessory sex glands are conspicuous outgrowths of the genital tract found only in mammals. The major accessory sex glands are formed by a pair of seminal vesicles, the prostate, and the bulbourethral glands, also called the Cowper's glands (Leeson *et al.*, 1985). The secretions of these glands are essential for the reproductive functioning of the male reproductive system (Junqueira and Carneiro, 2003).

2.1.11.1. Seminal vesicles

Each seminal vesicle is a tortuous, elongated diverticulum of the ductus deferens at the termination of the ampullary portion, situated posterior to the prostate gland. The wall consists an external connective tissue adventitia containing numerous elastic fibers, a smooth muscle coat thinner than that of the ductus deferens and consisting of inner circular and outer layers, and a mucosa which is marked with many infoldings. These primary folds of the mucosa branch into secondary and tertiary structures, which project into the lumen and merge with one another frequently. As a result, numerous compartments of different sizes are formed. The lamina propria is a loose connective tissue that is highly vascularized. It is rich in elastic fibers and forms a continuous layer around the vesicle. The epithelium typically shows many variations. It is usually pseudostratified but may be formed by simple columnar epithelial cells. The cytoplasm of the basal cells found in this gland contains granules and a yellowish lipochrome pigment (Kelly *et al.*, 1984; Leeson *et al.*, 1985).

2.1.11.2. Prostate gland

The prostate gland surrounds the urethra at its origin from the bladder. Embryologically, it is derived from a series of small peri-urethral glands and a larger series of lobules that form the greater bulk of the prostate gland. This gland can be separated into a central portion of short glands proximal to the urethra, and a more peripheral portion. The peripheral portion is an aggregate of 30-50 small compound

tubulo-alveolar glands that drain into the prostatic urethra by 15-30 small excretory ducts. The glandular elements are distributed in three different areas, more or less concentrically arranged around the urethra. Small glands lie in the mucosa and these are surrounded by submucosal glands. The principal glandular elements lie peripherally and constitute the bulk of the gland. The gland is surrounded by a fibro-elastic capsule containing some smooth muscle fibers on its inner aspect and an extensive plexus of veins, and the glandular components are embedded in an abundant, dense stroma which is continuous with the periphery of the capsule (Kelly, *et al.*, 1984; Leeson *et al.*, 1985).

2.1.11.3. Bulbo-urethral glands

The bulbo-urethral glands (Cowper's glands) are paired bodies, each the size of a pea, lying in the connective tissue behind the membranous urethra. Each is a compound tubulo-alveolar gland whose duct enters the posterior portion of the cavernous segment of the urethra. The bulbo-urethra glands are surrounded by a connective tissue capsule, external to which are skeletal muscle fibers. Septa pass into the gland to divide it into lobules. The secretory end pieces are variable, being either alveolar, saccular, or tubular. The epithelium is variable as well, being either cuboidal or columnar (Leeson *et al.*, 1985).

2.1.12. Structure of the spermatozoon

The mammalian spermatozoon consists of the head, neck, and tail. The basic structure of the sperm involves packaging of genetic material in the head, which is very poorly supplied with cytoplasm, and energy-producing midpiece wrapped with mitochondria, the energy source, and a motile tail. In general, the form of the sperm nucleus is somewhat paddle shaped and relatively symmetrical, except in certain rodent families. Despite this similarity, a relatively wide variety of minor characteristics are superimposed upon this basic structure. The greatest variation in morphology has been shown to involve the size and shape of the acrosomal

membrane and the number, size and organization of the mitochondria in the sperm midpiece (Gould, 1980). The length of the sperm is species-specific as outlined in Table 2.1.

The head consists of the acrosome and nucleus which are surrounded by the plasma membrane. The acrosomal cap that covers the anterior two-thirds of the nucleus contains enzymes such as hyaluronidase, neuraminidase, acid phosphates, and trypsin-like proteases called acrosin, hydrolases, and esterases. These enzymes are important in the digestion of the zona pellucida and the corona radiata. The nucleus contains condensed genetic information (Pesch and Bergmann, 2006). The shape of the head is species-specific and can take many forms, from total flat shape (Orang utang) to broad, to paddle-shaped (human) forms (Gould, 1980).

The neck which has a length of approximately 1 μm , is a connection between the flagellum and the head. The short neck contains a pair of centrioles and nine segmented columns that appear to merge with the nine dense outer dense fibers of the rest of the tail. On the anterior side, the neck is attached to the basal plate and posteriorly it is attached to outer dense fibers of the flagellum (Pesch and Bergmann, 2006).

The tail is the longest part of the sperm and consists of the midpiece, principal piece, and the end piece. The midpiece has a length of 5 μm in humans and is characterized by mitochondrial sheath that surrounds the axonemal complex (Pesch and Bergmann, 2006). It is possible to determine the exact number of mitochondria in the middle piece. The number of gyres shows small variation within sperm by great differences in total length within species. In man and bull there are 10 to 12 (Fawcett, 1958; Fawcett, 1970), in the dog 15-17, (Bretschneider, 1950), in mouse there are 90 and about 350 in rat (André, 1962).

At the end of the mitochondrial sheath in all mammalian spermatozoa is a dense ring called the annulus. The annulus develops in intimate relation to the plasma membrane where the latter is reflected from the cell body of the spermatid onto the flagellum. The mitochondria are arranged end to end in helices around the contractile elements for high flexibility. Distal to the middle piece, a fibrous sheath

consisting of two longitudinal columns and numerous connecting ribs surrounds the nine longitudinal fibers of the principal piece and extends nearly to the end of the flagellum. This short segment of the tail distal to the fibrous sheath is the end piece (Ross *et al.*, 1995). The principal piece is that segment of the mammalian sperm flagellum which is enclosed by the fibrous sheath. It is by far the longest segment of the flagellum and the most effective in motility. The principal piece measures about 40 μ m long in human sperm and contains the fibrous sheath external to the coarse fibers and the axonemal complex. The end piece, around the last 5 μ m of the flagellum in the mature sperm, contains only the axonemal complex (Ross *et al.*, 1995).

Table 2. 1. The lengths of spermatozoa in different mammalian species according to Gould (1980), Schnoor (1996), Pesch and Bergmann (2006), and modified.

Species	Length (μ m)
Man	50-60
Chimpanzee	57
Gorilla	61
Vervet Monkey	66
Rhesus Monkey	73
Ruffed Lemur	104
Bull	75-90
Dog	60

In the subsequent chapters, the light microscopy and the electron microscopy (both SEM and TEM) of the selected tissues of the vervet monkey will be described. Chapter 3 discusses the gross morphology and light microscopy of the entire reproductive system of the vervet monkey. Chapter 4 discusses the ultrastructure of

the epididymis. Chapter 5 addresses the scanning electron microscopy of the testis but then focuses on the transmission electron microscopy of the non germinal cells. Chapters 6 addresses details of spermatogenesis and staging using transmission electron microscopy and light microscopy, and chapter 7 deals with a special comparison of the male reproductive system of the vervet monkey and humans.



2.2. REFERENCES

André, J. 1962. Contribution à la connaissance du chondriome; Etude de ses modifications ultrastructurales pendant la spermatogénèse. *J. Ultrastruct. Res.* Suppl. **3**:1-185.

Bloom, W. and Fawcett, D. W. 1994. A Textbook of Histology. 12th Ed. Chapman and Hall. New York. London. pp 768-813.

Bretschneider, L. H. 1950. Elektronenmikroskopische Untersuchungen an spermien. *Koninklijke Nederlandse Akademie van Wetenschappen proceedings.* **53**:531-543.

Camatini, M., Franchi, P. and Decurtis, I. 1981. Ultrastructure of the Leydig cells in the African green monkey. *J. Ultra. Res.* **76**:224-234.

Dym, M. 1972. The fine structure of the monkey (*Macaca*) Sertoli cell and its role in maintaining the blood-testis barrier. *Anat. Rec.* **175**:639-656.

Eroschenko, V. P. 1996. Atlas of Histology with Functional Correlations. 8th Ed. Williams and Wilkins. Baltimore. pp 275

Fawcett, D. W. 1958. The structure of the mammalian spermatozoon. *Int. Rev. Cytol.* **7**:195-234.

Fawcett, D. W. 1970. A comparative view of sperm ultrastructure. *Biol. Reprod.* **2**:90-127.

Gould, K. G. 1980. Scanning electron microscopy of the primate sperm. *Int. Rev. Cyt.* **63**: 323-355.

- Guyton, A. C. and Hall, J.E. 1996. Textbook of Medical Physiology. 9th Ed. W.B Saunders. Philadelphia. pp 1003-1015.
- Junqueira, L. C., Carneiro, J. and Contopoulos, A. N. 1983. Basic Histology. 4th Ed. Lange Medical Publications. California. pp 451-467.
- Junqueira, L. C. and J. Carneiro. 2003. Basic Histology: Text and Atlas, 10th Ed. Lange Medical Books McGraw-Hill. New York. pp 443-444.
- Kelly, D. E., Wood, R. L. and Enders, A. C. 1984. Bailey's Textbook of Microscopic Anatomy. 18th Ed. Williams and Wilkins. Philadelphia. pp 687-722.
- Krause, W. J. and Cutts, J. H. 1986. Concise Text of Histology. 2nd Ed. Lippincott Williams and Wilkins. Baltimore. pp 409-439.
- Leeson, C. R., Leeson, T. S. and Paparo, A. A. 1985. Textbook of Histology. W. B. Saunders Co. Philadelphia. pp 492-517.
- Leydig, F. 1850. Zur Anätomie der Mannlichen Geschlechtsorgane and Analdrüsen der Säugethiere. *Z. Wissenschaftliche Zool.* **2**:1-57.
- Pesch, S. and Bergmann, M. 2006. Structure of mammalian spermatozoa in respect to viability, fertility and cryopreservation. *Micron* **37**:597-612.
- Ross, M. H., Romrell, L. J. and Kaye, G. I. 1995. Histology: A Text and Atlas. 3rd Ed. Lippincott Williams and Wilkins. Philadelphia. pp 636-665.
- Schnoor, B. 1996. Embryology of domestic animals. Enke. *Stuttgart* 10-13.

Sertoli, E. 1865. Dell 'esistenza di particolari cellule ramificate nei canalicoli seminiferi del testicolo umano. *Morgagni*. 7:31-39.

Sherwood, L. 2004. Human Physiology: From Cells to Systems. 5th Ed. Brooks/Cole. USA. pp 751-755.

Smithwick, E. B. and Young, L. G. 2001. Histological effects of androgen deprivation on the adult chimpanzee epididymis. *Tissue Cell*. 33:450-461.



CHAPTER 3: GROSS MORPHOLOGY AND LIGHT MICROSCOPY OF THE MALE REPRODUCTIVE SYSTEM OF THE VERVET MONKEY

3.1. INTRODUCTION

Nonhuman primates have been a relevant model for human biomedical research because of the physiological and genetic similarities among the members of the primate order. The study of the anatomy and morphology of the male reproductive tract and spermatogenesis in a species is fundamental for establishing the physiological patterns that will make possible the determination of the protocols for assisted reproduction. Although the mouse model has contributed extensively to the understanding of basic mammalian reproduction, nonhuman primates may appear to be a more ideal research model in relation to humans. Rhesus monkey (*M. mulatta*) (Clermont and Leblond, 1959; de Rooij *et al.*, 1986; Majumdar *et al.*, 1998), cynomolgus monkey (*M. fascicularis*) (Fouquet and Dadoune, 1986), and common marmoset (*Callithrix jacchus*) (Kumar and Phillips, 1991; Weinbauer *et al.*, 2001), are some of the common nonhuman primates species used in reproductive research studies. In the present study the vervet monkey will be used as a potential model, and probably for future studies in male human reproduction.

The biology of reproduction has intrigued the scientific community and public alike for centuries, and knowledge of reproductive physiology is obligatory for the ultimate goal of being able to control reproductive process in terms of promoting or preventing pregnancies. Lack of knowledge is often an impediment as the reproductive strategies within the animal kingdom are highly divergent, and most research is conducted only on a few well-studied species (Barfield *et al.*, 2006). Promoting research on reproduction is important for propagating animal species, especially those threatened by extinction. Reproductive research in human should also be encouraged because of the growing world-wide problem of infertility, especially in men. Every year thousands of couples struggle with the inability to conceive spontaneously and attempt various fertility treatments (Barfield *et al.*, 2006). Human tissues, embryos, and gametes are being frozen on regular basis for subsequent Assisted Reproduction Techniques (ART) such as *in vitro* fertilization

and intracytoplasmic sperm injection, both of which are well established techniques in humans (Barfield *et al.*, 2006). These studies are undertaken in order to understand and regulate the reproductive processes taking place in humans.

Contraception affords couples the ability to delay or space the births of their children. Access to a wide range of effective methods of contraception is an important element of reproductive health. The development of new methods of contraception, such as the combined oral contraceptive pill in the 1960s and more recently medicated intrauterine devices (IUDs) and long term implants, has been mainly female directed. Despite this one-sided approach to contraceptive provision, a third of couples practicing contraception world-wide use a male method, the condom (United Nations, 1994). Lack of demand for more advanced reversible male methods is frequently advocated as a reason for limiting the already meagre research effort in this field (Potts, 1996). The use of contraceptives for family planning has played a major role in curbing the birth rate of some populations over the past 40 years (e.g. in China). The prospect of a contraceptive for men within the next few years will be a welcome addition to the limited possibilities currently available to men (condoms, vasectomy, withdrawal, periodic abstinence). Studies show that couples would like the male partner to play a more active role in family planning and that the willingness of men to take a contraceptive is high in many countries (Barfield *et al.*, 2006). This new avenue of growth is sure to spawn many new contraceptive strategies directed at the males. Martin, *et al.*, (2000), suggested that the current emphasis that men should have greater involvement in family planning will be substantiated when appropriate contraceptive methods are made available.

This chapter will provide the gross morphology and histology of the male reproductive system of the vervet monkey. The ultrastructure (SEM and TEM) of the testis and the epididymis will follow in subsequent chapters. The rationale behind the inclusion of this chapter is to establish differences and similarities that can be obtained between the vervet monkeys and humans, and maybe between vervet monkeys and other mammals.

3.1.1. Objectives

- To provide the gross morphology of the selected organs of the male reproductive system of the vervet monkey.
- Histological description of the male reproductive tract of the vervet monkey.
- To reassess and re-evaluate the vervet monkey as a possible experimental model for research in human reproduction.

3.2. MATERIALS AND METHODS

3.2.1. Study animals

The study was performed using twenty-nine (29) male vervet monkeys which were obtained from the National Research Institute for Nutritional Diseases at the South African Medical Research Council, Tygerberg, Cape Town. The animals were housed permanently indoors and fed with a basic diet consisting of precooked maize meal with a protein-vitamin and mineral concentrate, which was mixed to a stiff porridge with water and fed in the mornings. Wholewheat brown bread was provided at noon, and apples and carrots, washed in chlorinated water, are fed in the afternoon. Drinking water was supplied *ad libitum* via an automatic device (Seier, 1986). Ethical clearance was obtained from the Medical Research Council's Ethical Committee for this study.

The ages of the animals ranged from 5-11 years. Animals were weighed to the nearest 100 g and subsequently anaesthetized with intramuscular injection of Ketamine (Ketalar at 10 mg/kg body mass). Immediately after sacrificing, their reproductive tracts were excised and the following structures were studied: the testes, the epididymis, the vas deferens, the seminal vesicle, the prostate gland, and the penis. Tissues were processed for both light and electron microscopy. However, this chapter deals with light microscopy only.

3.2.2. Sample collection and fixation

Upon their removal, each of the structures of the tract, excluding the penis, was weighed. Excess fat and blood were carefully removed and the samples were divided and fixed according to specific procedures as described below:

3.2.2.1. Testes

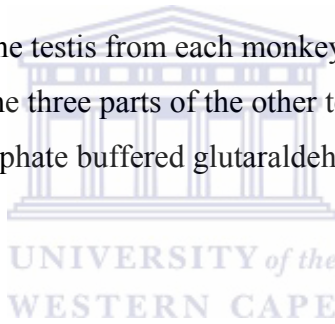
Each testis was dissected into three parts:

T1: The part situated to the end of the testis proximal to the point of attachment of the epididymis.

T2: The part that forms the middle section of the testis.

T3: The part located at the end of the testis distal to the point of attachment of the epididymis.

T1, T2, and T3 of one of the testis from each monkey were fixed in neutral buffered formalin. Sections from the three parts of the other testis were fixed in Bouin's fluid and 2.5% Sorenson's phosphate buffered glutaraldehyde for electron microscopy.



3.2.2.2. Epididymis

The epididymis of each monkey was divided into three parts:

E1: The head section of the epididymis attached to the testis (caput).

E2: The body/middle section of the epididymis (corpus).

E3: The tail section of the epididymis leading to the vas deferens (cauda).

E1, E2, and E3 of one epididymis were each fixed in neutral buffered formalin for light microscopic studies. Other sections of E1, E2, and E3 from the epididymis were fixed in 2.5% Sorenson's phosphate buffered glutaraldehyde for electron microscopy.

3.2.2.3. Vas deferens

The vas deferens was divided into three random parts, approximately equal in length:

V1: The section proximal to the epididymis.

V2: The section in the middle.

V3: The section distal to the epididymis.

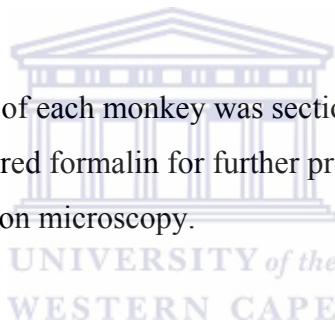
The three parts from one vas deferens of each monkey were fixed in neutral buffered formalin for further processing. Due to the manner in which the tissue was excised, the ampullary region of the vas deferens was not included.

3.2.2.4. Seminal vesicles

One seminal vesicle from each monkey was fixed in neutral buffered formalin for further processing. No part of the seminal vesicle was fixed for electron microscopy.

3.2.2.5. Prostate Gland

The prostate gland of each monkey was sectioned longitudinally. The gland was fixed in neutral buffered formalin for further processing. No part of the prostate gland was fixed for electron microscopy.



3.2.2.6. Penis

Whole penises from five monkeys were fixed in neutral buffered formalin. Due to the presence of a bony structure (os penis) in the penis, these samples were placed overnight in 20% formic acid to decalcify the os penis, prior to processing. This process allowed for easy sectioning for light microscopy. Penises from the remaining monkeys were sectioned into two parts; *viz*, P1 (glans penis) and P2 (shaft of the penis). These sections were each fixed in 2.5% Sorenson's phosphate buffered glutaraldehyde.

3.2.3. Light microscopy

3.2.3.1. Tissue processing

The samples fixed in neutral buffered formalin and Bouin's fluid, were used for the light microscopic study. Samples from each region of the reproductive tract were individually placed into labeled tissue containers (cassettes) and then placed in an automatic tissue processor (Shandon Elliot), which processed the tissue within 20 hours.

At the onset of processing, the tissue was placed in formaldehyde, which served as a secondary fixative. It was then dehydrated through 70%, 80%, 90%, and three changes of 100% alcohol. The tissue was cleared in two changes of xylene and finally transferred to two changes of molten paraffin wax.

The processed tissue was removed from the wax and placed into a metal mould. Molten paraffin wax was then dispensed from a tissue embedding center (Tissue Tek II) into the mould, covering the tissue. The wax in the mould was allowed to solidify and then the mould was removed, resulting in tissue being embedded in a solid wax block.

The embedded tissue was sectioned using a microtome (American optical, 820 Spencer rotating microtome) and section thickness was set at 4 μm (Reichert-Jung knife). The sections were floated on water in an electrothermal paraffin section bath to allow them to flatten out completely. They were then picked up onto glass slides and incubated at 37°C for 30 minutes.

The sections on the slides were stained by haematoxylin and eosin, using the following procedures:

- The sections were cleared in two changes of xylene (5 minutes each).
- They were then placed in absolute alcohol for 5 minutes and hydrated *via* 90%, 80%, and 70% alcohol.
- Sections were stained in haematoxylin for 10 minutes, rinsed in water, and differentiated in 1% acid-alcohol (2 dips).

- They were rinsed once more, blued in Scott's tap water, rinsed again, and counter stained with eosin for 1 minute.
- Finally, they were dehydrated via 70%, 80%, 95%, and two changes of 100% alcohol and cleared in two changes of xylene. The stained sections were then mounted with coverslips using Kanada balsam.

The slides were viewed by means of a Universal transmitted-light research microscope (Zeiss) and photographs were taken at various magnifications using an MC 63 automatic photomicrographic camera (for 35mm film) which was mounted on the microscope.

3.2.4. Flexible image processing system (FIPS)

The flexible image processing system (FIPS) (CSIR - Council for Science and Industrial Research) captures, characterizes, and stores video images, using a basic personal computer. It is able to analyze an image automatically according to the colour of the image, ranging from black to white. It can also save these images as printed or as computer files. Measurements made on the screen image are actually related to the actual physical dimensions.

FIPS was used to measure the inner and outer diameters of the seminiferous tubules of the testis and that of the epididymal ducts. Slides prepared for light microscopy and stained with haematoxylin and eosin, were used for this purpose. The slides were studied using a Universal transmitted-light research microscope (Zeiss) and FIPS obtained video images from these slides via a Grundig video camera, which was attached to the microscope. Slides from the testis (T1, T2, and T3) and epididymis (E1, E2, and E3) from eight monkeys were used.

3.2.5. Statistical Analysis

In order to establish significant differences in the number of basal, principal, and apical cells in the caput, corpus, and cauda epididymis, the obtained data were compared using one way ANOVA. The same test was used in comparing the epithelial height in the three regions of the epididymis. *P*-value of less than 0.05 was

considered to be statistically significant. All data were expressed as the mean \pm SEM.

3.3. RESULTS

3.3.1. General macro-anatomical description of the male reproductive tract

The average mass of the animals, sperm density, pH, testicular mass and gonadosomatic index (testicular weight expressed as a percentage of body mass) are indicated in Table 3.1. (van der Horst, 1995, per permission).

Table 3. 1. Average mass, sperm density, pH, testicular mass and gonadosomatic index (testicular weight expressed as a percentage of body mass) of vervet monkey (this study and van der Horst, 1995, per permission).

Mass of the animals (kg) (\pm SEM)	Sperm density 10^6 Sperm/ml (\pm SEM)	pH	Testicular mass (left and right) g (\pm SEM)	Gonadosomatic Index (GSI) (\pm SEM)
5.87 (0.13)	248.45 (52.3)	8.16 (0.11)	21.07 (1.07)	0.36 (0.02)

The external genitalia of the vervet monkey, *Chlorocebus aethiops*, consist of a small rosy pink to scarlet penis with a helmet-shaped light orange prepuce. The scrotum of *Chlorocebus aethiops* appears to be pendulous pouch situated at the base of the penis. It has a pale blue colour and divided into two compartments. The testes are paired and slightly oval as indicated in Figure 3.1 (showing one testis). They are found outside the abdomen in each of the two scrotal compartments.

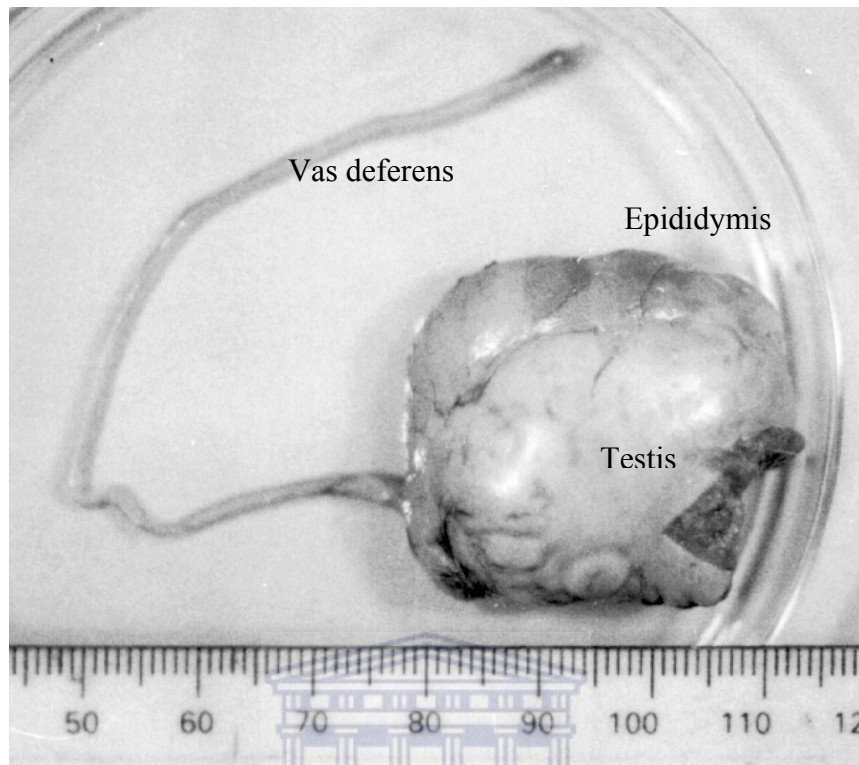


Figure 3. 1. Photograph showing the testis, the epididymis and the vas deferens of the vervet monkey, *Chlorocebus aethiops*. Scale in mm.

The epididymal tubules are attached to the posterior side of each testis (Figure 3.1). They are divided into three regions, caput epididymis, corpus epididymis, and the cauda epididymis (Figure 3.2). The broad caput epididymis (head) at the upper pole of the testis gave rise to a narrower, shorter corpus epididymis (body). The epididymis terminates at the lower pole of the testis when it widened slightly again to form a coiled cauda epididymis (tail). The cauda epididymis turns sharply and continues as the vas deferens (ductus deferens) (Figure 3.2).

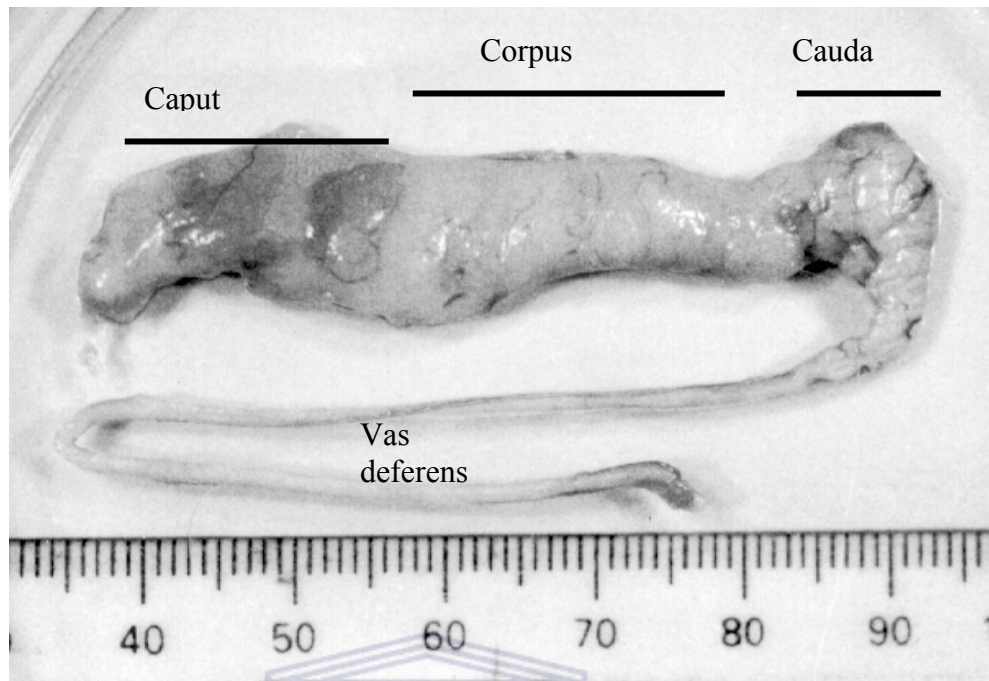


Figure 3. 2. Photograph showing three regions of the epididymis with the vas deferens of the vervet monkey, (*Chlorocebus aethiops*), been spread out. Scale in mm.

The vas deferens is a long, straight duct and is considerably narrower than the epididymis (Figure 3.2). The seminal vesicle has a coiled, pear shaped structure which appeared to consist of two lobes fused together in the centre (Figure 3.3). It is posteriorly attached to the prostate gland by connective tissue (Figure 3.3).

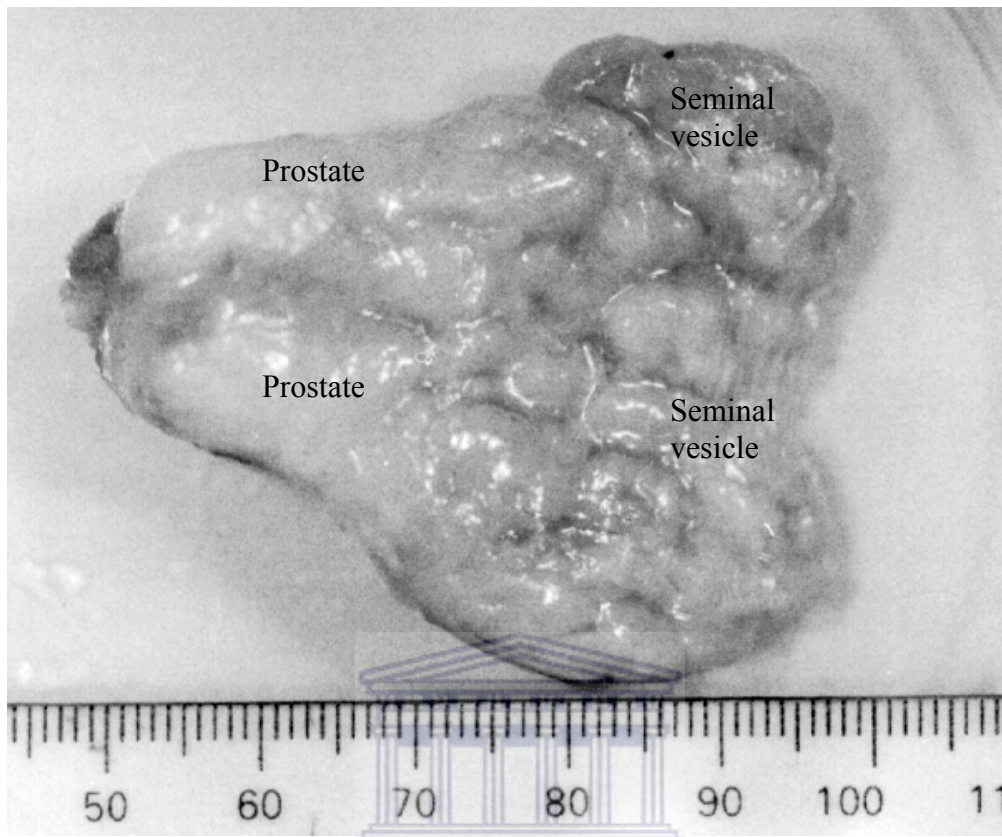


Figure 3.3. Photograph showing the seminal vesicles of the vervet monkey, *Chlorocebus aethiops*. Scale in mm.

The prostate gland forms a firm mass of tissue with a lobular appearance. It is situated in contact with the bladder and surrounds the urethra.

The penis has a straight, cylindrical structure which broadens at the tip to form a helmet-shaped glans penis (Figure 3.4). When in a flaccid state, the glans penis is covered by a fold of skin, prepuce. In the erect state, the prepuce moves back to expose the rosy-coloured glans. An os penis is present along the length of the penis. It is not seen in histological sections due to the fact that the tissue was decalcified during processing to make sectioning easier (Figure 3.4).

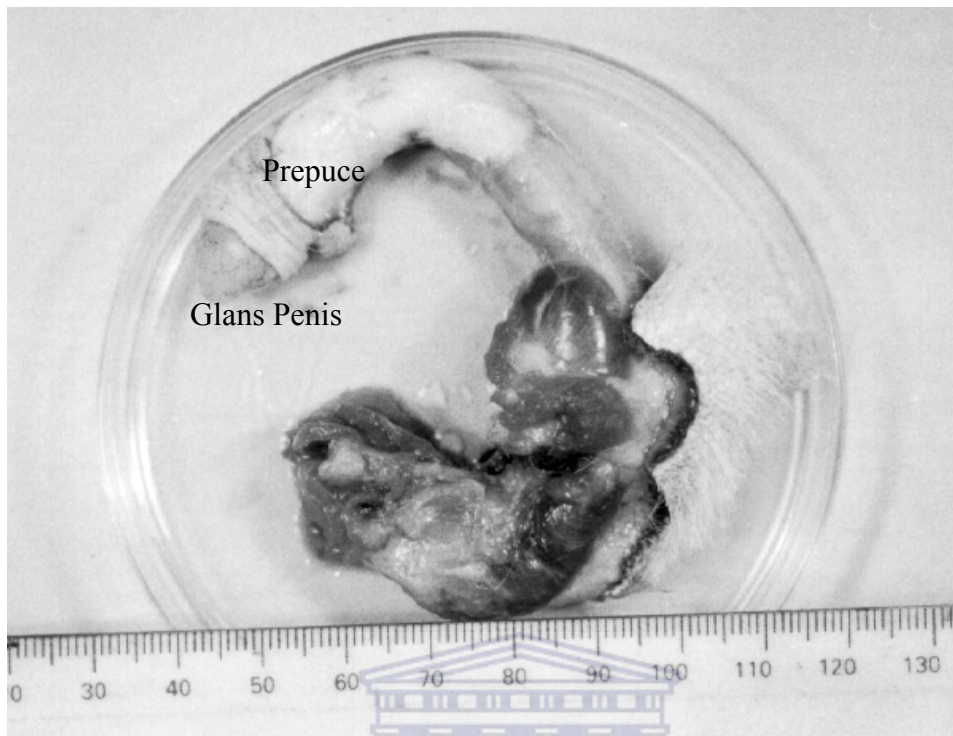


Figure 3. 4. Photograph showing the penile organ and associated structures of the vervet monkey, *Chlorocebus aethiops*. Scale in mm.

3.3.2. Histological description of the male reproductive tract of the vervet monkey

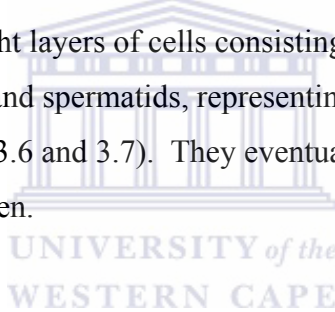
3.3.2.1. Testis

The testis is surrounded by a thick layer of dense connective tissue, the tunica albuginea. Immediately outside the layer, lies a simple squamous epithelial layer, the tunica vaginalis. Unlike the tunica albuginea, it does not surround the entire testis, but it is restricted to the anterior and lateral surfaces. Interiorly, the testis is divided into lobules by fibrous partitions called septa. They radiate from the posterior portion of the testis where the tunica albuginea thickens to form the mediastinum. These structures will be clearly illustrated in subsequent Chapters. Within each lobule there are several coiled seminiferous tubules (Figure 3.5).

3.3.2.2. Seminiferous tubules

These tubules are highly convoluted and are intertwined with each other within a lobule. In a cross-section view, they are seen in different planes (Figure 3.5). Each seminiferous tubule is lined by a complex germinal epithelium which rested on a thin basement membrane and is enveloped in a fibrous tunica propria which consists of several layers of fibroblasts. The seminiferous tubules are embedded in a loose connective tissue which contains blood vessels, nerves and specifically, interstitial endocrinocytes or cells of Leydig (Figure 3.8).

Within the seminiferous tubules, there are two specific categories of cells, viz. spermatogenic cells and sustentacular or Sertoli cells (Figure 3.6). The spermatogenic cells occupy the spaces between the Sertoli cells, extending from the basement membrane to the lumen of the seminiferous tubule. They are arranged in rows of approximately eight layers of cells consisting of spermatogonia, primary and secondary spermatocytes and spermatids, representing stages in the process of spermatogenesis (Figures 3.6 and 3.7). They eventually give rise to spermatozoa at the free surface of the lumen.



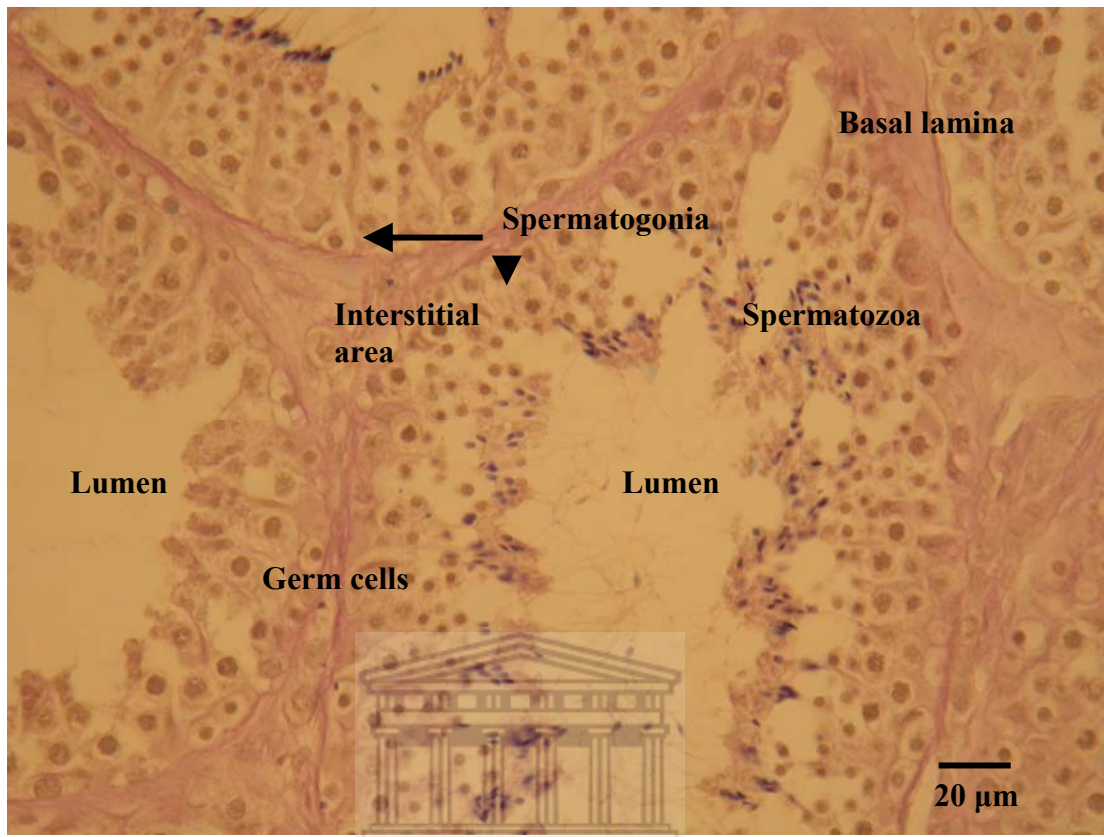


Figure 3. 5. The light micrograph showing the general lay-out of the seminiferous tubules of the vervet monkey, *Chlorocebus aethiops*.

3.3.2.2.1. Sertoli Cells

The Sertoli cells span the germinal epithelium and form a continuous sheath surrounding the lumen. Their bases rest on the basement membrane of the seminiferous tubule and their apices reach the luminal surface. They form invaginations and envelop the spermatogenic cells of the germinal epithelium and thus have an irregular outline. Developing spermatids at the lumen have their heads buried in the Sertoli cells and their flagellar tails extend into the lumen. A pale-staining, slightly triangular nucleus containing a prominent nucleolus is situated in the basal portion of the Sertoli cell, slightly above the basement membrane (Figures 3.6 and 3.7). The Sertoli cell nuclei are more clearly noticeable in sections than the rest of the cell. The Sertoli cell is a tall columnar cell extending from the base of the

seminiferous epithelium to the tubule lumen. It consists of a stem resting on the basal lamina, an intermediate portion which provides lateral processes around which the spermatocytes and spermatids are arranged, and apical projections which enclose the late spermatids prior to their release into the tubule lumen (Figure 3.6).

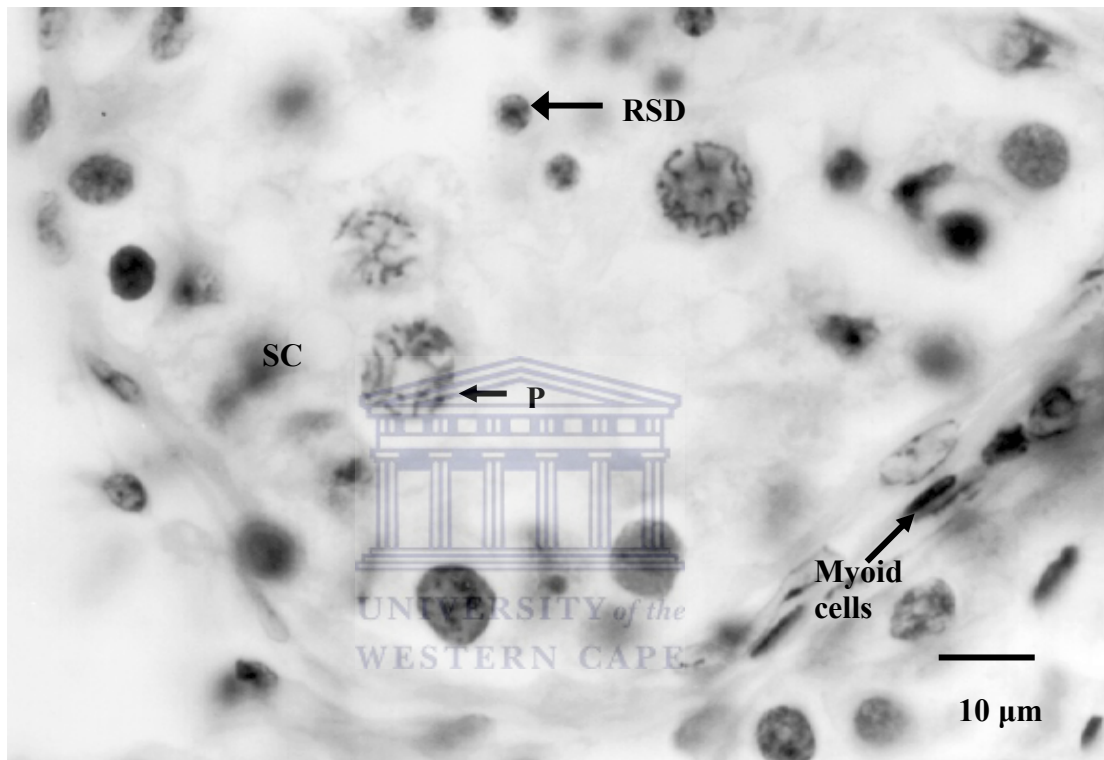


Figure 3. 6. The light micrograph showing the Sertoli cells and associated spermatogenic cells in the seminiferous tubules of the vervet monkey, *Chlorocebus aethiops*.

P - Pachytene spermatocyte, RSD – Round Spermatid, SC – Sertoli Cell.

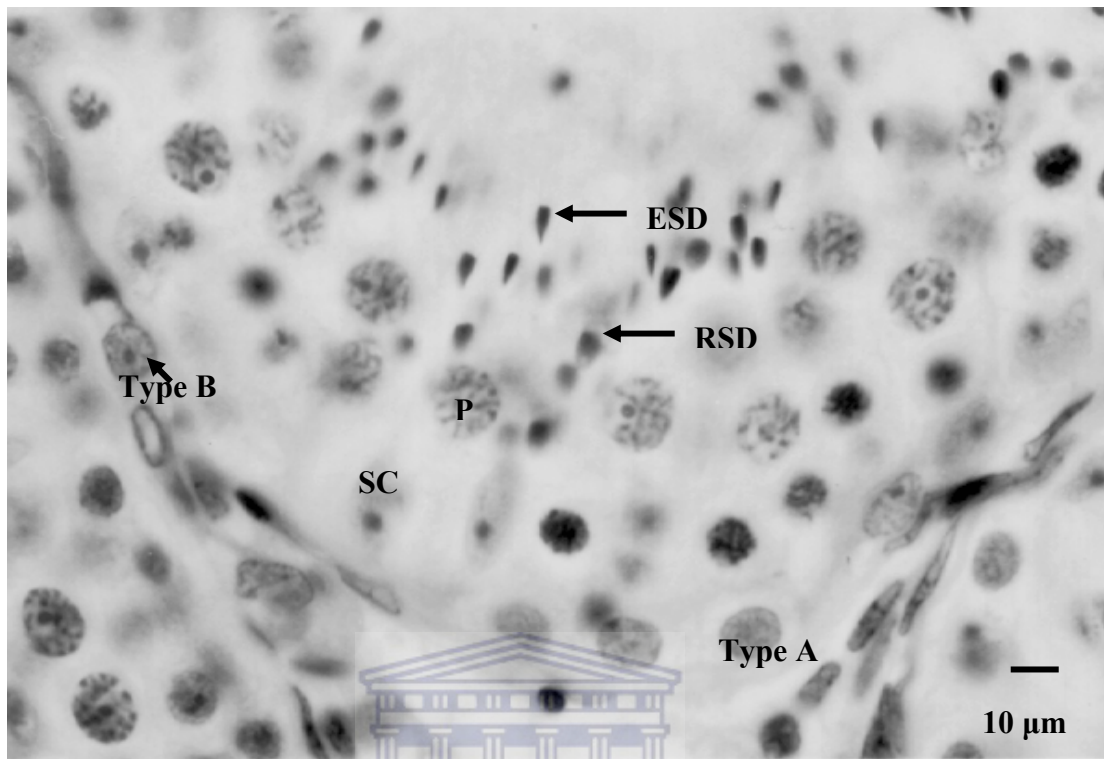


Figure 3. 7. The light micrograph showing the Sertoli cells in the seminiferous tubules of the vervet monkey, *Chlorocebus aethiops*.

ESD – Elongated spermatid, P - Pachytene spermatocyte, RSD - Round spermatid, SC – Sertoli cell, Type A - Type A Spermatogonium, and Type B – Type B spermatogonium.

3.3.2.2.2. Interstitial (Leydig) cells

The interstitial cells or the Leydig cells are found between the seminiferous tubules in the interstitial area or intertubular area (Figure 3.8). Leydig cells can either occur singly or in groups. These cells are large, round or polygonal. They formed groups of three to five. They have a granular cytoplasm and a distinct round nucleus.

3.3.2.2.3. Myoid cells

Myoid cells are elongated, thin cells with abundant actin filaments (Figure 3.6). The nucleus contains one or two nucleoli peripherally situated, and the cytoplasm encloses poorly developed cell organelles.

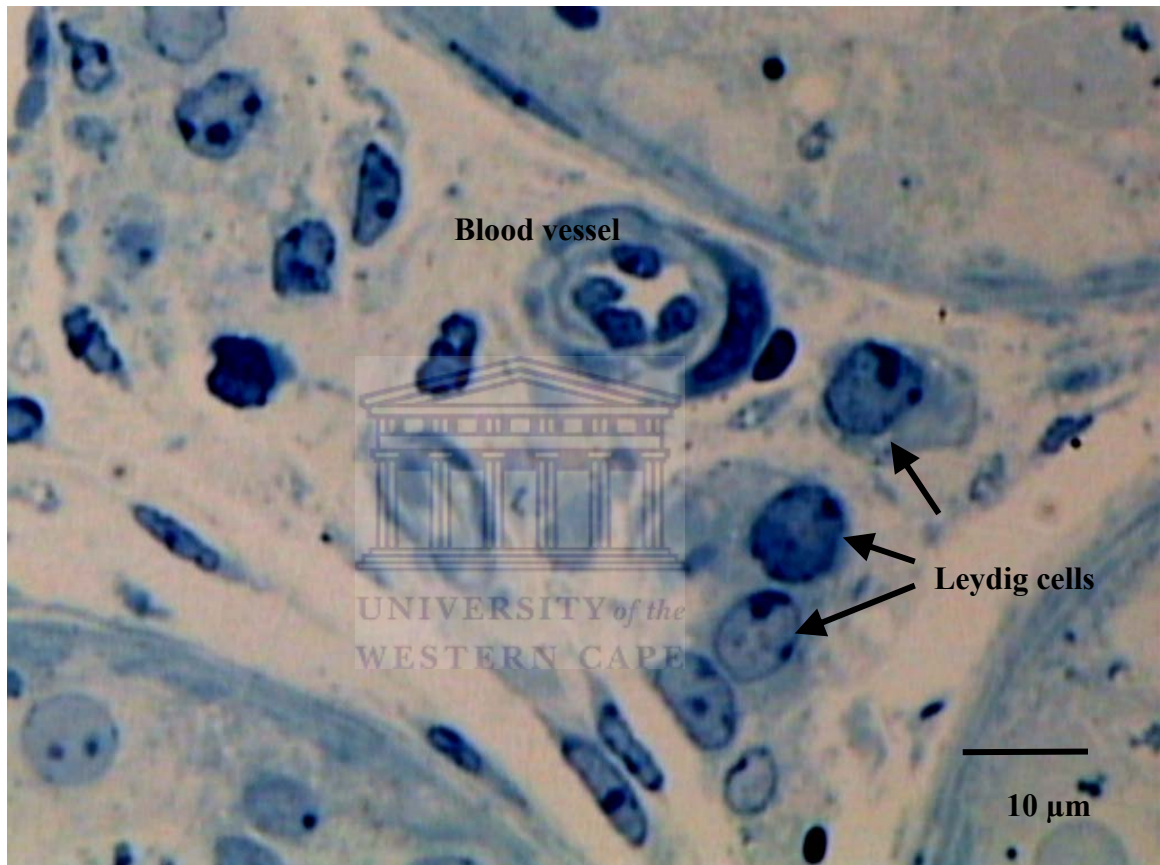


Figure 3. 8. Light micrograph showing intertubular region with the Leydig cells and blood vessels of the testis of the vervet monkey, *Chlorocebus aethiops*.

3.3.2.3. Ductus Epididymis

3.3.2.3.1. Caput epididymis (E1)

The caput epididymis could be histologically divided into three zones. Zone 1 contains the epididymal tubules, which developed from the efferent ductules. It occupies a very short part of the caput and then gives rise to zone 2. Zone 1 differs from zone 2 in that most of the epididymal tubules here are empty and free of clumps

of spermatozoa, while the zone 2 epididymal tubules all contain spermatozoa (Figure 3.10). Furthermore the tubules in both zones are similar in size and structure, having very tall principal cells and long stereocilia. Zone 3 has a star shaped lumen with spermatozoa inside. The intertubular area of the caput epididymis is composed of loose connective tissue and blood vessels. Principal cells contain a light stained cytoplasm, an ovoid light staining nuclei and prominent nucleoli. Basal cells are observed lying adjacent to the basement membrane. The basal cells are characterized by a light staining, round and big nuclei. Compared to the principal cells, the basal cells are found in reduced numbers.

3.3.2.3.2. Corpus epididymis (E2)

The tubules in the corpus epididymis are closely packed and appear to be slightly larger compared to both the caput and corpus epididymal regions. Their lumens are wider and contain varying amounts of spermatozoa (Figure 3.11). The principal cells lining the corpus epididymis have ovoid or elongated dark staining nuclei, prominent nucleoli and a distinct brush border. The stereocilia at their apical ends are shorter and less branched than in the caput epididymis. The layer of smooth muscle surrounding each tubule is found to be thick. Basal cells are also observed in the corpus epididymis. Spermatozoa are observed in the lumen of the corpus epididymis.

3.3.2.3.3. Cauda epididymis (E3)

Three different zones have been reported in this part of the epididymis, namely, zones 1, 2, and 3 (Figure 3.12). The tubules in zone 1 arise from the corpus epididymis (Figures 3.13). The height of the epithelium of the tubules is lower than in the corpus epididymis and the stereocilia are shorter too as illustrated in Tabel 3.2. The nuclei of the principal cells are more elongated. The outer smooth muscle layer is also thicker. The intertubular area of the cauda epididymis is composed of loose connective tissue and blood vessels. The epididymal tubules in zone 2 have the greatest diameter in the ductus epididymis (Figure 3.14). They have large lumens that are filled with spermatozoa. The epithelium is markedly reduced, having very

short principal cells with elongated nuclei, which seem to span half the cell, and short stereocilia. The cytoplasm appears to contain fewer and smaller lipid droplets. The smooth muscle layer surrounding the basement membrane is thicker and clearly visible. The tubules in zone 3 are found at the very end of the ductus epididymis, just before it gave rise to the ductus deferens (Figure 3.15). In this region, the epididymal tubules start changing in shape. They reduce in size and the principal cells in the epithelium vary in height. The stereocilia at the apical ends of the principal cells are very short and difficult to distinguish. The outer contour of the tubules remain even, but due to the variation in cellular height, their luminal surface presents an uneven, folded contour that eventually gives the lumen a star-shaped appearance. Progressing closer to the ductus deferens, less and less sperm cells are present in the lumen. The outer smooth muscle consists of many layers and is markedly thicker.



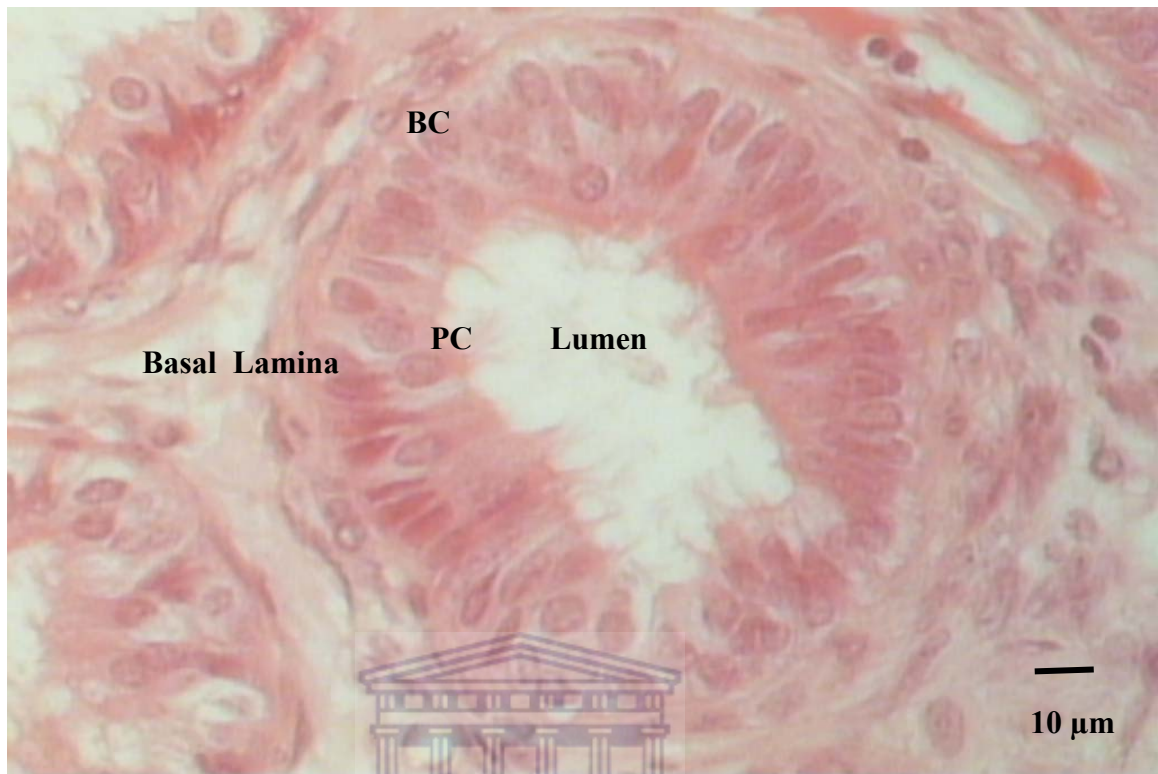


Figure 3. 9. Light micrograph showing the caput epididymis of the vervet monkey, *Chlorocebus aethiops*.

BC - Basal cell, PC - Principal cell.

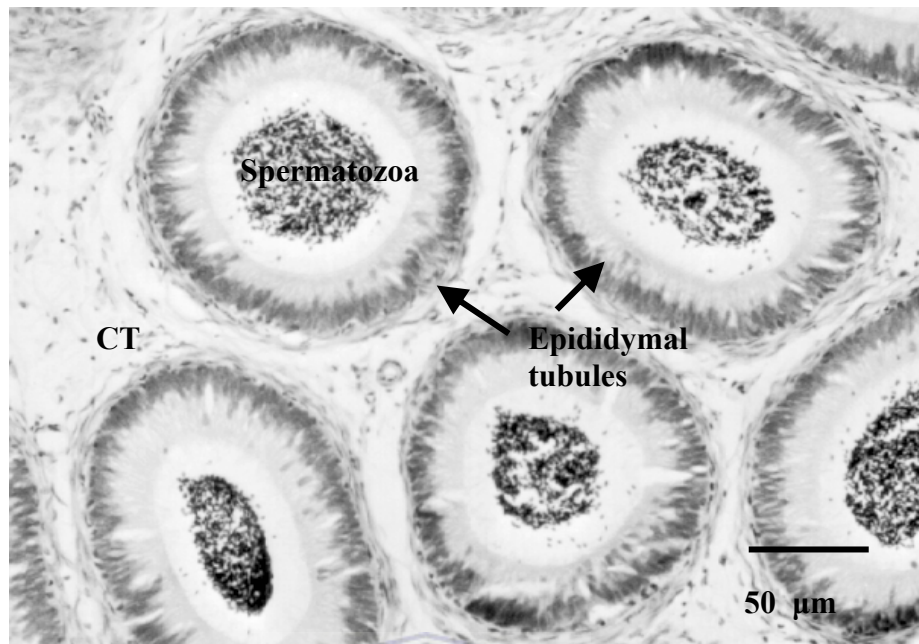
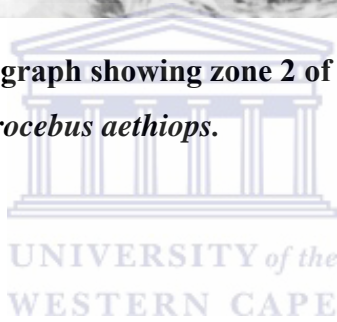


Figure 3. 10. Light micrograph showing zone 2 of the caput epididymis (E1) of the vervet monkey, *Chlorocebus aethiops*.

CT- Connective tissue.



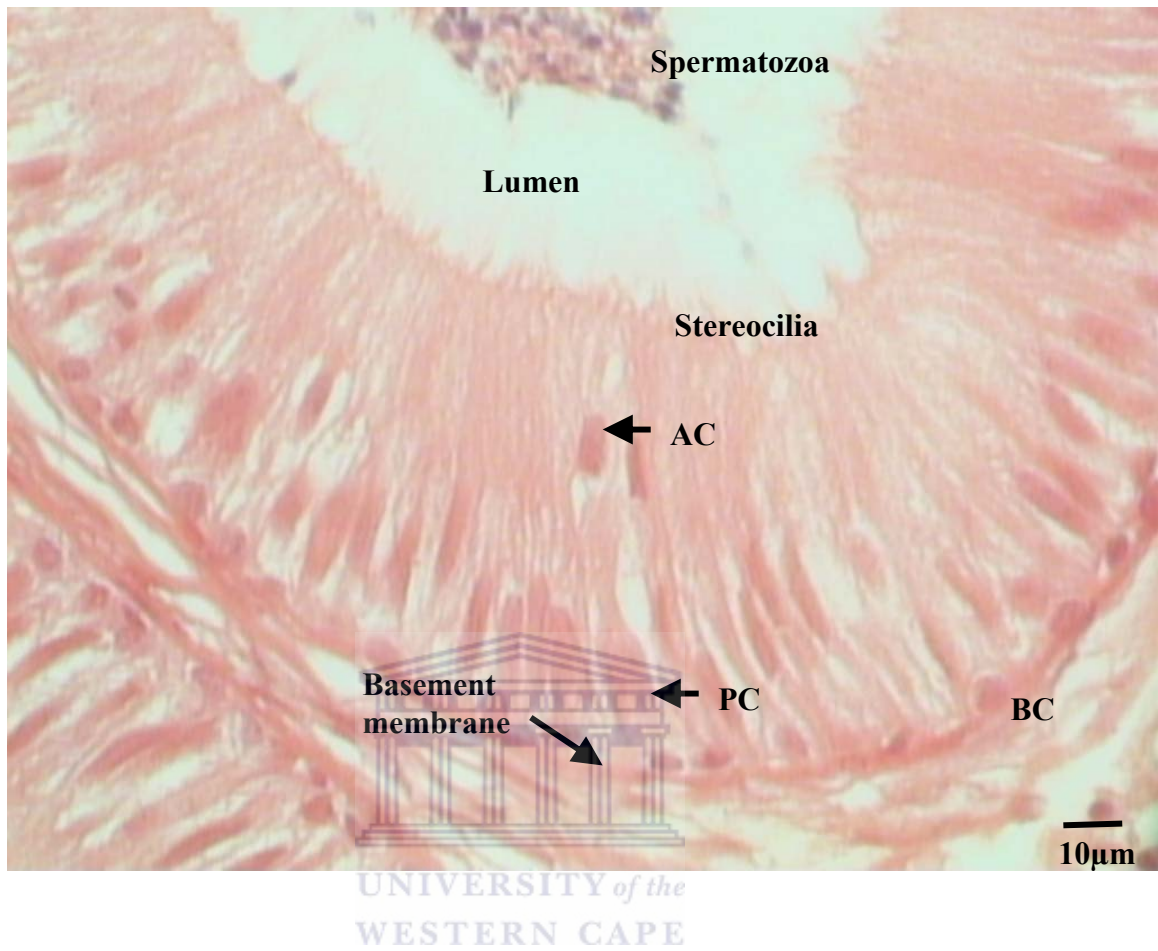


Figure 3. 11. Light micrograph showing the corpus epididymis of the vervet monkey, *Chlorocebus aethiops*.

AC - Apical cell, BC - Basal cell, and PC – Principal cell.

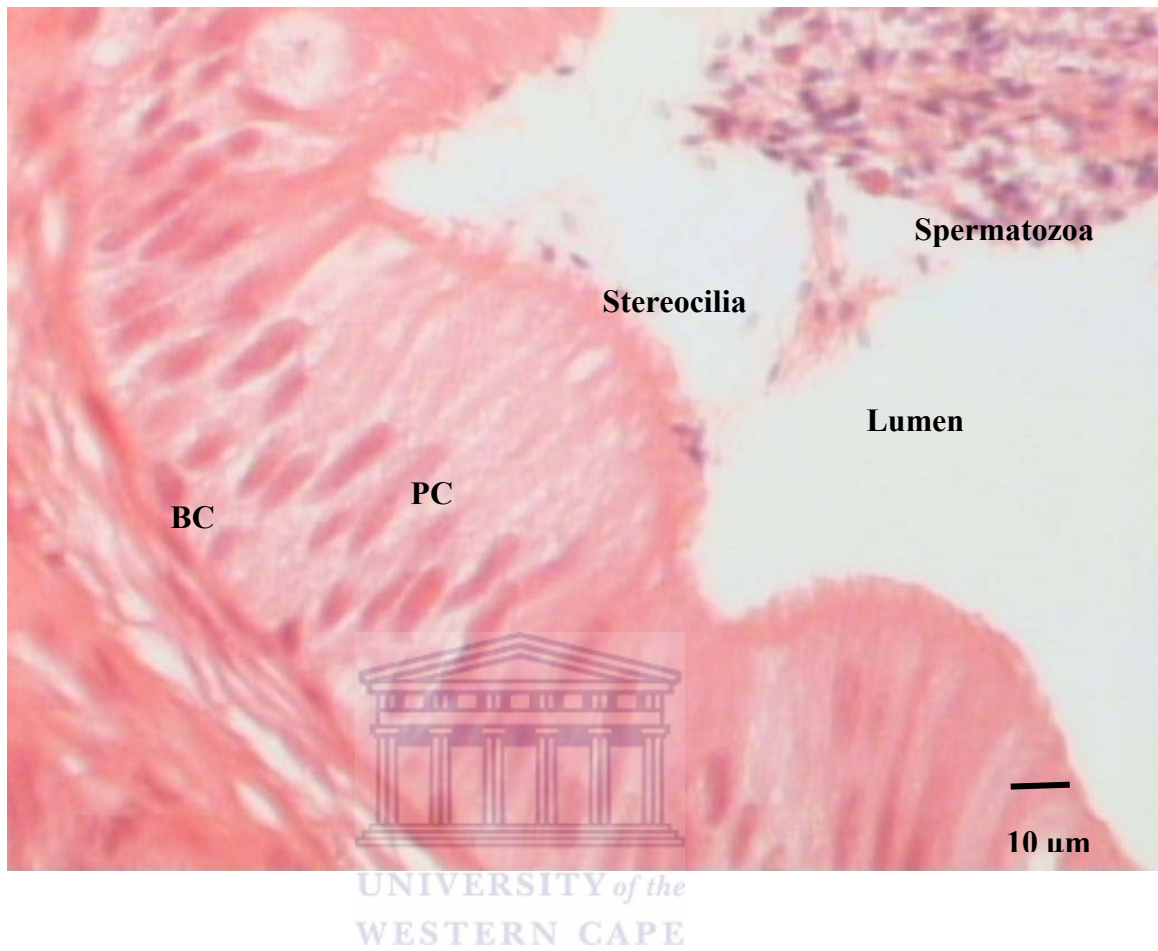


Figure 3. 12. Light micrograph showing the cauda epididymis of the vervet monkey, *Chlorocebus aethiops*.

BC - Basal cell, PC – Principal cell.

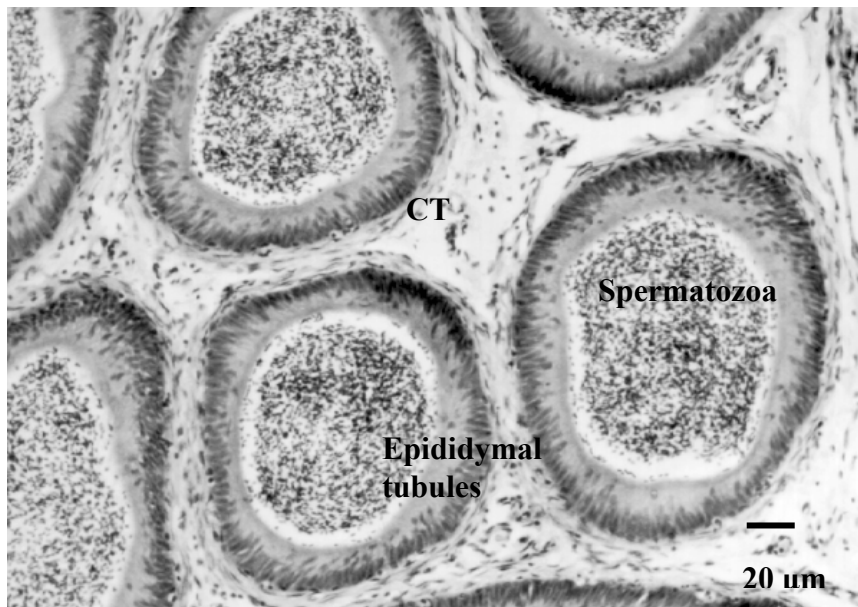


Figure 3. 13. Light micrograph showing zone 1 of the cauda epididymis (E3) of the vervet monkey, *Chlorocebus aethiops*.

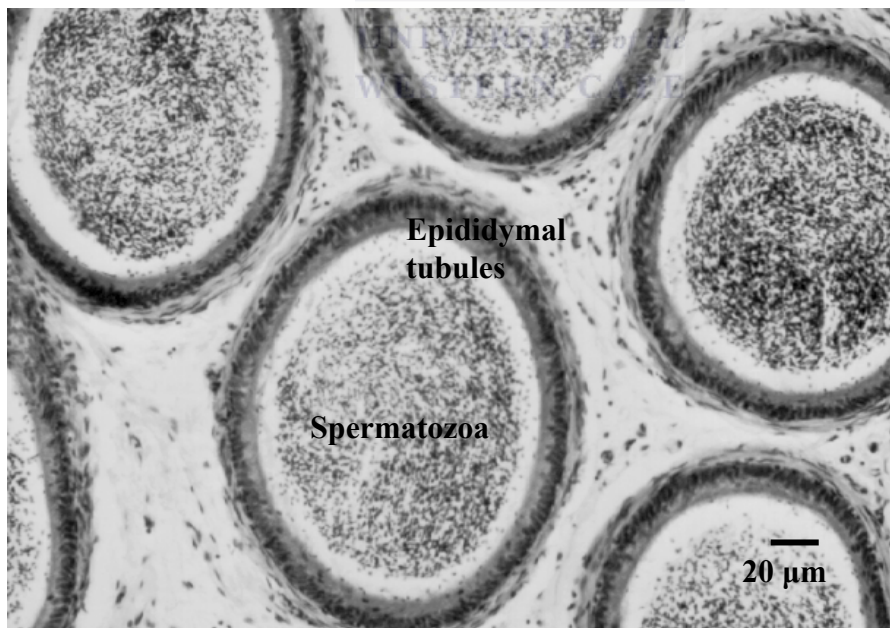


Figure 3. 14. Light micrograph showing zone 2 of the cauda epididymis (E3) of the vervet monkey, *Chlorocebus aethiops*.

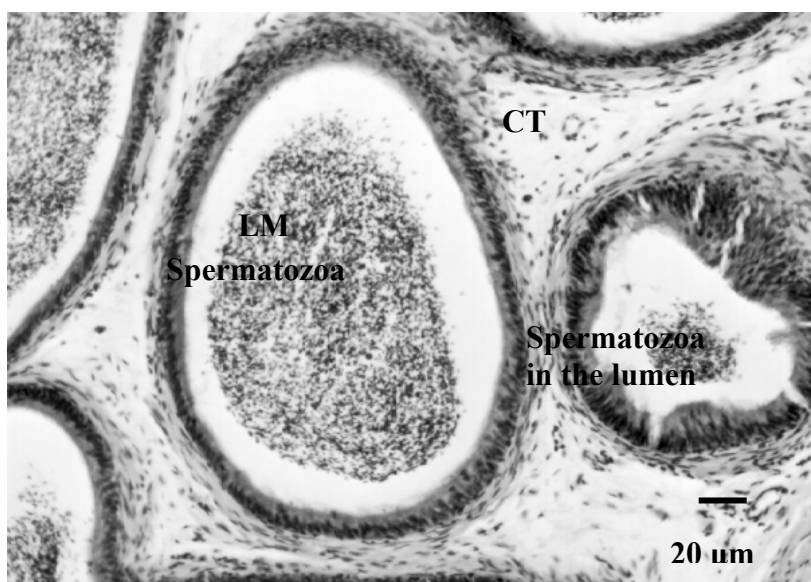


Figure 3. 15. Light micrograph showing zone 3 of the cauda epididymis (E3) epididymis of the vervet monkey, *Chlorocebus aethiops*.

Table 3. 2. The epithelial height of the epididymis (from basal lamina to the stereocilia), in three different regions of the epididymis in the vervet monkey.

Caput (μm) (\pm SEM)	Corpus (μm) (\pm SEM)	Cauda (μm) (\pm SEM)
38.89 \pm 3.69	67.89 \pm 1.84	29.67 \pm 2.33

Note - No significant difference was observed.

Table 3. 3. The number of three different cells found in three different regions of the epididymis of the vervet monkey in an area of 1000 μm^2 (\pm SEM).

	Basal *	Principal	Apical
Caput	1.01 \pm 0.01	3.31 \pm 0.42	0.61 \pm 0.12
Corpus	1.36 \pm 0.15	3.49 \pm 0.27	0.81 \pm 0.17
Cauda	1.47 \pm 0.16	3.26 \pm 0.52	0.88 \pm 0.31

* - Significantly different in its distribution – $P = 0.01$.

3.3.2.4. Vas deferens

At the end of the cauda epididymis, the ductus epididymis straightens out and becomes continuous with the vas deferens (Figures 3.2 and 3.16). The middle vas deferens is more irregular and somewhat narrower than the proximal region, apparently due to the increase in cell size and epithelial infoldings, although the length of the microvilli decreases. The histology of the vas deferens differs in its entire length, because of the presence of some specialized cells (e.g. principal cells) and apical structures in the epithelium (Figure 3.16).

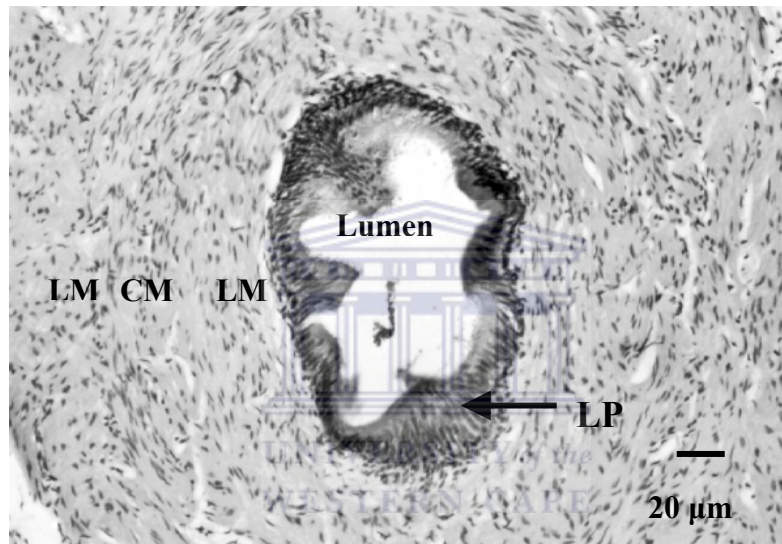


Figure 3. 16. Light micrograph showing the vas deferens of the vervet monkey, *Chlorocebus aethiops*.

CM- Circular muscle, **LP -** Lamina propria, **LM -** Longitudinal muscle.

Also cited by Van der Horst (2005).

3.3.2.10. Seminal vesicles

Histologically, the seminal vesicles contain a highly convoluted simple columnar epithelium which is thrown into mucosal folds (Figure 3.17). The wall of the seminal vesicle consists of a mucosa, a lamina propria, a smooth muscle coat and an adventitia. The mucosa lines the lumen of the seminal vesicle and was thrown into numerous large primary folds and finer secondary and tertiary folds. These folds

project into the lumen and subdivide it into many small, irregular compartments (Figures 3.17 and 3.18). The mucosal folds are lined by a secretory epithelium, which varies in appearance.

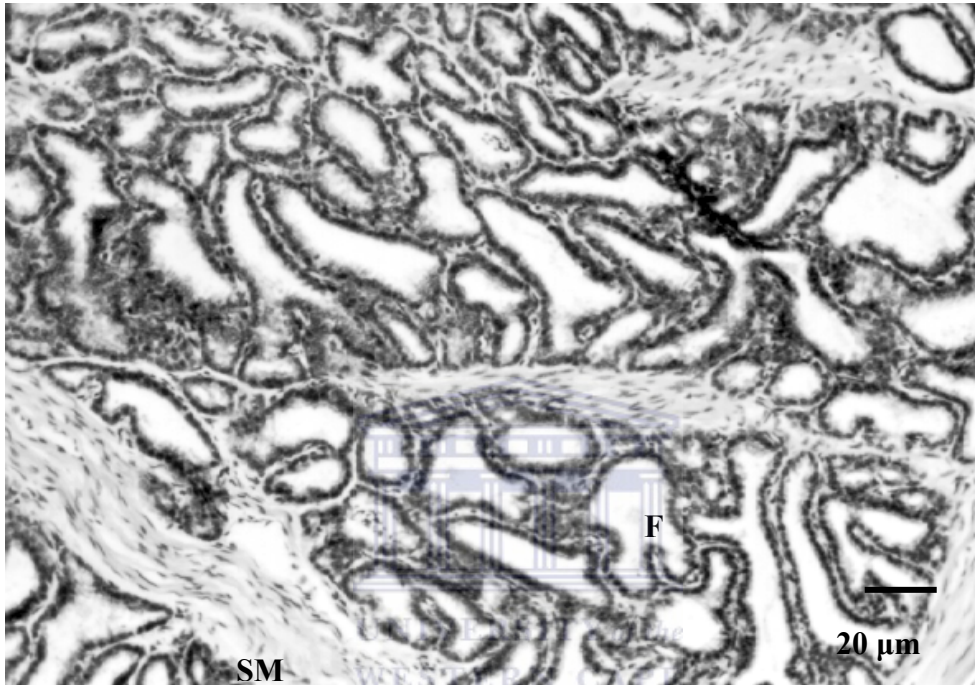


Figure 3. 17. Light micrograph showing the seminal vesicles of the vervet monkey, *Chlorocebus aethiops*.

SM - Smooth muscle, F - Folds

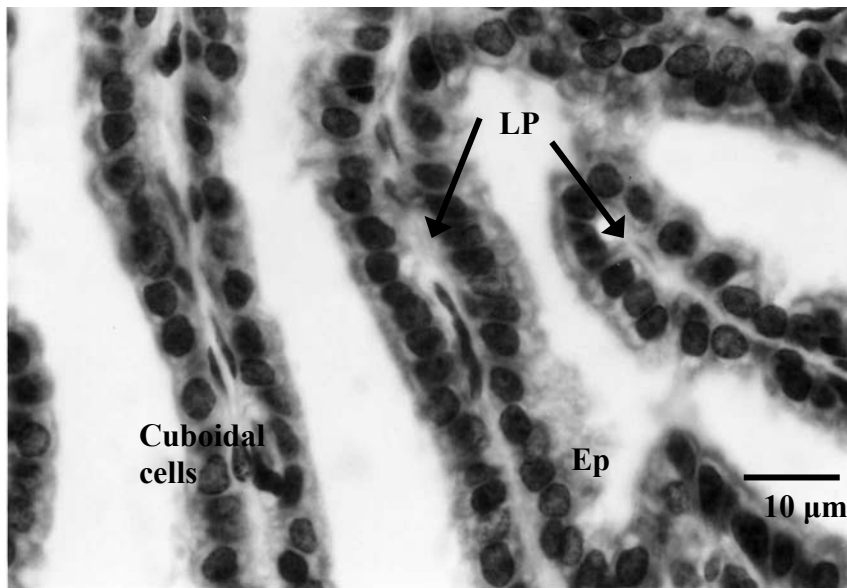
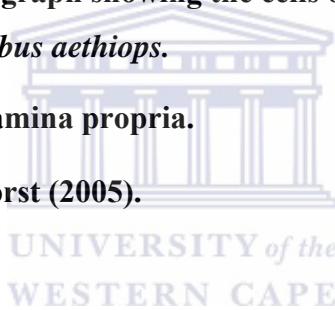


Figure 3. 18. Light micrograph showing the cells of the seminal vesicles of the vervet monkey, *Chlorocebus aethiops*.

Ep – Epithelium, LP - Lamina propria.

Also cited by Van der Horst (2005).



3.3.2.6. Prostate

The prostate appears to be a collection of small, irregular tubulo-alveolar glands. It is surrounded by a fibroelastic capsule rich in smooth muscle (Figure 3.19). This capsule consists of septa that penetrate the prostate and forms a stroma that contained smooth muscle and elastic fibers. The prostatic glands are embedded in this stroma. The epithelium of the prostate consists of cuboidal and low columnar cells with areas that also appear pseudostratified (Figure 3.20 and 3.21). Some of these prostatic cells form aggregations known as nuclear clusters (Figure 3.21). The nuclei of the epithelial cells are also darkly stained. No distinct basement membrane is distinguished between the epithelium and the stroma. The secretions of the prostate are observed as granules in the lumina of some of the prostatic alveoli.

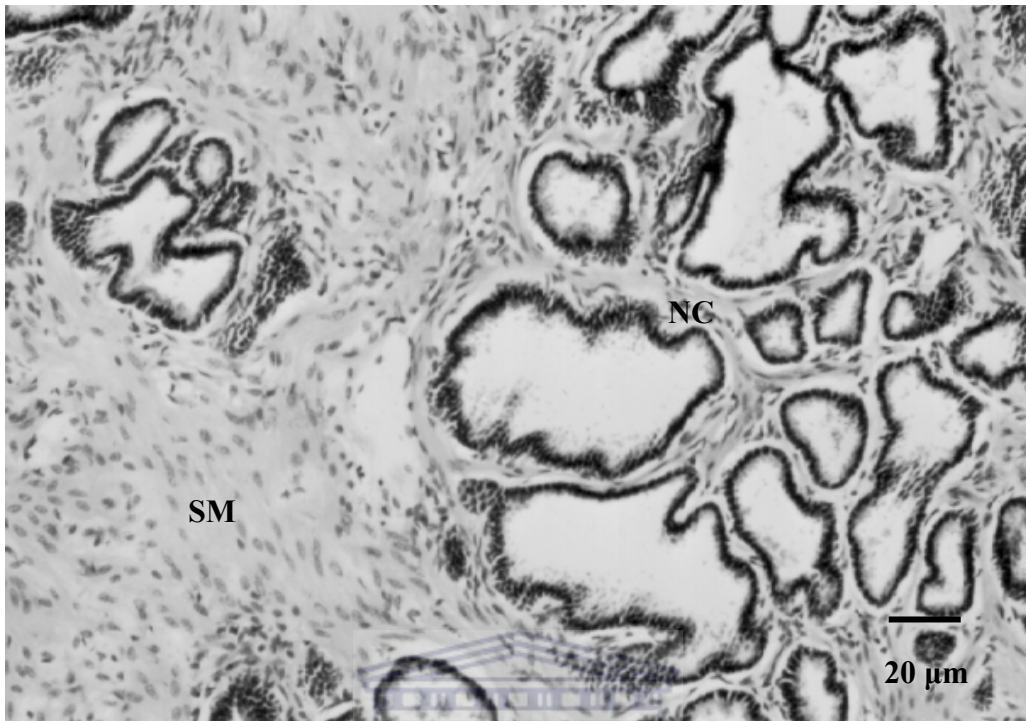


Figure 3. 19. Light micrograph showing the prostate of the vervet monkey *Chlorocebus aethiops*.

SM – Smooth muscle, NC - Nuclear clusters

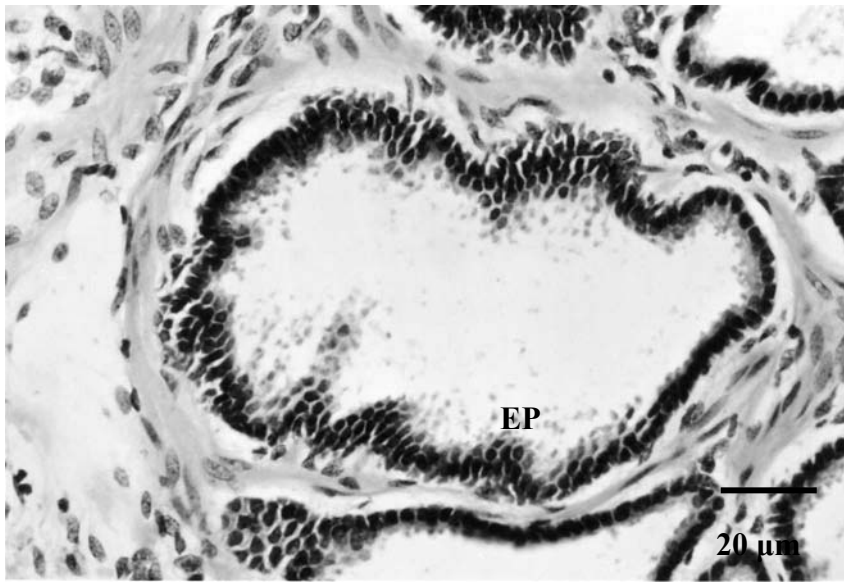


Figure 3. 20. Light micrograph showing the cells of the prostate gland of the vervet monkey, *Chlorocebus aethiops*.

EP - Epithelium (Pseudostratified)

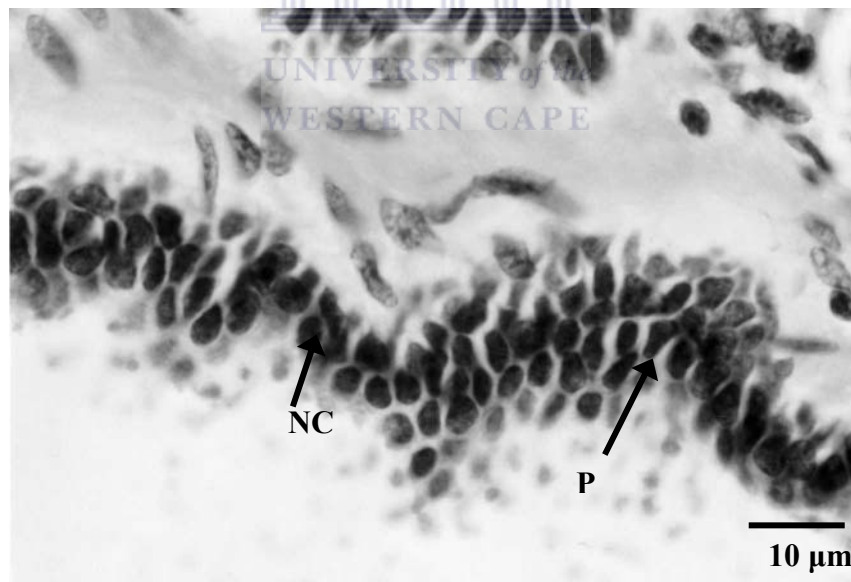


Figure 3. 21. Light micrograph showing the cells of the prostate gland of the vervet monkey, *Chlorocebus aethiops*.

NC - Nuclear clusters, P - Pseudostratified epithelial cells

3.3.2.7. Penis

Two cylindrical masses of erectile tissue are present. These cylinders, the corpora cavernosa, are situated adjacent to one another, while the third mass, corpora spongiosum is situated ventrally within the penile shaft. The corpora cavernosa are each surrounded by a thick layer of dense connective tissue, the tunica albuginea. Between these two corpora, the tunica albuginea forms a common layer, the median septum. Trabeculae consisting of collagenous, elastic, and smooth muscle fibers, extend into the corpora from the tunica albuginea and divide them into numerous cavernous spaces or sinuses (veins). These spaces are lined with squamous endothelium. The ventral corpus spongiosum, although smaller is structurally similar to the dorsal corpora cavernosa, except that its tunica albuginea is thinner and contains more elastic tissue. The cavernous spaces are small and almost uniform in size.

3.3.2.8. Cavernous urethra

This section is characterized by an irregular lumen lined with pseudostratified or stratified columnar epithelium tissue with round, dark staining nuclei (Figures 3.21A and 3.21B).

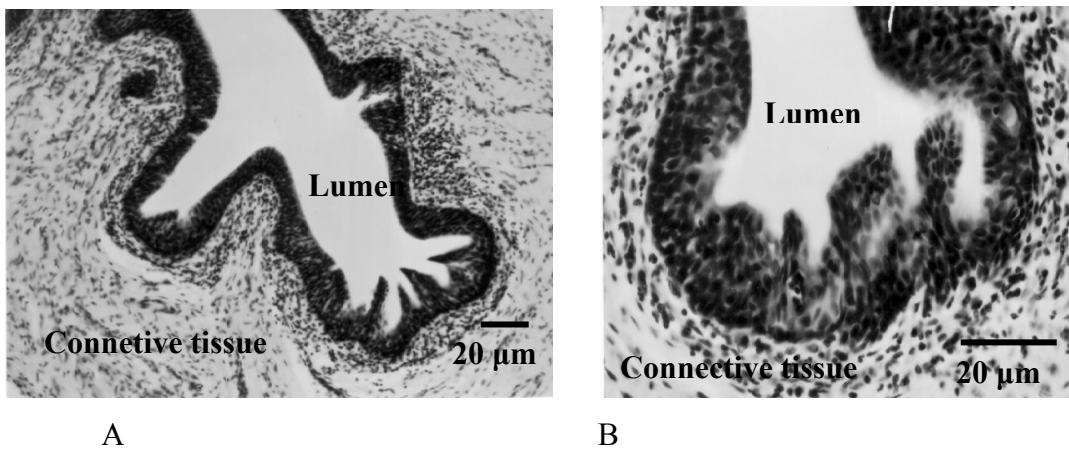


Figure 3. 22. (A and B). Light micrograph showing the corpus spongiosum urethra with lamina propria, and erectile tissue of the vervet monkey, *Chlorocebus aethiops*.

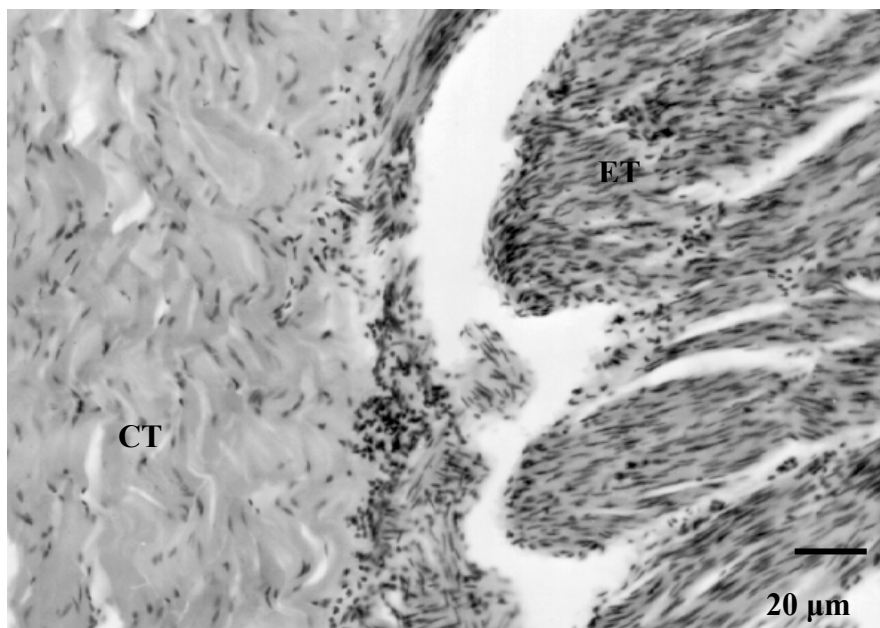


Figure 3. 23. Light micrograph showing the corpus cavernosum showing the erectile tissue in the vervet monkey, *Chlorocebus aethiops*.

CT- Connective tissue, ET – Erectile tissue.

3.4. DISCUSSION

The male reproductive tract of a typical non-human primate is almost similar to that found in man (Van der Horst, *et al.*, 1999; van der Horst, 2005). Harcourt *et al.*, (1981), reported the combined testes weight of the vervet monkey to be 13.00 g, the body weight of 4.9 kg, and the ratio of 0.26%. The smaller testicular weights recorded by Harcourt *et al.*, (1981), could be due to the age of the animals used.

The testes produce testosterone, a male hormone necessary for spermatogenesis, development and maintenance of the accessory glands of the male reproductive system, and the secondary male sex characteristics (Eroschenko, 1996). The interstitial tissue contained vascular elements, connective tissue, Leydig cells, macrophages, and peritubular myoid cells. Leydig cells occurred mostly in clusters of polymorphic cells, and they were usually associated with small blood vessels. Vascularization of this area is essential because these cells are regarded as endocrine

cells. Macrophages were usually detected close to and adherent to Leydig cells. These clusters of Leydig cells together with other types of cells were partly covered with a thin layer of squamous lymphatic endothelium, which was continuous with that of the peritubular myoid cells at sites where clusters of Leydig cells were in close apposition to the seminiferous tubules. Leydig cells had a large spherical nucleus or slightly elongated nucleus, which usually possessed a prominent nucleolus and frequently deep indentation of nuclear envelope. This was also observed in rats (Ichihara *et al.*, 2001). Rey *et al.*, (1996), found that mature Leydig cells in cebus monkey, were polygonal with round, euchromatic nuclei (6-7 μm) and few heterochromatic granules attached to the nuclear envelope, and conspicuous nucleoli. The cytoplasm was abundant and showed either a pale or a dark staining appearance. Nistal *et al.*, (1986) reported that in men, peritubular fibroblasts (myoid cells), differentiated into interstitial fibroblasts and partially differentiate into Leydig cells, which complete their differentiation into the adult Leydig cells. Rey *et al.*, (1996), also showed in the monkey testis that myoid cells are differentiated into Leydig cells during postnatal development. Rana and Bilaspuri (2000) reported that in the Murrah buffalo, the myoid cells are differentiated into fibroblasts and mesenchymal cells, which are then differentiated into adult Leydig cells (Figure 3.8).

The population of Leydig cells in the adult human testis represents the third and final phase of their developmental history, preceded by distinct neonatal and earlier fetal Leydig cell generations. Human Leydig cells are irregular in outline, deeply staining with basophilic dyes and exhibit a characteristic circular or ovoid nucleus. Crystals of Reinke of up to 30 μm in length are often noted in the Leydig cell cytoplasm in humans although their function remains unknown (Kerr, 1992).

The epididymis is a long, highly coiled tube consisting of the caput (E1), corpus (E2), and the cauda (E3) parts and has the total length of 6 cm compared to the epididymis of the adult macaque monkey which has a length of 6-8 cm, and is situated primarily at the dorso-lateral region of the testis, the same position as in humans. The ductuli efferentes, which may vary in number from 8 to 16, emerge from the apical pole of the testis and open into the highly coiled initial segment of the

epididymis at various sites of the caput region. Ramos and Dym (1977), found that the absence of the adipose tissue around the epididymis serves as a unique gross anatomical feature of the monkey epididymis, compared to the rodents and other mammals. In many other species, the width measurements of the different sections (caput, corpus, and cauda) of the epididymis differ markedly from one another, whereas in the Macaque monkey epididymis, the thickness is more uniform throughout the whole length of the duct (Ramos and Dym, 1977). In section, the vervet monkey epididymal ducts in these regions have an even contour, both inside and outside, since the epithelium, unlike that of the ductus efferentes, is uniform in height (Table 3.2). The general morphology of the epididymis in the vervet monkey was found to be similar to the ones in the three Macaque species (*Macaca mulatta*, *Macaca fascicularis*, and *Macaca arctoides*), studied by Ramos and Dym (1977). The pseudostratified epithelium consists of four distinct cell types, viz: principal cells, apical cells, basal cells, and halo cells (intraepithelial lymphocytes). Bajpai *et al.*, (1985), also reported the pseudostratified epithelium of the rhesus monkey which consisted of the three distinct cells, viz: principal cells, apical cells, and the basal cells. They also reported a gradual reduction in the height of the stereocilia of the principal cells which is accompanied by an increase in tubular and luminal diameter along the length of the epididymal duct. The ducts are lined by pseudostratified columnar epithelium, which rests on a basement membrane. The basal cells stain dark and can clearly be distinguished along the basement membrane, distributed intermittently between the principal cells. They have a low cuboidal structure and contain small rounded nuclei. The principal cells are more numerous in both the corpus and caudal regions of the vervet monkey epididymis (Table 3.3.). The basal cells and the apical cells are few in numbers in all the regions of the epididymis. There were significant differences in the basal cell distributions among three regions of the epididymis (Table 3.3). The principal cells extend from the basement membrane to the lumen of the tubule. These tall cells have elongated nuclei, which are situated at different levels above the basement membrane, but most of them lie close to the membrane. Their nuclei are vacuolated and contain a dark-staining

nucleolus. At their luminal surface the principal cells have irregular, branched stereocilia which extend into the lumen. Many lipid droplets are present in the cytoplasm of both the principal cells and the basal cells. Intraepithelial lymphocytes are scattered within the epithelium close to the luminal surface. Surrounding the basement membrane is a lamina propria with circularly arranged smooth muscle fibers. Outside this layer of smooth muscle, the tubules are surrounded by connective tissue rich in blood vessels. There are numerous arterioles and capillaries that penetrated directly into the epithelium from the underlying connective tissue. The stereocilia in the caput and corpus epididymides appeared to be more pronounced than in the caudal region. This concurs with what was reported by Ramos and Dym (1977), in the Macaques.

Alsum and Hunter, (1978), found that the epididymal epithelial and stereocilial height was maximal in the caput region (caput section 3 = 69.6 μm) and minimal in the caudal region (cauda section 7 = 40.2 μm) in the rhesus monkey (*Macaca mulatta*). This suggests a slight difference in the morphological appearance of the epididymis in the primate group. Connell and Donjacour (1985), reported that the epithelial height and diameter of the tubules of the corpus epididymis of prepubertal dogs were greater than those of the caput region. The smallest tubular diameter recorded were those of the cauda. The width of the epithelium was reported as $24.0 \pm 4.2 \mu\text{m}$ in the caput, $33.0 \pm 5.4 \mu\text{m}$ in the corpus, and $48.2 \pm 3.7 \mu\text{m}$ in the caudal region. The tubular diameter was $95.5 \pm 16.2 \mu\text{m}$ in the caput, $122.2 \pm 11.8 \mu\text{m}$ in the corpus and $232.9 \pm 29.1 \mu\text{m}$ in the caudal region. Sprando *et al.*, (1999) reported a significantly larger diameter in the caudal region ($173.5 \pm 32.3 \mu\text{m}$) of the 12.5 month-old sand rat and lower diameter in the caput region ($111.0 \pm 19.0 \mu\text{m}$) in the rat of the same age. The corpus diameter was reported to be $129.2 \pm 2.1 \mu\text{m}$.

Ramos (1979) divided the vas deferens structure of the Macaques species into four distinct regions, viz: proximal, middle, distal and ampulla. The prostate end of the monkey vas deferens is thicker than the testicular end. The lumen of the vas deferens is lined by epithelium separated by a thick basal lamina from the underlying lamina propria. Ramos (1979) recorded the length of 19 cm in two Macaque species

and the luminal diameter is about 450-490 μm in the proximal end and the distal end is approximately 260-350 μm . Leong and Singh (1990) reported that the testicular end is composed of pseudostratified tall columnar cells with stereocilia protruding into the lumen in the *Macaca fascicularis*. This concurs with the findings in this study as outlined in Figure 3.16. The epithelial cells of the monkey vas deferens are capable of secretion. Leong and Singh (1990) suggested that the vas deferens may not function simply as a conduit for the transport of spermatozoa. It could play some role in the absorption of fluid from the lumen of the vas deferens in the maturation of the spermatozoa and in spermiophagy which occurs mostly at the prostatic end of the vas deferens (Murakami *et al.*, 1982). Leong and Singh (1990) further reported stellate cells which were found interspersed between columnar cells. In addition to these cells, there were other cells which most likely were the intraepithelial lymphocytes which have been constantly reported in the vas deferens of the rat and monkey (Dym and Romrell, 1975) and in man (Hoffer, 1976).

The vas deferens has a thick, irregular lumen, which is surrounded by a thick wall consisting of a mucosa, a muscularis and an adventitia. The mucosa is thrown into longitudinal folds that project into the lumen, resulting in an irregular luminal contour. The epithelium rests on a thin basement membrane and is surrounded by the lamina propria which contains numerous elastic fibers. Light microscopic examinations revealed that the epithelial cells of the vas deferens are capable of secretion. This will mean that the vas deferens performs other important physiological functions more than just as a passive conduit for the transport of spermatozoa (Ramos, 1979). Hoffer (1976) reported that the fine structure of the human ductus deferens surgically removed during vasectomy demonstrated the infoldings and complexity of the epithelium. The portion of the human vas deferens studied was probably the proximal segment because vasectomy is normally performed in the region of the scrotum. Furthermore, the epithelial lining of the vas deferens has a heterogenous cell population, an indication that the epithelium can actively modify the luminal contents by selective absorption and secretion (Ramos, 1979).

The muscularis forms the bulk of the wall of the vas deferens and consists of three layers of smooth muscle in the vervet monkey. The inner and outer layers are arranged longitudinally, while the middle layer is arranged in circular manner. The muscularis is surrounded by the adventitia which consists of fibrous connective tissue containing numerous blood vessels and nerves. Sperm cells and macrophages are found in great abundance in the lumen of the prostatic end of the vas deferens. Leong and Singh (1990) also observed these structures and concluded that such features occur most frequently in the accessory lumen arising from the central zone. It appears that the accessory lumen is a reservoir wherein excess spermatozoa are phagocytosed.

The seminal vesicles of the vervet monkey are highly convoluted with simple columnar epithelium which is folded. These folds are lined by secretory epithelium. Badia *et al.*, (2006) also observed the same features when they described seminal vesicles of the boar as a compact glandular tissue arranged in multiple lobules containing a system of ramified secretory tubules with well-developed lumina. It consists of low columnar and cuboidal cells, while in some regions the epithelium appears pseudostratified, consisting of spherical basal cells intermittently positioned between cuboidal cells. The nuclei of the columnar cells are slightly elongated and those of the cuboidal cells are more ovoid (Figure 3.18). Badia *et al.*, (2006), reported two types of columnar cells in the seminal vesicle of the boar, namely: principal cells and dense cells. The principal cells contained an elongated or rounded euchromatic nucleus located in basal or mid-basal cytoplasm with one or two nucleoli. Dense cells were scarce and irregularly distributed, mostly singly and occasionally in small groups. These dense cells had elongated heterochromatic nuclei (Badia *et al.*, 2006). They stain darkly and possess a round nucleolus. Lipid droplets are also present in the epithelial cytoplasm. The epithelium rests on a thin lamina propria of loose connective tissue with many elastic fibers. These features were also observed by Sprando *et al.*, (1999), in the male sand rat, *Psammomys obesus*. The lamina propria projects into the mucosal folds and forms the core of the primary folds and thin stroma of the smaller folds. Surrounding the lamina propria is a muscular

coat which is thinner than the muscularis of the ductus deferens. External to the muscle coat is a layer of loose connective tissue rich in elastic fibers, adventitia.

Most of the features of the male reproductive tract of the vervet monkey tend to be similar to that found in humans. Table 3.4 indicates the comparison of the vervet monkey to humans and other mammals.

Table 3. 4. Comparison of the vervet monkey, humans and other mammals on selected features of the reproductive tract.

Feature	Vervet	Humans	Other Mammals	References (if necessary)
Tunica albuginea	+	+	+	
Seminiferous tubule layers	4 -5	5	2	(Dym, 1972)
Myoid cells	+	+	+	
Interstitial area	+	+	+	
Seminiferous tubules	+	+	+	
Sertoli cells and germ cells	+	+	+	
Stages	Multistage	Multistage	Multistage and Unistage	
Stage / Cross section	3-4	1-5 (average 3)	1 (rat, rhesus monkey)	Millar <i>et al.</i> , (2000)

+ - Present

3.5. CONCLUSIONS

The general microanatomy of the male reproductive system of the vervet monkey, *Chlorocebus aethiops*, was found to be similar to that documented in other mammals, especially in the nonhuman primates such as chimpanzees and Macaques. The light microscopic studies revealed that the testes had numerous seminiferous tubules and these tubules have two different types of cells, namely, the germ cells (spermatogonia, spermatocytes, spermatids, and the spermatozoa) and the somatic

cells (Sertoli cells). The testosterone-secreting cells, the Leydig cells are found in between the seminiferous tubules. The myoid cells (peritubular cells) constitute the cellular component of the boundary tissue around the seminiferous epithelium. These cells have nuclei which contains one or two nucleoli which are peripherally situated. The boundary tissue also contains a relatively thick basal lamina and elastic collagen fibrils which are visible at the light microscopic level.

The testis empties into the the straight tubules, commonly known as the tubuli recti, which later form the rete testis. The rete testis will then form the ductuli efferentes, which will anastomose to form the epididymis. The epididymis like in other mammals is subdivided into three regions, the caput, corpus and the cauda epididymis. The initial segment, which is the proximal part of the caput epididymis is commonly reported as the fourth region in most of the literature on monkey epididymis. Like in other primates, the vervet monkey epididymis consists of a pseudostratified epididymal epithelium, which consists of the four major cell types, namely, principal cells, apical cells, the basal cells and the intraepithelial lymphocytes (halo cells). In this study, the corpus epididymis was found to have a greater width compared to the other two sections. In Macaques, the thickness is uniform throughout the length, whereas in other mammals the epididymis tapers as it enters the vas deferens. Apical cells are fewer in number and their luminal surface is free of stereocilia. In contrast, principal cells are the dominant type throughout the length of the epididymal duct and it is their variations in height that create regional differences in the gross morphology of the epithelium.

In summary, the present study provides basic light microscopy information on the structure and histology of some of the most important parts of the male reproductive system of the vervet monkey. However, in some aspects such as the testicular structure the vervet monkey appears to be more closely related to humans than other mammalian species. However, more detailed investigations are required at electron microscopic level to establish further relationships with humans and/or other mammals.

3.6. REFERENCES

Alsum, D. J. and Hunter, A. G. 1978. Regional histology and histochemistry of the ductus epididymis in the rhesus monkey (*Macaca mulatta*). *Biol. Reprod.* **19**:1063-1069.

Badia, E., Briz, M. D., Pinart, E., Sancho, S., Garcia-Gil, N., Bassols J., Pruneda, A., Bussalleu, E., Yeste, M., Casas, I. and Bonet S. 2006. Structural and ultrastructural features of boar seminal vesicles. *Tissue Cell.* **38**:79-91.

Bajpai, V. K., Shipstone, A. C., Ratna Kumar, B. V., Qaisar, J. and Setty, B. S. 1985. Ultrastructure of the epididymal epithelium of Rhesus monkey (*Macaca mulatta*). *Acta Euro. Fertil.* **61**:207-217.

Barfield, J. P., Nieschlag, E. and Cooper T. G. 2006. Fertility in wildlife: humans as a model. *Contraception* **73**:6-22.

Clermont, Y. and Leblond, C. P. 1959. Differentiation and renewal of spermatogonia in the monkey, *Macaca rhesus*. *Am. J. Anat.* **104**:237-274.

Connell, C. J. and Donjacour, A. 1985. A morphological study of the epididymides of control and estradiol-treated prepubertal dogs. *Biol. Reprod.* **33**:951-969.

de Rooij, D. G., van Alphen, M. M. A. and van de Kant, H. J. G. 1986. Duration of the cycle of the seminiferous epithelium and its stages in the rhesus monkey (*Macaca mulatta*). *Biol. Reprod.* **35**: 587-591.

Dym, M. 1972. The fine structure of the monkey (*Macaca*) Sertoli cell and its role in maintaining the blood-testis barrier. *Anat. Rec.* **175**:639-656.

Dym, M. and Romrell, L. J. 1975. Intraepithelial lymphocytes in the male reproductive tract of rats and rhesus monkeys. *J Reprod. Fertil.* **42**:1-7.

Eroschenko, V. P. 1996 Atlas of Histology with Functional Correlations. 8th Ed. Williams and Wilkins. pp 275.

Fouquet, J. P. and Dadoune, J. P. 1986. Renewal of spermatogonia in the monkey (*Macaca fascicularis*). *Biol. Reprod.* **35**:199-207.

Harcourt, A. H., Harvey, P. H., Lawson, S. G., and Short, R. V. 1981. Testis weight, body weight and breeding systems in primates. *Nature* **293**:55-57.

Hoffer, A. P. 1976. The ultrastructure of the ductus deferens in man. *Biol. Reprod.* **14**:425-443.

Ichihara, I., Kawamura, H., Nakano, T. and Pelliniemi, L. J. 2001. Ultrastructural, morphometric, and hormonal analysis of the effects of testosterone treatment on Leydig cells and other interstitial cells in young adults rats. *Ann. Anat.* **183**:413-426.

Kerr, J. B. 1992. Functional cytology of the human testis. Baillière 's *Clin Endo. Met.* **6**:235-250.

Kumar, R. A. and Phillips D. M. 1991. Spermiation and sperm maturation in the marmoset. *Anat. Rec.* **229**:315-320.

Leong, S. K. and Singh, G. 1990. Ultrastructure of the monkey vas deferens. *J. Anat.* **171**:85-92.

Majumdar, S. S., Winters, S. J. and Plant, T. M. 1998. Procedures for the isolation and culture of Sertoli cells from the testes of infant, juvenile, and adult rhesus monkeys (*Macaca mulatta*). *Biol. Reprod.* **58**:633-640.

Martin, C. W., Anderson, R. A., Cheng, L., Ho, P. C., van der Spuy, Z., Smith K. B., Glasier, A. F., Everington, D. E. and Baird D. T. 2000. Potential impact of hormonal male contraception: cross-cultural implications for development of novel preparations. *Human Reprod.* **15**:637-645.

Millar, M. R., Sharpe, R. M., Weinbauer, G. F., Fraser, H. M. and Saunders P. T. K. 2000. Marmoset spermatogenesis: organizational similarities to the human. *Int. J. Androl.* **23**:266-277.

Murakami, M., Sugita, A. and Hamasaki, M. 1982. Scanning electron microscopic observations of the vas deferens in man and monkey with special reference to spermiphagy in its ampullary region. *Scan. Electr. Micro.* **111**:1333-1339.

Nistal, M., Panigua, R., Regadera, J., Santamaria, L. and Amat, P. 1986. A quantitative morphological study of human Leydig cells from birth to adulthood. *Cell Tissue Res.* **246**:229-236.

Potts, M. 1996. The myth of a male pill. *Nature Med.* **2**:38-399

Ramos, A. S. 1979. Morphologic variations along the length of the monkey vas deferens. *Arch. Androl.* **3**:187-196.

Ramos, A. S. and Dym, M. 1977. Fine structure of the monkey epididymis. *Am. J. Anat.* **149**:501-532.

- Rana, B. K. and Bilaspuri, G. S. 2000. Changes in interstitial cells during development of buffalo testis. *Vet. J.* **159**:179-185.
- Rey, R. A. Nagle, C. A. and Chemes, H. 1996. Morphometric study of the testicular interstitial tissue of the monkey *Cebus apella* during postnatal development. *Tissue Cell.* **28**:31-42.
- Seier, J. V. 1986. Breeding vervet monkeys in a closed environment. *J. Med Primatol.* **15**:339-349.
- Sprando, R. L., Collins, T. F. X., Black, T. N., Olejnik, N., Rorie, J. I., West, L. J., Bower, J. O., Sass, N. and Robl, N. 1999. Light microscopic observation on the reproductive tract of the male sand rat, *Psammomys obesus*. *Tissue Cell.* **31**:99-115.
- United Nations. 1994. World Contraceptive use. UN Department for Economic and Social Information and Policy Analysis, Population Division. (ST/ESA/SER.A/143). New York.
- Van der Horst, G. 1995. Computer aided sperm motility analysis of selected mammalian species. Unpublished PhD Thesis. University of Stellenbosch. pp 278.
- Van der Horst, G., Seier, J. V., Spinks, A. C. and Hendricks, S. 1999. The maturation of sperm motility in the epididymis and vas deferens of the vervet monkey, *Cercopithecus aethiops*. *Int. J. Androl.* **22**:197-207.
- Van der Horst, G. 2005. Reproduction. In: The Handbook of Experimental Animals. The Laboratory Primate. (ed. S. Wolfe-Coote). Chapter 31, Elsevier Academic Press. Amsterdam. pp 527-536.

Weinbauer, G. F., Aslam, H., Krishnamurty, H., Brinkwork, M. H., Einspanier, A. and Hodges, J. K. 2001. Quantitative analysis of spermatogenesis and apoptosis in the common marmoset (*Callithrix jacchus*) reveals high rates of spermatogonial turnover and high spermatogenic efficiency. *Biol. Reprod.* **64**:120-126.



CHAPTER 4: ULTRASTRUCTURE OF THE EPIDIDYMIS OF THE VERVET MONKEY

4.1. INTRODUCTION

4.1.1. Ultrastructure of the epididymis

The epididymis (pl-epididymides), from the Greek *epi* (on) and *-didymoi* (twins or testicules) is an elongated organ located on the testis surface. It is a long, single, convoluted tubule that conveys spermatozoa from the vasa efferentia to the vas deferens (Sullivan *et al.*, 2005). Anatomically, the epididymis can be divided into four sections: the initial segment, caput, corpus and the cauda. In some species, an initial segment is incorporated in the caput (Hermo *et al.*, 1994; Cooper, 1998). In humans, the caput epididymis is not well defined and is mainly formed by vasa efferentia, whereas the cauda segment is not as bulbous as in other mammalian species (Yeung *et al.*, 1991; Cooper, 1993). There are clear changes from the caput region to the cauda regions in terms of epithelial height, stereocilial height, and nuclear membrane infoldings (Dym, 1983). The caput region readily absorbs fluid and particulate matter, the cauda acts as sperm reservoir and can contract forcefully upon appropriate nervous stimulation (Dym, 1983). It is also believed that gycerylphosphoryl choline is synthesized in the caput region and carnitine is concentrated from the blood by epithelial cells throughout the organ (Marquis and Fritz, 1965).

From studies of many species, the epididymal epithelium is known to be composed of principal cells, basal cells, and apical cells, with white blood cells (including lymphocytes, macrophages, and monocytes) interposed among the epithelial cells (Robaire and Hermo, 1988). The pseudostratified epithelium of the monkey, like with many other mammals, consists of four main cell types; principal cells, apical cells, basal cells, and intraepithelial lymphocytes (Ramos and Dym, 1977b). The luminal surface of the epithelium bears long non-motile microvilli (stereocilia). The height of these structures decreases from 80 μm in the caput to 40 μm in the caudal region. Alsum and Hunter (1978) indicated that in male rhesus monkeys, epididymal epithelial cells and stereocilia appear to reach maximum height

in the caput region and minimal at the caudal region and the luminal diameter to be the reverse. However, in the bonnet monkey (*Macaca radiata*), the height of the epididymal epithelium and lumen diameter are maximal in caput and minimal in the cauda (Flechon *et al.*, 1976).

The principal cells are the most abundant cells and are characterized by large supranuclear Golgi apparatus and rough endoplasmic reticulum in the basal cytoplasm (Dym, 1983). Some dense granules and mitochondria are present in the basal region of the principal cells of several mammalian species, including man. Hoffer (1976) indicated that in different organs, cells rich in mitochondria are believed to be involved in the production of acidic secretory products and in resorption of water from the lumina. The apical cytoplasm contains numerous micropinocytotic vesicles, multivesicular bodies and lysosomes, lipid droplets, coated vesicles, and mitochondria (Dym, 1983). The principal cells have been associated with absorptive and digestive functions hence the presence of pinocytic vesicles and vacuoles in the apical region (Ramos and Dym, 1977b). In addition, the principal cells have a key role in creating and maintaining the unique regional characteristics of the luminal fluid (Amann, 1987; Robaire and Hermo, 1988). Intraepithelial lymphocytes are located at all levels in the epithelium. In rodents and monkeys, the intraepithelial lymphocytes represent about 2% of the total cell population (Dym, 1983). The elaborate infoldings of the nuclear membrane and the large nucleoli may also be interpreted as a sign of highly intense metabolic activity (Ramos and Dym, 1977b).

There are spheres that were observed in the principal cells of the Macaque monkey epididymis. They could be involved in the transportation of cellular products into the lumen. These spheres were associated with endocytosis and exocytosis processes. In addition, the degradation products of luminal spermatozoa are perhaps transported in the epithelial cells via the spheres (Ramos and Dym, 1977b).

Basal cells may play a role in stabilizing and giving rigidity to the epithelium because of their strategic location between the bases of principal cells and their complex interdigitations with the latter's plasma membrane.

This chapter will provide the ultrastructural information on the epididymis of the vervet monkey. This information is essential in examining the cell types and cell organelles responsible for sperm maturation.

4.2. OBJECTIVES

- To study the ultrastructure of the three regions of the epididymis of the vervet monkey.
- To compare the ultrastructure of the epididymis of the vervet monkey to the epididymis of the human.

4.2. MATERIALS AND METHODS

Study animals and their maintenance, sample collection, and dissection procedures were the same as in previous chapter. Ethical clearance was obtained from the Medical Research Council's Ethical Committee for this study.

4.2.1. SCANNING ELECTRON MICROSCOPY (SEM)

The samples fixed in 2.5% Sorenson's phosphate buffered glutaraldehyde were used for the purpose of SEM. The specimens were dehydrated in ethanol. Graded alcohol (70%, 80%, 96% and absolute) was used to achieve dehydration. After dehydration the specimens were sonicated in absolute alcohol for approximately 1 minute to loosen the smear layer caused by cutting during sampling. The specimens were dried at the critical point of medical wet carbon dioxide, after which they were mounted and fixed onto standard SEM pin type aluminium stubs with double-sided tape. The specimens were sputter-coated with gold for 2 minutes at 12mA under vacuum and in the presence of argon gas. The coating procedure was repeated from different angles to reduce the effects of charging when rotating and

tilting the specimen stage (holder). All cut surfaces of the specimens were viewed in a Leica Stereoscan 420 SEM at 6-8 kV with 3-12 mm working distances.

Although the working distances varied to the tilting of the specimen stage, good resolution and contrast were obtained by optimally manipulating the beam of electrons. The accelerating voltages varied proportionately to the working distances during tilting. The specimens were tilted from 0°-90° and rotated from 0°-360° thus covering all planes of the X,Y,Z axes through the specimens. The tilting and rotation was performed for the sole purpose of obtaining the maximum anatomical exposure of the surface of each tissue. The contrast was set to 14% whilst the brightness was kept at 32%. A 30 µm aperture was placed in the path of the beam to lessen the negating effects of diffraction and interference of the accelerated electrons. Micrographs were recorded as tagged information files (*.tif) and later printed on to Hewlett Packard (Premium Glossy Photographic Paper with a Hewlett Packard 1120C Professional Series printer) (Turner, 2003).

4.2.2. TRANSMISSION ELECTRON MICROSCOPY (TEM)

Samples were fixed in 2.5% buffered gluteraldehyde and then cut in cubes of 1 mm³ before placed in 1% O_sO₄ for contrasting. The tissues were then rinsed in buffer for 15 minutes. Specimens were dehydrated through the following ethanol series:

- 50% Ethanol – 15 minutes
- 70% Ethanol – 15 minutes
- 80% Ethanol – 15 minutes
- 90% Ethanol – 15 minutes
- 96% Ethanol – 15 minutes
- 100% Ethanol – 15 minutes (X2)

The specimens were placed in 1:1 mixture of propylene oxide: resin overnight for infiltration. The next morning the specimens were placed in 1:3 mixture of propylene oxide and resin for 2 hours. The specimens were then placed in fresh 100% resin under vacuum for 2 hours. The procedure was followed by embedding specimens in

fresh resin. The specimens were then placed in an embedding oven at 70 °C for curing. Specimens were sectioned for thin sections of approximately 1µm thickness, then placed on glass slides, stained with 1% toluidene blue and viewed by a light microscope. Area for thin sectioning was selected and trimmed to appropriate size. Gold sections (70 nm) were placed on copper grids and left to dry. Grids were contrasted or stained using heavy metal stains e.g. lead citrate and uranyl acetate. Grids were viewed by means of a Jeol JEM1010 (Jeol Inc., Tokyo) transmission electron microscope (TEM). Selected areas were photographed and micrographs printed for examination.

4. 3. RESULTS

The results observed in this investigation showed the fine structure of the three regions of the epididymis of the vervet monkey. The distribution of different cells in specific regions was also investigated.

4.3.1. Ultrastructure of the epididymal duct of the vervet

The SEM micrograph of the caput epididymis shows features of a distinct coiled tube with different lumen sizes (Figure 4.1). From this micrograph it will be difficult to distinguish different cell types found in the layers of the epididymal tubules. Figure 4. 2 shows basal cells which are found on the thick basement membrane. The principal cells with microvilli are also observed. Sperm tails are observed in the lumen of the epididymal tube.

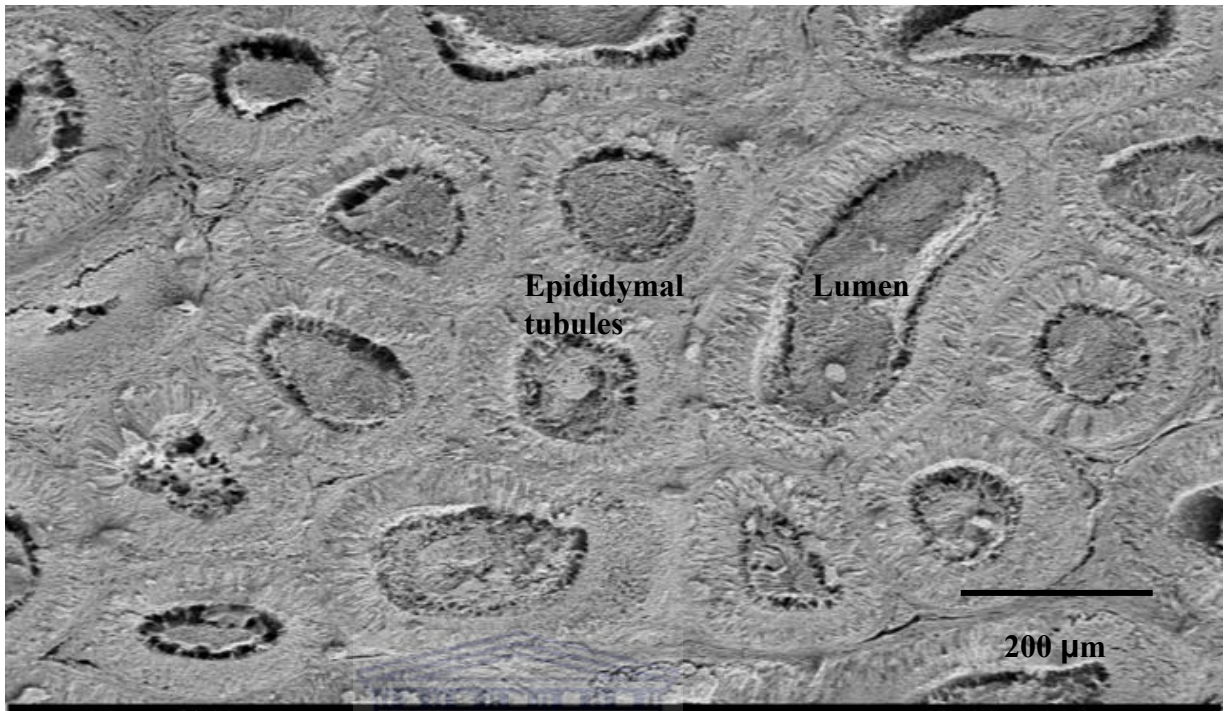


Figure 4. 1. SEM micrograph showing the general lay-out of the caput epididymis of the vervet monkey, *Chlorocebus aethiops*.

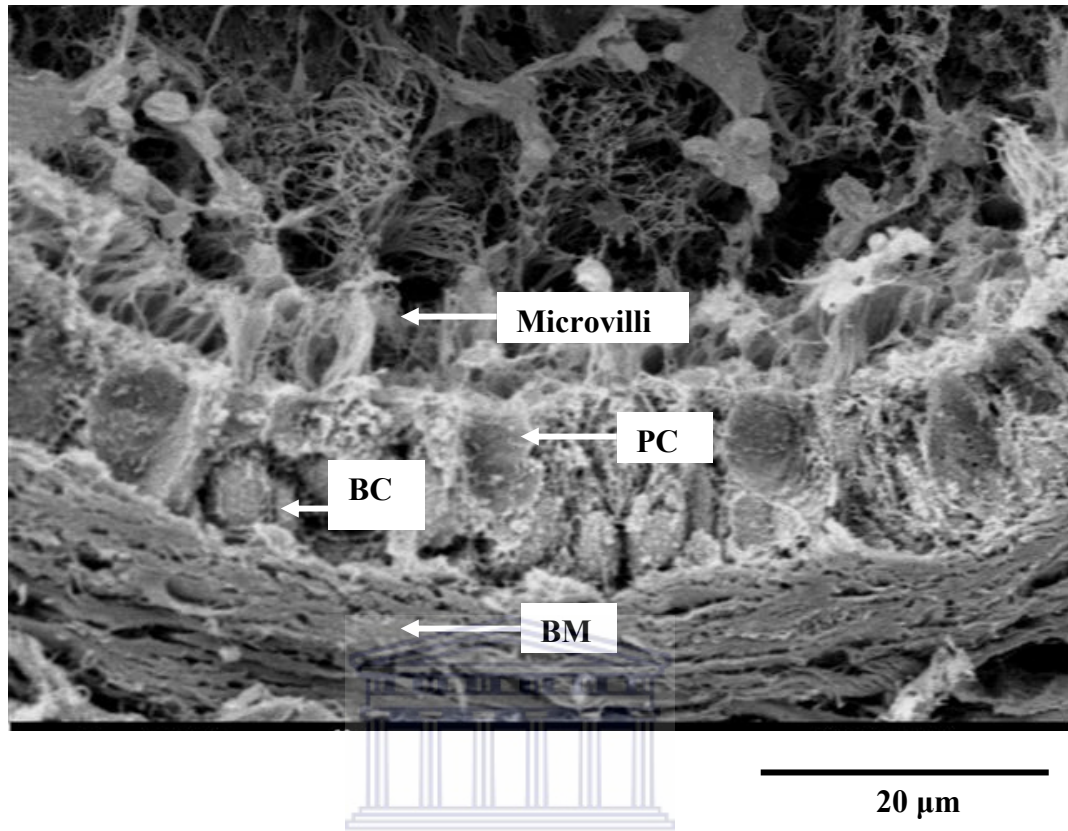


Figure 4. 2. SEM micrograph showing the microvilli in the caput region of the epididymis of the vervet monkey, *Chlorocebus aethiops*.

BC - Basal cell, PC - Principal cell, BM - Basement membrane.

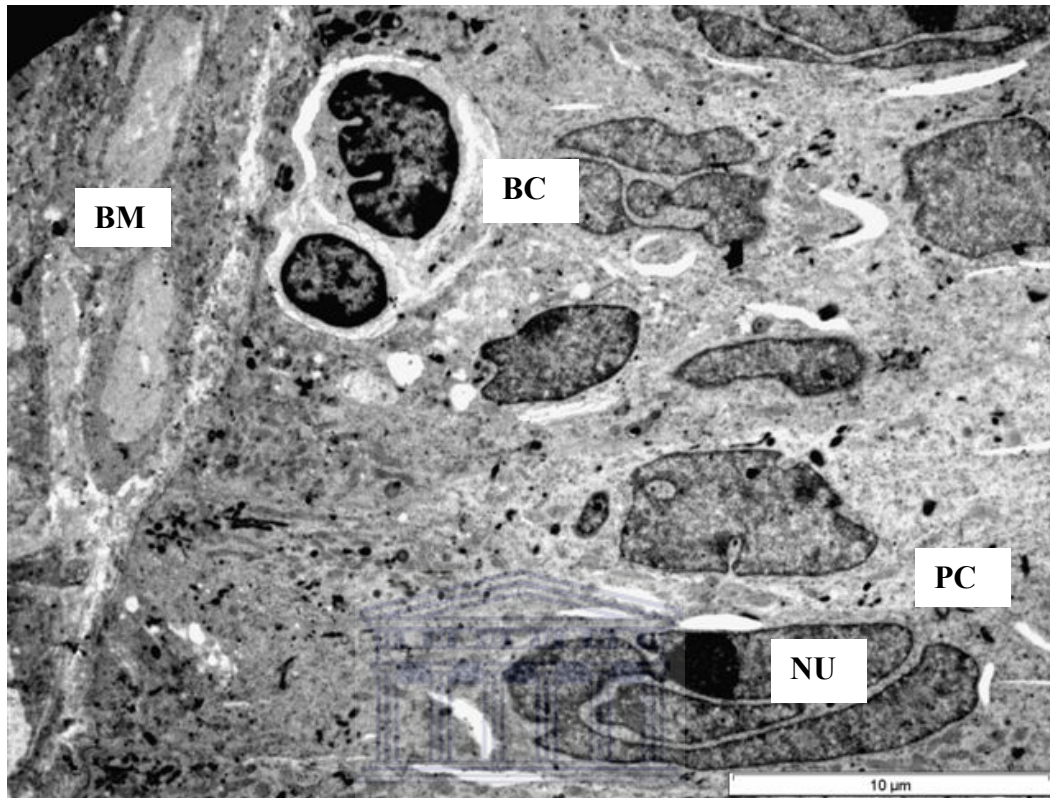


Figure 4. 3. TEM micrograph showing the basal cells of the corpus epididymis of the vervet monkey, *Chlorocebus aethiops*.

BC - Basal cell, BM - Basement Membrane, Nu - Nucleus, and PC - Principal cell.

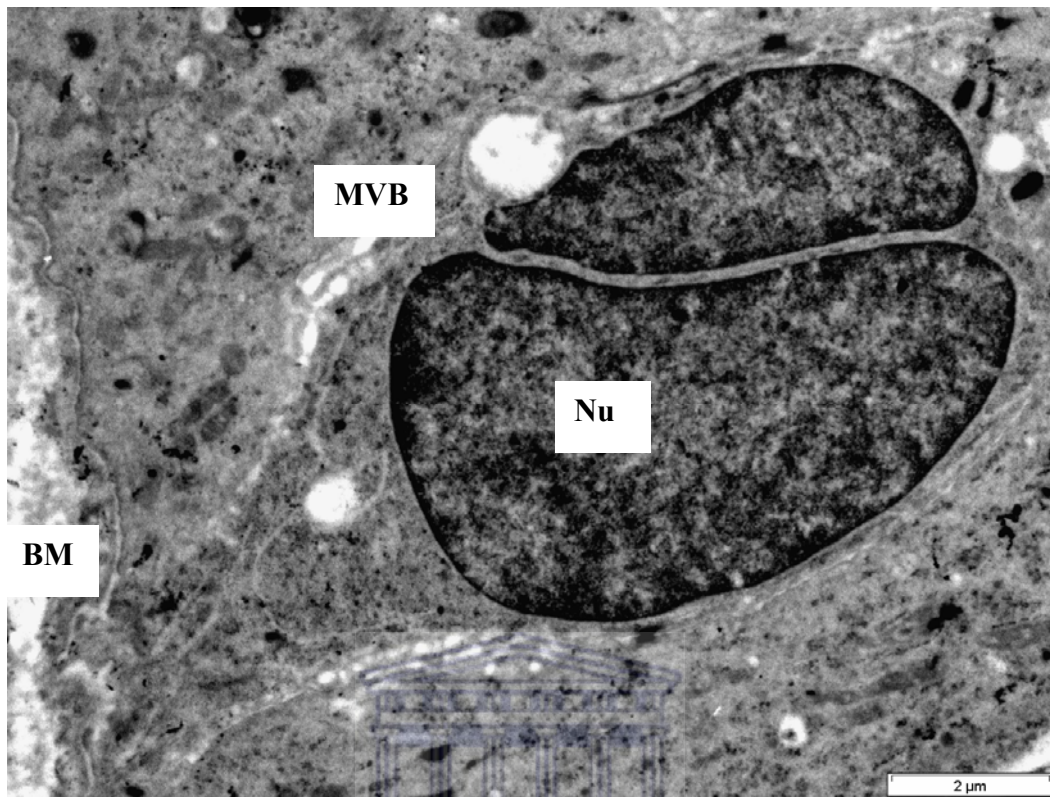


Figure 4. 4. TEM micrograph showing the basal cell of the corpus epididymis of the vervet monkey, *Chlorocebus aethiops*.

BM - Basement Membrane, MVB – Multivesicular body, and Nu - Nucleus.

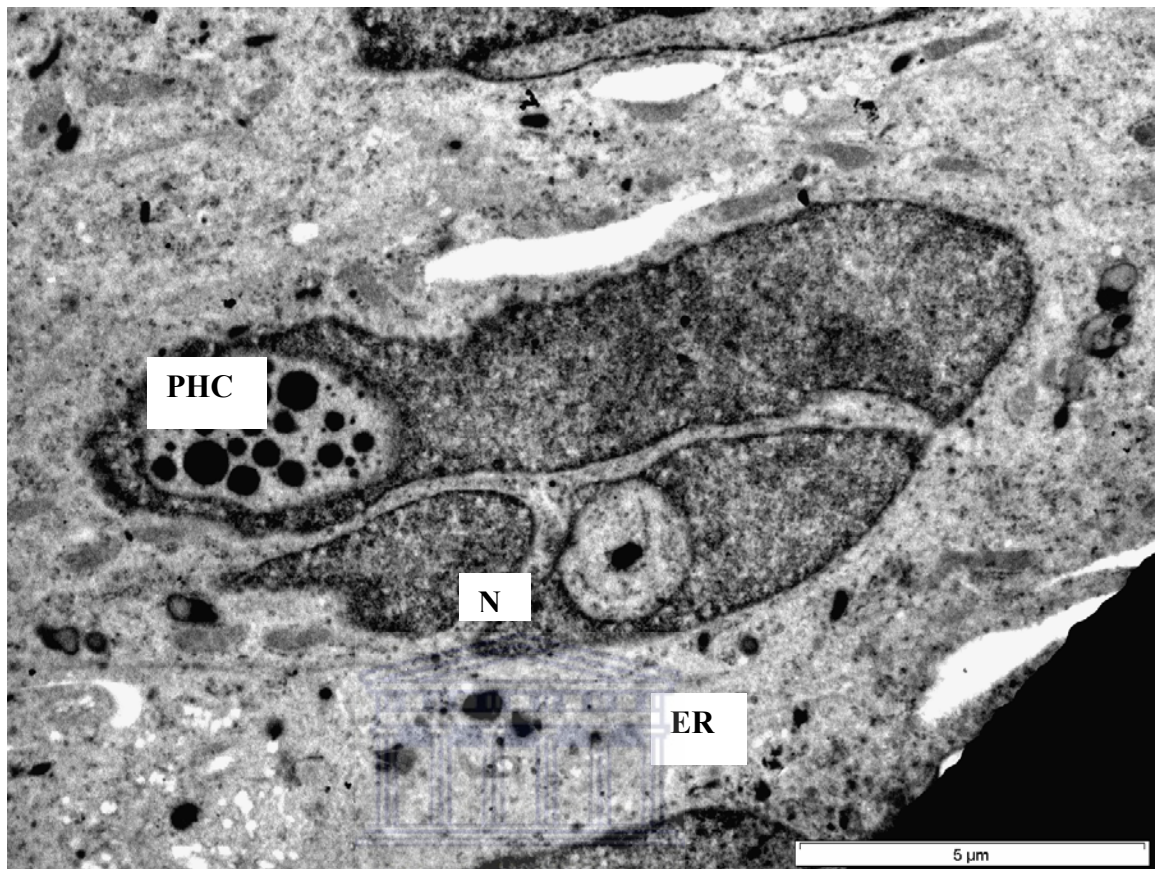


Figure 4. 5. TEM micrograph showing the principal cell of the corpus epididymis of the vervet monkey, *Chlorocebus aethiops*.

ER – Endoplasmic reticulum, N - Nucleus, and PHC - Phagocytic vesicle.

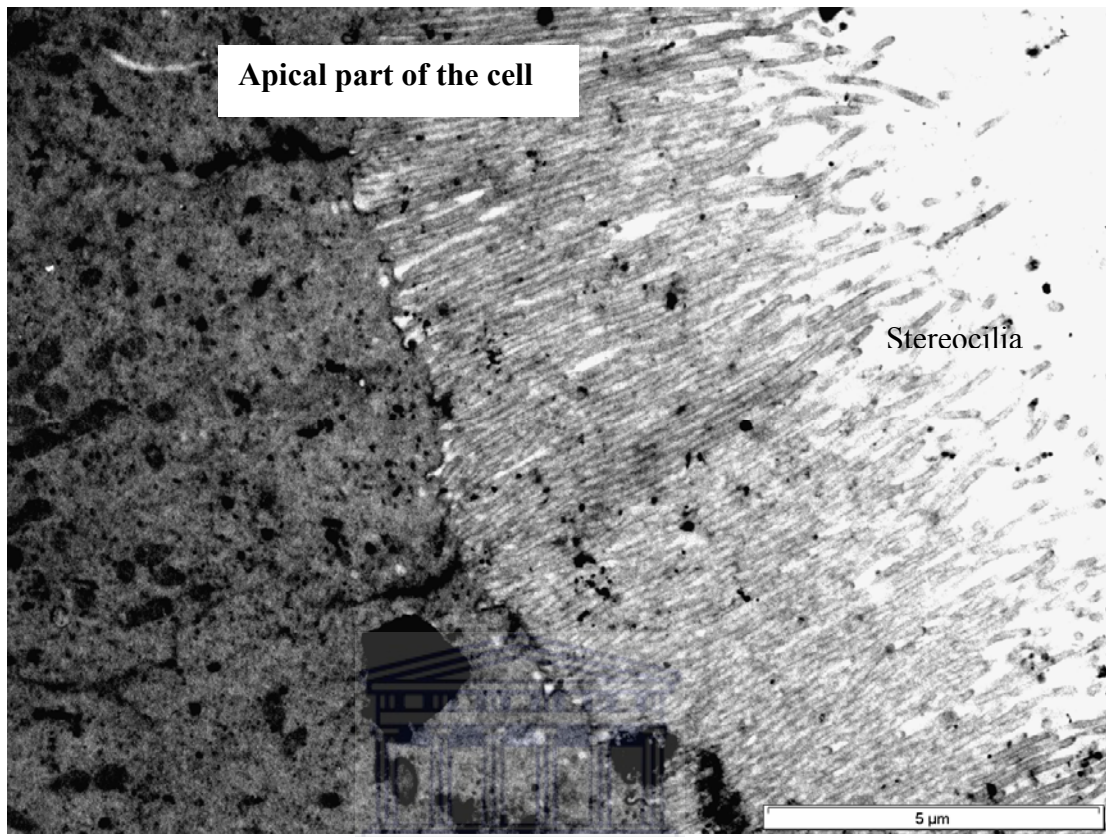


Figure 4. 6. TEM micrograph showing the microvilli of the principal cells in the corpus region of the epididymis of the vervet monkey, *Chlorocebus aethiops*.

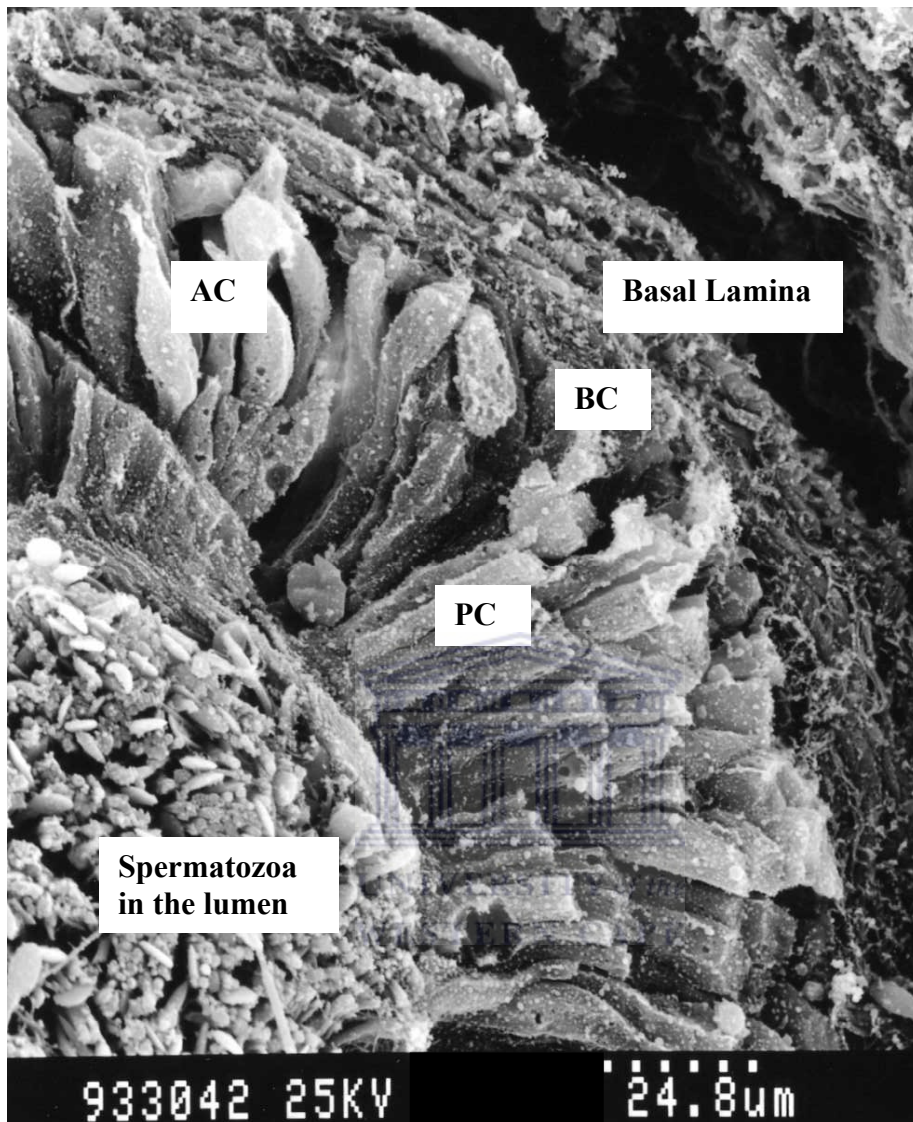


Figure 4. 7. SEM micrograph showing the corpus epididymis of the vervet mokey, *Chorocebus aethiops*.

AC - Apical cell, BC – Basal cell, PC – Principal cell

4.3.1.1. Principal cells

These are tall columnar cells which extend from the basal lamina to the lumen. The lateral cell membranes are relatively straight in the apical two-thirds of the cell but exhibit infoldings and interdigitations in the lower regions. The adjacent cells are held together by numerous desmosomes and present well developed junctions. Several smooth surfaced vesicles are present in the vicinity of caveolae (Figures 4.2; 4.3; 4.5; 4.7). The nucleus, which is multi-lobed and show variations in its infoldings in different segments of the epididymis, is oval, elongated and is oriented along the long axis of the cell. In general, the nuclei possess more euchromatin with prominent nucleoli located at the periphery (Figures 4.3; 4.8; 4.9; 4.10).

The cytoplasm is characterized by a well developed system of vesicular and tubular rough and smooth endoplasmic reticulum, Golgi complexes and dense granules. The multivesicular bodies are very conspicuous, especially in the corpus region of the epididymis (Figure 4.4). The localization of different organelles is similar in the principal cells in different segments but their relative amount varies from one region to another.

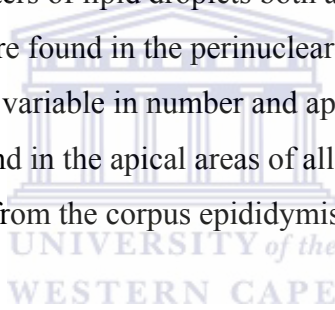
Mitochondria of varying sizes and shapes are seen scattered throughout the cytoplasm. Numerous membrane-bound dense granules also tend to concentrate in the cytoplasm. In places tubular profiles of endoplasmic reticulum are seen in continuation with the dense granules (Figure 4.5).

In the caput regions the luminal surface of the principal cells exhibited the presence of numerous microvilli which were long, finger-like cytoplasmic projections and are arranged irregularly (Figure 4.2 and 4.6). Their sizes and shapes show variations in different regions of the epididymal duct membrane bound vesicles. These membrane bound vesicles are usually located in between the microvilli as well as adjacent to the apical membrane of the principal cells. The luminal surface of the principal cells display irregular contours, presence of numerous coated deep pit-like invaginations or caveolae, vesicles in different stages of formation and vacuoles of various sizes are conspicuous features in the caput and

corpus segments of the epididymis (Figures 4.3; 4.5). The appearance of these features in a sequential order from the luminal surface through the apical cytoplasm was suggestive of occurrence of endocytosis in these cells. The apical pole of the principal cells is characterized by one or occasionally two multivesicular bodies. Infoldings are clearly visible on the nuclear membrane of the nuclei of the principal cells. Phagocytic vesicles are conspicuous throughout the length of the epididymis. The greatest concentration of vesicles is in the perinuclear region of principal cells, although some vesicles are associated with the apical region and Golgi complex (Figures 4.3; 4.5). In the subnuclear region, small irregularly shaped, electron-dense vesicles usually are present (Figure 4.8).

The perinuclear region of the principal cells is distinctive in that it contained grape-like clusters of lipid droplets both above and below the nucleus (Figure 4.11). Vesicles are found in the perinuclear region of principal cells of the corpus and are extremely variable in number and appearance.

Stereocilia are found in the apical areas of all sections of the epididymis. In this study, the stereocilia from the corpus epididymis was investigated (Figure 4.6).



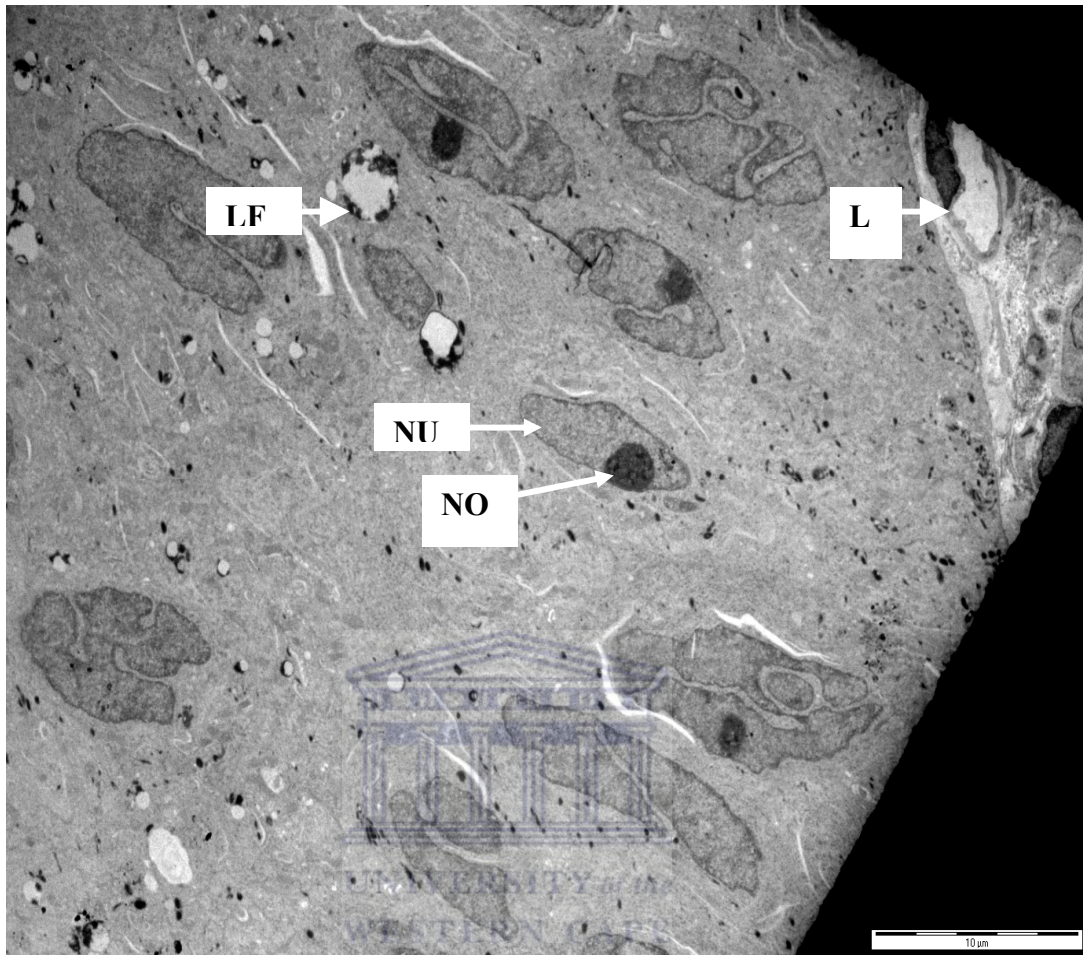


Figure 4. 8. TEM micrograph showing the principal cells of the cauda epididymis of the vervet monkey, *Chlorocebus aethiops*

L - Lysosome, LF - Lipofuscin, NU - Nucleus, and NO - Nucleolus.

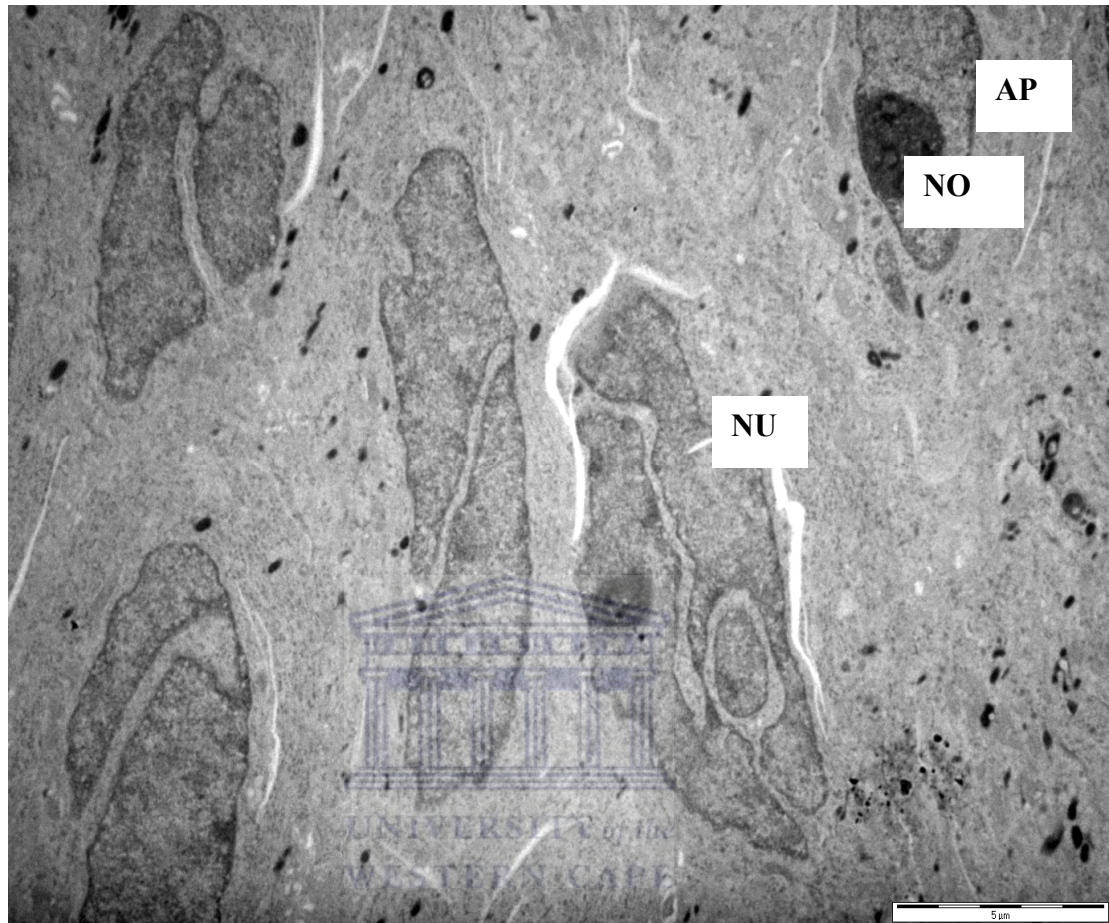


Figure 4. 9. TEM micrograph showing the principal cells of the cauda epididymis of the vervet monkey, *Chlorocebus aethiops*.

AP - Apical cell, NO - Nucleolus, and NU - Nucleus,

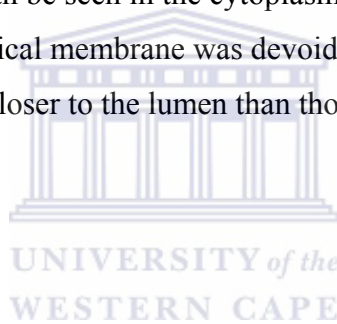
4.3.1.2. Basal cells

These cells are found close to the basement membrane of the epididymal epithelium, and in between the basal parts of the principal cells. The nuclei of these cells are ovoid or round in shape, with or without deep indentation or lobed and occupy a major portion of the cell (Figure 4.4). Heterochromatin regions are more prominent towards the periphery of the nuclear membrane, though a few patches are also scattered throughout the karyoplasm. The cytoplasm of these cells is poorly

developed and the organelles are scarce. Only a few mitochondria, profiles of endoplasmic reticulum and numerous free ribosomes are evident in the cytoplasm. Occasionally, lipofuscin-like pigment and electron dense bodies are also observed (Figure 4.8).

4.3.1.3. Apical cells

The cytoplasm of the apical cells extends right from the basement membrane to the lumen. It is wide towards the apex, sometimes projecting into the lumen. The nuclei of these cells are round or oval in shape and are situated towards the apex. The heterochromatin is patchy and tends to aggregate near the nuclear membrane. Other organelles are poorly developed. Lipid droplets and lamellar profiles of rough endoplasmic reticulum can be seen in the cytoplasm. The most prominent feature of these cells is that their apical membrane was devoid of microvilli. Apical cells have spherical nuclei located closer to the lumen than those of the principal cells (Figure 4.9).



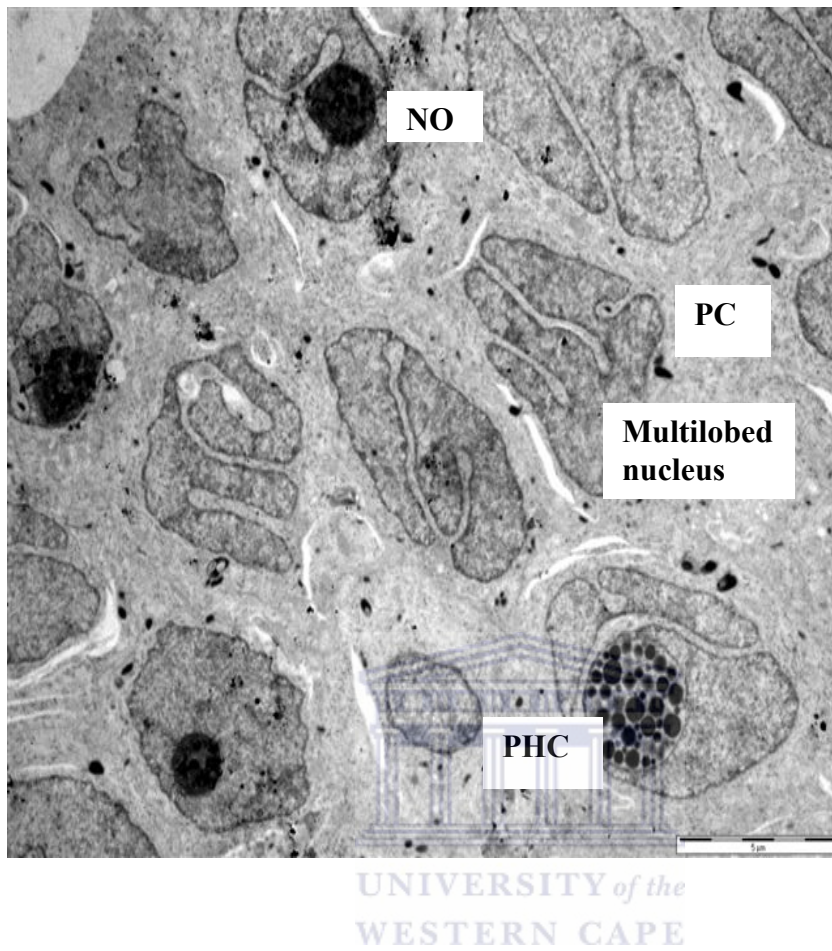


Figure 4. 10. TEM micrograph showing the principal cells of the cauda epididymis of the vervet monkey, *Chlorocebus aethiops*.

NO - Nucleolus, PC - Principal cell, PHC - Phagocytic vesicle.

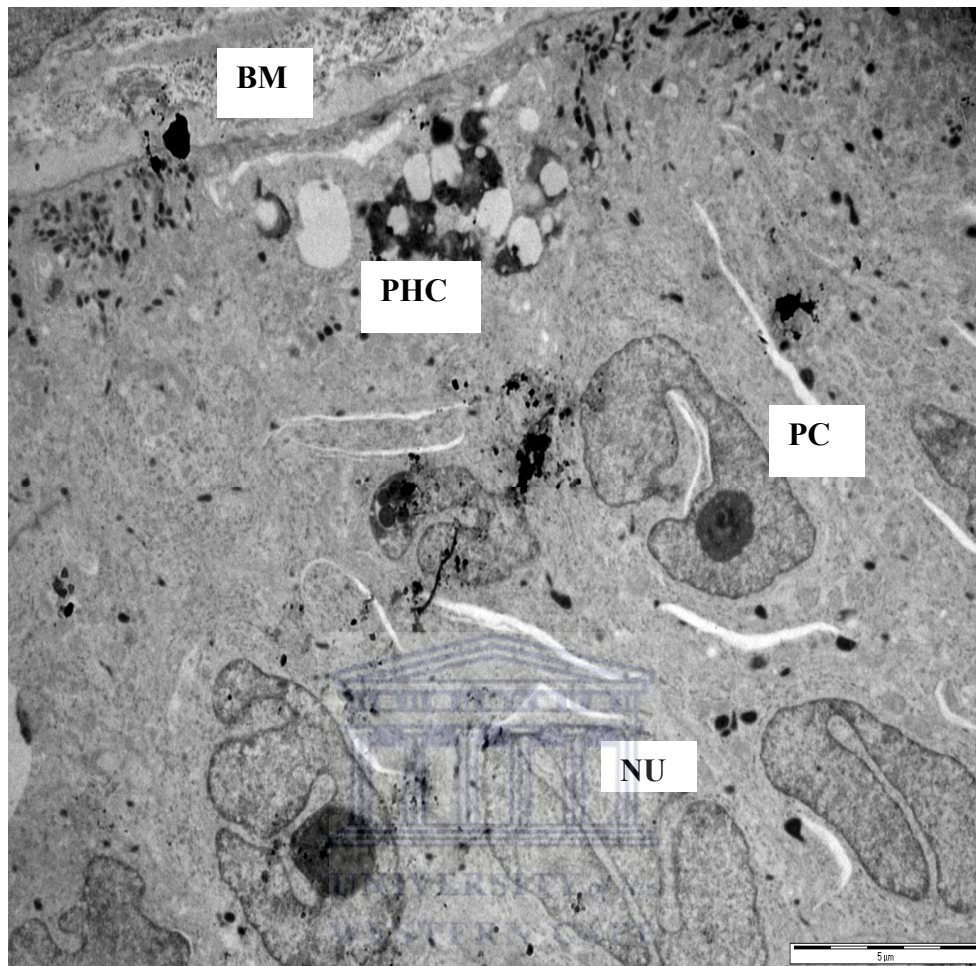


Figure 4. 11. TEM micrograph showing the principal cells of the cauda epididymis of the vervet monkey, *Chlorocebus aethiops*.

BM - Basement membrane, NU – Nucleus of principal cell lobed, PC - Principal cell, PHC - Phagocytic vesicle.

4.3.1.4. Intraepithelial Lymphocytes

A few intraepithelial lymphocytes are observed at different segments along the epithelium, and they possess densely heterochromatic nuclei, large mitochondria, and scattered endoplasmic reticulum (Figure 4.5). The cells are characterized by irregular shape as a result of irregular structures which are labeled as pseudopodia by Aruldas *et al.*, (2006). Neither basal cells nor intraepithelial macrophages contain lipofuscin material.

4. 4. DISCUSSION

Principal cells of the epididymal epithelium are rich in organelles that are responsible for secretion, synthesis and absorption, whereas basal cells are often described as cells abutting the basal lamina that have little cytoplasm and sparse organelles (Yeung *et al.*, 1994). The human basal cells of the epididymal epithelium appeared to be mostly round and oval, to be approximately 12µm across, and almost completely line the basal membrane. Yeung *et al.*, (1994), also reported that a large area of the cell was occupied by the nucleus, which in contrast to the oblong euchromatic nucleus of the principal cell, was round and slightly heterochromatic. The mitochondria found in the basal cells of the human epididymis showed a large diameter and more circular cross-sections. The endoplasmic reticulum, lysosomes, microfilament bundles and endocytic vesicles were also observed. The Golgi apparatus was seldom seen. The ultrastructure also revealed peritubular macrophages which were similar to basal cells in the appearance of their nucleus, cytoplasmic organelles and processes, dense bodies and lipofuscin inclusions. Lipid-like droplets in basal cells have been described as a common feature in human epididymis (Yeung *et al.*, 1994).

Lysosomes are known to contain an array of hydrolytic enzymes which are primarily concerned with the digestion of cell nutrients, cell protein turnover, tissue remodeling, lysis of foreign particles, and autolysis of cells. Presumably, the high lysosomal turnover is required for digestion of materials which are being endocytosed by the principal cells. It is pertinent to note that the receptor-ligand complexes accumulated in the coated pits are transported within membrane bound compartments to lysosomes, wherein they are degraded (Bajpai *et al.*, 1985).

The principal cells accounted for about 70% of the epithelial cells whereas basal cells and apical cells constituted 25% and 1% respectively in all the regions studied. This concurred with the study carried out by Marengo and Amann (1990) on the ovine epididymis. The same observations were reported by Bajpai *et al.*, (1985), in their study on the rhesus monkey. Bajpai *et al.*, (1985) further reported that principal cells are the predominant type throughout the length of the epididymal duct

and it is the variations in their height that create regional differences in the gross morphology of the epithelium. The same arrangement was observed in the vervet monkey. White blood cells accounted for approximately 2% of all the cells regardless of the region.

It has been reported that the principal cells are capable of phagocytosing dead spermatozoa (Sutovsky *et al.*, 2001). The digestion of the spermatozoa acquired into the principal cytoplasm is incomplete and results in lipofuscin material. Because the principal cells do not possess the mechanism to process the huge quantity of lipofuscin material, the latter is discharged into the intercellular spaces to be acquired by the basal cells and the intraepithelial macrophages (Aruldas *et al.*, 2006).

There was a high density of lipid droplets located perinuclearly in the corpus region of the vervet monkey. The same observation was made by Wagley, *et al.*, (1984) in ram epididymis. The epididymis is apparently involved in secretion of lipids, including glycerylphosphoryl choline (Crabo, 1965; Amann, 1987). Apparently, the epididymis synthesizes glycerylphosphoryl choline from phosphatidyl choline derived from blood lipoproteins (Hammerstedt and Rowan, 1982; Cooper, 1986). The aggregates of lipids reflect uptake and synthesis of lipid secreted into the lumen, or elimination of lipid available as a result of the remodeling of sperm membranes and removal from the luminal fluid (Parks and Hammerstedt, 1985).

The present ultrastructural study on the principal cells demonstrated the extensive absorptive function in the caput and the corpus regions, the latter being the more active. The characteristic features that support their absorptive function include presence of long microvilli, numerous coated pit-like invaginations on the luminal surface, various stages of endocytotic vesicles in the cytoplasm and abundance of multivesicular bodies in the supranuclear and Golgi regions of the cytoplasm (Bajpai *et al.*, 1985).

One of the most striking observations made was the presence of caveolae at the basal plasmalemma of the principal cells, which lie closely apposed to the subepithelial stroma and capillaries. This may be indicative of an intracellular

transepithelial transport of macromolecules from the stroma into the lumen of the duct. This mode of transport is likely to occur due to the presence of well-developed tight junctions which suggests the existence of a blood epididymis barrier (Bajpai *et al.*, 1985).

The presence of numerous membrane bound dense bodies and multivesicular bodies (MVBs) indicates a higher lysosomal turnover in the principal cells as observed by Bajpai *et al.*, (1985). Lysosomes are known to contain an array of hydrolytic enzymes which are primarily concerned with the digestion of cell nutrients, cell protein turnover, tissue remodeling, lysis of foreign particles, and autolysis of cells (Bajpai *et al.*, 1985). The presence of visible phagosomes throughout the epididymal epithelium indicated that phagocytosis was taking place. In vervet monkey the phagosomes were observed in the caudal region of the epididymis.

The basal cells were located on top of the basal lamina in such a way that the epithelium appeared pseudostratified. This arrangement was also observed by Aruldas *et al.*, (2006), in bonnet monkeys (*Macaca radiata*), and in this study. Irrespective of the segments, that is, caput, corpus, or caudal regions, the epididymal epithelium possessed very few basal cells and intraepithelial macrophages. The same distribution amongst regions was also observed by Aruldas *et al.*, (2006) in bonnet monkeys. This is in contrast to the distribution of basal cells in the gerbil, where these cells were predominantly observed in the proximal regions of the epididymis (Domeniconi *et al.*, 2007) and had been considered to be stabilizing elements of the epididymal epithelium structure (Hamilton 1975).

The basal cells had the characteristic arrangement abutting the basal lamina and possessed heterochromatic round or irregular nuclei occupying almost the entire cell, leaving only little cytoplasm around it. The cytoplasm consisted of few organelles such as mitochondria, endoplasmic reticulum, lysosomes, and endocytic vesicles. These features were also observed by Aruldas *et al.*, (2006). Both the intraepithelial macrophages appeared to acquire the lipofuscin material from the principal cells, produced as a result or partial digestion of spermatozoa, which were

phagocytosed through apical plasma membrane in the bonnet monkey (Aruldas *et al.*, 2006).

The basal cells are the second largest population of epithelial cell type that is common to all segments of the epididymis after the principal cells (Yeung *et al.*, 1994). Consistently found in the epididymal epithelium of different mammalian species, the basal cells are established only after the other cell types (Seiler *et al.*, 1998). The basal cells have been shown to express macrophage antigens in humans (Yeung *et al.*, 1994) and in monkey and mouse (Seiler *et al.*, 1998; Seiler *et al.*, 2000), suggesting that the basal cells may be derived from the monocytes, which arrive at the epididymal epithelium for transformation into macrophages. The ultrastructural similarities between basal cells and interstitial macrophages also support that suggestion (Yeung *et al.*, 1994). The relative abundance of lipofuscin material in the basal cells is a reflection of the extent of scavenging of sperm antigens (Aruldas *et al.*, 2006).

These basal cells could have been monocytes recruited from the blood that aerates the epididymis (Holschbach and Cooper, 2002). Furthermore, basal cells in the human epididymal epithelium stained with a monoclonal antibody against macrophages, suggesting that basal cells might phagocytose sperm antigens and subsequently leave the epithelium to be replenished by macrophages from the peritubular tissue (Yeung *et al.*, 1994).

Leung *et al.*, (2004) reported that the basal cells play an active role by serving as humoral regulators of electrolytes and water transport across the epithelium. They are thus integral to the formation of the epididymal fluid.

Apical cells were richly supplied with mitochondria. These cells are involved with the transport system mechanisms of the epithelia. Apical cells are few in number and their luminal surface is free of stereocilia in rhesus monkey (Bajpai *et al.*, 1985). Brown and Montesano (1980) indicated that cells in the initial segment, presumed to be narrow cells or apical cells, as there is no distinction between the two types of cells (Adamali and Hermo, 1996), have been shown by histochemical studies to contain carbonic anhydrase. Furthermore, freeze-fracture analysis of the apical

plasma membrane of these cells revealed elongated intramembranous particles. Brown and Montesano (1980) concluded that the apical cells could be involved in the transport of fluid and electrolytes in the proximal region of the epididymis.

The distribution of lymphocytes was not constant within a given epididymal region or within a given tubule cross-section and were difficult to identify. All regions show the white blood cells, however they accounted for approximately 2% of all the cells regardless of the region, which is similar to the 5% found in the rat epididymis. T lymphocytes detected by immunocytochemistry in the rat epithelium may correspond to halo cells (Flickinger *et al.*, 1997). Ramos and Dym, (1977a), reported that the ductuli efferentes in monkeys consisted primarily of ciliated and nonciliated cells and occasionally basal cells, macrophages and intraepithelial lymphocytes. In this study numerous phagocytic vesicles were identified in almost all the regions of the epididymis. This will explain the immunological function of the epididymis in protecting the spermatozoa as they go through this structure.

Table 4.1 shows some similarities between the vervet monkey and human epididymis in terms of their appearance, structure and functions. Despite many similarities in terms of cell types between the vervet monkey and humans, there are also distinct differences. The main differences being that the caput region is well defined in vervets and apparently not well defined in humans (Table 4.1).

Cells of the immune system have been detected in the epididymal epithelium as well as in the interstitial connective tissue surrounding the duct (Flickinger *et al.*, 1997). Light microscopic studies revealed that the normal epididymal epithelium contains small round cells, with dense nuclei and pale cytoplasm, which were referred to as halo cells and were considered to be lymphocytes, agranular leukocytes or monocytes. Both lymphocytes and macrophages were identified on the basis of ultrastructural characteristics in the epithelium of the human epididymis rather than in the more proximal parts (Hamilton, 1972; Dym and Romrell, 1975; Wang and Holstein, 1983; Robaire and Hermo, 1988).

Table 4. 1. Comparisons of the vervet monkey, humans, and other mammals on the selected features of the epididymis.

Feature	Vervet	Humans	Other Mammals	References (if necessary)
Caput epididymis	Well defined	Not well defined	Well defined	Yeung <i>et al.</i> , (1991)
Cauda epididymis	Less bulbous	Not bulbous	Bulbous	Yeung <i>et al.</i> , (1991)
Phagocytosis	+	+	+	

+ - Present

4.5. CONCLUSIONS

The ultrastructure of the epididymis seems to be similar in rats, humans, and other primates. Epididymal function is not only confined to maturation, but also plays an important role in the protection of the reproductive tract. Numerous phagocytic vesicles were found along the length of the epididymis. Future investigations should look into the specific regions of the epididymis where phagocytosis takes place and its mechanisms. The ultrastructure of the epididymis epithelium in mammals reflected the main functions exerted by epithelial cells inside the epididymal luminal compartment (Robaire and Hermo, 1988; Arrighi *et al.*, 1993), especially concerning the ultrastructural features of the principal cells.

Thus it is essential to evaluate both the quantitative and qualitative aspects of ultrastructure to critically evaluate morphological features of epididymal cells for interpretation of cellular function.

4. 6. REFERENCES

- Adamali, H. I. and Herno, L. 1996. Apical and narrow cells are distinct cell types differing in their structure, distribution, and functions in the adult rat epididymis. *J. Androl.* **17**:208- 222.
- Amann, R. P. 1987. Function of the epididymis in bulls and rams. *J. Reprod. Fertil.* (Suppl.) **34**:115-131.
- Alsum, D. J. and Hunter, A. G. 1978. Regional histology and histochemistry of the ductus epididymis in the rhesus monkey (*Macaca mulatta*). *Biol. Reprod.* **19**:1063-1069.
- Aruldhas, M. M., Subramanian S., Sekhar, P., Vengatesh, G., Govindarajulu, P. and Akbarsha, M. A. 2006. In *vivo* spermatotoxic effect of chromium as reflected in the epididymal epithelial principal cells, basal cells, and intraepithelial macrophages of a nonhuman primate (*Macaca radiata*, Geoffroy). *Fertil. Steril.* **86**:1097-1105.
- Arrighi, S., Romanello, M. G. and Domeneghini, C. 1993. Ultrastructure of epididymal epithelium in *Equus caballus*. *Ann. Anat.* **175**:1-9.
- Bajpai, V. K., Shipstone, A. C., Ratna Kumar, B. V., Qaisar, J. and Setty, B. S. 1985. Ultrastructure of the epididymal epithelium of Rhesus monkey (*Macaca mulatta*). *Acta Euro. Fertil.* **61**:207-217.
- Brown, D. and Montesano, R. 1980. Membrane specialization in the rat epididymis. I. Rod-shaped intramembrane particles in the apical (mitochondria-rich) cell. *J. Cell Sci.* **45**:187-198.

Cooper, T. G. 1986. The Epididymis, Sperm Maturation, and Fertilization. Springer Verlag. New York. pp 117-230.

Cooper, T. G. 1993. The human epididymis-Is it necessary? *Int. J. Androl.* **16**:245-300.

Cooper, T. G. 1998. Epididymis. In: Encyclopedia of Reproduction. (ed. N. J. Knobil). Academic Press. San Diego. pp 1-17.

Crabo, B. 1965. Studies on the composition of epididymal content in bulls and boars. *Acta Vet. Scand.* (Suppl) **5**: 1-94.

Domeniconi, R. F., Orsi, A. M., Beu, C. C. L. and Felisbino, S. L. 2007. Morphological features of the epididymal epithelium of gerbil, *Meriones unguiculatus*. *Tissue. Cell.* doi:10.1016/j.tice.2007.01.002 (in press).

Dym, M. 1983. The male reproductive system. In: Histology: Cell and Tissue Biology. 5th Ed. (ed. L. Weiss). Macmillan Press. New York. pp 1000-1053.

Dym, M. and Romrell, L. J. 1975. Intraepithelial lymphocytes in the male reproductive tract of rats and rhesus monkey. *J. Reprod. Fertil.* **42**:1-7.

Flechon, J. E., Bustos-Obregon, E., Steger, R. W. and Hafez, E. S. 1976. Ultrastructure of the testes and excurrent ducts in the bonnet monkey (*Macaca radiata*). *J. Med. Primatol.* **5**:321-335.

Flickinger, C. J., Bush, L. A., Howards, S. S. and Herr, J. C. 1997. Distribution of leukocytes in the epithelium and interstitium of four regions of the Lewis rat epididymis. *Anat. Rec.* **248**:380-390.

Hamilton, D. W. 1972. The mammalian epididymis. In: Reproductive Biology. (eds. H. Balin and S. Glasner) Excerpta Media. Amsterdam. pp 268-337.

Hamilton, D. W. 1975. Structure and function of the epithelium lining the ductuli efferentes, ductus epididymidis, and ductus deferens in the rat. In: (Eds. Greep, R. O. Astwood, E. B. Handbook of Physiology. Sect. 7. Endocrinology, Male Reproductive System. American Physiology Society. 5. pp 259-301.

Hammerstedt, R. H. and Rowan, J. E. 1982. Phosphaditylcholine of blood lipoproteins is the precursor of glycerylphosphorylcholine found in seminal plasma. *Biochim Biophys Acta* **710**:370-406.

Hermo, R., Oko, R. and Morales, C. R. 1994. Secretion and endocytosis in the male reproductive tract: a role in sperm maturation. *Int. Rev. Cytol.* **154**:106-189.

Hoffer, A. P. 1976. The ultrastructure of the ductus deferens in man. *Biol. Reprod.* **14**:425-443.

Holschbach, C. and Cooper, T. G. 2002. A possible extratubular origin of epididymal basal cells in mice. *Reproduction* **123**:517-525.

Leung, G. P. H., Cheung, K. H., Leung, C. T., Tsang, M. W. and Wong, P. Y. D. 2004. Regulation of epididymal principal cell functions by basal cells: Role of transient receptor potential (Trp) proteins and cyclooxygenase-1 (COX-1). *Mol. Cell. Endocrinol.* **216**:5-13.

Marengo, S. R. and Amann, R. P. 1990. Morphological features of principal cells in the ovine epididymis: a quantitative and qualitative study. *Biol. Reprod.* **42**:167-179.

Marquis, N. R., and Fritz, I. B. 1965. Effects of testosterone on the distribution of carnitine, acetylcarnitine and carnitine acetyltransferase in tissue of the reproductive system of the male rat. *J. Biol. Chem.* **240**:2197-2200.

Parks, J. E. and Hammerstedt, R. H. 1985. Developmental changes occurring in the lipids of ram epididymal spermatozoa plasma membrane. *Biol. Reprod.* **32**:653-668.

Ramos, A. S. and Dym, M. 1977a. Ultrastructure of the ductuli efferentes in monkeys. *Biol. Reprod.* **17**:339-349.

Ramos, A. S. and Dym, M. 1977b. Fine structure of the monkey epididymis. *Am. J. Anat.* **149**:501-532.

Robaire, B. and Hermo, L. 1988. Efferent ducts, epididymis and vas deferens: Structure, functions, and their regulation. In: *The Physiology of Reproduction* (Eds. Knobil, E. and Neill, J). Raven Press. New York. pp 999-1080.

Seiler, P., Wenzel, I., Wagenfeld, A., Yeung, C. H. and Nieschlag, E. 1998. The appearance of basal cells in the developing murine epididymis and their temporal expression of macrophage antigens. *Int. J. Androl.* **21**:217-226.

Seiler, P., Cooper, T. G. and Nieschlag, E. 2000. Sperm number and condition affect the number of basal cells and their expression of macrophage antigen in the murine epididymis. *Int. J. Androl.* **23**:65-76.

Sullivan, R., Saez, F., Girouard, J. and Frenette, G. 2005. Role of exosomes in sperm maturation during the transit along the male reproductive tract. *Blood Cells. Mol. Dis.* **35**:1-10.

Sutovsky, P. Moreno, R., Ramalho-Santos, J., Dominco, T., Thompson, W. E. and Schatten, G. 2001. A putative, ubiquitin-dependent mechanism for the recognition and elimination of defective spermatozoa in the mammalian epididymis. *J. Cell. Sci.* **114**:1665-1675.

Turner, M. L. 2003. The micromorphology of the blesbuck louse *Damalinia (Damalinia) crenelata* as observed under the scanning electron microscope. *Koedoe* **46**:65-71.

Wagley, L. M., Vershuis, T. D. Brown, D. V. and Amann, R. P. 1984. Culture of principal cells from the ram epididymis: a comparison of the morphology of principal cell in culture and in situ. *J. Androl.* **5**:389-408.

Wang, Y. F. and Holstein, A. F. 1983. Intraepithelial lymphocytes and macrophages in the human epididymis. *Cell Tissue Res.* **233**:517-521.

Yeung, C. H., Cooper, T. G., Bergmann, M. and Schulze, H. 1991. Organization of tubules in the human caput epididymis and the ultrastructure of their epithelia. *Am. J. Anat.* **191**:261-279.

Yeung, C. H., Nashan, D., C. Sorg, F. Oberpenning., H. Schulze., Nieschlag, E. and Cooper, T. G. 1994. Basal cells of the human epididymis—antigenic and ultrastructural similarities to tissue-fixed macrophages. *Biol. Reprod.* **50**:917-926.

CHAPTER 5: ULTRASTRUCTURE OF THE TESTES OF THE VERVET MONKEY, WITH SPECIAL REFERENCE TO THE NON-GERMINAL CELLS

5.1. INTRODUCTION

5.1.1. Ultrastructure of the testis

The mammalian testis consists of three major cell types, namely, Sertoli cells, Leydig cells, and germinal cells. The somatic cells of the testis are peritubular myoid cells, endothelial cells, and fibroblasts. Before sexual differentiation, primordial germ cells, which originate from the proximal epiblast, migrate from the base of the allantois *via* the gut mesentery and populate the genital ridge. These bipotential cells colonise the primitive undifferentiated gonads that are beginning to form and become gonocytes (Capel, 2000; de Rooij and Russell, 2000). The pre-Sertoli cell is the first somatic cell type to differentiate in the testis. The Sertoli cell presumably originates from the coelomic epithelium and its precursors are thought to express the male sex determining gene SRY in the short arm of the Y chromosome (Karl and Capel, 1998). Previously, Sertoli cells have been proposed to arise from the mesonephros, the coelomic epithelium, or both (Byskov, 1986). Sertoli cells are thought to be present in the gonad itself by 11.5 days post coitum, since Müllerian Inhibiting Substance (MIS), a Sertoli cell-specific product, could be detected in the medium when 11.5 days post coitum gonads were cultured separate from the mesonephros (Merchant-Larios *et al.*, 1993). In this regard, Sertoli cells play a crucial role in directing testis differentiation, which occurs at 11.5 days of gestation in mice (Capel, 2000), and 27 days in pigs (Pelliniemi, 1975), and 56 days in humans (Pelliniemi *et al.*, 1993). Peritubular myoid cells and endothelial cells have been shown to arise from the mesonephros. The mesonephros is a mesenchymal tissue derived from the intermediate mesoderm (Buehr *et al.*, 1992).

It is well documented in the literature on mammals that FSH is the major hormone responsible for postnatal Sertoli cell proliferation (Orth, 1993; Heckert and Griswold, 2002), whereas thyroid hormone (T_3) is responsible for the change of these cells from mitotic to non-mitotic status that occurs before puberty (Cooke *et*

al., 1994; Franca *et al.*, 1995). Research showed that in rodents, proliferation of Sertoli cells starts after sex differentiation, decreasing steadily after birth. Sertoli cell mitosis in these species ceases completely approximately 2-3 weeks after birth (Vergouwen *et al.*, 1991; Joyce *et al.*, 1993; Orth, 1993). However, a different pattern of Sertoli cell proliferation after birth is observed in non-rodent species such as pigs and some primates, including man, in which puberty takes place several months or years after birth (Sharpe *et al.*, 2003). In general, in these species, Sertoli cells present two distinct and prominent mitotic phases; the first phase continues for a variable period of time after birth, depending on the species considered, and the second phase takes place just before puberty (Sharpe *et al.*, 2003).

The peritubular interstitium contains clusters of Leydig cells that possess LH receptors and are the primary sites of synthesis of androgenic steroid hormones, including testosterone (Russell *et al.*, 1990; Bloom and Fawcett, 1994). The seminiferous epithelium is composed of Sertoli cells and of germinal cells in various developmental steps from the most undifferentiated stem cell spermatogonia to structurally mature sperm newly released into the tubular lumen. Sertoli cells possess receptors for FSH and various androgens, including testosterone, and secrete regulatory substances, including estrogen, androgen-binding protein, inhibin, activin, mitogens, and transferrin that are essential for germ cell development (Russell *et al.*, 1990; Shupnik and Schreihof, 1997).

5.1.2. Ultrastructure of the Sertoli cell

The coelomic epithelium contributes to the Sertoli cell population in the mouse (Karl and Capel, 1998). However, they could rule out the possibility that the Sertoli cells could be derived from more than one region as previously reported. A dual Sertoli cell system has been proposed consisting of two types of Sertoli cells with different functions, one of which is to inhibit the germ cells in the male testis from undergoing meiosis (Wartenberg *et al.*, 1991).

Ramos and Dym (1979) showed that the cytoplasm of the Sertoli cells contains a large amount of smooth endoplasmic reticulum in addition to mitochondria

with tubular cristae, lipid droplets, lysosomes and other inclusion bodies. These cell organelles and inclusions also increase in number towards sexual maturity. These structural features of the mature Sertoli cell cytoplasm, particularly the smooth endoplasmic reticulum, are characteristics of a typical steroid producing cell. The presence of a large number of Golgi profiles within the Sertoli cell is suggestive of a secretory function and the coincidental appearance of a tubule lumen. The formation of junctional complexes during the rapid growth period of the rat testis correlates fully with the testicular fluid production by the Sertoli cells. In man, characteristic inclusion bodies of Charcot–Böttcher are found in the basal cytoplasm. They measure 10 - 25 μm long and 1 μm wide and are quite visible in routine histologic preparations (Ross *et al.*, 1995).

Sertoli cells themselves are known to change functionally and morphologically during the spermatogenic cycle. Alterations of Sertoli cell ultrastructure on mitochondria, microtubules, and Golgi apparatus have been described qualitatively and alterations on various organelles such as lipid droplets and lysosomes have been described quantitatively (Chen and Yates, 1975; Fawcett, 1975). Ultrastructural observations have also revealed regional relationships between the germ cells and the Sertoli cells, such as new formation of Sertoli cell–Sertoli junctional specialization below the leptotene spermatocytes along with upward movement of the spermatocytes, formation of spermatid-Sertoli tubulobulbar complexes as devices for elimination of cytoplasm from the head region of the late spermatids, evolution of the endoplasmic reticulum in the Sertoli cell cytoplasm encapsulating the head of late spermatids (residual body) during spermiation (Ueno and Mori, 1990).

Ueno and Mori (1990) also reported that cytoplasmic components of Sertoli cells varied in volume and surface densities during the seminiferous epithelial cycle. In their study, there was an increase in volume density of mitochondria in stages VII and VIII in rats. The increase in size of the mitochondria has generally been considered to represent an active state of cells. There is a general pattern that an increase in volume of mitochondria coincided with that of the endoplasmic reticulum.

It has been suggested that the mitochondria may have a facilitatory influence on the development of the rough endoplasmic reticulum. The increase in rough endoplasmic reticulum implied that the cell is involved in active protein synthesis (Ueno and Mori, 1990).

Parvinen (1982) observed that the secretion of androgen binding protein, plasminogen activator, and a meiosis inducing substance increased at stages VII and VIII. Again, this close association of mitochondria with rough endoplasmic reticulum may provide energy for the rough endoplasmic reticulum and facilitate the synthesis of these proteins.

The topographical change of the Golgi apparatus during the seminiferous epithelial cycle is not clearly elucidated. The organelle is usually localized in the basal cytoplasm, whereas it was found to be located predominantly in the middle and apical cytoplasm at stages VII and VIII. The Golgi apparatus appears to move upwards to meet the need for increased lysosomes and plasma membrane at stages VII and VIII. Kerr (1988) found that the surface area of the Golgi apparatus in a whole Sertoli cell does not change significantly during the cycle. Primary lysosomes change their volume during the cycle with an inverse increase and decrease in the basal cytoplasm relative to that in the middle and apical cytoplasm. In the basal cytoplasm, the first consecutive increase occurred in the primary lysosomes at stage IV and in the secondary lysosomes at stage VI. The secondary lysosomes that increased in clusters near the plasma membrane at stage VI, seemed to engage in the digestion of tubulobulbar complexes consisting of interdigitations between Sertoli cells or cytoplasmic islands of type B spermatogonia invaginating into pits of Sertoli cells (Ueno and Mori, 1990).

Lipid droplets increase at stages II-IX with sharp peaks at stages XII or XIV, and lows at stages IV and VIII. Lipid droplets seem to be the last remnants of digested residual bodies. Accumulated lipid droplets may have rapidly decreased at stage II because they were used for nourishing germ cells. Lipid constituting the plasma membrane of spermatids and lipid droplets appearing in the spermatid cytoplasm at stage II, may at least in part be provided from the Sertoli cells. The

secretion of the plasminogen activator by Sertoli cells has been reported to decrease when the preleptotene spermatocytes decrease markedly in number (Vihko *et al.*, 1984). In addition, the androgen binding protein secretion increases when Sertoli cells are cocultured with pachytene spermatocytes (Galdieri *et al.*, 1977).

5.1.3. Ultrastructure of the Leydig cell

The rat testis consists of two distinct populations of Leydig cells, *viz.*, the fetal Leydig cells and the adult Leydig cells. These two types of cells differ both in morphology and physiological function (Hardy *et al.*, 1989; Haider and Servos, 1998; Haider, 2004). The precursors for the fetal Leydig cells seem to be the mesenchymal fibroblasts. The peritubular cells of mesenchymal origin build the wall of the testicular cords. The formation of testicular cords starts first at the cortex of the gonad and progresses gradually toward the hilus near the mesonephros. It has been speculated that the peritubular fibroblasts contribute to the trigger mechanisms that initiate fetal Leydig cell differentiation via local growth factors from the endothelial cells (Skinner, 1991). Two sources for the precursors of fetal Leydig cells have been reported in the literature, *viz.*, mesenchymal fibroblasts from the mesonephros and mesenchymal fibroblasts from the gonadal ridge (Byskov, 1986; Buehr *et al.*, 1992; De Kretser and Kerr, 1994; Merchant-Larios *et al.*, 1993; Nishino *et al.*, 2001). The special cell contacts between perivascular fetal Leydig cells and the endothelial cells of blood capillaries are often observed. Gap junctions and special desmosome-like cell contacts are observed between adjacent fetal Leydig cells. Kuopio *et al.*, (1989), described three consecutive developmental stages in prepubertal rats, *viz.*, fetal (fetal Leydig cells in the fetal testis), early juvenile (fetal Leydig cells during neonatal stage to early juvenile), and juvenile adult (adult Leydig cells before and after puberty).

Adult Leydig cells are classified into the three stages, *i.e.*, progenitor stage, immature stage, and mature stage (Hardy *et al.*, 1989). Progenitor stage includes Leydig cells originating from the mesenchymal-like fibroblasts and produce androsterone as the predominant androgen end product. Immature stage includes those cells that produce small amounts of testosterone and metabolize most of the

testosterone. The predominant androgen end product is the 5α -androstane- 3α , 17β -diol. Mature stage will be formed by cells which actively produce testosterone as an androgen end product and are fully functional in the sexually mature animal.

Fibroblasts lying in the outer peritubular layer as well as in the perivascular region are regarded as the precursors of the adult Leydig cells. Prince (2001) suggested that gonadotrophic hormones are primary regulators of neonatal Leydig cell development in primates, for example, in the common marmoset.

The clusters of Leydig cells are located in the angular spaces among the seminiferous tubules and are frequently associated with blood vessels. These cells have a spherical or irregularly polyhedral shape and are about 20 μm in diameter. The nuclei are usually rounded and the cell surface is characterized by microvilli. The most prominent cytoplasmic organelles in these cells are abundant smooth endoplasmic reticulum, mitochondria with tubular cristae, lipid droplets, and lipofuscin bodies. These features are characteristics of steroid producing cells (Dym, 1983; Camatini *et al.*, 1981). In humans, conspicuous cytoplasmic crystals of Reinke are characteristic features. The crystals vary widely in size and form, but are often rectilinear and may be 2 μm long and 3 μm in thickness. With the use of advanced histochemical techniques, the Leydig cells have been shown to contain cholesterol, ascorbic acid, lipases, esterases, leucylamino peptidases, succinic dehydrogenase, cytochrome oxidase, and 3-B-ol dehydrogenase. In addition, it has been reported that Leydig cells secrete glycoprotein for export (Dym, 1983).

5.2. OBJECTIVES

- To study the ultrastructure of the testis of the vervet monkey and compare it with the testis of the human. Particular attention in this regard is paid to an overview of the testis by making use of scanning electron microscopy.
- To study the ultrastructure of the Sertoli cells and Leydig cells and their organelles, as well as the other non germinal cells.
- To provide information that may be valuable in applied reproduction such as evaluating male contraceptives or potential substances toxic to the testis.

5.3. MATERIALS AND METHODS

Study animals and their maintenance, sample collection, and dissection procedures were the same as in previous chapters. Ethical clearance was obtained from the Medical Research Council's Ethical Committee for this study.

5.3.1. SCANNING ELECTRON MICROSCOPY (SEM)

The procedures are the same as in previous chapter.

5.3.2. TRANSMISSION ELECTRON MICROSCOPY (TEM)

The procedures are the same as in previous chapter.

5.4. Results

5.4.1. Ultrastructure of the testis of the vervet monkey

Figures 5.1 to 5.5 are scanning electron micrographs showing various features of the vervet monkey testis. The thick tunica albuginea, approximately 300 μm in diameter, can be seen in Figure 5.1. Seminiferous tubules in both transverse and longitudinal planes are depicted in Figures 5.2 and 5.3. The interstitial septum is clearly discernable in both these Figures.

Figures 5.4 and 5.5 show more detail of the organization of the testis compartment and show some testicular cells as viewed by SEM. It is, however, difficult to distinguish between different types of spermatogonia, spermatocytes and spermatids, but the outline and position of these cells as viewed by SEM makes it possible to identify Sertoli and Leydig cells as well as spermatogonia and spermatocytes in general.

Figures 5.6 and 5.8 show the sleeve-like processes. There are more perforations in these structures in Figure 5.6 than Figure 5.7 or Figure 5.8. It is conceivable that more perforations per sleeve-like pocket are present in late stages of spermiogenesis (Figure 5.6) than in very young stages of spermiogenesis (Figure 5.7).

These pockets finally erode because of the amalgamation of all perforations, for the release of spermatozoa



Figure 5. 1. SEM micrograph showing the tunica albuginea of the testis of the vervet monkey, *Chlorocebus aethiops*.

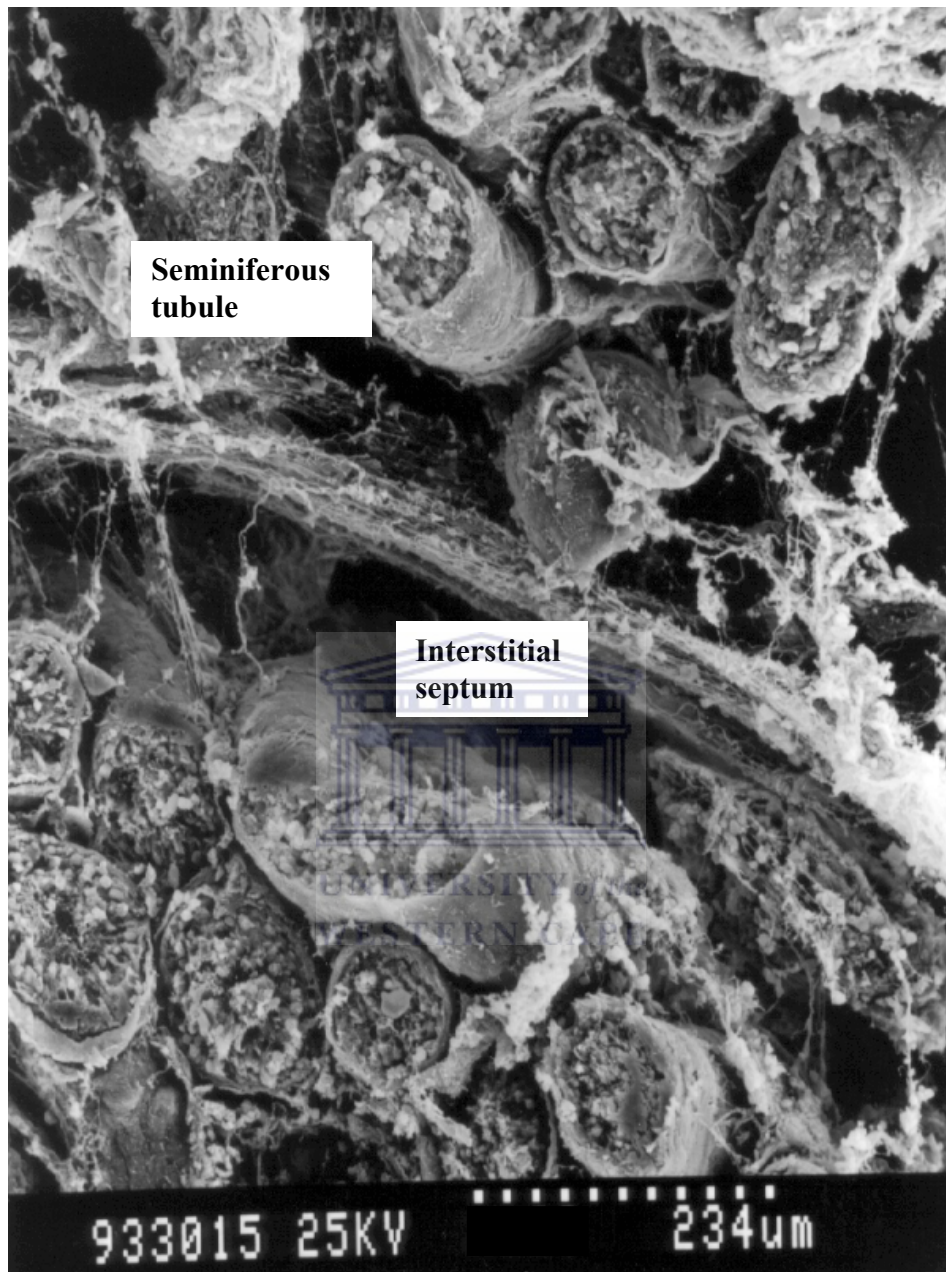


Figure 5. 2. SEM micrograph showing the interstitial septum of the testis of the vervet monkey, *Chlorocebus aethiops*.



Figure 5. 3. SEM micrograph showing at low magnification of external appearance of the seminiferous tubules in the testis of the vervet monkey, *Chlorocebus aethiops*. Line shows approximate position of septum.

Also cited by Van der Horst (2005).

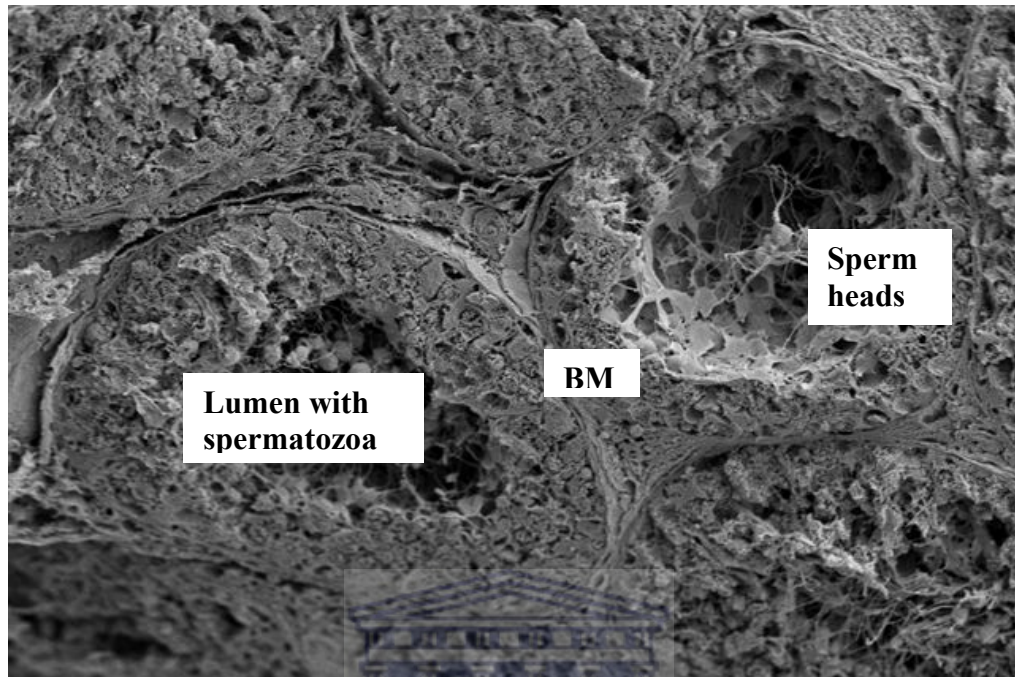


Figure 5. 4 . SEM micrograph showing seminiferous tubules in transverse section from the medial testis of the vervet monkey, *Chlorocebus aethiops*.

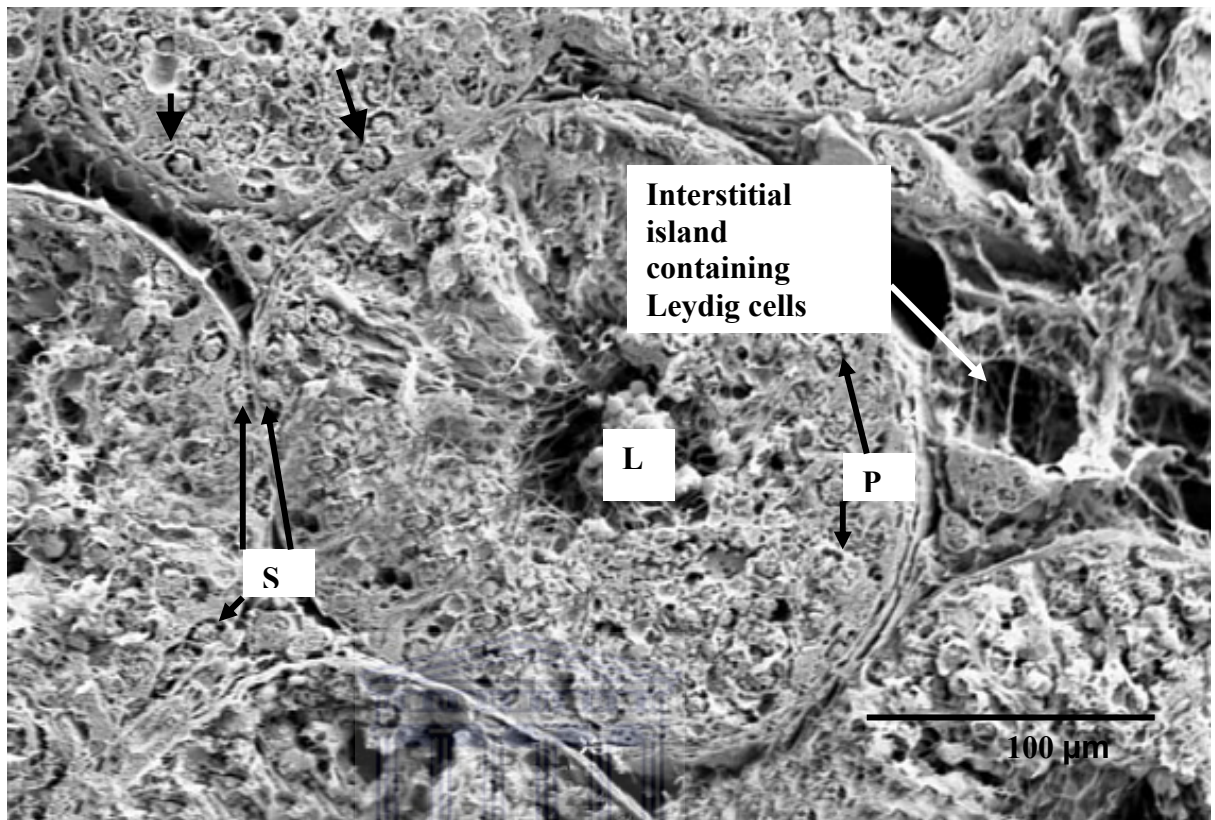


Figure 5. 5. SEM micrograph showing the seminiferous tubules of the medial testis of the vervet monkey, *Chlorocebus aethiops*.

Arrows- Spermatogonia, L- Lumen, P- Primary Spermatocyte, S- Sertoli cell

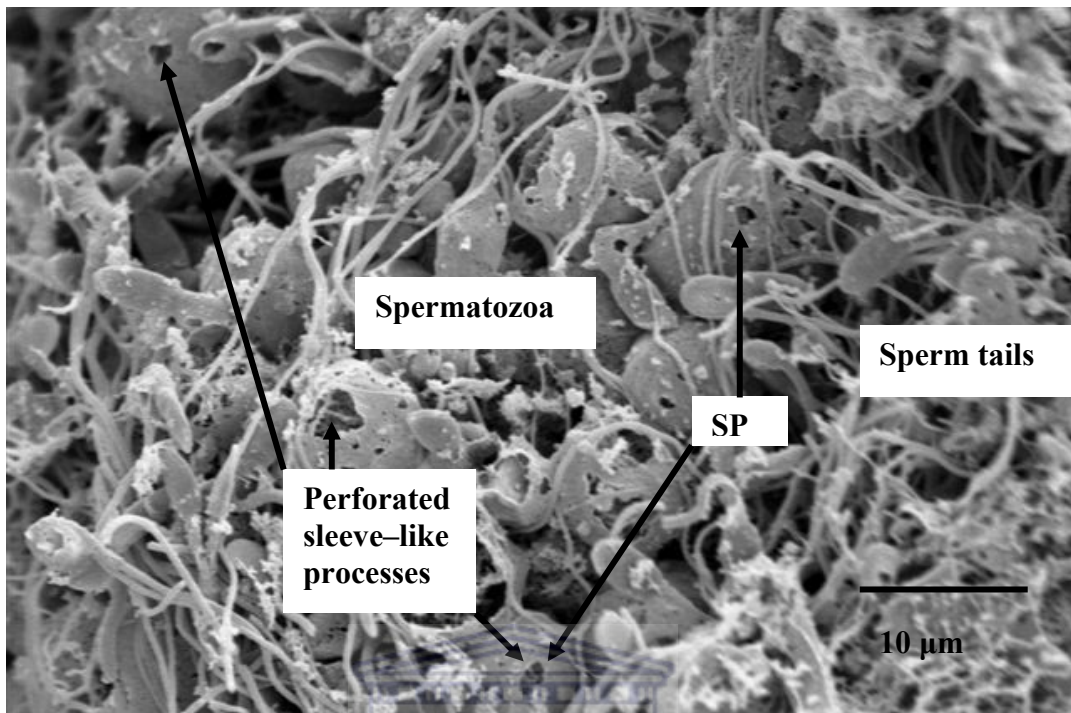


Figure 5. 6. SEM micrograph showing the sleeve –like processes found in the Sertoli cells of the middle testis, of the vervet monkey, *Chlorocebus aethiops*.

SP - Sleeve-like pouches.

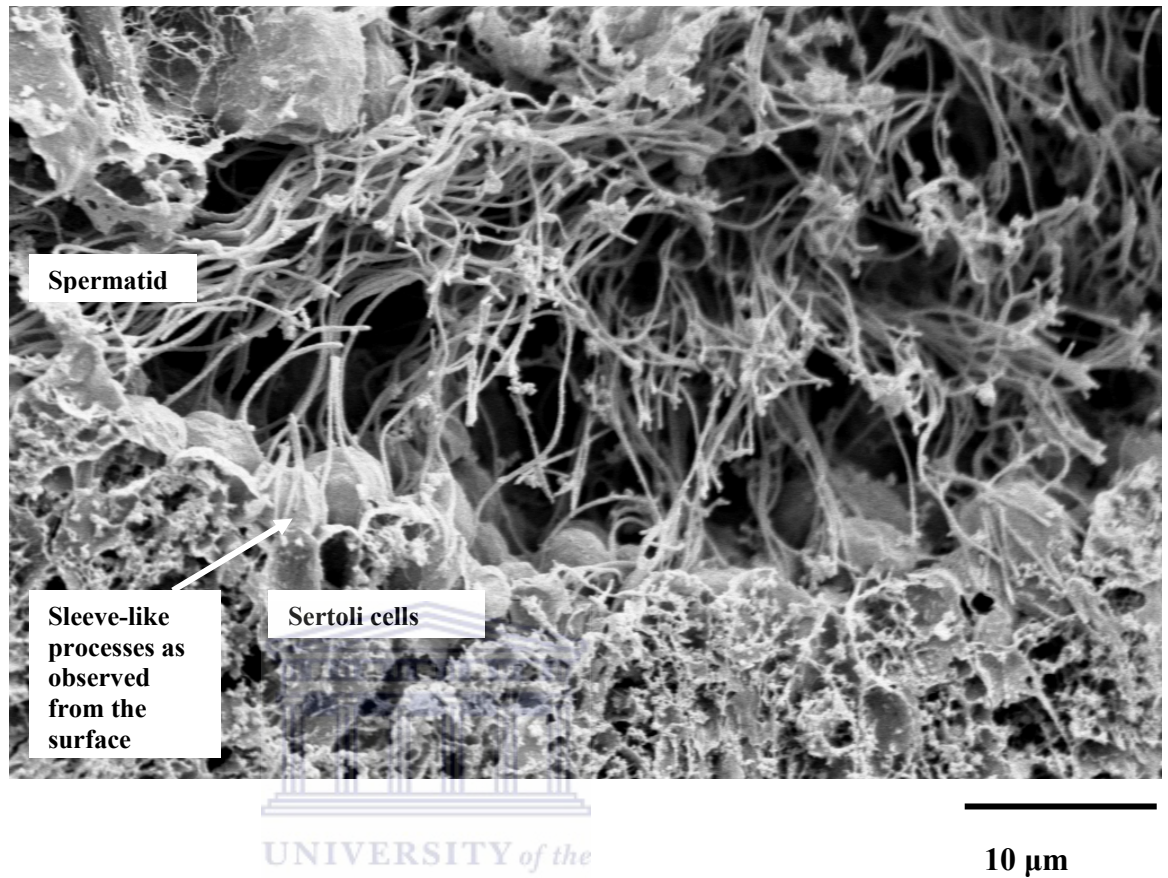


Figure 5. 7. SEM micrograph showing the sperm tail and sleeve like processes in the testis of the vervet monkey, *Chlorocebus aethiops*.

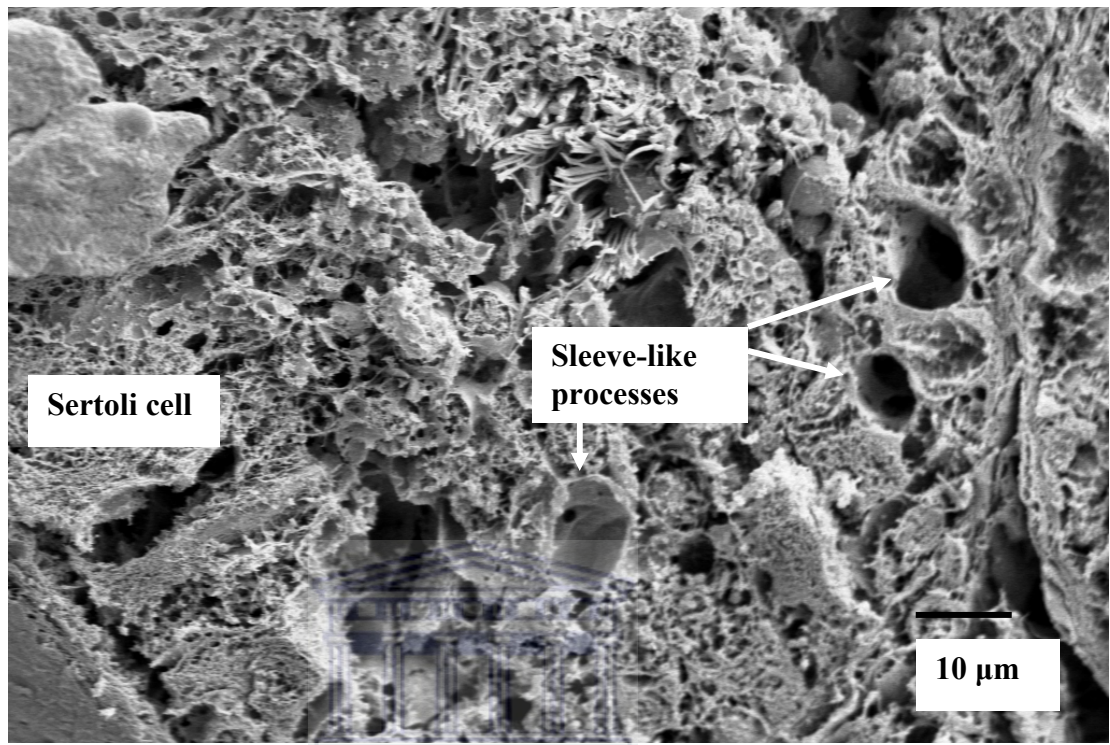


Figure 5. 8. SEM micrograph showing the sperm tail and sleeve like processes in the testis of the vervet monkey, *Chlorocebus aethiops*.

Figures 5.9 and 5.10 show different layers of the seminiferous tubules and the interstitial region of the testis of the vervet monkey. The three layers observed are from inside, the basement membrane, myoid cell layer and the glycoprotein layer. The type B spermatogonium rests on the basement membrane. The phagosomes are found on the basal side of the pachytene spermatocytes. The endothelial cell layer is also observed. The lymphatic vessel is also observed between the two seminiferous tubules (Figure 5.10).

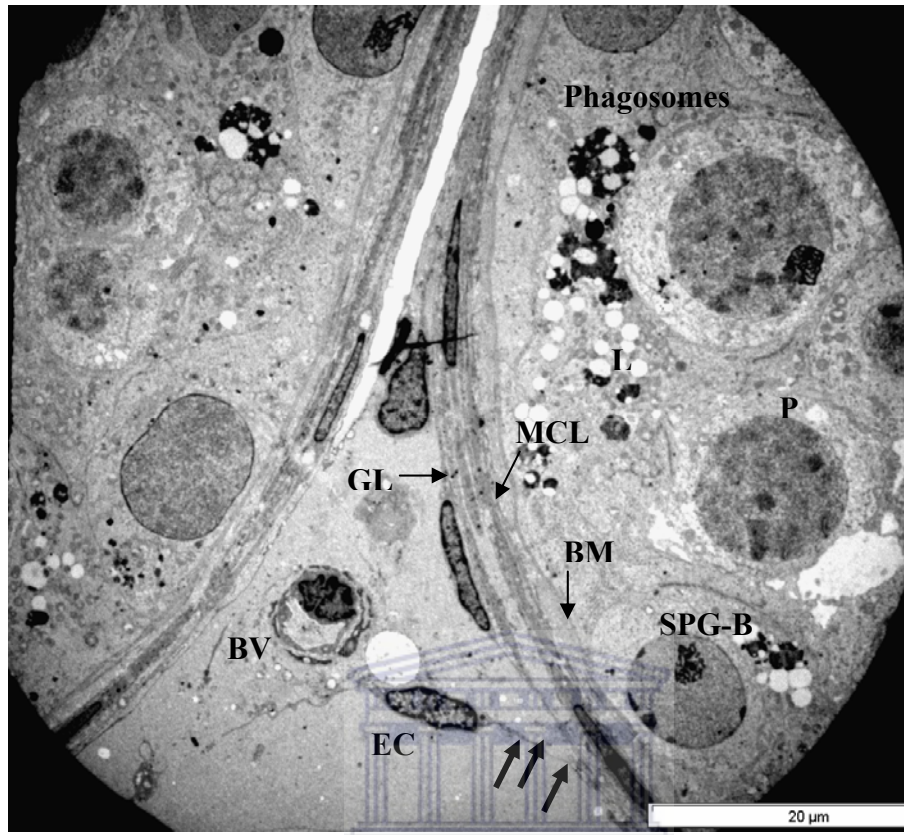


Figure 5. 9. TEM micrograph showing the interstitial region of the testis and the three layers of the seminiferous tubules of the vervet monkey, *Chlorocebus aethiops*.

Arrows (thick) – Endothelial cell layer, BM – Basement membrane, EC - Endothelial cell, BV- Blood vessel, GL – Glycoprotein layer, L - Lipid droplets, MCL – Myoid cell layer, P - Early pachytene, SPG -B- Spermatogonium Type B.

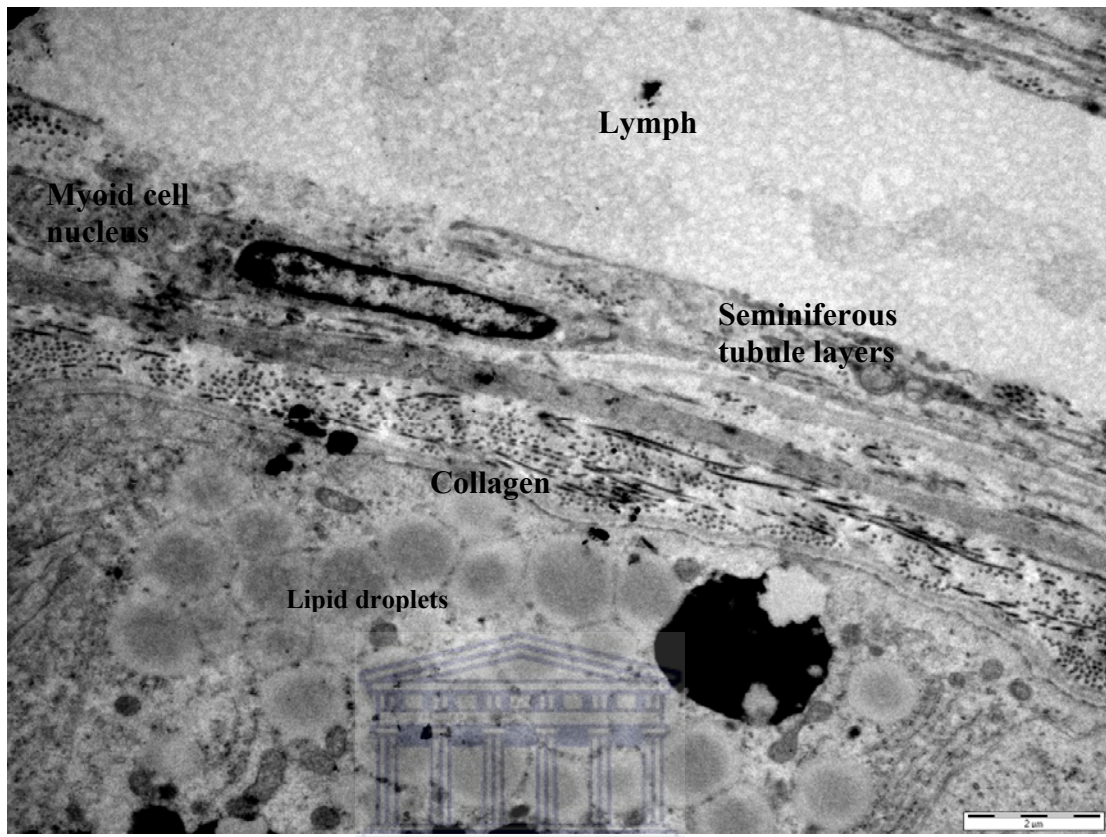


Figure 5. 10. TEM micrograph showing myoid cells and lipid droplets in the interstitial tissue of the testis of the vervet monkey, *Chlorocebus aethiops*.

5.4.2. Ultrastructure of the Sertoli cell of the vervet

Figures 5.11 to 5.13 show transmission electron micrographs of the Sertoli cells. The Sertoli cell, a tall columnar cell extends from the base of the seminiferous tubule to the lumen. The Sertoli cell has a large nucleus, with numerous infoldings and characterized by a homogenous nucleoplasm and a distinctive nucleolus. It occupied a significant portion of the basal region of the cell. Sertoli cell nuclei have 4-5 lobes. The distribution of chromatin clearly shows the high activity of these cells. A prominent nucleolus is quite distinct in one of the Sertoli cells (Figure 5.12). Near the nucleus, there were many profiles of the smooth endoplasmic reticulum. Free ribosomes are also scattered throughout the Sertoli cytoplasm (Figure 5.12). Well developed Golgi apparatus was clearly observed in the cytoplasm (Figure 5.13). Lipid droplets and numerous spherical and elongated mitochondria are observed (Figure 5.12). The mitochondria are found to be more abundant in the basal side compared to the apical side. There is phagocytic activity in the Sertoli cells as can be seen by numerous phagosomes. Desmosomes are also observed between the Sertoli cells (Figure 5.13). The SER and GER were observed in the cytoplasm of the Sertoli cell nucleus.

Residual bodies and degenerating germ cells are evident and appearing to be membrane bound. Near the base of the seminiferous epithelium are the junctional complexes. Specialized Sertoli cell junctions were found between lateral extensions of the Sertoli cell cytoplasm.

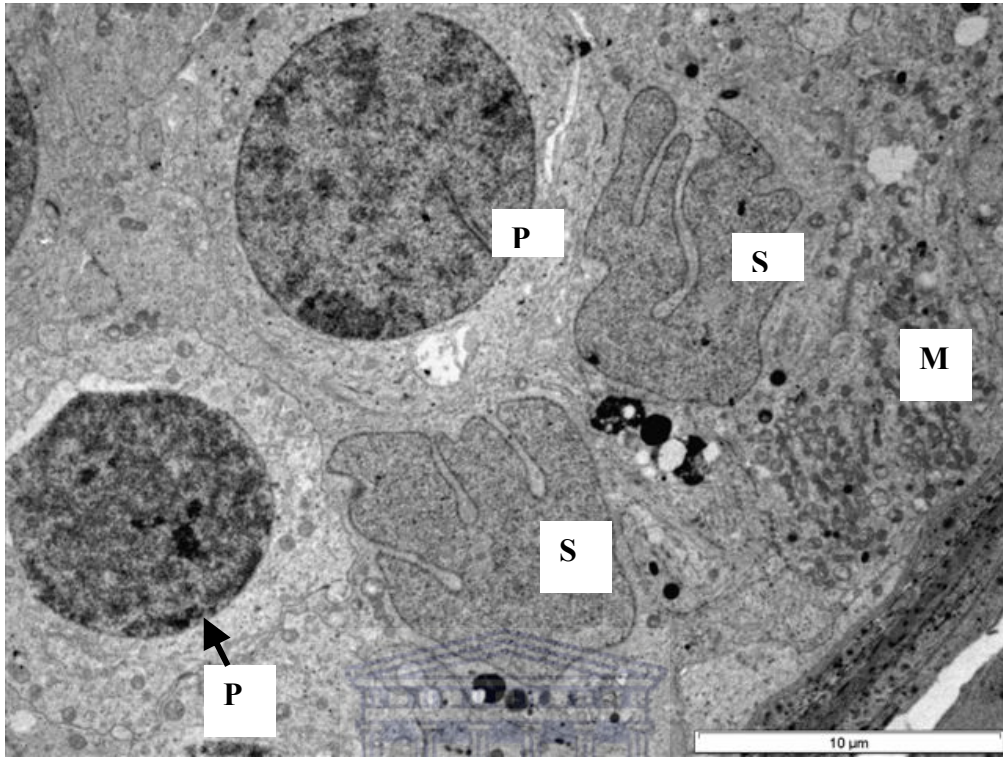
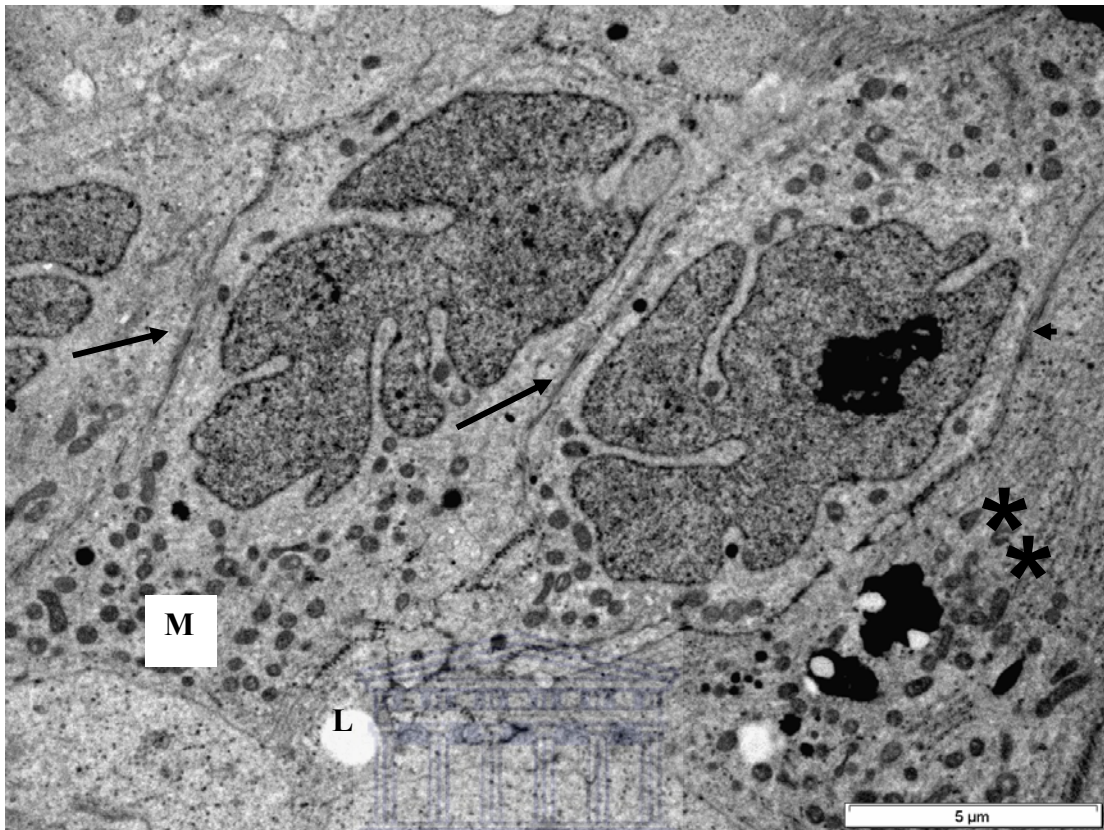


Figure 5. 11. TEM micrograph showing the Sertoli cells with primary spermatocytes (early pachytene) of the vervet monkey, *Chlorocebus aethiops*. M - Mitochondria, P - early pachytene, S - Sertoli cell nucleus.



UNIVERSITY of the
Figure 5. 12. TEM micrograph showing the Sertoli cell tight junctions, lipid complex in the seminiferous tubules of the vervet monkey, *Chlorocebus aethiops*. Arrows - tight junctions between Sertoli cells, asterisk - endoplasmic reticulum, L - Lipid droplets, M- Mitochondria,

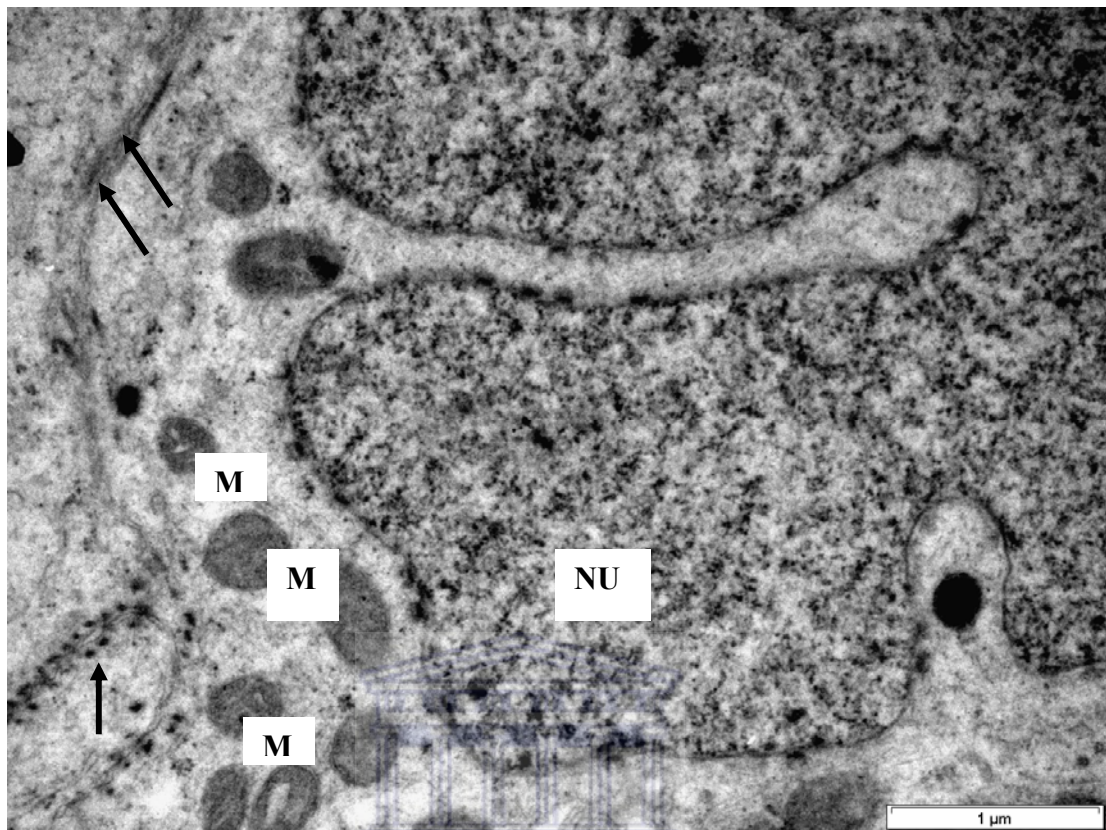


Figure 5. 13. TEM micrograph of the Sertoli cells, showing mitochondria and tight junction in the seminiferous tubules of the vervet monkey, *Chlorocebus aethiops*. Prominent is the dispersed chromatin in the nucleus indicating the high cellular activity.

Arrows – Desmosomes, M - Mitochondria, NU - Nucleus of the Sertoli cells.

5.4.3. Ultrastructure of the Leydig cell of the vervet

Figures 5.14 to 5.19 show Leydig cells which occur mostly in clusters of polymorphic cells, and they are usually associated with small blood vessels and abundant loose connective tissue.

Leydig cells have large spherical or slightly elongated nuclei, which usually possessed prominent nucleoli and frequently deep indentations of nuclear envelope (Figure 5.19). The cytoplasm contains small Golgi - apparatus, round or oval lysosome-like structures, some mitochondria containing tubular or lamellar cristae, small patches of rough endoplasmic reticulum as short cisternae, and a large dense network of interconnecting tubular smooth endoplasmic reticulum (Figures 5.18; 5.19). The peroxisomes are generally spherical and often had indistinct protrusion of the membrane and are closely apposed to smooth endoplasmic reticulum (Figure 5.19).

A number of cytoplasmic inclusions were frequently found, including lipid droplets and lysosomes. However, crystals of Reinke were not observed in this study. Crystals of Reinke are regarded as one of the distinguishing features in the human Leydig cell. Collagen fibers were observed in the cytoplasm of the Leydig cells (Figures 5.14; 5.18).

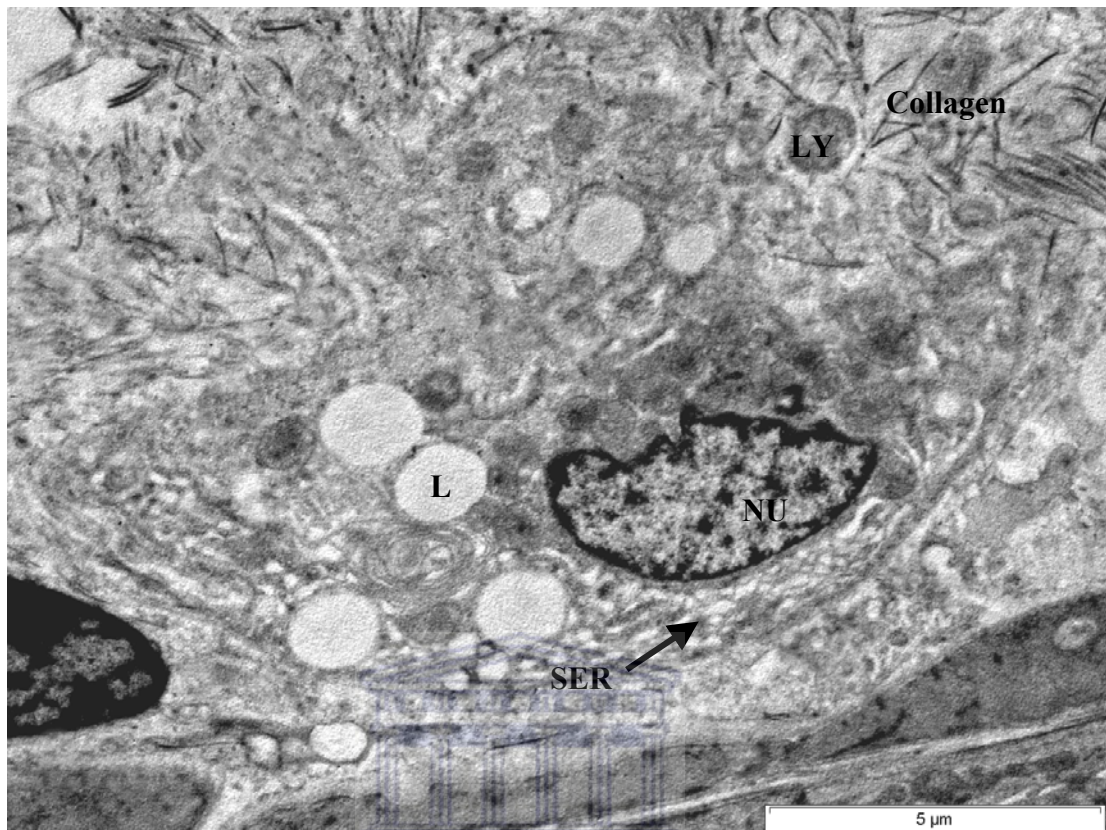


Figure 5. 14. TEM micrograph showing the Leydig cells, showing mitochondria, lipid droplets, and SER in the interstitial region of the testis of the vervet monkey, *Chlorocebus aethiops*.

L - lipid droplet, LY -Lysosome, NU – Nucleus, and SER - Smooth endoplasmic reticulum.

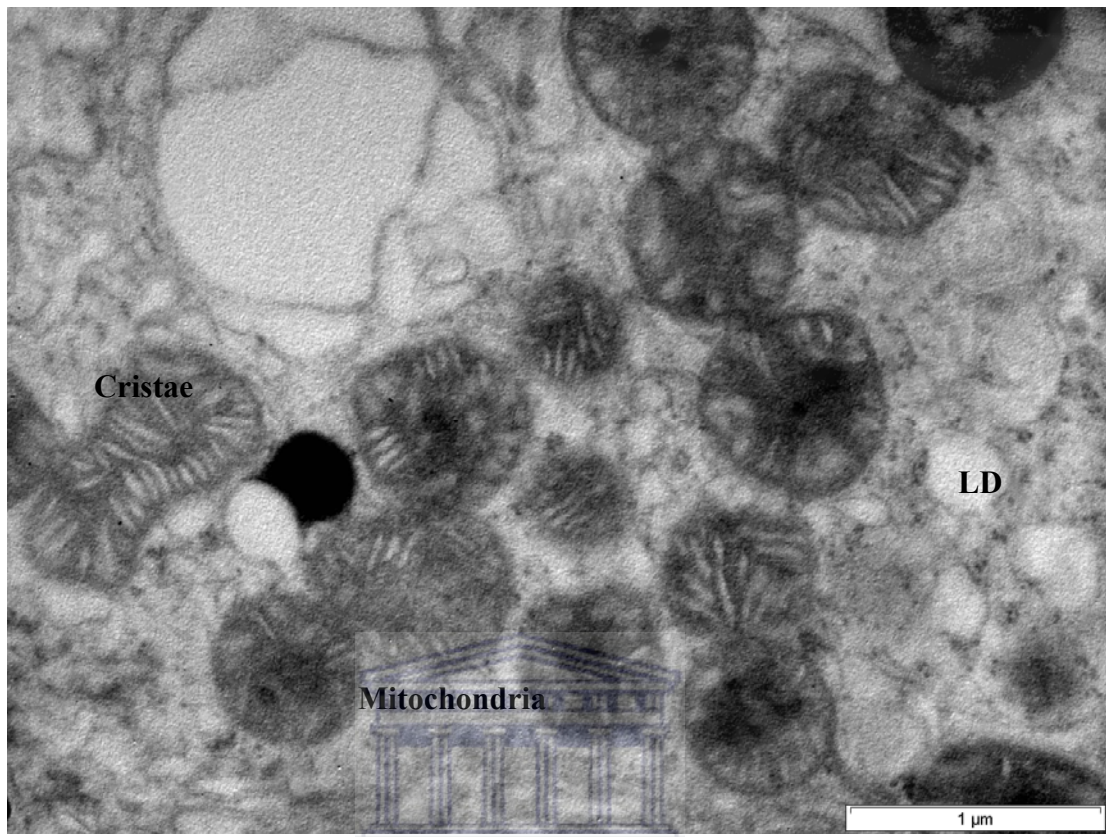


Figure 5. 15. TEM micrograph of the Leydig cells, showing mitochondria with characteristics and extensive cristae, and lipid droplets in the interstitial region of the testis of the vervet monkey, *Chlorocebus aethiops*.

LD - Lipid droplets

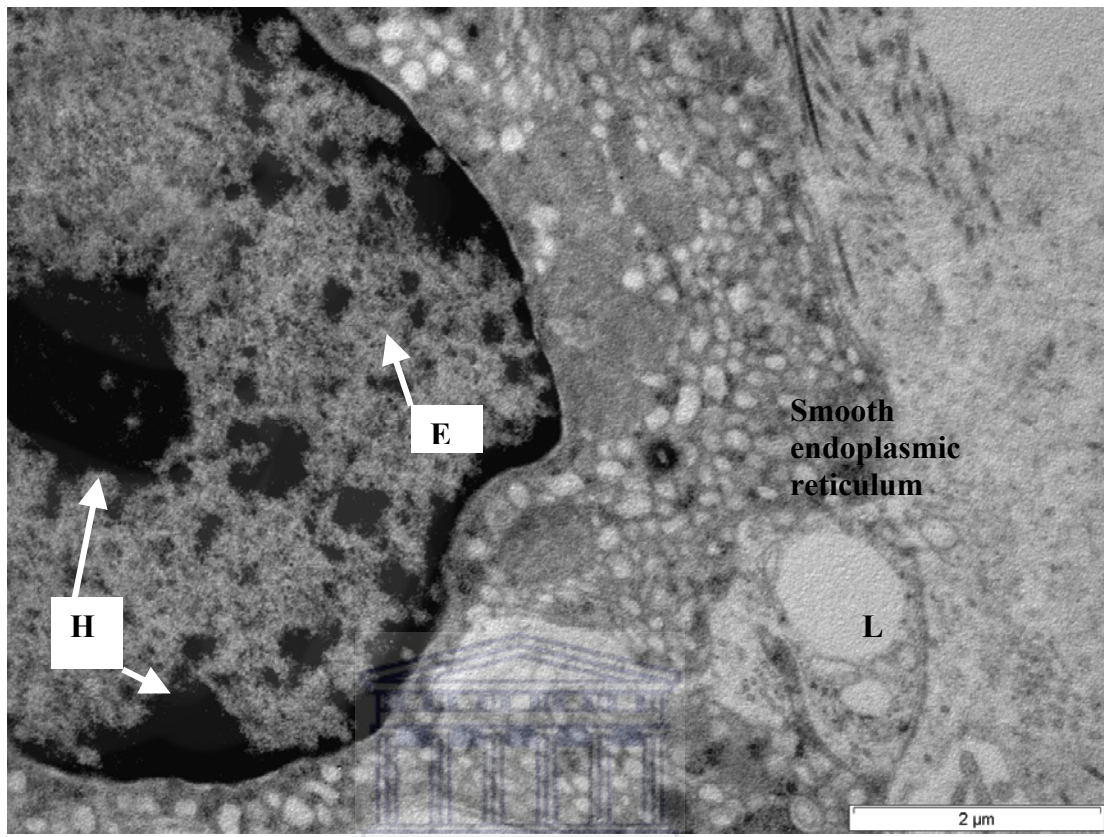


Figure 5. 16. TEM micrograph showing the Leydig cell nucleus with its heterochromatin and euchromatin regions, and lipid droplets in the interstitial region of the testis of the vervet monkey, *Chlorocebus aethiops*.

E - Euchromatin, H - Heterochromatin, and L - Lipid droplet.

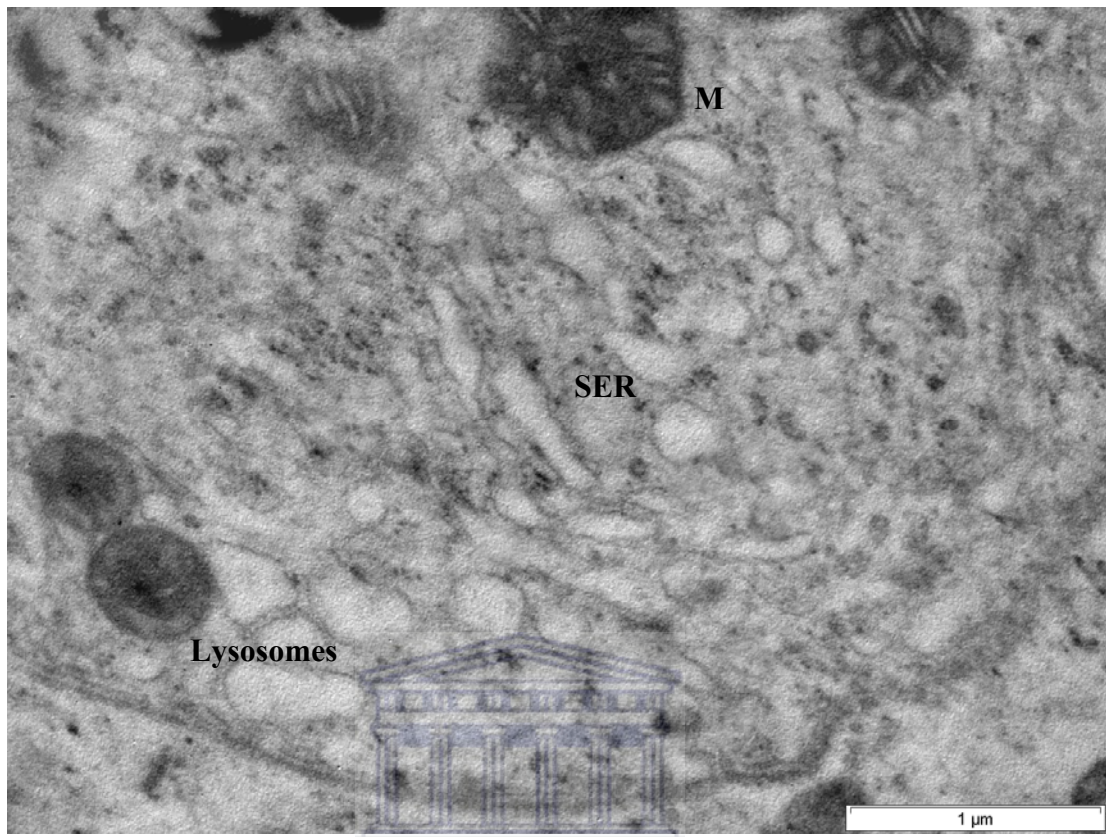


Figure 5. 17. TEM micrograph of the Leydig cell, showing mitochondria, lipid droplets, and SER in the interstitial region of the testis of the vervet monkey, *Chlorocebus aethiops*.

M - Mitochondria, SER - Smooth Endoplasmic Reticulum

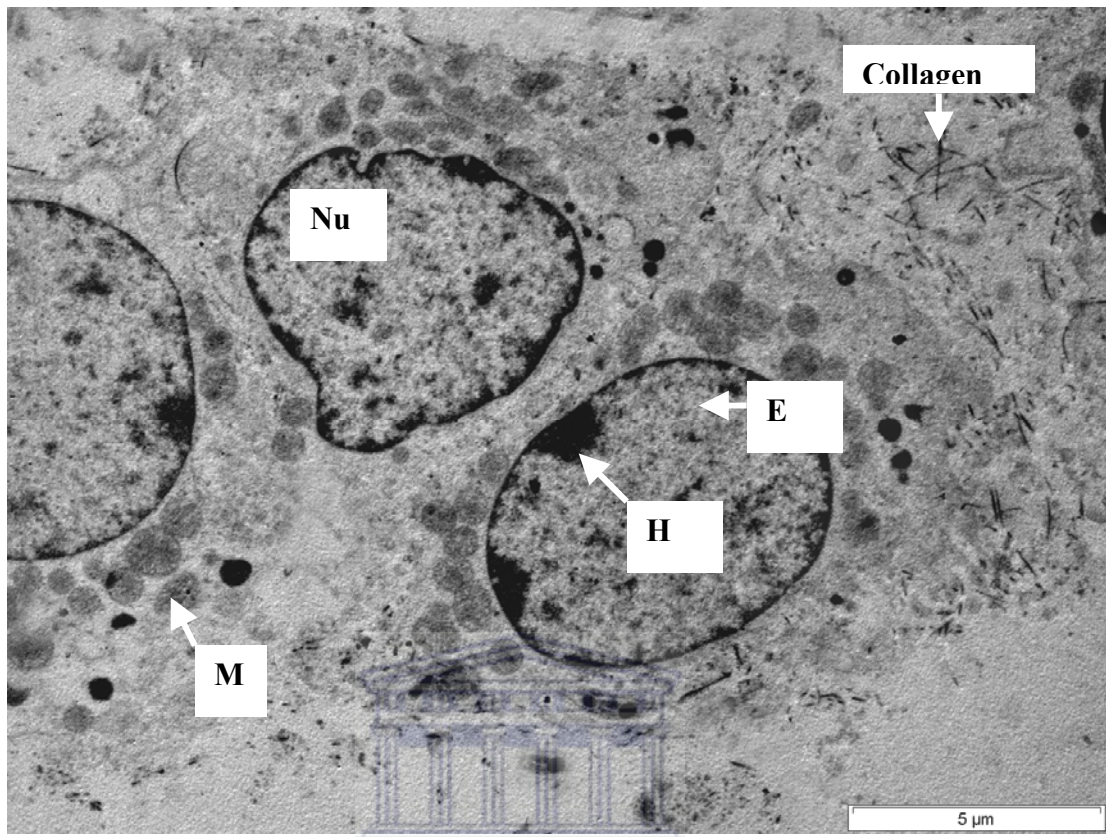


Figure 5. 18. TEM micrograph showing a cluster of Leydig cells, mitochondria, and lipid droplets in the interstitial region of the testis of the vervet monkey, *Chlorocebus aethiops*. In this instance there appears to be less lipid droplets. E -Euchromatin, H - Heterochromatin, M - Mitochondria, and NU - Nucleus.

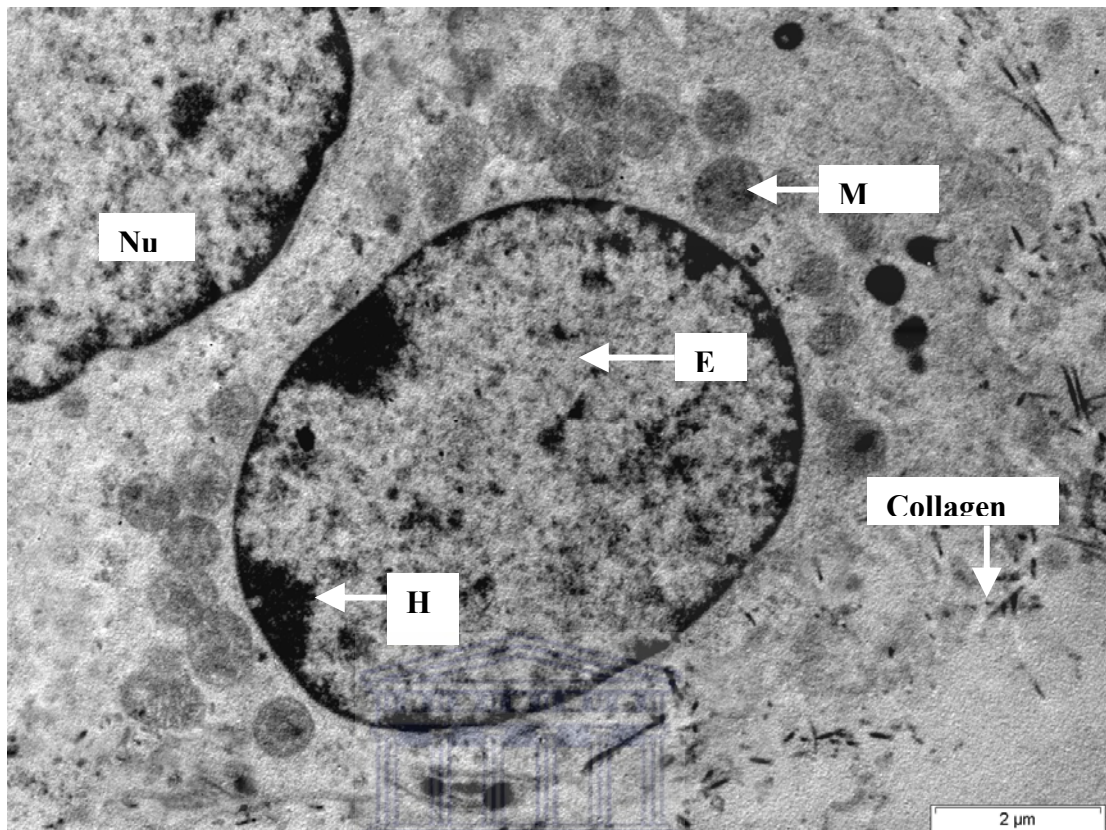


Figure 5. 19.TEM micrograph showing the Leydig cell nucleus with its heterochromatin and euchromatin regions, and lipid droplets in the interstitial region of the testis of the vervet monkey, *Chlorocebus aethiops*.

E -Euchromatin, H - Heterochromatin, NU – Nucleus, and M – Mitochondria.

5.4.4. Ultrastructure of other cells of the interstitial tissue (excluding Leydig cells).

Figures 5.20 to 5.24 show the electromicrograph of cells outside the seminiferous tubules excluding the Leydig cells. The interstitial tissue contains vascular elements, connective tissue matrix, macrophages, peritubular myoid cells, and lymphatic endothelial cells. The macrophages are characterized by finger-like projections as observed in Figure 5.21. The macrophages also possess collagen fibers as observed in Figures 5.22 and 5.23.

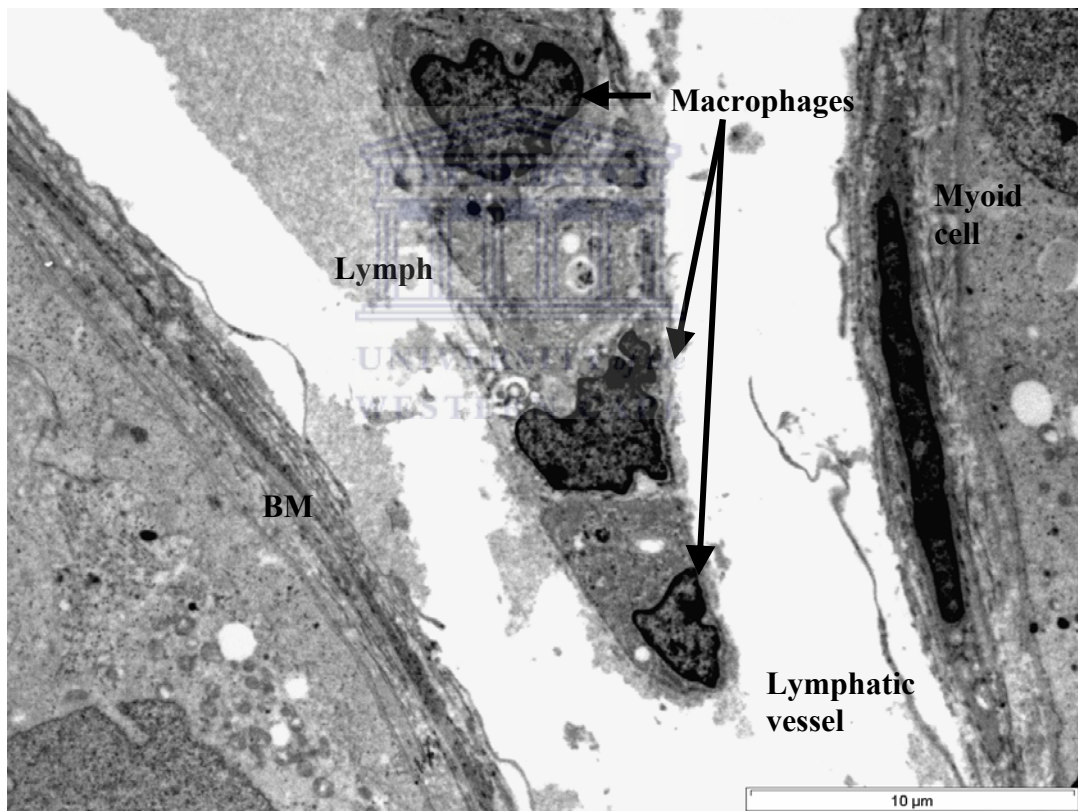


Figure 5. 20. TEM micrograph showing the interstitial area, lymphatics and Sertoli cell nucleus, and two seminiferous tubules of the vervet monkey, *Chlorocebus aethiops*.

BM- Basement membrane

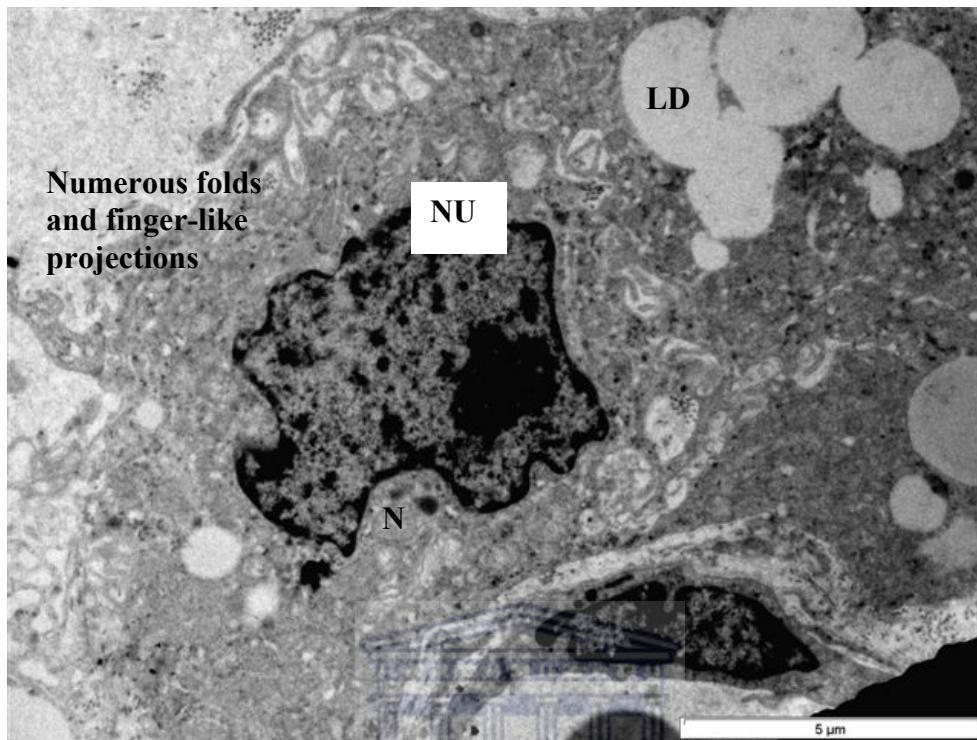


Figure 5. 21. TEM micrograph showing the nucleus of the macrophage in the interstitial tubule of the vervet monkey, *Chlorocebus aethiops*.

LD - Lipid droplets, NU - Nucleus.

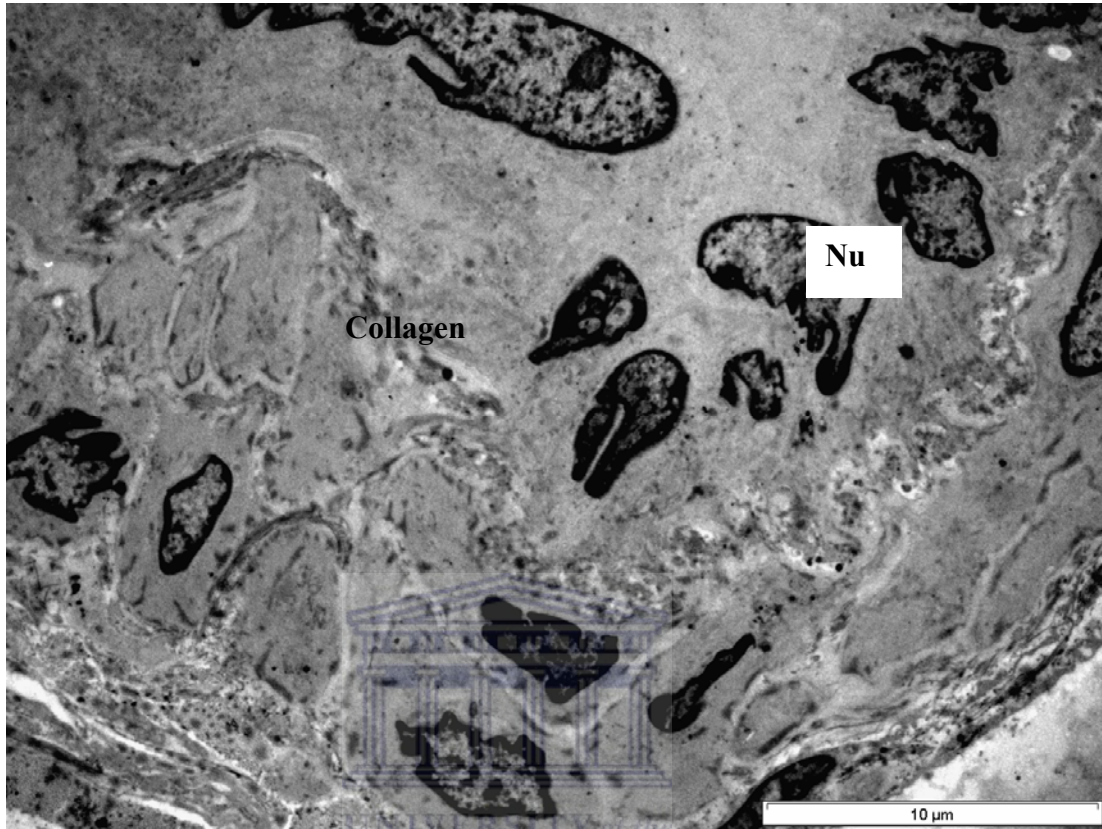
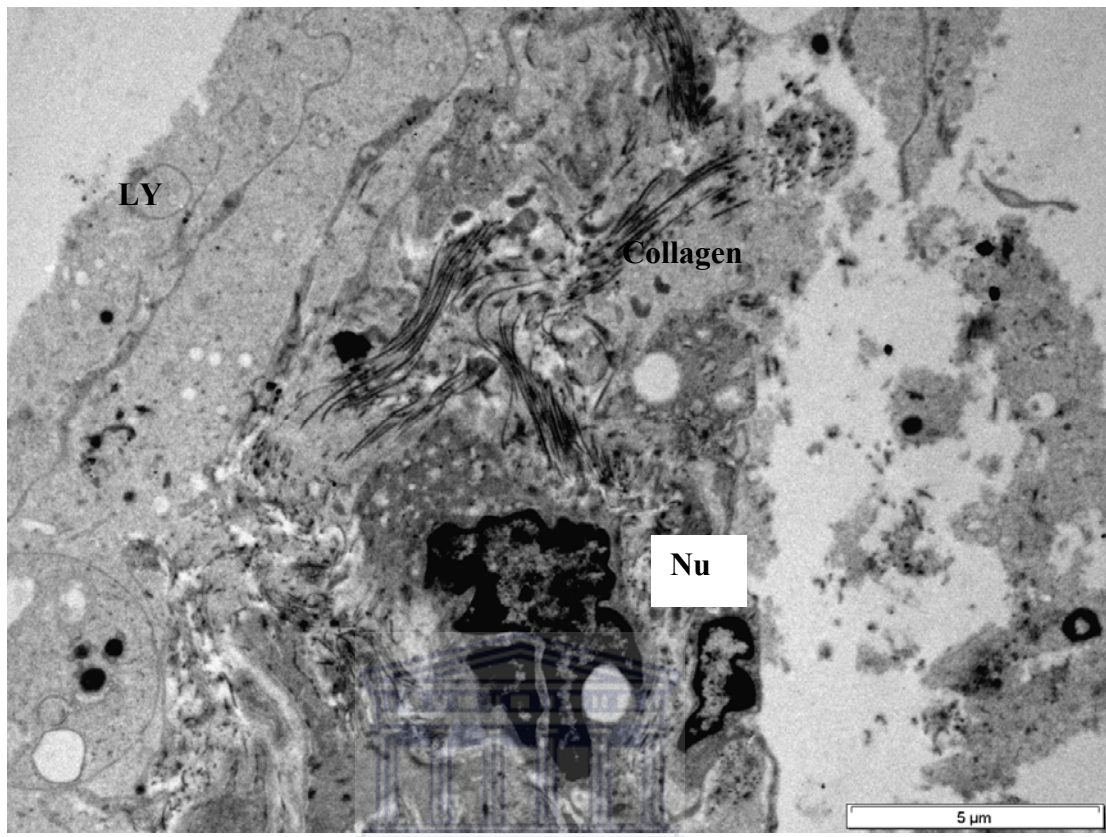


Figure 5. 22. TEM micrograph showing the macrophages at different stages of development in the interstitial area of the testis of the vervet monkey, *Chlorocebus aethiops*.

NU - Nucleus.



**Figure 5. 23. TEM micrograph showing the macrophage in the testis of the
vervet monkey, *Chlorocebus aethiops*.**

LY - Lysosomes, Nu - Nucleus.

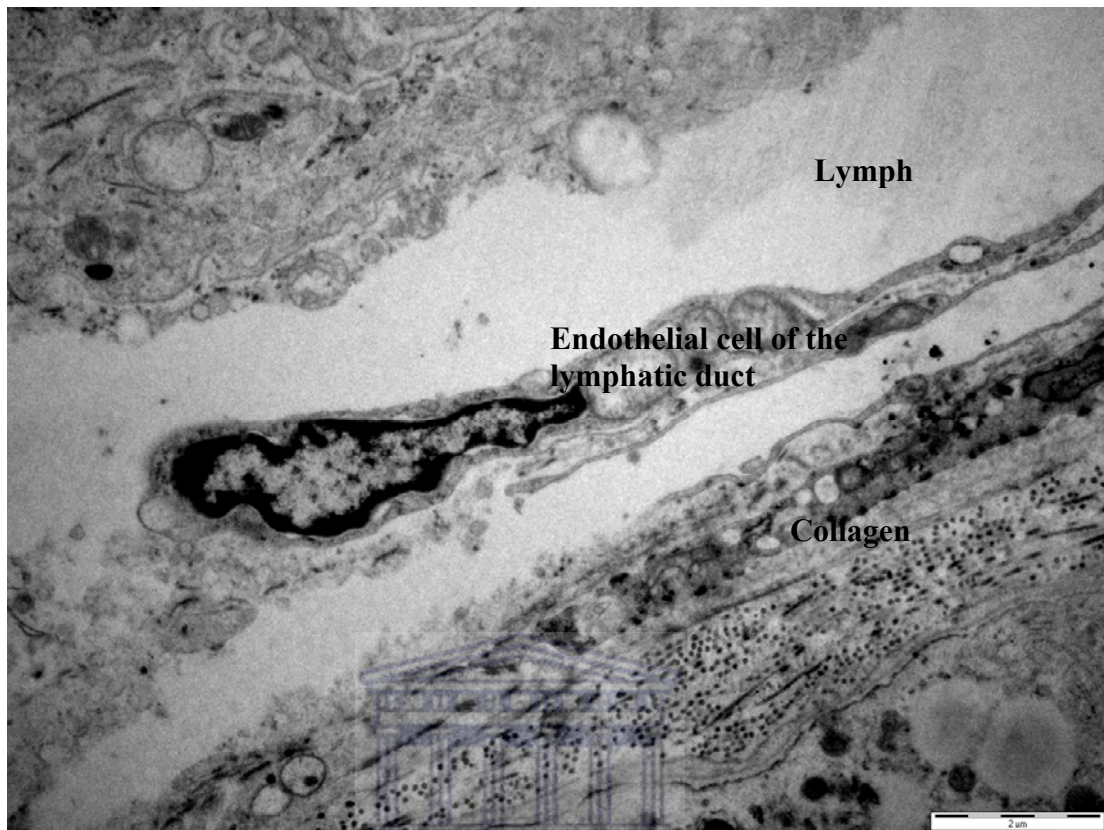


Figure 5. 24. TEM micrograph showing the endothelial cell of the interstitial tissue of the vervet monkey, *Chlorocebus aethiops*.

5.4.5. Ultrastructure of the tissue immediately outside the testis in the coni vasculosi area.

Figure 5.25 shows the ultrastructure of the extratesticular tissue of the testis close to the coni vasculosi. Many lipid droplets were in close association with myelinated neurons with distinct Schwann cells. These neurons have a diameter of approximately 3 μm . The collagen fibers appear to be forming the epineurium.

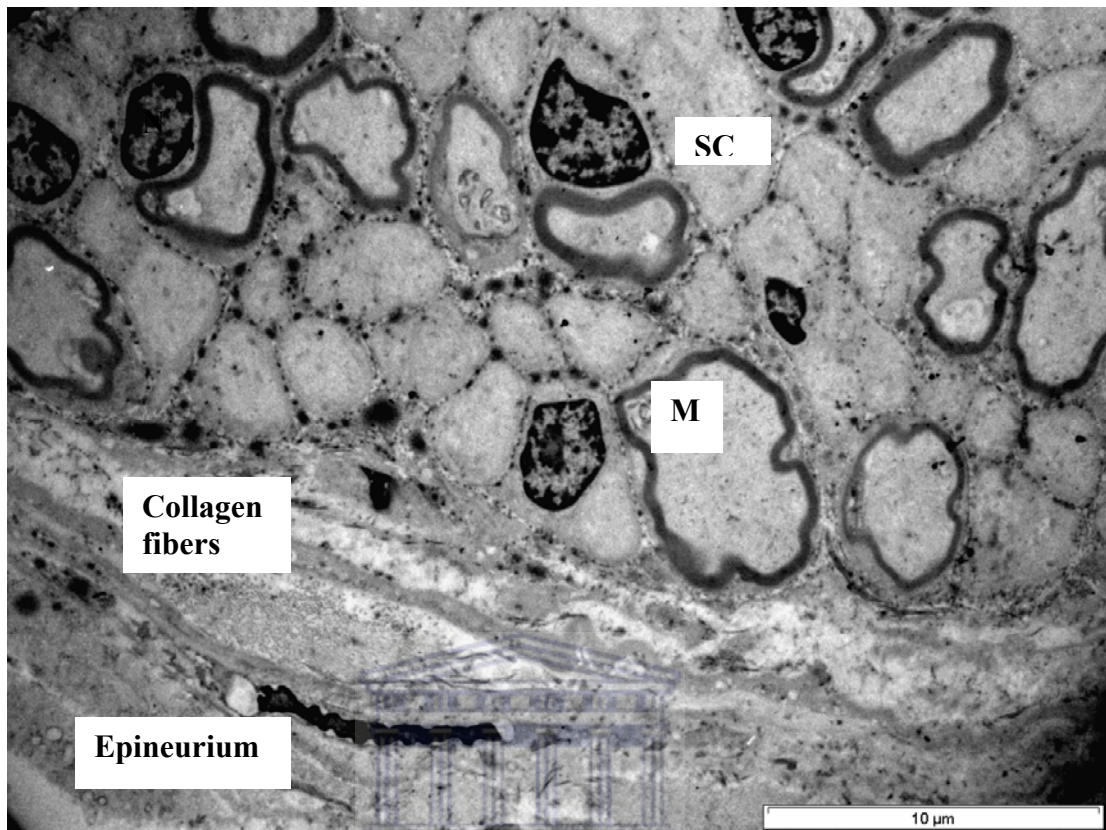


Figure 5. 25. TEM micrograph showing nerves immediately outside testis in the conus vasculosus area of the vervet monkey, *Chlorocebus aethiops*..

M- Myelin sheath, SC- Schwann cell nucleus.

5.5. DISCUSSION

Dym, (1972), reported that the tunica propria of the seminiferous tubules in monkeys is markedly different from that found in the rodents and more closely resembles the patterns observed in humans. It was found that in rodents, two layers of flattened cells surround the seminiferous tubules, whereas monkeys exhibit up to five circumferentially arranged cell layers each one overlapping the other. In this study four to five layers were observed (Figure 5.9). The innermost cell layer immediately adjacent to the seminiferous tubules of subhuman primates contains the abundant filaments and is probably contractile, whereas the more peripherally placed cell exhibit fewer filaments and are fibrocyte-like. This is in contrast to rodents where the outer cell layer is the endothelium of large interstitially placed lymphatics (Dym, 1972).

Sertoli cells support and control the development of the germinal cells of the seminiferous tubules. Elongated spermatids of mammals, as they differentiate into mature spermatozoa, are located within deep recesses in the supranuclear cytoplasm of Sertoli cells and the greater surface of the spermatid is closely covered by the Sertoli cell cytoplasm. Wong and Russell (1983), revealed that the three-dimensional reconstruction of Sertoli cells show many processes which encapsulate the spermatid. Such processes have been considered as structures that hold the spermatids within the Sertoli cell recesses and contribute to the separation of the residual cytoplasm from the spermatozoon at the time of spermiation (Morales and Clermont, 1982). The same processes of the Sertoli cells were reported in bandicoots and rams (Sapsford and Rae, 1969). These processes were clearly observed in this study. The invading Sertoli cell processes are finger-like projections containing mitochondria, microtubules, lysosomes, and small vesicles. According to Morales and Clermont (1982), some of the invading Sertoli cell processes are pinched off to form isolated vacuoles that collapse to form mixed bodies consisting of small vacuoles and endoplasmic reticulum. Sakai *et al.*, (1988) reported that Sertoli cell processes start invading spermatid cytoplasm at the acrosomal phase of development and undergo considerable change at the maturation phase of development. Sakai *et al.*, (1988),

labelled these processes as the canal complex based on the manner in which the structures extend in various directions. Morales and Clermont (1982), defined this processes as mixed bodies. Sakai *et al.*, (1988), however, indicated that the mixed bodies could possibly be specialized parts of the canal complex. If they arise directly from invading Sertoli cell processes instead of isolated vacuoles then they are actually part of the canal complex. Morales and Clermont (1982), reported that they possibly served as a route for the passage of material from the Sertoli cells to the differentiating spermatids.

The organization of the intertubular tissue observed on the vervet monkey is similar to that described in man and other nonhuman primates such as the *Macaca mulatta* (Christensen, 1975; Camatini *et al.*, 1981). The ultrastructural characteristics of Leydig cells of *C. aethiops* observed in this study follow the general pattern clearly found in other adult active mammalian Leydig cells, including those found in humans. SER, RER and many mitochondria were observed in the cytoplasm of the Leydig cells. The same features were observed by Camatini *et al.*, (1981). Camatini *et al.*, (1981) further outlined that an extensive and polymorphic aspect of the smooth endoplasmic reticulum could be regarded as a distinguishing characteristic of the Leydig cells in the vervet monkey. This finding concurs with results in this study. Human Leydig cells possess a tubulovesicular system of the smooth endoplasmic reticulum, which represents a uniform morphology throughout the cell. Pleomorphism of the smooth endoplasmic reticulum has been described in other mammals. Numerous complexes of whorl formations with smooth endoplasmic reticulum in lamellar and tubulovesicular arrays have also been described in normal adult mouse Leydig cells.

Leydig cells are important in the biosynthesis of testosterone from cholesterol. The cholesterol esters are first stored in lipid droplets. Cholesterol, the substrate for all steroid-hormones, is transferred from cellular stores into the outer membrane of mitochondria by protein kinase A. There are two transport proteins involved in the transfer of cholesterol from the outer membrane to the inner membrane, the steroid acute regulator and the peripheral-type benzodiazepine receptor (Haider, 2004).

Abundant peroxisomes are present in the steroid-producing cells and are involved in the β -oxidation of fatty acids, and in the biosynthesis and metabolism of cholesterol. Peroxisomes contain thiolase and mevalonate kinase, two enzymes necessary for the initial steps of cholesterol synthesis (Haider, 2004).

As expected in many mammals, the close association of the smooth endoplasmic reticulum and mitochondria is involved in androgen synthetic pathways. Mitochondria had extensive cristae as observed by Camatini *et al.*, (1981) in vervets and again in this study. In this respect the results of the current study concur with these findings. Camatini *et al.*, (1981), further reported a very extensive rough endoplasmic reticulum which coexisted with the smooth endoplasmic reticulum. Their study could not elucidate the association of the two organelles.

The Golgi apparatus was surrounded by small vesicles. This was associated with the secretory process in the cells. No crystals of Reinke were observed in this study. The crystals of Reinke seem to be confined to humans because even in previous studies on the nonhuman primates there seem to be no literature which explains their presence in Leydig cells. This was one of the striking differences between the vervet Leydig cells and the human Leydig cells. Camatini *et al.*, (1981), suggested that the existence of some of the morphological features of organelles can be associated with the sexual maturity of those animals. Since the physiological functions of the crystals of Reinke are not well documented, it could be suggested that these structures could well be one of the few features confined to human Leydig cells. However, Prince (1999) reported the presence of inclusions with much similarity to the crystals of Reinke within the Leydig cells of the marmoset monkey. This will suggest that in this respect marmoset monkey is closer to human than the vervet monkey.

Rey *et al.*, (1996) reported that the interstitial tissue of the Capuchin monkey, (*Cebus apella*), which is a New World monkey, is similar to that of Old World monkeys and humans. Rey *et al.*, (1996), reported that there are similarities in the ultrastructural characteristics of immature and mature Leydig cells. Immature and mature Leydig cells are present from birth to late puberty in *Cebus*.

Myofibroblasts of the peritubular tissue are the main source of Leydig precursors in primates (Rey *et al.*, 1996).

Macrophages were observed in the interstitial region of the testis. These cells were characterized by numerous finger-like projections. The nuclei of these cells showed euchromatin regions which signified an intense cellular activity. Furthermore, different stages of development were also observed which indicated that these cells undergo continuous development in the interstitial region of the testis. No reference has been found in the literature which relates to macrophages inside the mammalian testis. Lipid droplets were also found in the cytoplasm of these cells.

The extratesticular tissue of the testis, found close to the conus vasculosus was characterized by lipid droplets and myelinated neurons. These neurons had a diameter of approximately 3 μm . This signified that they were A-delta neurons which were typically involved in temperature and fast pain conduction (Despopoulos and Silbernagl, 1986).

5.5.1. Human Leydig Cells

Cells of the outer layer of peritubular cells may probably serve as precursors for Leydig cells. Prince (2001), proposed a triphasic nature of Leydig cell development in humans and other primates in contrast to the biphasic nature in rodents. The three phases are classified as follows: a) between the 14-19 weeks of fetal life, b) from the second and third month after birth, and c) from puberty throughout adult life. Numerous non-human primates such as the rhesus monkey, common marmoset, crab-eating monkey, and the chimpanzees, have been shown to exhibit fetal, neonatal, and pubertal periods of testosterone secretion (Winter *et al.*, 1976; Steiner and Bremner, 1981; Fouquet *et al.*, 1984; Dixson, 1986; Lunn *et al.*, 1994).

Table 5. 1. Comparisons of vervet monkey, humans, and other mammals on selected features of the testis.

Feature	Vervet	Humans	Other mammals	References (if necessary)
Sleeve like process	Defined	Not defined	Well defined in marmoset	Kumar and Phillips (1991)
Lysosomes	+	+	+	
Mitochondria	+	+	+	
Sertoli cell nucleus	4-5 lobes	3 lobes	Less lobed	
Charcot-Böttcher bodies	-	+	-	Ross <i>et al.</i> , (1995)
Collagen	+	+	+	(Fawcett <i>et al.</i> , 1973)
Crystals of Reinke	-	+	Reinke-like inclusions in marmoset	Prince (1999)

+ - Present and - - Absent



5.6. CONCLUSIONS

The ultrastructure of the vervet monkey testis was found to be similar to that reported in other nonhuman primates and showed many similarities with humans. The spermatogenic cells observed in this study are also similar to the ones observed in nonhuman primates and humans. This study could not identify the three populations of Leydig cells as reported by other researchers because only the adult reproductively mature animals were selected for this study. The absence of the crystals of Reinke in this animal model further suggests that these structures are confined to humans and not to any of the nonhuman primates studied. The fine structure of the Sertoli cells of the vervet monkeys was found to be different from that found in the humans, especially the nuclear shape. In the vervet monkey the Sertoli cell nucleus typically had four to five lobes. In humans the Sertoli cell

nucleus had three lobes. The multi-lobed nature of the Sertoli cell may be species specific in primates.



5. 6. REFERENCES

Bloom, W. and Fawcett, D. W. 1994. A Textbook of Histology. 12th Ed. Chapman and Hall. New York. London. pp 768-813.

Buehr, M., Gu, S. and McLaren, A. 1992. Mesonephric contribution to testis differentiation in the fetal mouse. *Development* **117**:273-281.

Byskov, A. 1986. Differentiation of mammalian embryonic gonad. *Physiol. Rev.* **66**:77-112.

Camatini, M., Franchi, P. and Decurtis, I. 1981. Ultrastructure of the Leydig cells in the African green monkey. *J. Ultra. Res.* **76**:224-234.

Capel, B. 2000. The battle of the sexes. *Mech. Dev.* **92**:89-103.

Chen, I. L., and Yates, R. D. 1975. The fine structure and phosphatase cytochemistry of the Golgi complex and associated structures in the Sertoli cells of Syrian hamsters. *Cell Tissue Res.* **157**:227-238.

Christensen, A. K. 1975. Leydig cells. In: Handbook of Physiology, Endocrinology V (eds. R. O. Greep and E. R. Asterwood). Williams and Wilkins Co. Baltimore. pp 1-19.

Cooke, P. S., Kirby, J. D., Bunick, D. and Hardy, M. P. 1994. Neonatal propylthiouracil treatment as a model system for studying factors controlling testis growth and sperm production. In: Function of somatic cells in the testis. (ed. A. Bartke) Springer Verlag. Norwel. pp 400-406.

De Kretser, D. M. and Kerr, J. B. 1994. The cytology of the testis. In: The Physiology of Reproduction. (eds. E. Knobil and J. D. Neil.) Raven Press. New York. pp 1177-1290.

De Rooij, D. G. and Russell, L. D. 2000. All you wanted to know about spermatogonia but were afraid to ask. *J. Androl.* 2000. **21**:776-798.

Despopoulos, A. and Silbernagl, S. 1986. Color Atlas of Physiology. 3rd Ed. Thieme Inc. New York. pp 28-29.

Dixson, A. F. 1986. Plasma testosterone concentrations during postnatal development in the male common marmoset. *Folia Primatol.* **47**:166-170.

Dym, M. 1972. The fine structure of the monkey (*Macaca*) Sertoli cell and its role in maintaining the blood-testis barrier. *Anat. Rec.* **175**:639-656.

Dym, M. 1983. The male reproductive system. In: Histology: Cell and Tissue Biology. 5th Ed. (ed. L. Weiss) Macmillan Press. New York. pp 1000-1053.

Fawcett, D. W. 1975. Ultrastructural and function of the Sertoli cell. In: Handbook of Physiology. (eds. D. W. Hamilton and R. O. Greep) Sect &, vol. 5. American Physiology Society. Washington, D. C. pp 21-55.

Fawcett, D. W., Neaves, W. B. and Flores, M. N. 1973. Comparative observations on intertubular lymphatics and the organization of the interstitial tissue of the mammalian testis. *Biol. Reprod.* **9**:500-532.

Fouquet, J. P., Meusy-Dessole, N. and Dang, D. C. 1984. Relationships between Leydig cells morphometry and plasma testosterone during postnatal development of the monkey, *Macaca fascicularis*. *Reprod. Nutri. Dev.* **24**:281-296.

Franca, L. R., Hess, R.A., Cooke, P. S. and Russell, L. D. 1995. Neonatal hypothyroidism causes delayed Sertoli cell maturation in rats treated with propylthiouracil: evidence that the Sertoli cell controls testis growth. *Anat. Rec.* **242**:57-69.

Galdieri, M. Monaco, L. and Stefanini, M. 1977. Secretion of androgen binding protein by Sertoli cells is influenced by contact with germ cells. *J. Androl.* **5**:409-415.

Haider, S. G. 2004. Cell biology of Leydig cells in the testis. *Int. Rev. Cytol.* **233**:181-241.

Haider, S. G. and Servos, G. 1998. Ultracytochemistry of 3 β -hydrosteroid dehydrogenase in Leydig cell precursors and vascular endothelial cells of the postnatal rat testis. *Anat. Embryol.* **198**:101-110.

Hardy, M. P., Zirkin, B. R. and Ewing, L. L. 1989. Kinetics studies on the development of the adult population of Leydig cells testes of the pubertal rat. *Endocrinol.* **124**:762-770.

Heckert, L. L. and Griswold, M. D. 2002. The expression of the follicle-stimulating hormone receptor in spermatogenesis. *Recent. Prog. Horm. Res.* **57**:129-148.

Joyce, K. L., Porcelli, J. and Cooke, P. S. 1993. Neonatal goitrogen treatment increases adult testis size and sperm production in the mouse. *J. Androl.* **14**:448-455.

Karl, J. and Capel, B. 1998. Sertoli cells of the mouse testis originate from the coelomic epithelium. *Dev. Biol.* **203**:323-333.

Kerr, J. B. 1988. An ultrastructural and morphometric analysis of the Sertoli cell during the spermatogenic cycle in the rat. *Anat. Embryol.* **179**:191-203.

Kuopio, T., Tapanainen, J., Pelliniemi, L. J. and Huhtaniemi, I. 1989. Developmental stages of fetal-type Leydig cells in pubertal rats. *Development* **107**:213-220.

Kumar, R. A. and Phillips, D. M. 1991. Spermiation and sperm maturation in the marmoset. *Anat. Rec.* **229**:315-320.

Lunn, S. F., Recio, R., Morris, K. and Fraser, H. M. 1994. Blockade of the neonatal rise in testosterone by a gonadotrophin-releasing hormone antagonist: Effects on timing of puberty and sexual behaviour in the male marmoset monkey. *J. Endocrinol.* **141**:439-447.

Merchant-Larios, H., Moreno-Mendoza, N. and Buehr, M. 1993. The role of the mesonephros in cell differentiation and morphogenesis of the mouse fetal testis. *Int. J. Dev. Biol.* **37**:407-417.

Morales, C. and Clermont, Y. 1982. Evolution of Sertoli cells processes invading the cytoplasm of rat spermatids. *Anat. Rec.* **203**:233-244.

Nishino, K., Yamanouchi, K., Naito, K. and Tojo, H. 2001. Characterization of mesonephric cells that migrate into the XY gonad during testis differentiation. *Exp. Cell. Res.* **267**:225-232.

Orth, J. M. 1993. Cell biology of testicular development in fetus and neonate. In: *Cell Biology and Molecular Biology of the Testis.* (eds. C. Desjardins and L. Ewing) Oxford University Press. New York. pp 3-42.

Parvinen, M. 1982. Regulation of the seminiferous epithelium. *Endocrinol. Rev.* **3**:404-417.

Pelliniemi, L. J. 1975. Ultrastructure of the early ovary and testis in pig embryos. *Am. J. Anat.* **144**:89-111.

Pelliniemi, L. J., Frojzman, K. and Paranko, J. 1993. Embryological and prenatal development and function of Sertoli cells. In: *The Sertoli Cell.* (eds. L.D. Russell and M. D. Griswold) Clearwater, Cache River Press. Florida. pp 87-114.

Prince, F. P. 1999. A Reinke-like inclusion within the Leydig cells of the marmoset monkey (*Callithrix jacchus*). *J. Anat.* **195**:311-313.

Prince, F. P. 2001. The triphasic nature of Leydig cell development in humans, and comments on nomenclature. *J. Endocrinol.* **168**:213-216.

Ramos, A. S. and Dym, M. 1979. Ultrastructural differentiation of rat Sertoli cells. *Biol. Reprod.* **21**:909-922.

Rey, R. A., Nagle, C. A. and Chemes, H. 1996. Morphometric study of the testicular interstitial tissue of the monkey *Cebus apella* during postnatal development. *Tissue Cell.* **28**:31-42.

Ross, M. H., Romrell, L. J. and Kaye, G. I. 1995. *Histology: A Text and Atlas.* 3rd Ed. Lippincott and Wilkins. Philadelphia. pp 636-665.

Russell, L. D., Ettlin, R.A., Sinha Hikim, A. P. and Clegg, E. D. 1990. *Histological and Histopathological Evaluation of the Testis.* Cache River Press. Clearwater. Florida.

Sakai, Y., Nakamoto, T. and Yamashina, S. 1988. Dynamic changes in Sertoli cell Processes invading spermatid cytoplasm during mouse spermiogenesis. *Anat. Rec.* **220**:51-57.

Sapsford, C. S. and Rae, C. A. 1969. Ultrastructural studies on Sertoli cells and spermatids in the bandicoot and ram during the movement of mature spermatids into the lumen of the seminiferous tubule. *Aust. J. Zool.* **17**:415-445.

Sharpe, R. M., McKinnell, C., Kivlin, C. and Fischer, J. S. 2003. Proliferation and functional maturation of Sertoli cells cells, and their relevance to disorders of testis function in adulthood. *Reproduction* **125**:769-784.

Shupnik, M. A. and Schreihofner, D. A. 1997. Molecular aspects of steroid hormone action in the male reproductive axis. *J. Androl.* **18**:341-344.

Skinner, M. K. 1991. Cell-cell interactions in the testis. *Endocrinol. Rev.* **12**:45-77.

Steiner, R. A. and Bremner, W. J. 1981. Endocrine correlates of sexual development in the male monkey, *Macaca fascicularis*. *Endocrinology* **109**:914-919.

Ueno, H. and Mori, H. 1990. Morphometrical analysis of Sertoli cell ultrastructure during the seminiferous epithelial cycle in rats. *Biol. Reprod.* **43**:769-776.

Van der Horst, G. 2005. Reproduction. In: *The Handbook of Experimental Animals. The Laboratory Primate.* (ed. S. Wolfe-Coote). Chapter 31. Elsevier Academic Press. Amsterdam. pp 527-536.

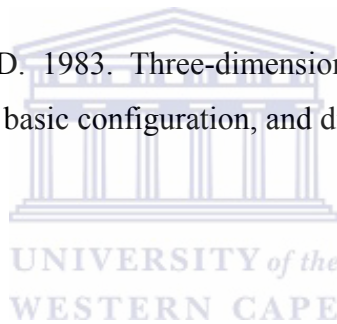
Vergouwen, R. P., Jacobs, S. G., Huiskamp, R., Davids, J. A. and De Rooij, D. G. 1991. Proliferative activity of gonocytes, Sertoli cells and interstitial cells during testicular development in mice. *J. Reprod. Fertil.* **93**:233-243.

Vihko, K. K., Souminen, J. J. O. and Parvinen, M. 1984. Cellular regulation of plasminogen activator secretion during spermatogenesis. *Biol. Reprod.* **31**:383-389.

Wartenberg, H., Kinsky, I., Viebahn, C. and Schmolke, C. 1991. Fine structural characteristics of testicular cord formation in the developing rabbit gonad. *J. Electron. Microsc. Tech.* **19**:133-157.

Winter, J. S. D., Hughes, I. A., Reyes, F. I. and Faiman, C. 1976. Pituitary gonadal relations in infancy. 2. Patterns of serum gonadal steroid concentrations in man from birth to two years of age. *J. Clin. Endocrinol. Metabol.* **42**:679-686.

Wong, V. and Russell, L. D. 1983. Three-dimensional reconstruction of a rat stage V Sertoli cell: I. Methods, basic configuration, and dimensions. *Am. J. Anat.* **167**:143-161.



CHAPTER 6: STAGING OF SPERMATOGENESIS IN THE VERVET MONKEY

6.1. INTRODUCTION

Spermatogenesis can be defined as a complex, synchronized, and very organized process by which undifferentiated germ cells, which are diploid are transformed into mature haploid spermatozoa. It lasts for about 30 to 75 days in mammals (Russell *et al.*, 1990; Hess and Chen, 1992). The process of spermatogenesis includes processes of mitotic divisions of spermatogonia, meiotic divisions of spermatocytes yielding germ cells, and the morphological differentiation and maturation of round spermatids into elongated spermatids (Weinbauer, *et al.*, 2001; Hess and Chen, 1992). The germ cells advance within the seminiferous epithelium, with the older cells being associated with younger ones in a specific cycle. The germ cell associations are known as the stages of spermatogenesis, and these stages vary in number and duration in a species-specific manner. Ideally, each stage should have three generations of spermatocytes and spermatids (Johnson *et al.*, 1992). However, the critical criterion for stage classification is based upon the morphological development of the spermatids (Clermont, 1972; Russell *et al.*, 1990). In addition, the formation of spermatids is based upon the changes in the development of nucleus, acrosome, and flagellum (Haider *et al.*, 1989). An exact description of phases of spermiogenesis is a prerequisite to define stages of spermatogenesis in a given species (Leblond and Clermont, 1952a).

In the mammalian group, there are two different types of topographical arrangements of the spermatogenic stages. The topographical arrangements are based on the number of stages in a given cross-section of the seminiferous tubule. In rodents, only one specific spermatogenic stage is seen in a round cross-section of a seminiferous tubule. An orderly succession of the consecutive stages along the tubules was discovered from the analysis of longitudinal tubular sections (stage I, followed by stage II, stage III, etc). This type of topographical arrangement is known as the wave of the spermatogenic process. In other species however, such as the chimpanzees, *Pan troglodytes* (Smithwick *et al.*, 1996) and humans, (Clermont 1963;

Heller and Clermont, 1964), more than one or several spermatogenic stages can be recognized within the same tubular cross section. In the cynomolgus monkey (*Macaca fascicularis*) and olive baboon (*Papio anubis*), an intermediate arrangement was observed. In the baboon, 60% of the tubule sections showed the presence of one stage and 40% showed presence of two or three stages. It has been proposed for the human testis that the presence of several stages results from a helical / spiral organization of spermatogenesis, which again is referred to as a random organization (Shulze and Rehder, 1984; Weinbauer *et al.*, 2001).

Clermont (1969), studied the process of spermatogenesis in vervet monkeys and highlighted 12 different stages. In his study, he reported the two main classes of spermatogonial stem cells: the type A₁ and the type A₂ spermatogonia. The same arrangement and types of spermatogonia are also observed in the olive baboon, *Papio anubis* (Chowdhury and Steinberger, 1976). The type A₁ spermatogonia seemed to be quiescent at all the stages of the cycle and they would not normally participate in the production of the primary spermatocytes. These cells were called the reserve stem cells. The type A₂ spermatogonia appeared to be elements that periodically at each cycle of the seminiferous epithelium entered into divisions and yielded new type A₂ spermatogonia and may thus be referred to as the renewing stem cells. The four generations of type B spermatogonia (B₁-B₄), committed to the production of spermatocytes should then be considered as differentiated spermatogonia (Clermont, 1969). The type A₂ spermatogonia would divide at stages IX-X of the cycle and yield a new pair of type A₂ spermatogonia, that would remain dormant until stage IX-X of the next cycle. The A₂ will yield a pair of type B₁ spermatogonia which in stage XII would provide type B₂ cells. Type B₂ spermatogonia would give rise to B₃ during stage II. In stage IV, the type B₃ spermatogonia will give rise to B₄ and finally B₄ will give rise to spermatocytes in stage VI (Clermont, 1969). However, other researchers challenged the 12 stage arrangement that was found in vervet, and presented criteria which clearly described primate spermatogenesis (Heller and Clermont, 1964; Dietrich *et al.*, 1986; Weinbauer *et al.*, 2001; McLachlan *et al.*, 2002). Each stage is represented by a specific group of germ cell associations. The

six stage spermatogenic process was also reported in vervet monkeys, but a clear description of those stages needs to be elucidated (Wistuba *et al.*, 2003). This study will focus on a nine-stage classifying system which was used by Holt and Moore (1984).

6.1.1. Type A Spermatogonia

Clermont (1969) identified two classes of the type A spermatogonia: type A₁ and type A₂. The type A₁ spermatogonia possess distinctive nuclear characteristics. They have a spherical or ovoid nucleus which contained a homogenous, finely granulated and deeply stained chromatin. The nuclear chromatin of type A₁ spermatogonia is retracted and separated by an irregular space from the nuclear membrane whereas type A₂ spermatogonia showed discoid nuclei containing pale stained coarse chromatin granulation. One or two globular nuclei associated with the nuclear membrane were separated from the chromatin by an unstained space. Most distinguishing feature of the type A cytoplasm is that larger areas may be found which contain only ribosomes, either free or clustered as polyribosomes. Round profiles of the smooth endoplasmic reticulum are scattered throughout the cell but they are not found in all sections. There is a moderate Golgi complex and its associated small vesicles are usually located in the supranuclear region. Round mitochondria with transverse cristae are located singly or in small groups at each end of the oblong nucleus. Lysosomes, dense granules and multi-vesicular bodies are also common organelles which are clearly observed in the cytoplasm of these cells. Certain fine structural modifications in the type A₂ were observed in stages IX, X, and XI. The nuclei increase in size accompanied by an increase in nuclear dimensions and flakes of chromatin appear along the nuclear membrane (Cavicchia and Dym, 1978).

6.1.2. Type B Spermatogonia

Clermont (1969) noted four categories of type B spermatogonia of similar ultrastructure. These rounded cells have a limited contact with the basal lamina and

are observed in all stages of the cycle except the VII, VIII, and IX. A striking observation made was the fact that the cytoplasm of type B spermatogonia contains more endoplasmic reticulum than the cytoplasm of the type A spermatogonia. Also, with the cytoplasm of the type B spermatogonia, there is a small Golgi apparatus and round mitochondria, many of them having dilated cristae (Cavicchia and Dym, 1978). The mitochondria are usually not clustered. There is a centrally located nucleus which is oval and spherical in outline. It contains discrete clumps of chromatin close to the nuclear envelope and one or two nucleoli in the central region. The nucleoplasm of the type B spermatogonium is relatively homogenous and consists of fine granules with a staining pattern similar to the type A spermatogonium (Cavicchia and Dym, 1978).

6.1.3. Preleptotene Spermatocytes

These cells have less contact with the basal lamina of the seminiferous epithelium than the type B spermatogonia. Many of these cells are completely detached from the tunica propria. The nucleoplasm is more clumped than the type B spermatogonia. It consists of irregular patches of light and dark regions clumps of chromatin that are associated with the nuclear envelope and the nucleolus. The nuclei are perfectly spherical and are located in the central part of the cell. The cytoplasm of the preleptotene spermatocytes resembles that of the type B spermatogonia (Cavicchia and Dym, 1978; Dym and Cavicchia, 1978).

6.1.4. Primary Spermatocytes

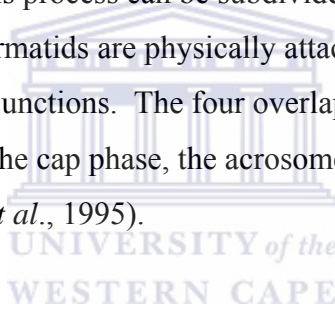
These cells are normally found in one of following four stages of the first prophase: leptotene, zygotene, pachytene, and diplotene. As meiosis proceeds through leptotene and zygotene, the nuclei enlarge and display a progressive increase in the amount of chromatin clumping. Spermatocyte differentiation during the long meiotic prophase is a very gradual process occupying approximately 16 days in monkeys. It is not possible to detect morphological differences between cells in continuous steps of differentiation, e.g. late leptotene and early zygotene because

these cells appear identical at the fine structural level (Dym and Cavicchia, 1978). The leptotene stage is characterized by chromosomes which become more apparent and appear as thin linear structures. In the zygotene stage, chromosomes are paired and become more condense within the nuclei. In addition, during the zygotene stage an unusual tripartite structure, the synaptonemal complexes become visible in the nuclei (Dym and Cavicchia, 1978). The pachytene stage which is regarded as the more distinct and prominent stage, is characterized by the completion of chromosomal pairing. The chromosomes will become shorter and thicker at the ends and will split longitudinally into chromatids, and the centromere remaining single in the pachytene stage. These four chromatids, from the two chromosomes constitute a bivalent. There is also a marked increase in nuclear and cellular volume as the cells progress through the pachytene stage. The pachytene stage is regarded as very long, occupying about 16 days in humans. Cells in the pachytene stage are therefore clearly visible and common in most cross sections of the seminiferous tubules. Diplotene stage, which is the last stage, is characterized by cells with comparatively large nuclei. The chromosomes in this stage will further shorten, broaden and ultimately coil (Weiss, 1983).

Much research has been conducted on the cycle of the seminiferous epithelium, its duration and the mode of renewal of spermatogonia in different primates. The cellular maturation steps characteristic of spermatogenesis, the cellular associations composing the various stages of the spermatogenic cycle, the distribution of these functional regions which compose the seminiferous tubular epithelium, and the pattern of spermatogenesis have been reported in *Macaca mulatta*, (de Rooij *et al.*, 1986); *Macaca arctoides* (Clermont and Antar, 1973); *Macaca fascicularis* (Kluin *et al.*, 1983; Fouquet and Dadoune, 1986); *Otolemur garnetti* (Ojoo *et al.*, 2005) and in humans (Clermont, 1963; Heller and Clermont, 1964; Johnson *et al.*, 2001). Certain comparisons will be made to serve as guidelines for classifying the germinal epithelium of *Chlorocebus aethiops*.

6.2. SPERMIOGENESIS AND ITS PHASES

Spermiogenesis is defined as the process of differentiation of the newly formed spermatids to mature spermatozoa just before their release into the lumen (Dym, 1983). This process involves complex morphological, biochemical, and physiological alterations of postmeiotic germ cells resulting in the formation of spermatozoa (Behr *et al.*, 2000). The major events in this extraordinarily complex process involve elaboration of the acrosome from the Golgi apparatus, condensation and elongation of the nucleus, formation of motile flagellum, and extensive shedding of the cytoplasm. In mammals, acrosome biogenesis begins with the fusion of proacrosomal granules synthesized by the Golgi apparatus in pachytene spermatocytes, similar to the formation of secretory granules in many other cell types (Moreno *et al.*, 2000). This process can be subdivided into four successive phases which occur while the spermatids are physically attached to the Sertoli cell plasma membrane by specialized junctions. The four overlapping phases reported are as follows: the Golgi phase, the cap phase, the acrosome phase, and the maturation phase (Dym, 1983; Ross *et al.*, 1995).



6.2.1. Golgi phase

During this phase, the acrosomal vesicle attaches to the nuclear envelope and grows as a result of the constant arrival and fusion of Golgi-derived vesicles (Moreno *et al.*, 2000). Furthermore, this phase is characterized by the appearance of the periodic acid Schiff–positive granules in the region of the Golgi apparatus. These proacrosomic granules are rich in glycoproteins, soon fuse within a membrane–bounded acrosomic vesicle, containing a single large granule, the acrosomic granule that becomes closely applied to the nuclear envelope (Dym, 1983).

In many species the mitochondria suddenly migrate towards the periphery of the cytoplasm to lie very close to the plasma membrane. The centrioles migrate from the juxtannuclear region to the posterior pole of the spermatid, where the distal centriole aligns at right angles to the plasma membrane. The distal centriole initiates

the synthesis of nine peripheral microtubule doublets and two central microtubules that constitute the axonemal complex of the sperm tail (Ross *et al.*, 1995).

6.2.2. Cap phase

The acrosomal vesicles spread to cover the anterior half of the nucleus and become further condensed. The acrosomal cap is derived from the reshaping of the membrane of the acrosomal vesicle. This cap consists of an outer and inner acrosomal membrane enclosing the acrosomal contents (Ross *et al.*, 1995).

6.2.3. Acrosome phase

The spermatid reorientates itself so that the head becomes deeply embedded in the Sertoli cell and points towards the basal lamina. The developing flagellum extends into the lumen of the seminiferous tubule. The cytoplasmic microtubule becomes organized into a cylindrical sheath, and the manchette extends from the posterior rim of the acrosome towards the posterior pole of the spermatid. It is during this phase whereby the nucleus begins to progressively flatten and elongate while the chromatin granules enlarge and become uniform in size and dispersed. The Golgi complex detaches itself from the anterior pole of the nucleus and migrates freely in the cytoplasm when the acrosome ceases growing (Dym, 1983; Ross *et al.*, 1995).

6.2.4. Maturation phase

The maturation phase is characterized by the pinching off and phagocytosis of excess cytoplasm by the Sertoli cells. The intercellular bridges that have characterized the developing gametes since the pre-spermatocyte stages remain with the residual bodies. The maturation phase is further characterized by the release of spermatids from the Sertoli cells, especially those that are no longer attached to one another (Ross *et al.*, 1995).

6.3. SERTOLI CELL ASSOCIATIONS AND ACTIVITY

The Sertoli cell has been extensively studied. However, some of the physiological functions of the Sertoli cells within the testis remain elusive. There is a clear anatomical and histological relationship between Sertoli cells and germ cells which has been reported as early as 1865 by Enrico Sertoli (1842-1910). Histochemical and morphological studies have indicated that Sertoli cells undergo cyclic changes in their metabolic activity related to specific stages in the cycle of the seminiferous epithelium. Thus, the Sertoli cell receptors for FSH and androgen, according to the differentiation stage of the guest germ cells at the moment, elicit complex Sertoli cell responses, leading to an increase of metabolic activity and nuclear–cytoplasmic transport (Kangasniemi *et al.*, 1990; Heckert and Griswold, 1991; Griswold, 1993; Cavicchia *et al.*, 1998). Stages VI, VII, and VIII are maximally androgen dependent whereas stages XIII, and XIV, and I are more influenced by FSH in rats (Sar *et al.*, 1993). These changes appear to be analogous to changes occurring in the granulosa cells during the follicular growth and maturation in the ovary (Ross, *et al.*, 1995). Russell and Peterson, (1985) reported that Sertoli cells can assume two broadly different shapes as they interact with germ cells during the cycle of the seminiferous epithelium. Sertoli cells with spermatids within deep crypts were designated as type A, and Sertoli cells where the crypts were absent because of the apical movements of spermatids destined for release were designated as type B. Experiments performed on three different animal models showed that the ratio of spermatids to Sertoli cells remained relatively constant (Hess *et al.*, 1993). The conclusion drawn was that the number of germ cells appears to be directly related to the number of Sertoli cells and probably to their synthetic capability.

Parvinen (1993) reported that there are techniques which were used to show that the secretions by Sertoli cells and thus the immediate environment in the seminiferous epithelium vary as a function of the stage of the cycle. Sertoli cells associated with germ cells at one stage of the cycle express genes different from those in the other parts of the cycle. Erickson-Lawrence *et al.*, (1991), showed that

cathepsin L is a protease and is secreted from Sertoli cells at stages VI and VIII, whereas cystatin is a protease inhibitor specific for cathepsin L and is secreted primarily at stages XII and II in the cycle of the seminiferous epithelium of the rat.

In this project, a general ultrastructural account will be given, supported by some light microscopic work, of the process of spermatogenesis in the vervet monkey. This will be accompanied by a proposed system of classification of spermatogenic steps, spermiogenesis and its phases, and Sertoli cell activity in different stages of the seminiferous epithelium. This is important for future studies which may involve toxicological, pharmacological or experimental research programs.

6.4. OBJECTIVES

- To determine the organization of the germ cells within the seminiferous epithelium of the vervet monkey.
- To study the specific types of spermatogenic cells and their associations in the vervet monkey.
- To study the process of spermiogenesis.
- To study some key features of the structure and cellular interactions in the vervet monkey testis.
- To compare the process of spermatogenesis in the vervet monkey to that of humans and other mammals.

6.5. MATERIALS AND METHODS

Study animals and their maintenance, sample collection, and dissection procedures were the same as in previous chapters. Ethical clearance was obtained from the Medical Research Council's Ethical Committee for this study.

Small pieces of testicular tissue were fixed in 2.5 % Sorenson 's phosphate buffered glutaraldehyde. After fixation, the tissues were post fixed in a mixture of 1% osmium tetroxide and 1.5% potassium ferrocyanide, dehydrated, embedded in

Epon and sectioned for electron microscopy. Sections were stained with uranyl acetate and lead citrate, and examined.

Some tissue samples were fixed in Bouin's and subsequently embedded in paraffin wax. Processing was done as in previous chapters. Sections (5 µm) were stained using the iron hematoxylin/periodic acid-Schiff technique for the demonstration of acrosomal structures.

For high resolution light microscopy, methacrylate resin embedded tissues were sectioned at a thickness of 1µm. Sections were stained with 1% toluidine blue to provide the fine nuclear detail essential for distinguishing the various stages of spermatid development because of less superimposition of structures.

6.6. STAGING OF SPERMATOGENESIS

Testes sections were viewed under a Universal transmitted-light research microscope (Zeiss) (100X oil immersion) using the haematoxylin and eosin slides prepared for light microscopy. Thirty seminiferous tubules were selected to investigate the stages present during spermatogenesis in *Chlorocebus aethiops*, in each of 10 vervet monkeys. Two random areas in each individual's seminiferous tubule were considered. The cellular associations clearly seen from the basement membrane to the lumen of the tubule in a specified order, within each area was thoroughly studied. Individual germ cells were identified using methacrylate resin sections, PAS stained sections, electron micrographs and use was made of the stage map published by Holt and Moore (1984). The different stages were recognized with the aid of the binary decision key and method of evaluation of stages used by Hess (1990). Stages of the seminiferous epithelium were identified, based on the changes in the morphology of acrosomes and nuclei of developing spermatids (Leblond and Clermont, 1952a), and the germ cell associations found within a given part of the epithelium (Ojoo *et al.*, 2005). In this way a table, similar to that produced by Clermont (1969), was constructed to illustrate the number of stages in the cycle of the seminiferous epithelium and the cellular composition of each stage. The different types of spermatogonial cells were defined by their nuclear and morphological

differences. Counts of the various types of spermatogonia per unit surface area of tubular wall were obtained.

6.7. STATISTICAL ANALYSIS

One way ANOVA was used to compare germ cell distribution in the lateral, medial, and middle regions of the testis. All data were presented as Mean \pm SEM, and $P < 0.05$ was considered statistically significant.

6.8. RESULTS

6.8.1. Staging of spermatogenesis

Spermatogenesis is a temporal event whereby relatively undifferentiated spermatogonia slowly evolve into highly specialized testicular spermatozoa over a specific time period (Figures 6.1 and 6.2). The photographic montage representing the progressing steps of spermatid development (steps 1-12) was established to aid in the staging of the spermatogenic cells (Figure 6.3.). In a mature testis, the rate at which germ cells develop is an absolute species-specific constant, and thereby, the duration of spermatogenesis is also constant. The seminiferous epithelium is composed of 5-6 generations of germ cells that are not randomly arranged but form cellular associations of fixed composition. Due to the precise and regular timing of the steps of spermatogenesis, spermatids at a given step of spermiogenesis are always associated with spermatocytes and spermatogonia at given steps of development. These cellular groupings which appear at regular intervals represent stages of a cycle of the seminiferous epithelium (Leblond and Clermont, 1952b).

Results will be represented in three groupings. The TEM micrographs will describe the process of spermiogenesis and spermatid development (Figures 6.4 to 6.13). The wax sections stained for PAS will elucidate the spermatid development and some of the stages (Figures 6.14 to 22). Lastly, the 1 μm methacrylate resin sections will describe the basic stages of spermatogenesis with all their cellular associations (Figures 6.23 to 6.32). The three above combined procedures are complimentary in order to elucidate the staging of spermatogenesis.

6.8.2. Electron Microscopy

6.8.3. Spermiogenesis

The developmental changes in spermatid structure during spermiogenesis were similar to those seen in other mammals, and were classified into twelve steps as outlined (Holt and Moore, 1984). The distinctions between steps were clearly studied by both light and electron microscopy. The schematic diagram of spermiogenesis in humans is illustrated in Figure 6. 2. Step 1 was characterized by the presence of a proacrosomal vesicle situated near the highly developed Golgi apparatus (Figure 6.4). Steps 2- 4 of spermiogenesis (Figure 6.5) involved flattening of the proacrosomal vesicle against one pole of the spermatid nucleus, and synthesis of acrosomal contents. Golgi apparatus consisted of several lamellae arranged in a crescent with its concavity facing the acrosome (Figures 6.4 to 6.13). The endoplasmic reticulum also observed near the Golgi apparatus, and numerous small vesicles were situated between these two organelles.

In steps 4 to 7, the spermatid nucleus becomes flattened, and some condensation of the chromatin granules occurred. The apical segment of the acrosome became extended anteriorly at about step 7. Nuclear condensation continued between steps 7-10, when it was virtually complete and the spermatid head had assumed its final shape (Figures 6.6 and 6.7).

Step 9 was characterized by the annulus that had not commenced its caudal migration and the mitochondria were not yet arranged helically about the axial filament (Figures 6.6 and 6.10). Steps 10-11 were characterized by the formation of the residual body. Spermiation occurred in the late step 11.

During the final development of the sperm tail, prior to the caudal migration of the annulus in steps 10-12, a swelling of the posterior middle piece became apparent (Figures 6.12 and 6.13), also refer to Table 6.1 which summarizes the description of spermatogenic stages.

Figures 6.14 to 6.22 represent light micrographs of wax sections stained for PAS. These results are important adjunct to define the various stages of

spermatogenesis on the basis of both spermatid development (PAS stains for glycoprotein of acrosome) and other spermatogenic cells. From these results stages I to III, VIII and XI could be elucidated (See description of stages in Table 6.1).

However, in order to give a comprehensive account of staging 1 μm methacrylate resin sections were used. These are represented in Figures 6.23 to 6.32. From these results stages I to VIII could be elucidated (See description of stages in Table 6.1).

Figures 6.33 and 6.34 represent the TEM micrographs showing the germ cellular associations with Sertoli cells. These micrographs assist in confirming the validity of cell types from 1 μm methacrylate resin sections.

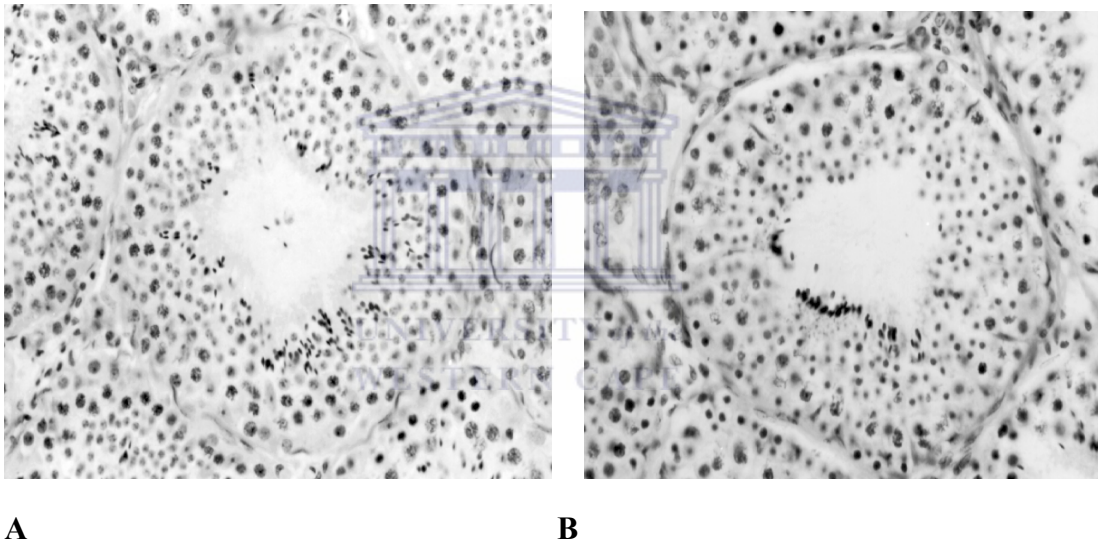


Figure 6. 1 (A and B). Light micrographs showing transverse sections through the seminiferous tubules of the vervet monkey, *Chlorocebus aethiops*.

The sections show the lumen, interstitial tissue, germinal epithelium, and peritubular tissue. The sections also show the general lay-out and arrangement of stages in a single cross-section of a seminiferous tubule.

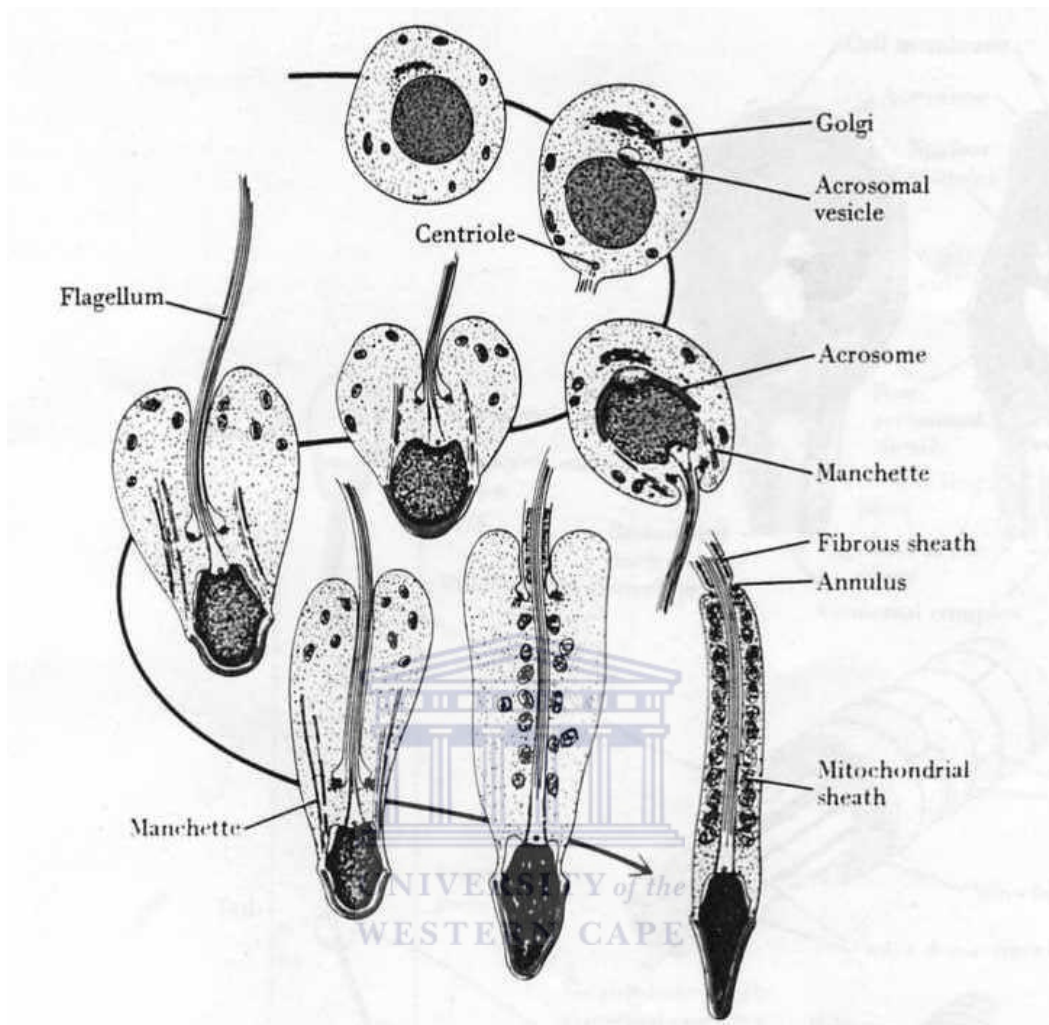


Figure 6. 2. Schematic diagram showing spermiogenesis in the human.

The basic changes in the structure of the key organelles of the spermatid are illustrated (Modified from Dym M: In: Cell and Tissue Biology, 1983. (ed. L. Weiss).

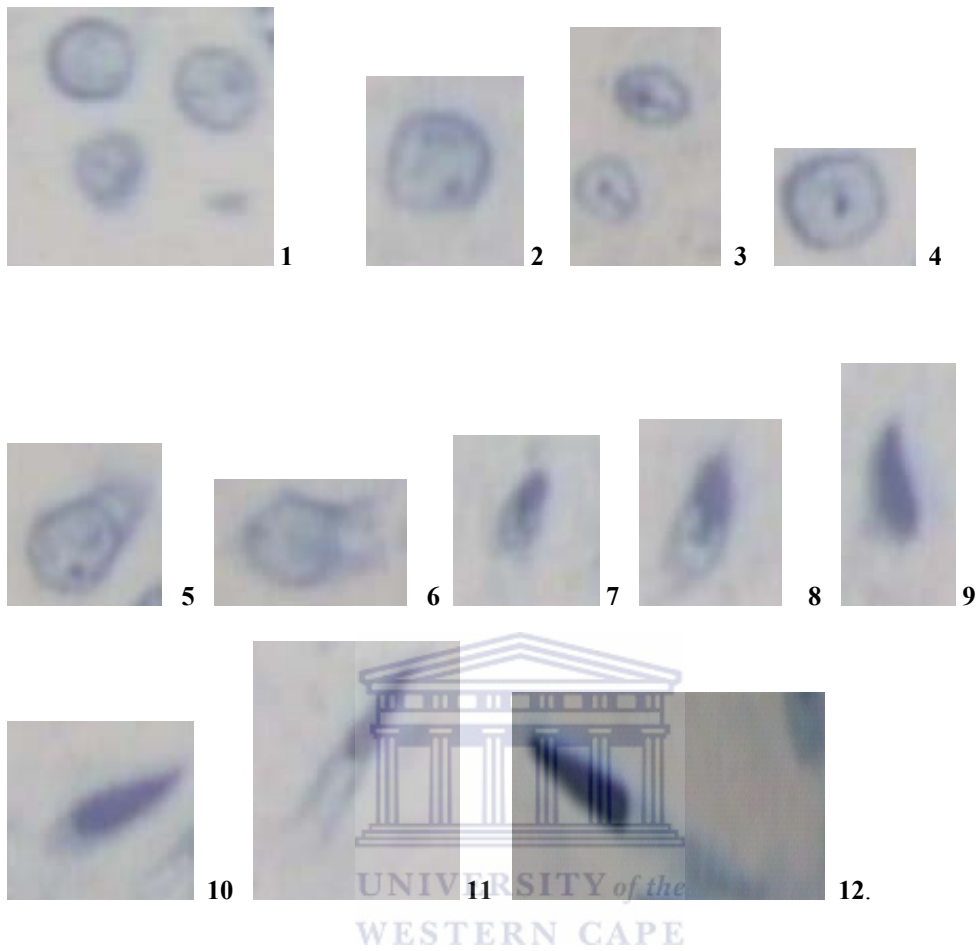
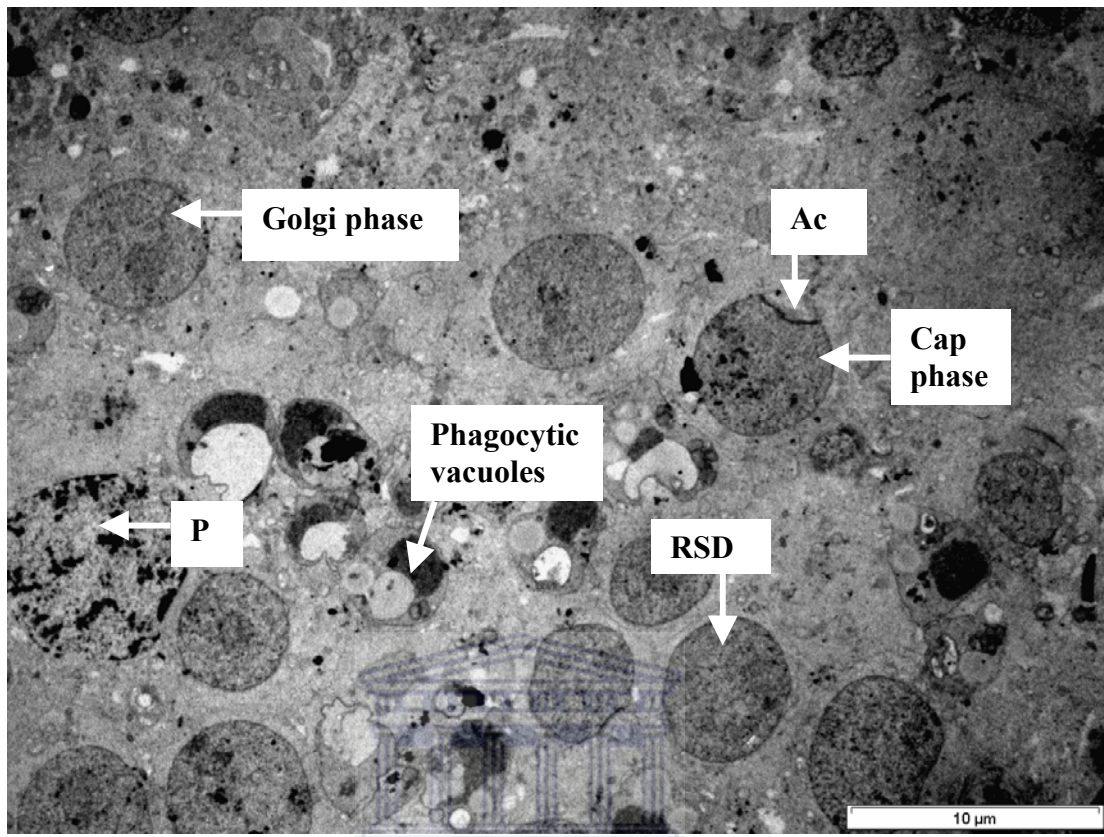


Figure 6. 3. Photographic montage representing the progressive steps of spermatid development (Steps 1-12) in the seminiferous tubules of the vervet monkey, *Chlorocebus aethiops*. using 1 μ m methacrylate resin sections.



UNIVERSITY of the

Figure 6. 4. TEM micrograph showing different phases of spermiogenesis and phagocytotic events in the seminiferous tubules of the vervet monkey, *Chlorocebus aethiops*.

AC - Acrosomal cap, P - Pachytene primary spermatocyte, and RSD - Round spermatid.

Steps 1 - 2 of spermatid development.

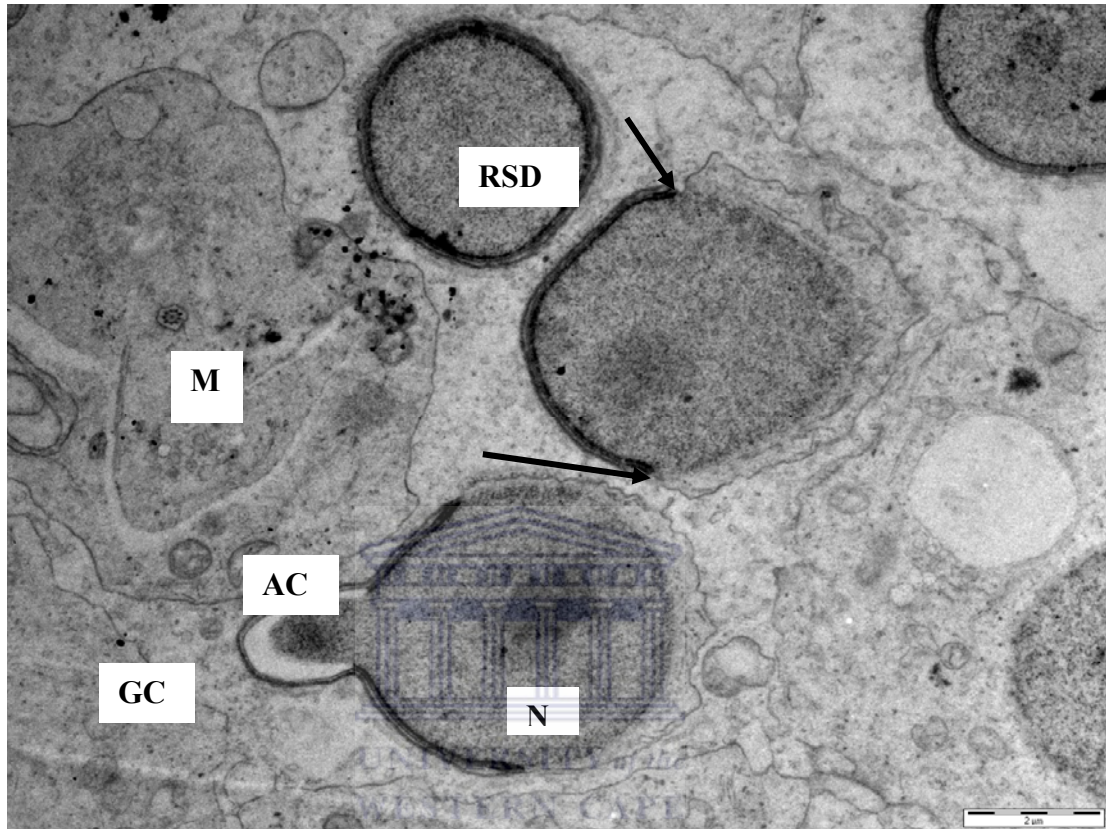


Figure 6. 5. TEM micrographs showing the different spermatids in their developing stages in the seminiferous tubules of the vervet monkey, *Chlorocebus aethiops*.

AC - Acrosomal cap, GC - Golgi complex, M - Mitochondria, N – Nucleus, RSD - round spermatids. arrows - spreading of the acrosomal vesicle. Steps 1 – 4 of spermatid development.

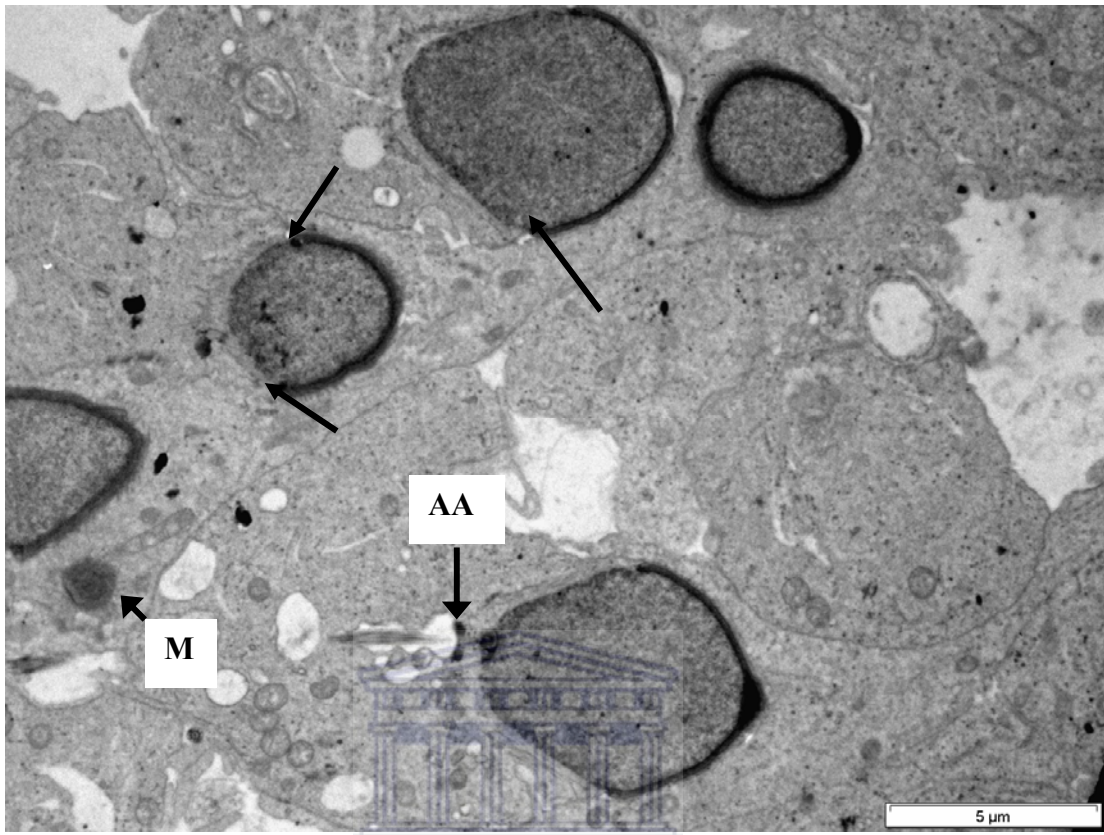


Figure 6. 6. TEM micrograph showing the different stages of the spermatids in seminiferous tubules of the vervet monkey, *Chlorocebus aethiops*.

Note the annulus anlage, manchette, and acrosomal vesicles.

**AA - Anlage of the future annulus, arrows - spreading of the acrosomal vesicle
M- Mitochondrion**

Steps 1 – 6 of spermatid development.

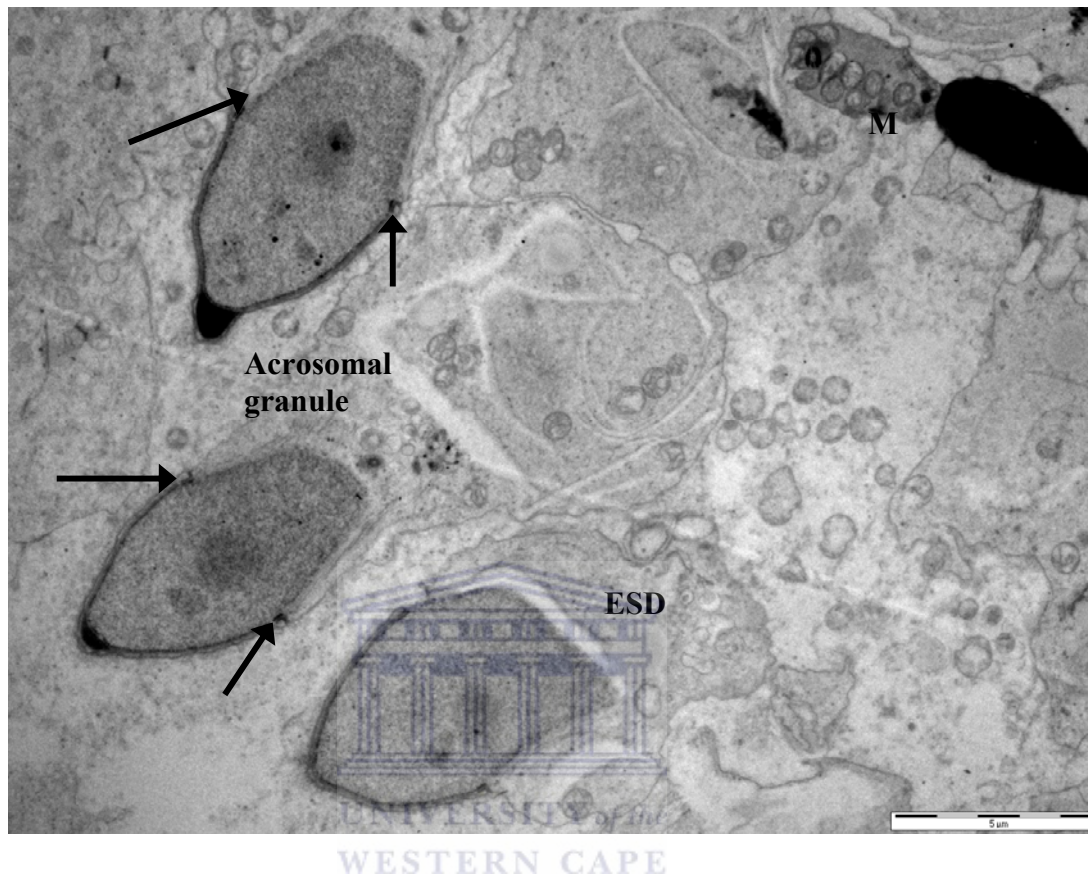


Figure 6. 7. TEM micrograph showing different stages of spermatids in a seminiferous tubule of the vervet monkey, *Chlorocebus aethiops*.

Arrows - spreading of the acrosomal vesicle, ESD – Elongated spermatid, M - Mitochondria.

Note the process of spermiogenesis.

Steps 6-8 of spermatid development.

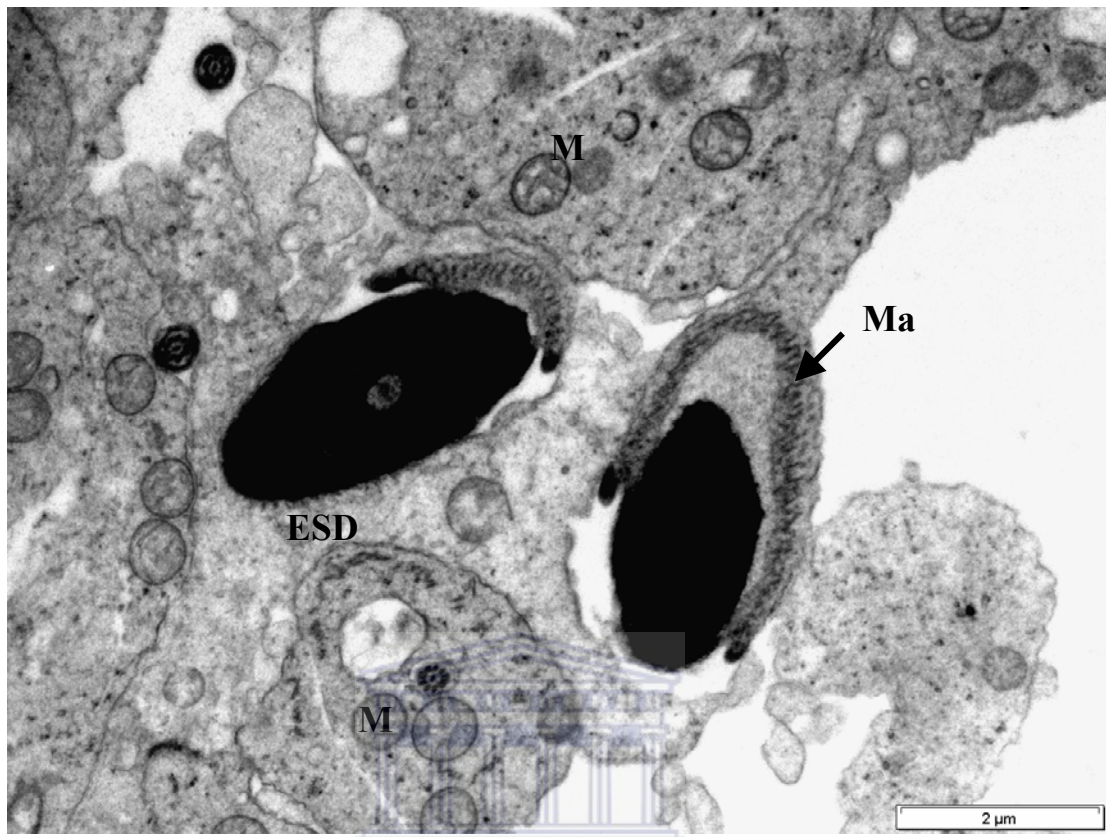


Figure 6. 8. TEM micrograph showing the manchette of the developing spermatid in the seminiferous tubules of the vervet monkey, *Chlorocebus aethiops*.

**ESD - elongated spermatid, M - Mitochondria, Ma - Manchette.
Step 9 – 10 of spermatid development.**

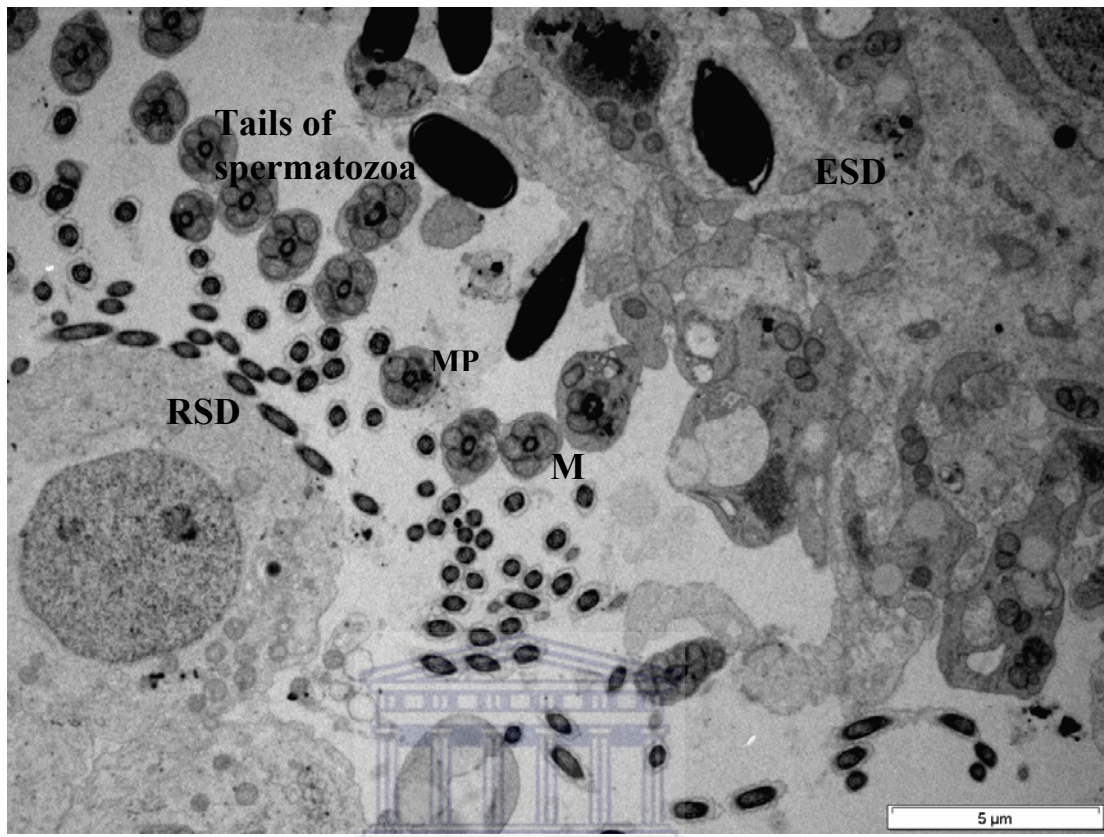


Figure 6. 9. TEM micrograph showing different phases of spermiogenesis in the seminiferous tubules of the vervet monkey, *Chlorocebus aethiops*.

ESD - Elongated spermatids, M - Mitochondria, MP – Midpiece, RSD - Round spermatids

Steps 1 and 11 of spermatid development

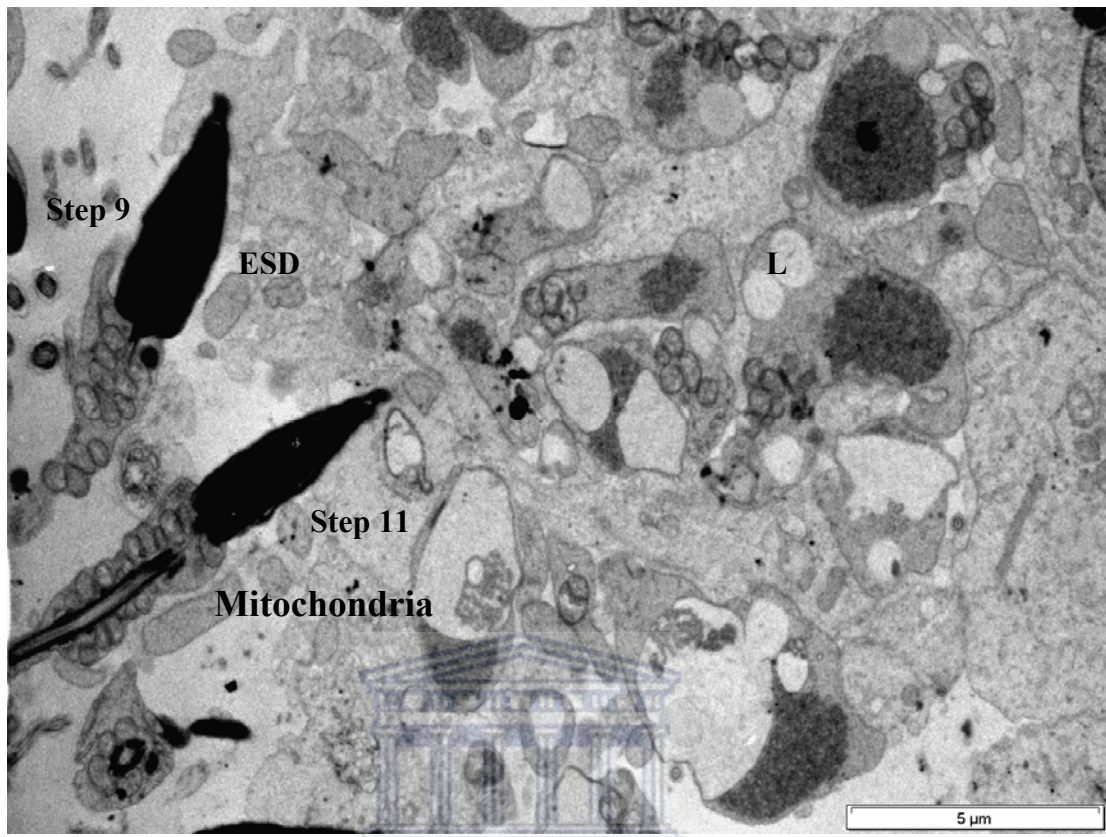


Figure 6. 10. TEM micrograph showing an elongated stage of the spermatid with helical mitochondrial arrangement in the seminiferous tubules of the vervet monkey, *Chlorocebus aethiops*.

ESD - Elongated spermatid, L - Lipid droplet

Steps 9 – 11 of spermatid development.

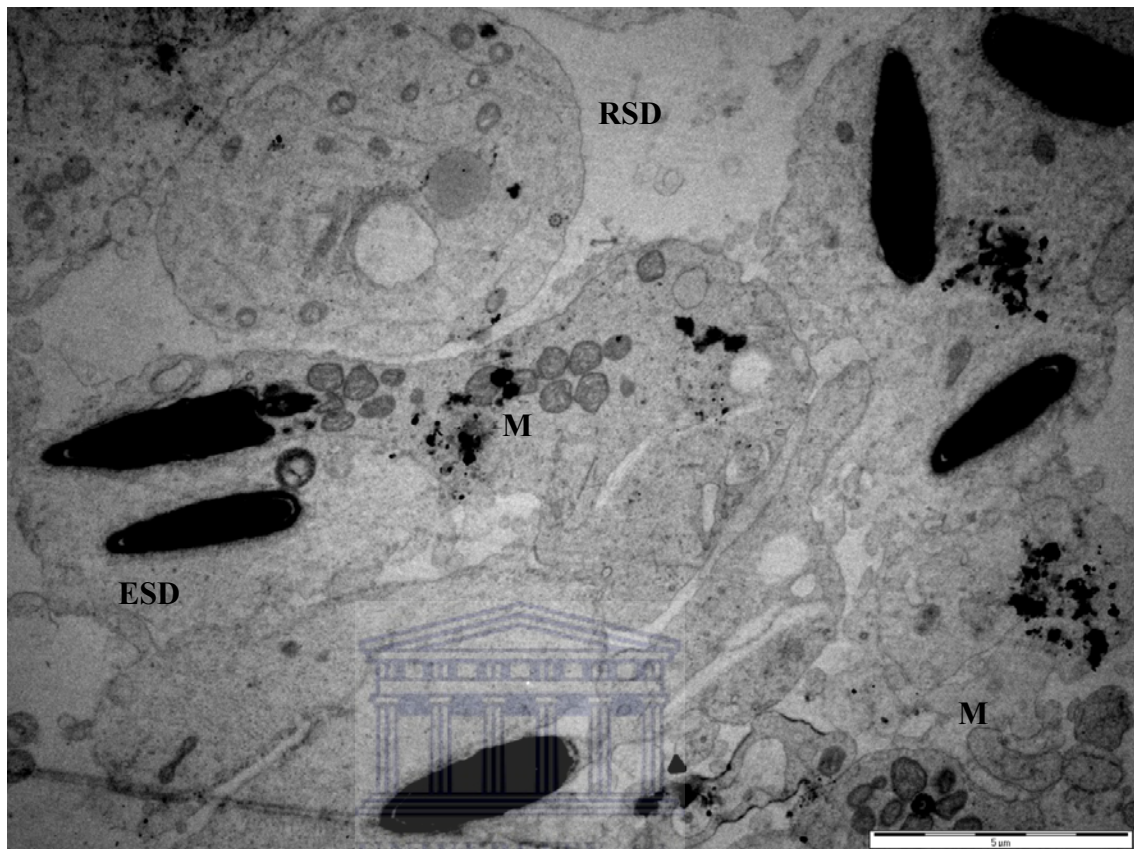


Figure 6. 11. TEM micrographs showing the different spermatids in their developing stages in the seminiferous tubules of the vervet monkey, *Chlorocebus aethiops*.

ESD - Elongated spermatids, M - Mitochondria, RSD - Round Spermatids

Steps 10 – 11 of spermatid development.

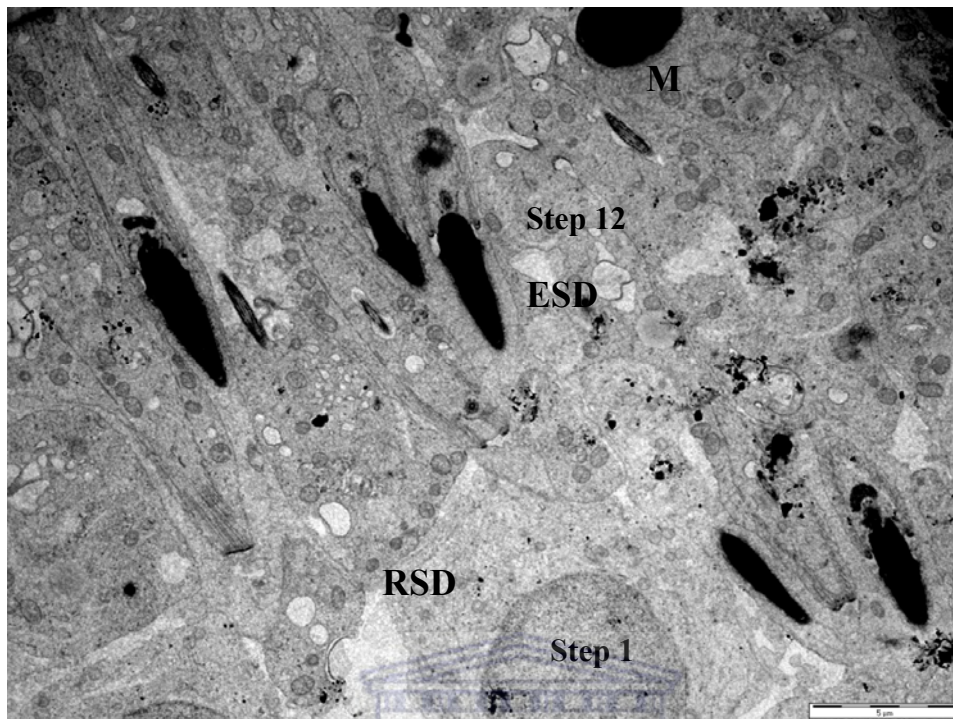


Figure 6. 12. TEM micrograph showing the elongated spermatids during spermiogenesis in the vervet monkey, *Chlorocebus aethiops*.

ESD - Elongated spermatids, RSD - Round Spermids

Step 1 and 12 of spermatid development

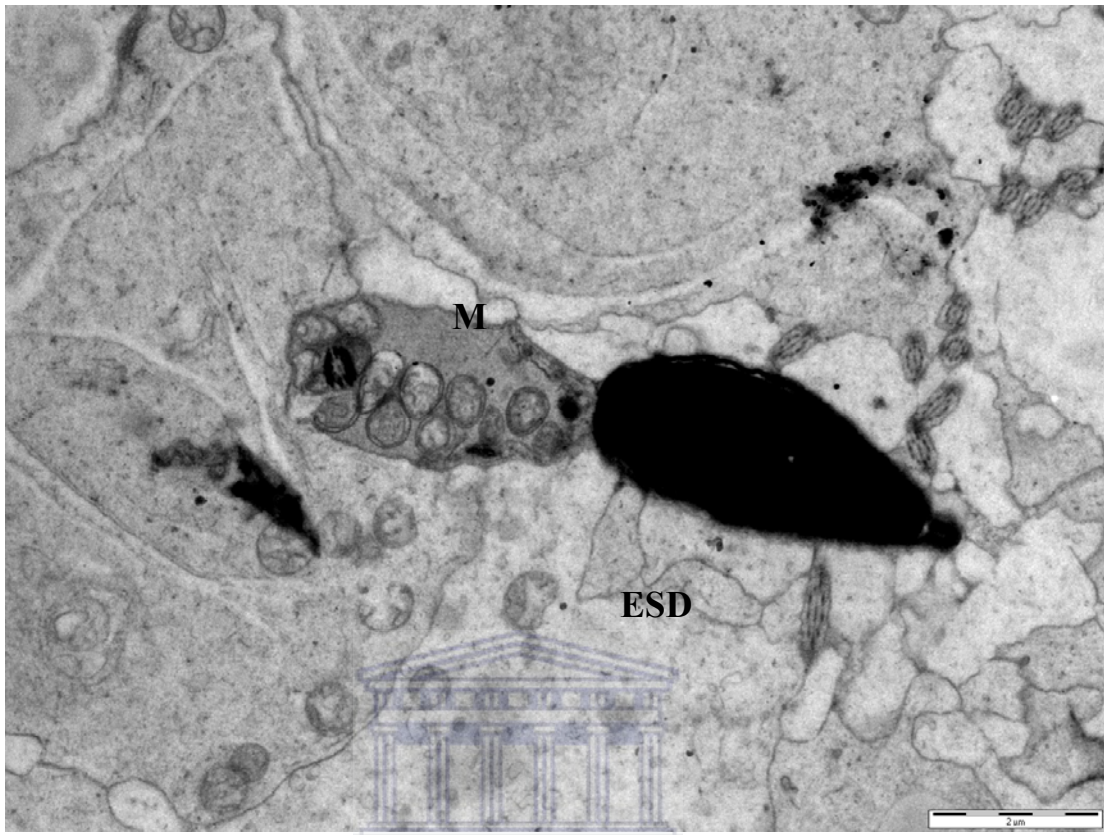


Figure 6. 13. TEM micrograph showing an elongated stage of the spermatid with spherical mitochondrial arrangement in the seminiferous tubules of the vervet monkey, *Chlorocebus aethiops*.

ESD - Elongated spermatids, M - Mitochondria

Step 11 of spermatid development.

Table 6. 1. Description of stages.

Stage I: This stage was characterized by the presence of two generations of the spermatids. The first generation comprised of newly formed spermatids with small spherical nuclei. The other generation consisted of older maturing and elongated spermatids. The seminiferous tubule epithelium also contained the early pachytene primary spermatocytes, which have just entered the long pachytene step of the meiotic phase (Figures 6.14 and 6.23). Type A and B spermatogonia were also present in this stage.

Stage II: There was a further maturation of the round spermatids in this stage, which resulted in their acrosomal vesicles making contact with the nuclei. These spermatids had a distinct well-formed mitochondrial sheath. Pachytene primary spermatocytes were clearly observed. It was difficult to make a clear distinction between stages I and II (Figures 6.15 and 6.25). They were distinguished from each other by their Golgi and acrosomic granule appearance.

Stage III: This stage was characterized by the acrosomic vacuole adhering to the nuclear membrane of spermatids. These spermatids still had a spherical nuclei, but the acrosome has developed a cap over the nuclei (cap phase). The pachytene primary spermatocytes were observed (Figures 6.16; 6.17; 6.18; 6.19, and 6.26). The seminiferous epithelium contained A and B spermatogonia.

Stage IV: The younger generation of spermatocytes was just entering the meiotic phase. This stage was characterized by the presence of the preleptotene primary spermatocytes. The nuclei of the preleptotene spermatocytes were finely granular with evenly distributed areas of chromatin condensation. The older generation of the spermatids associated with the residual bodies (Figures 6.27 and 6.28). The seminiferous epithelium consisted of A and B spermatogonia.

Stage V: The acrosome occupies a third of the circumference of the spermatids and flagella were occasionally seen. There were large pale leptotene primary spermatocytes present (Figure 6. 29). These cells can also be considered to be preleptotene spermatocytes as there was no clear distinction between the two types of spermatogenic cells. The presence of the types A and B were confirmed.

Table 6. 1. (Continues). Description of stages.

Stage VI: Large pale leptotene primary spermatocytes were predominant. Acrosomes pointed to the basal lamina. Pachytene spermatocytes were also present. The elongated spermatids were situated near the lumen of the seminiferous tubule, away from the Sertoli cell nucleus (Clermont, 1969). Both types A and B spermatogonia were observed (Figure 6. 30).

Stage VII: This stage was characterized by the emergence of the zygotene primary spermatocytes and again the presence of large pachytene primary spermatocytes with partially condensed chromatin. Only round spermatids were present. The acrosome head cap was more extended than in stage VI. The B spermatogonium type was occasionally observed. The type A spermatogonium was clearly observed (Figure 6. 31).

Stage VIII: Pachytene primary spermatocytes appeared to be large with condensed chromatin. Elongated spermatid cytoplasm was distinct and easily identified. The acrosomic head cap was not clearly visible. Residual bodies were seen along the lumen beneath the elongated spermatids. Spermatogonium type A was clearly observed. No type B spermatogonium was observed (Figures 6. 20; 6.32).

Stage IX: Elongated and round spermatids were present. The zygotene and the pachytene spermatocytes were observed. Leptotene spermatocytes were also evident in this stage. Nuclei of the spermatids were slightly pointed. Head of the spermatid still slightly translucent in occasional cells but nearly fully condensed. Divisions of primary and secondary spermatocytes were observed. Both the types A and B spermatogonia were present (Figures 6.21; 6.22).

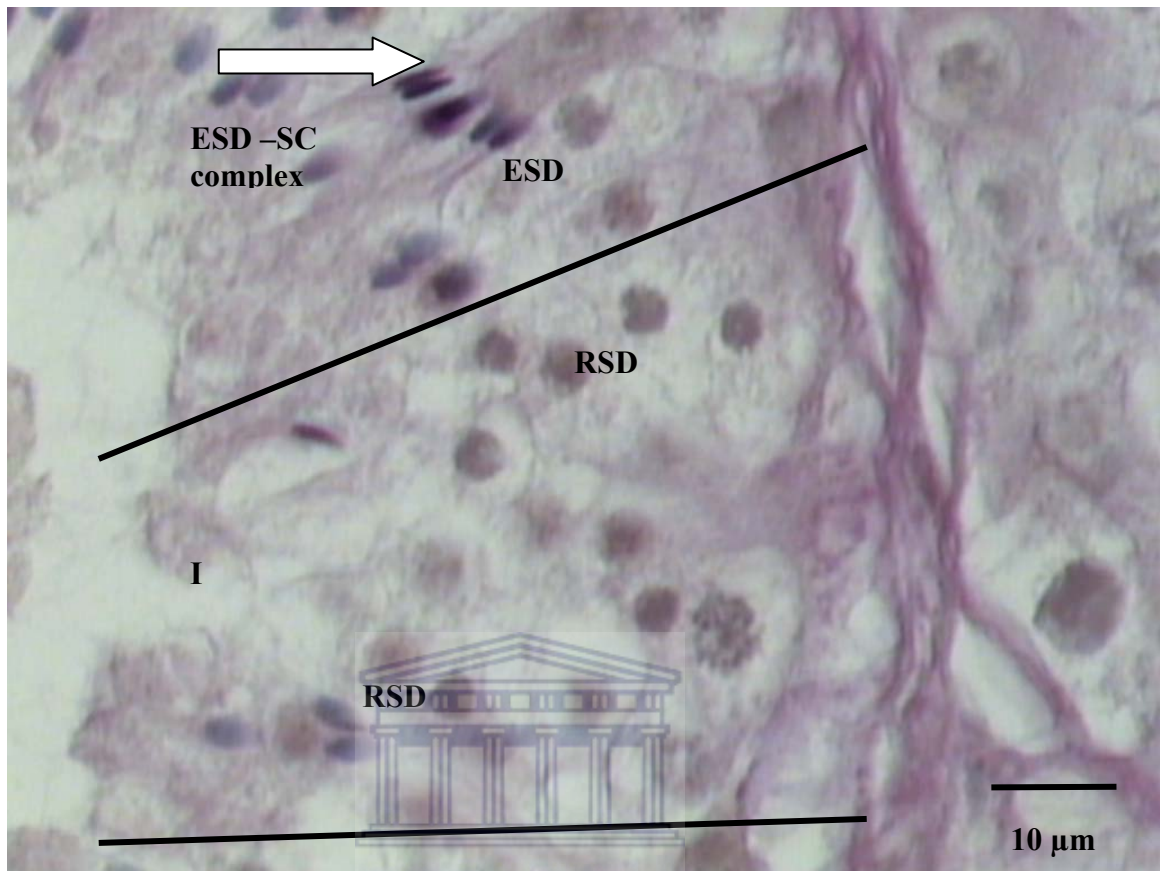


Figure 6. 14. Light micrograph of the lateral section of the testicular tissue of the vervet monkey, *Chlorocebus aethiops*, (Section 1 of the 4 sections).

ESD – Elongated spermatids, RSD – Round spermatids, ESD – SC complex (Arrow) - Elongated spermatids - Sertoli cell complex .

Note: Stage I

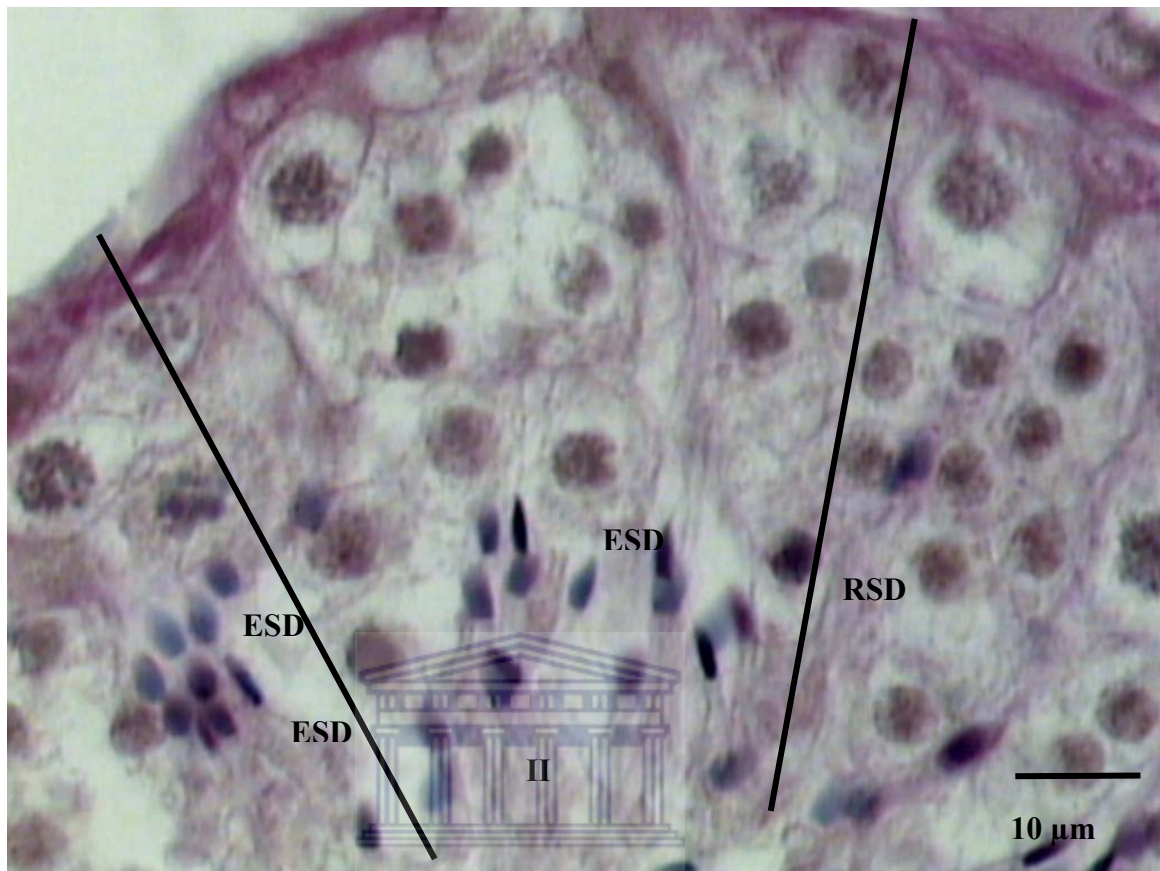


Figure 6. 15. Light micrograph of the lateral section of the testicular tissue of the vervet monkey, *Chlorocebus aethiops*, (Section 2 of the 4 sections).

ESD – Elongated spermatids, RSD – Round spermatids.

Note: Stage II

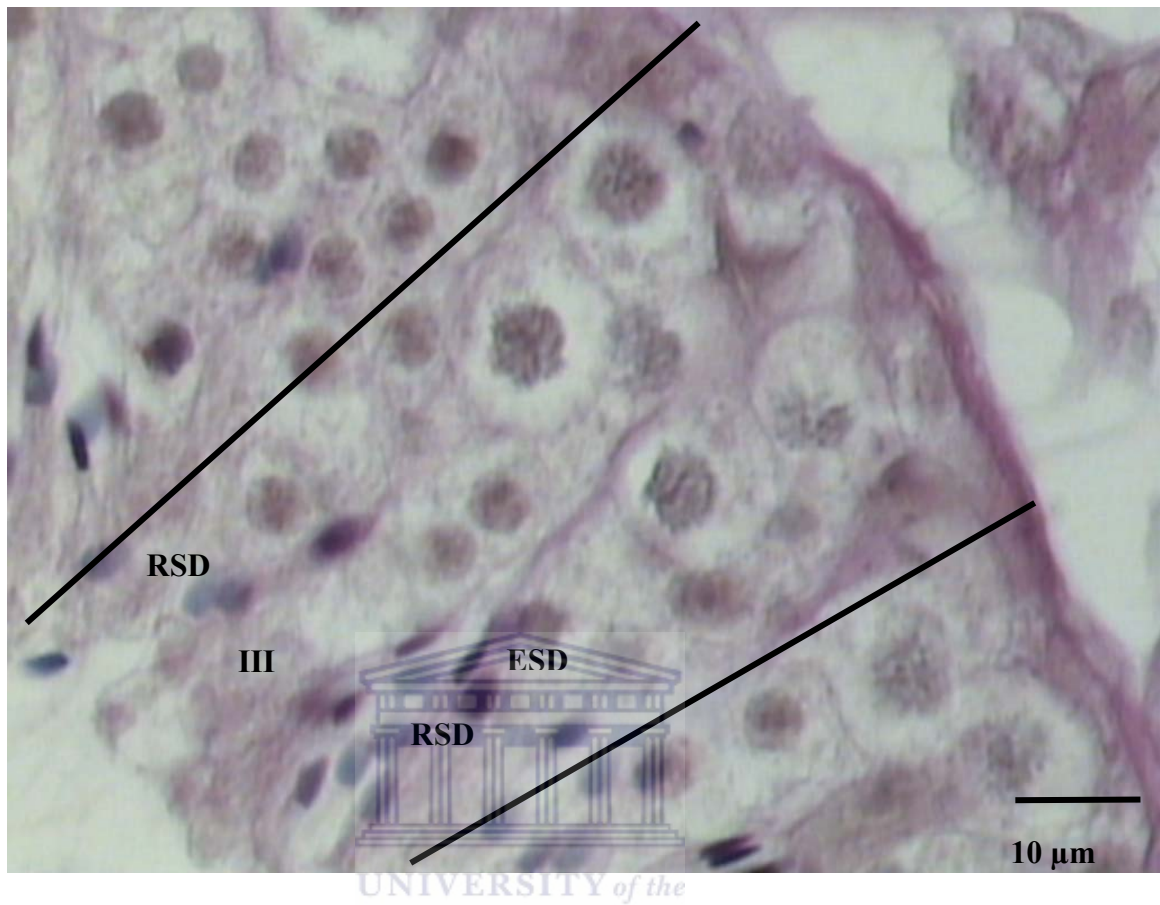


Figure 6. 16. Light micrograph of the lateral section of the testicular tissue of the vervet monkey, *Chlorocebus aethiops*, (Section 3 of the 4 sections).

ESD – Elongated spermatids, RSD – Round spermatids.

Note: Stage III

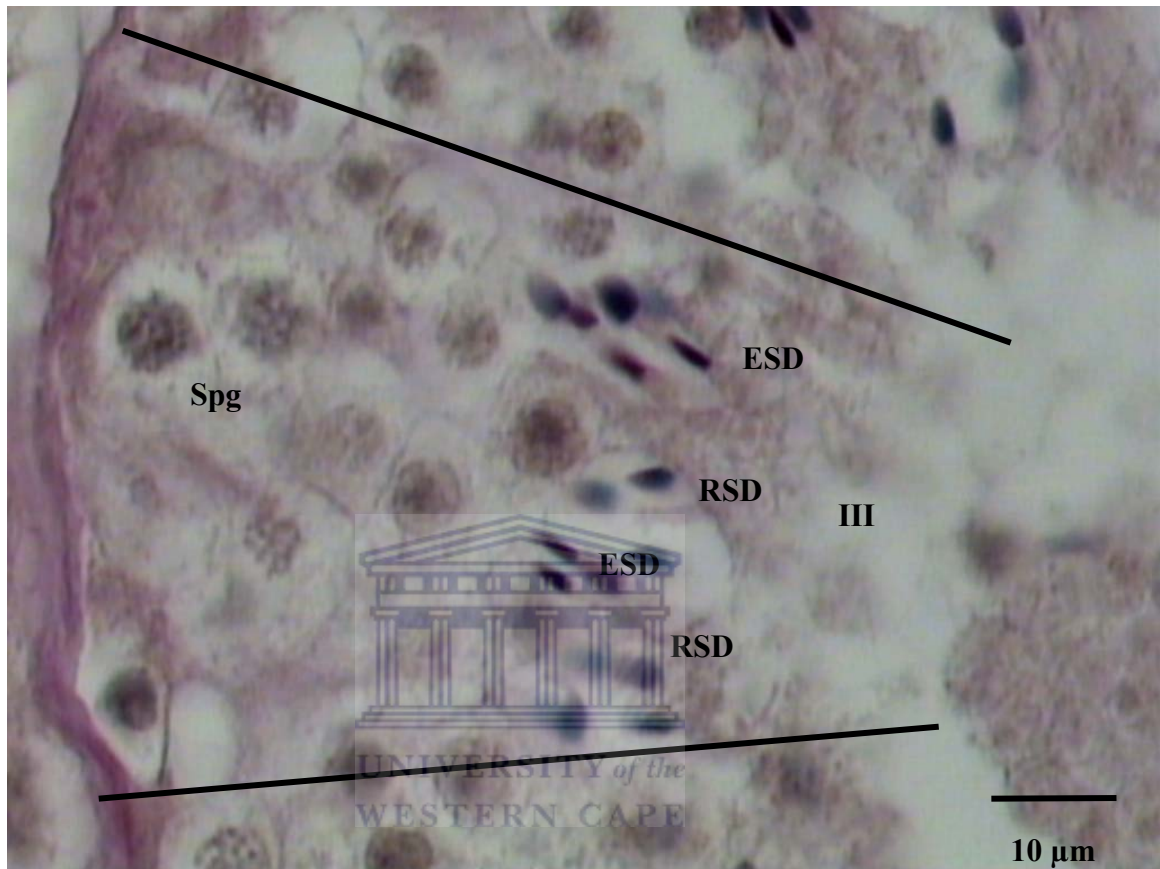


Figure 6. 17. Light micrograph of the lateral section of the testicular tissue of the vervet monkey, *Chlorocebus aethiops*, (Section 4 of the 4 sections).

ESD – Elongated spermatids, RSD – Round spermatids, Spg - Spermatogonium.

Note: Stage III



Figure 6. 18. Light micrograph of the lateral section of the testicular tissue of the vervet monkey, *Chlorocebus aethiops*.

PL – Preleptotene spermatocyte, Spg B - Type B spermatogonium, ESD – Elongated spermatids, RSD – Round spermatids, SC - Sertoli cell.

Note: Stage III

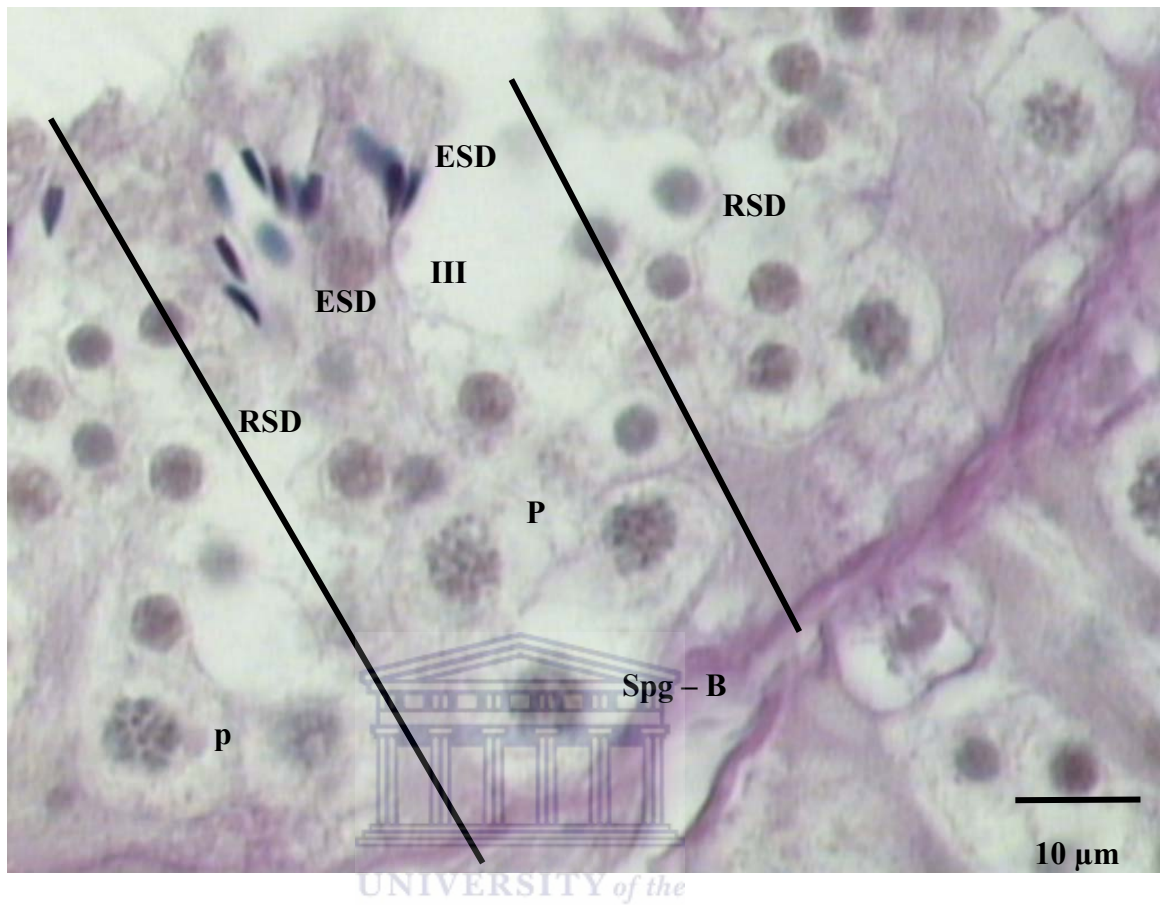


Figure 6. 19. Light micrograph of the lateral section of the testicular tissue of the vervet monkey, *Chlorocebus aethiops*.

ESD – Elongated spermatids, P- Pachytene stage, RSD – Round spermatids, Spg B - Type B spermatogonium.

Note: Stage III

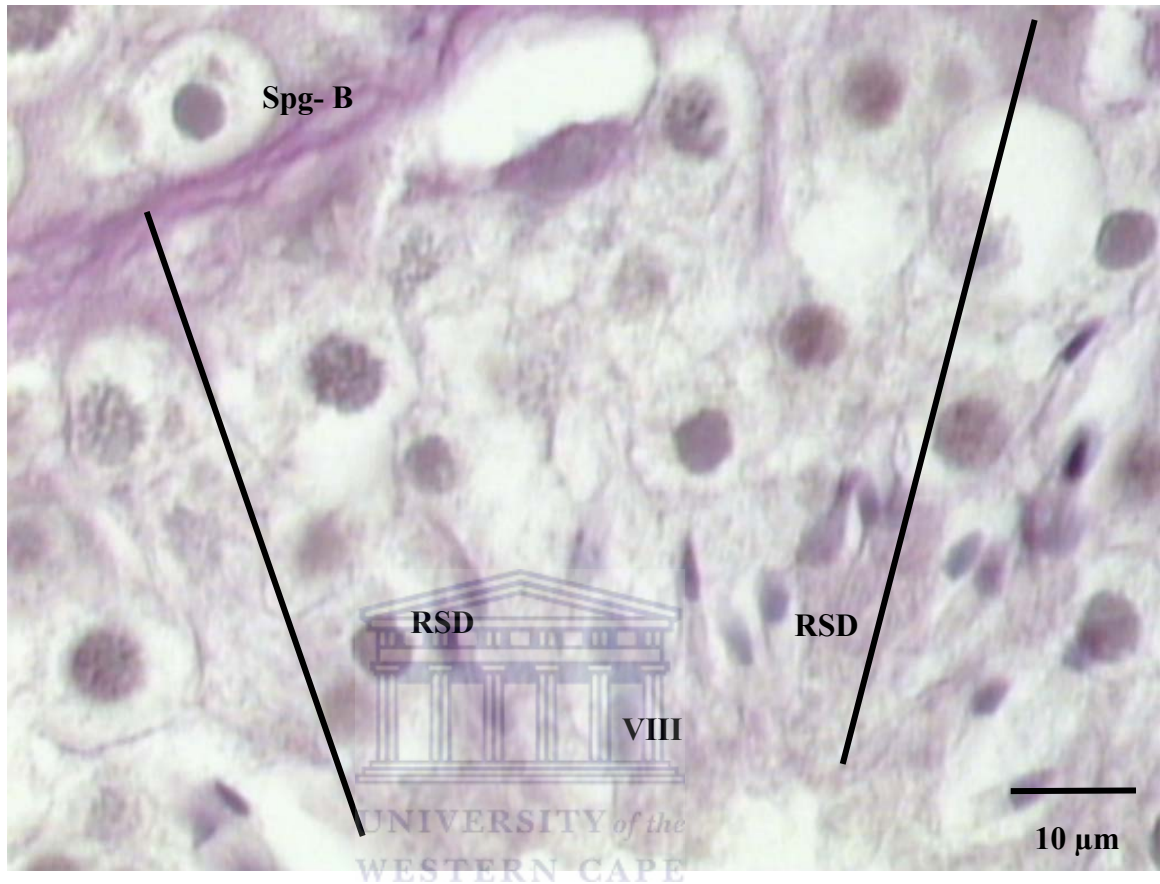


Figure 6. 20. Light micrograph of the lateral section of the testicular tissue of the vervet monkey, *Chlorocebus aethiops*.

ESD – Elongated spermatids, RSD – Round spermatids, Spg B - Type B spermatogonium.

Note: Stage VIII

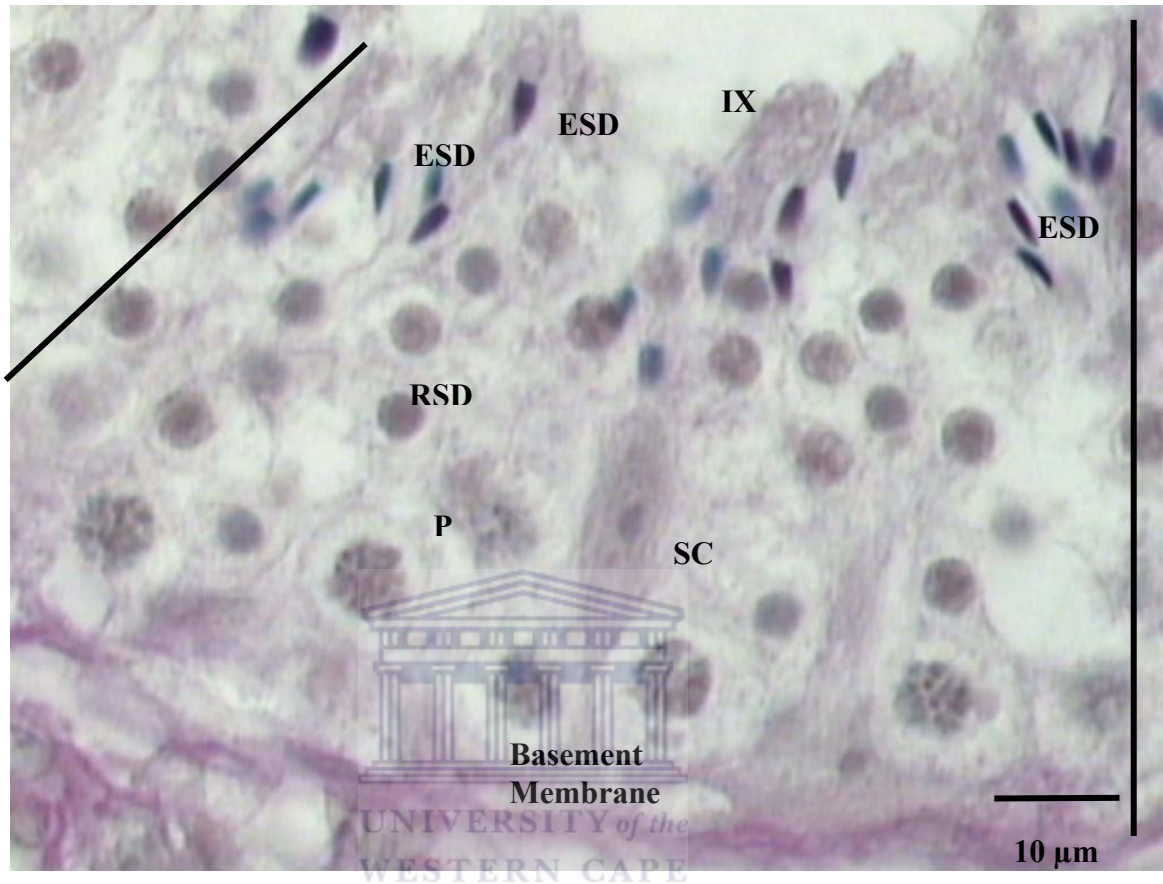


Figure 6. 21. Light micrograph of the lateral section of the testicular tissue of the vervet monkey, *Chlorocebus aethiops*.

ESD – Elongated spermatids, P - Pachytene stage, RSD – Round spermatids, SC- Sertoli cell.

Note: Stage IX

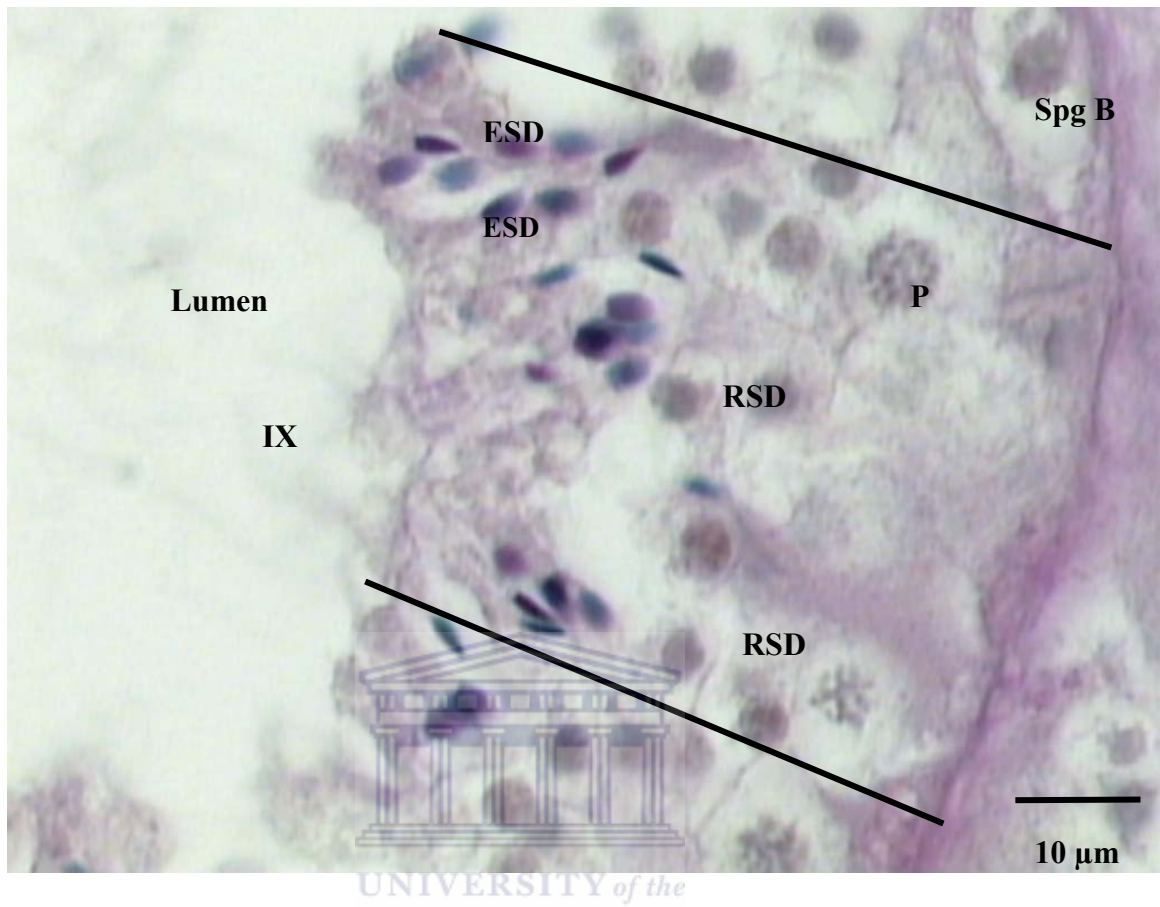


Figure 6. 22. Light micrograph of the lateral section of the testicular tissue of the vervet monkey, *Chlorocebus aethiops*.

Spg B - Type B spermatogonium, **ESD** – Elongated spermatids, **RSD** – Round spermatids, **P** - Pachytene stage.

Note: Stage IX

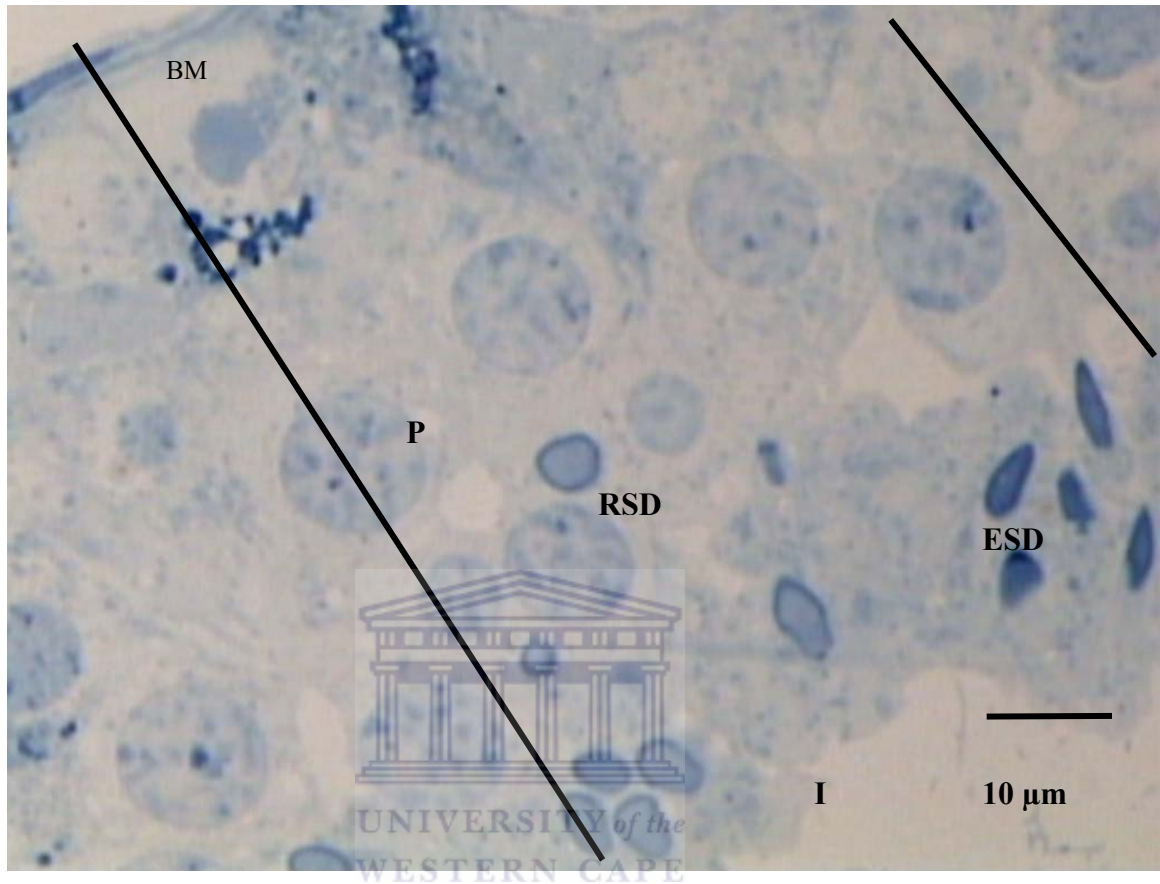


Figure 6. 23. Light micrograph of a methacrylate resin section showing a section of the testicular tissue (lateral) of the vervet monkey, *Chlorocebus aethiops*.

BM - Basement Membrane, P - Pachytene, ESD – Elongated spermatids, RSD – Round spermatids.

Note: Stage I

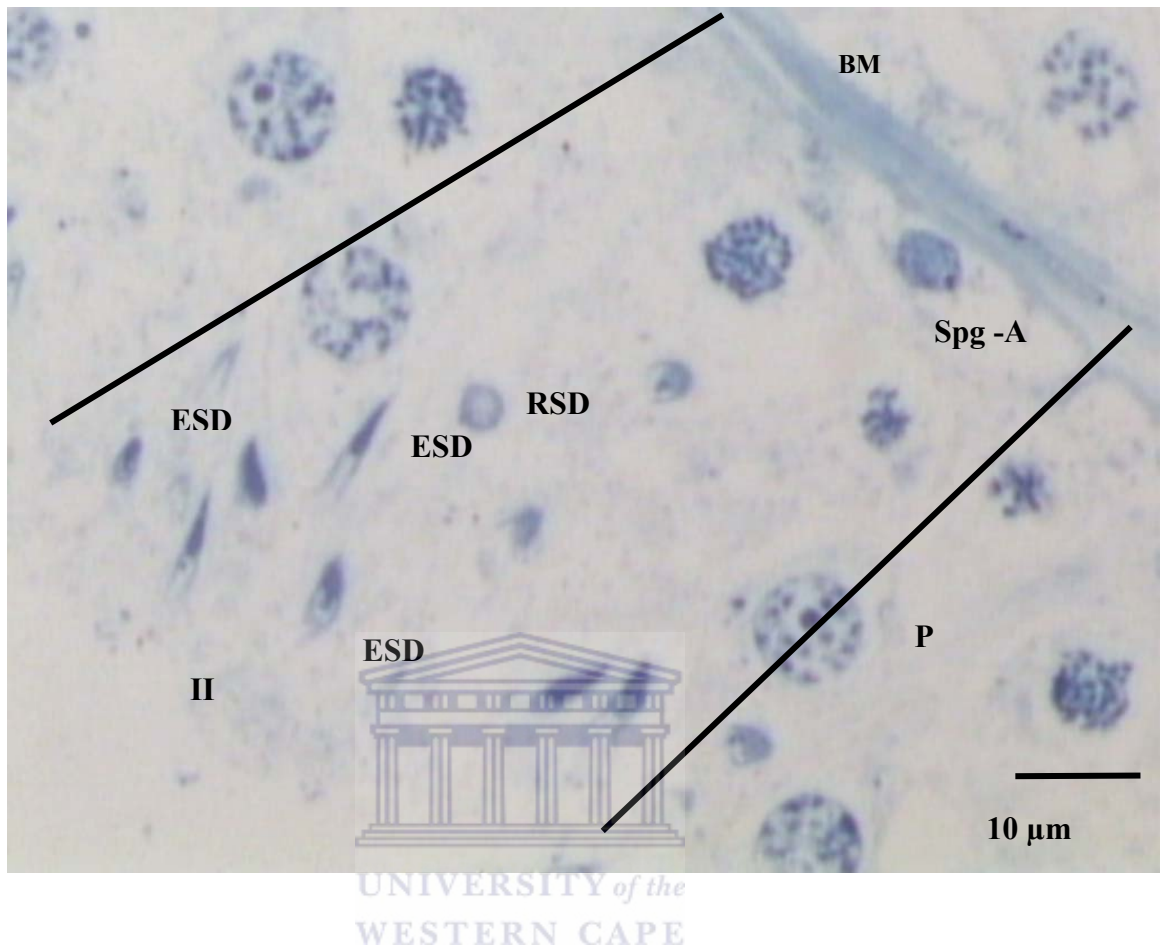


Figure 6. 24. Light micrograph of a methacrylate resin section showing a section of the testicular tissue (lateral) of the vervet monkey, *Chlorocebus aethiops*.

BM - Basement Membrane, P - Pachytene, Spg A - Type A spermatogonium, ESD – Elongated spermatids, RSD – Round spermatids.

Note: Stage II

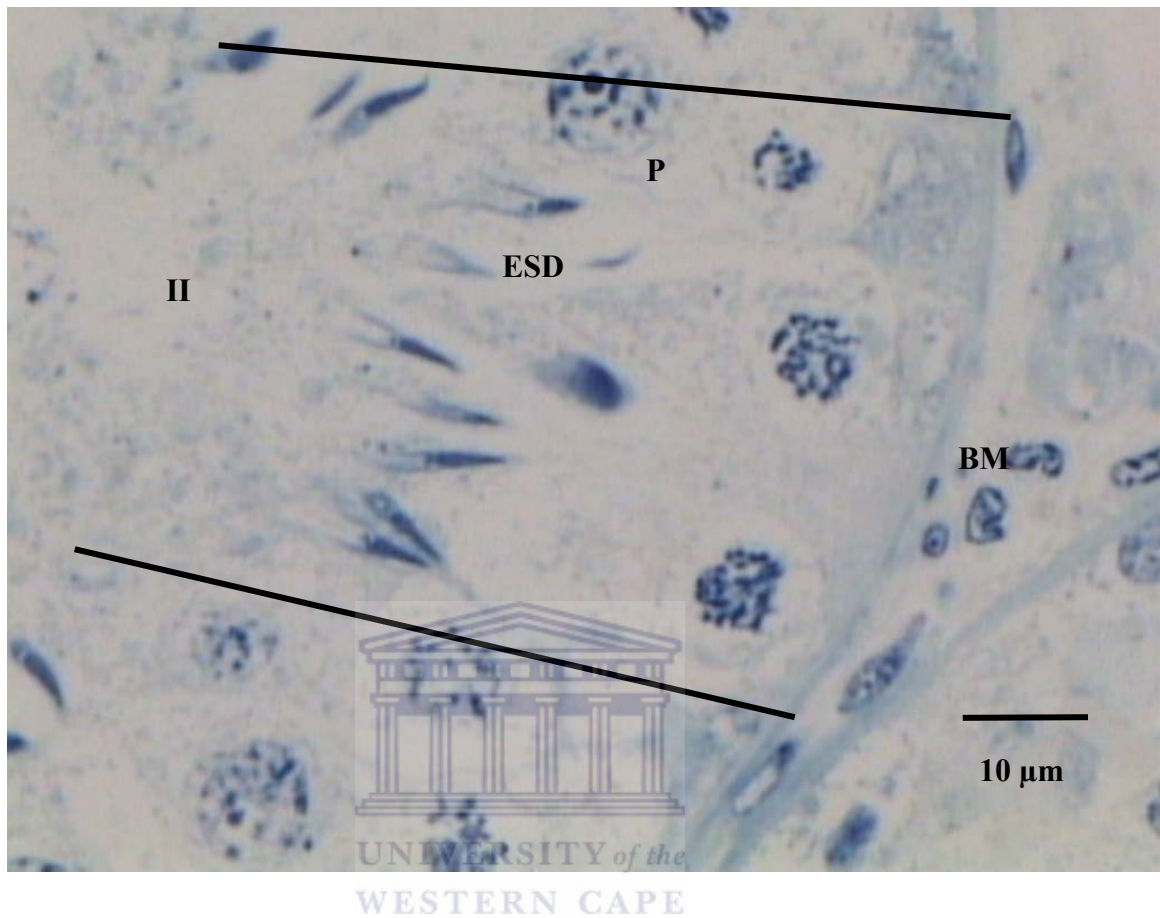


Figure 6. 25. Light micrograph of a methacrylate resin section showing a section of the testicular tissue (lateral) of the vervet monkey, *Chlorocebus aethiops*.

BM - Basement Membrane, P - Pachytene stage, ESD – Elongated spermatids.

Note: Stage II

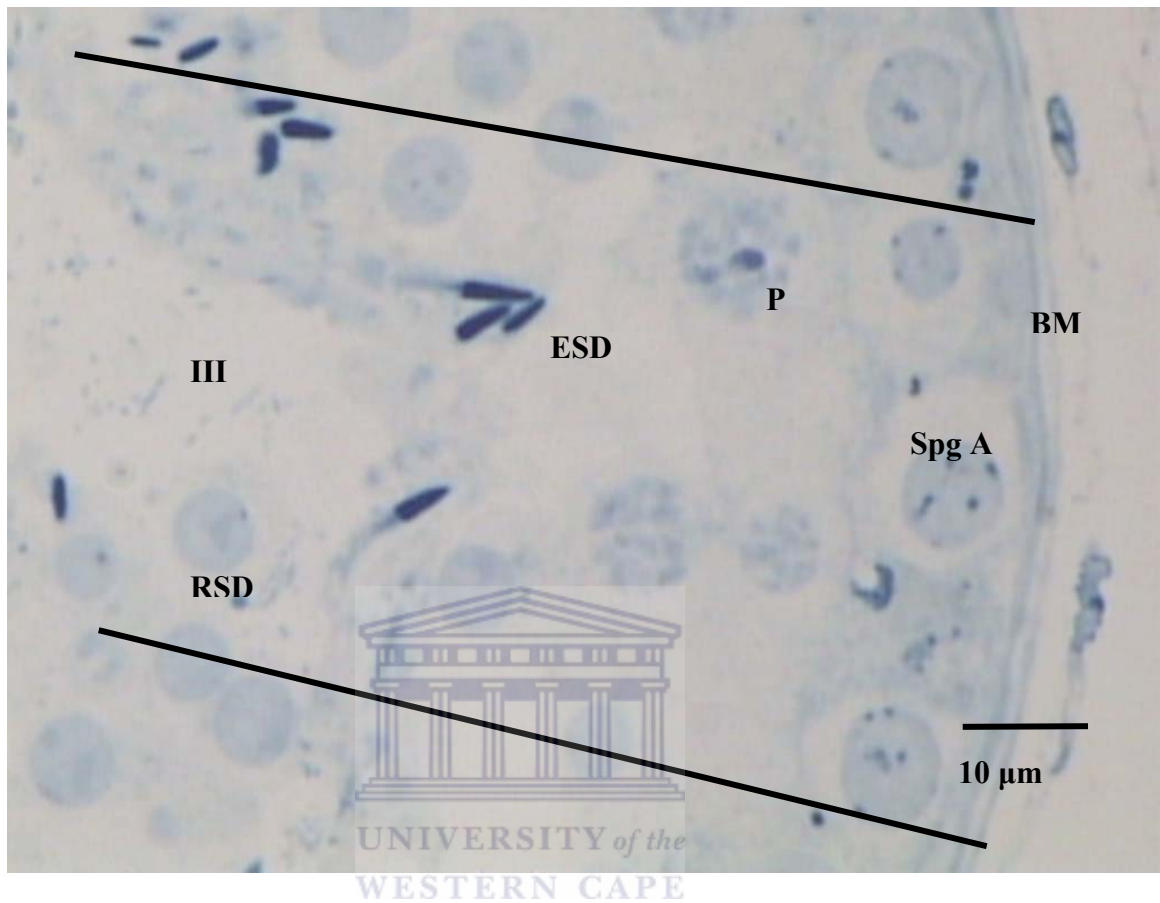


Figure 6. 26. Light micrograph of a methacrylate resin section showing a section of the testicular tissue (lateral) of the vervet monkey, *Chlorocebus aethiops*.

BM - Basement Membrane, P - Pachytene stage, Spg A - Type A spermatogonium, ESd – Elongated spermatids, RSd – Round spermatids.

Note: Stage III

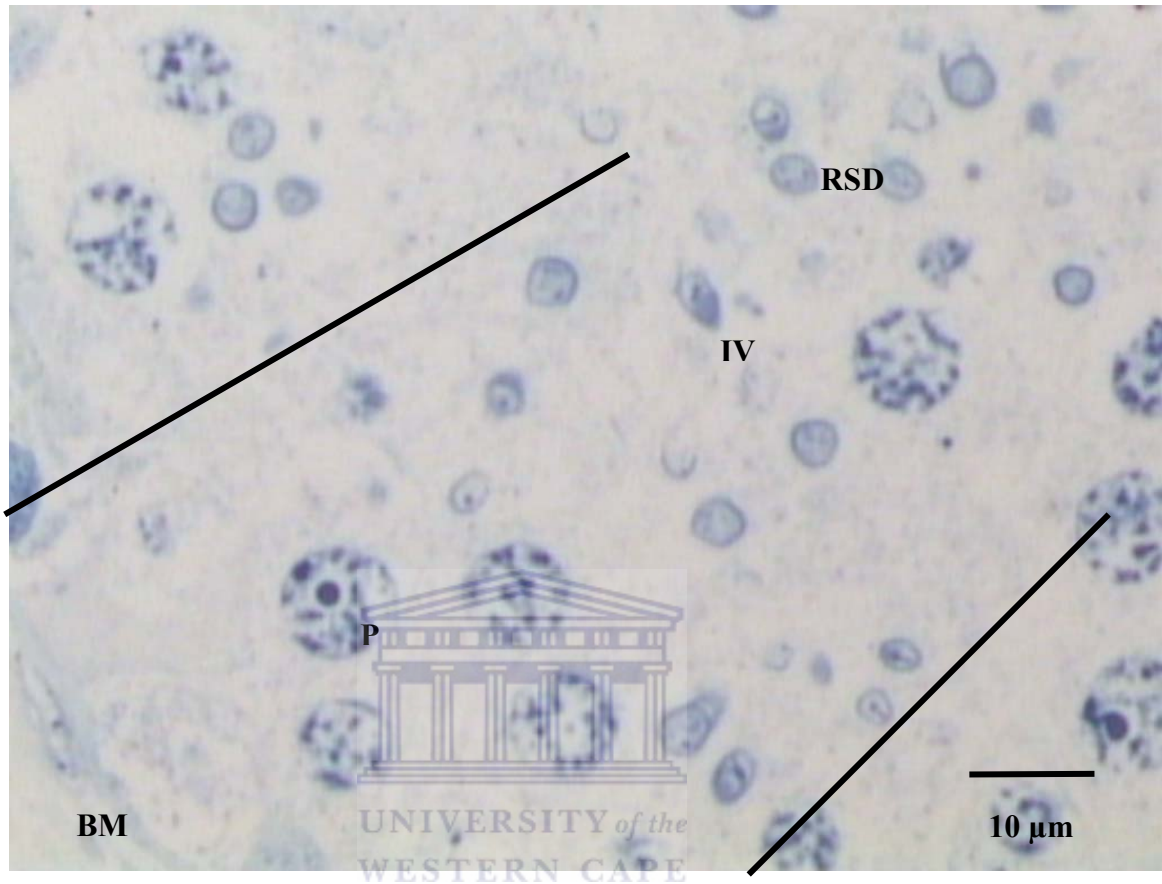


Figure 6. 27. Light micrograph of a methacrylate resin section showing a section of the testicular tissue (lateral) of the vervet monkey, *Chlorocebus aethiops*.

BM - Basement membrane, P - Pachytene stage, RSD – Round spermatids.

Note: Stage IV

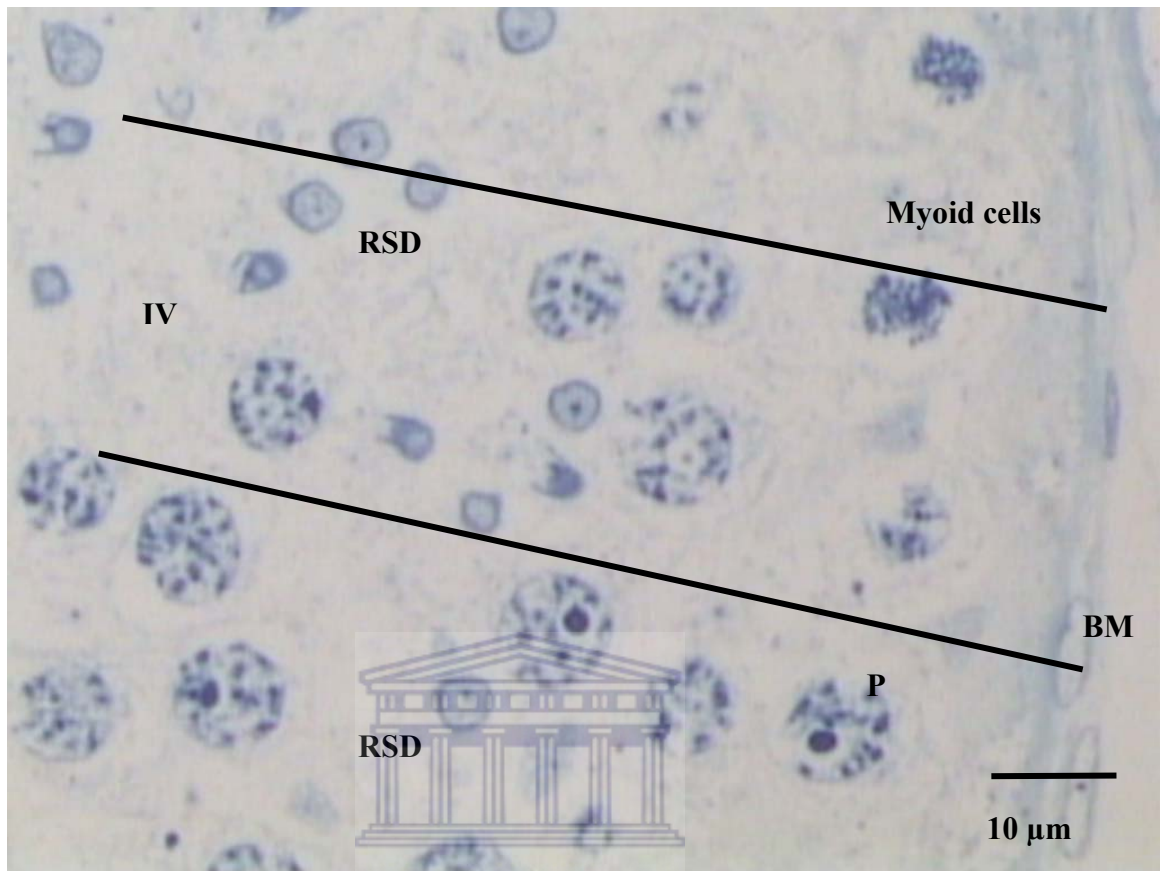


Figure 6. 28. Light micrograph of a methacrylate resin section showing a section of the testicular tissue (lateral) of the vervet monkey, *Chlorocebus aethiops*.

BM - Basement Membrane, P - Pachytene stage, RSD – Round spermatids.

Note: Stage IV

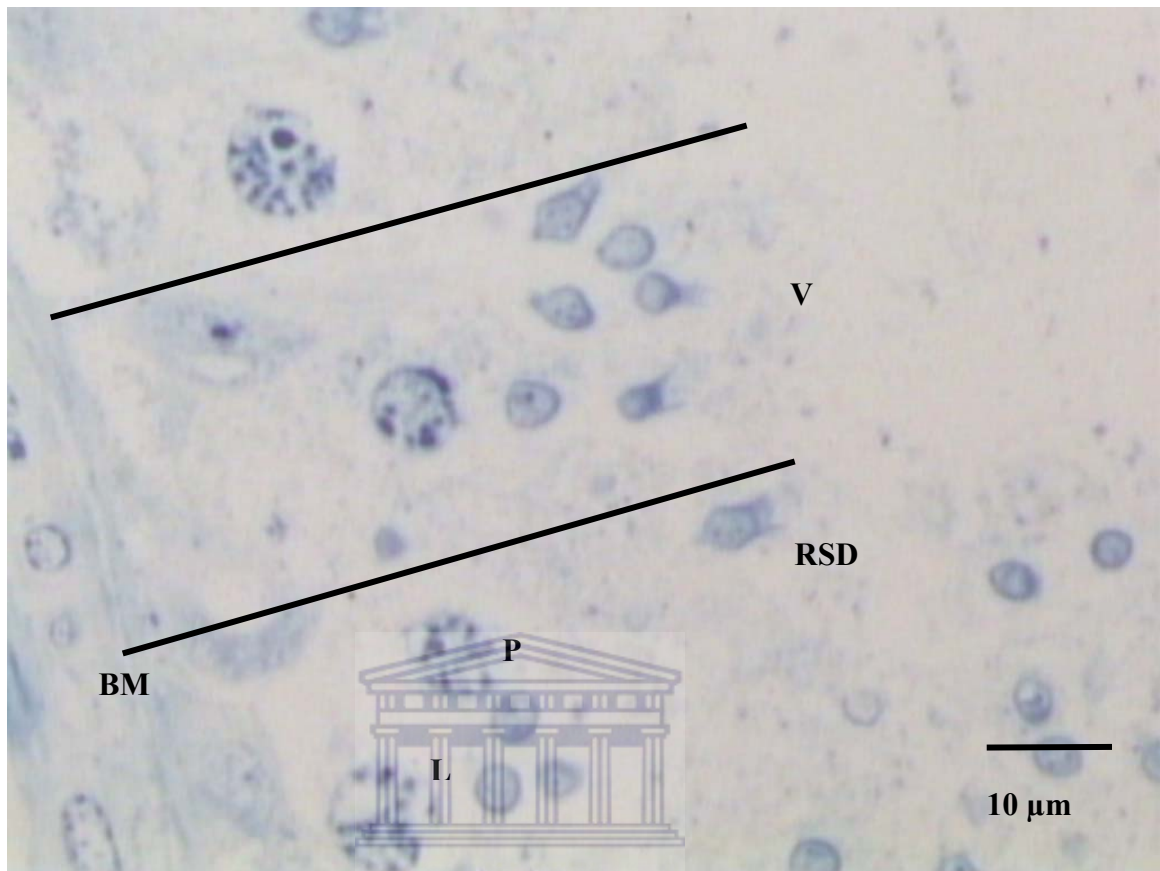


Figure 6. 29. Light micrograph of a methacrylate resin section showing a section of the testicular tissue (lateral) of the vervet monkey, *Chlorocebus aethiops*.

BM - Basement Membrane, P - Pachytene, RSD – Round spermatids.

Note: Stage V

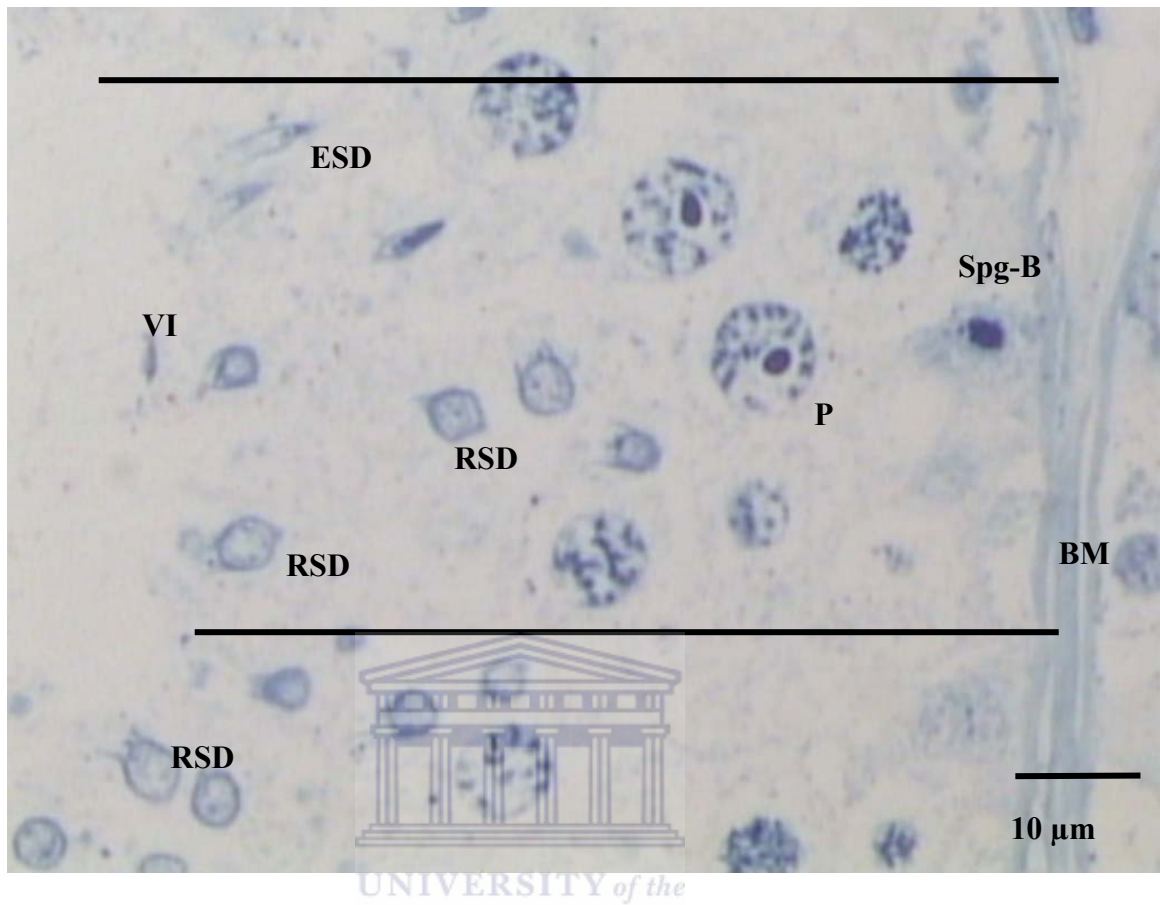


Figure 6. 30. Light micrograph of a methacrylate resin section showing a section of the testicular tissue (lateral) of the vervet monkey, *Chlorocebus aethiops*.

BM - Basement Membrane, P - Pachytene stage, Spg B - type B spermatogonium, ESD – Elongated spermatids, RSD – Round spermatids.

Note: Stage VI

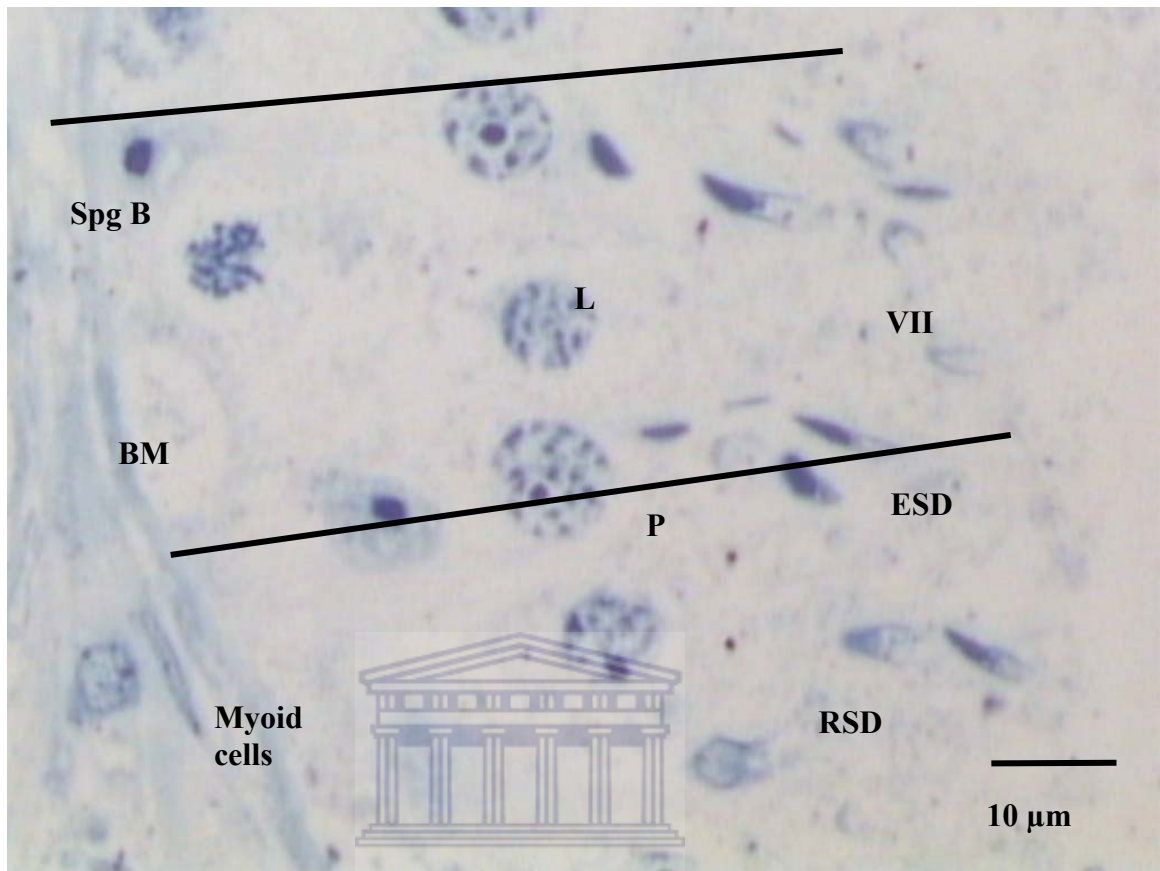


Figure 6. 31. Light micrograph of a methacrylate resin section showing a section of the testicular tissue (lateral) of the vervet monkey, *Chlorocebus aethiops*.

BM - Basement Membrane, L - Leptotene, P – Pachytene stage, Spg B - Type B spermatogonium, ESD – Elongated spermatids, RSD – Round spermatids.

Note: Stage VII

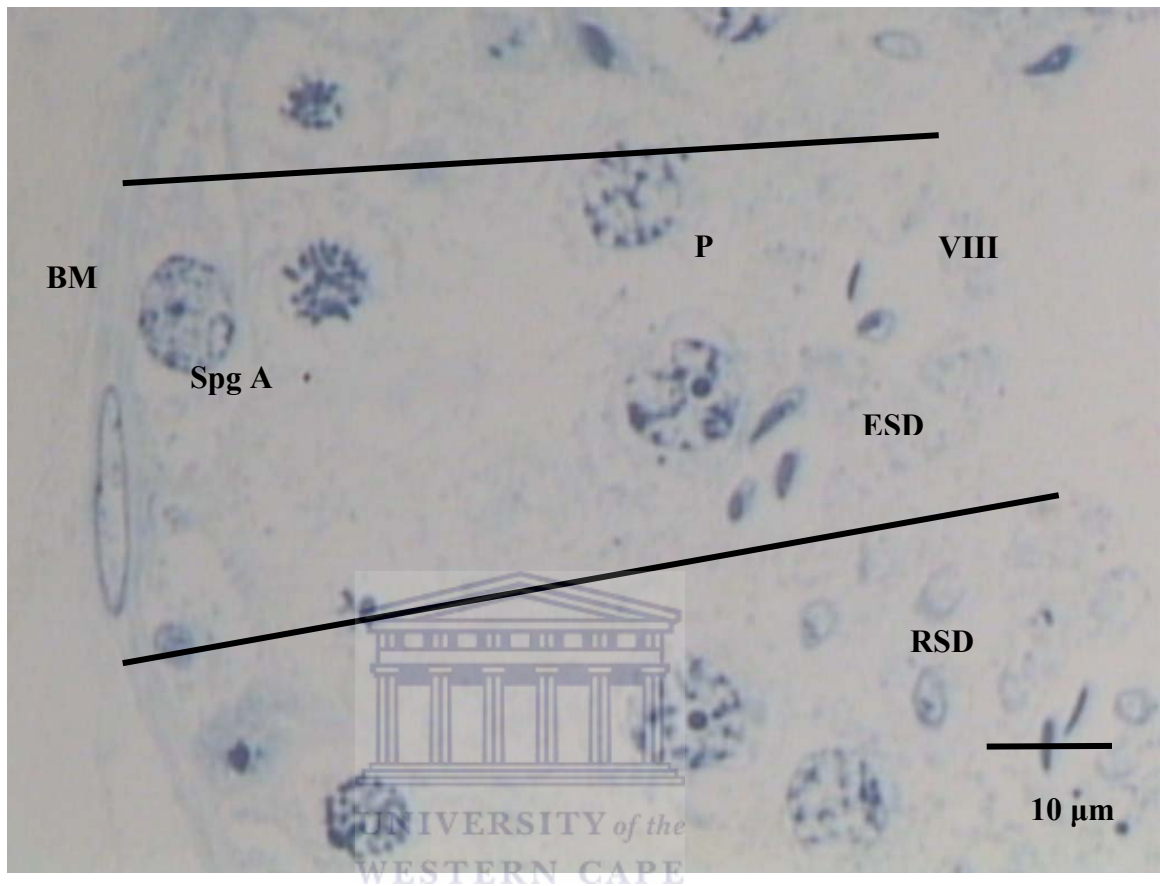


Figure 6. 32. Light micrograph of a methacrylate resin section showing a section of the testicular tissue (lateral) of the vervet monkey, *Chlorocebus aethiops*.

BM- Basement Membrane, **P-** Pachytene stage, **Spg A -** Type A spermatogonium, **ESD –** Elongated spermatids, **RSD –** Round spermatids.

Note: Stage VIII

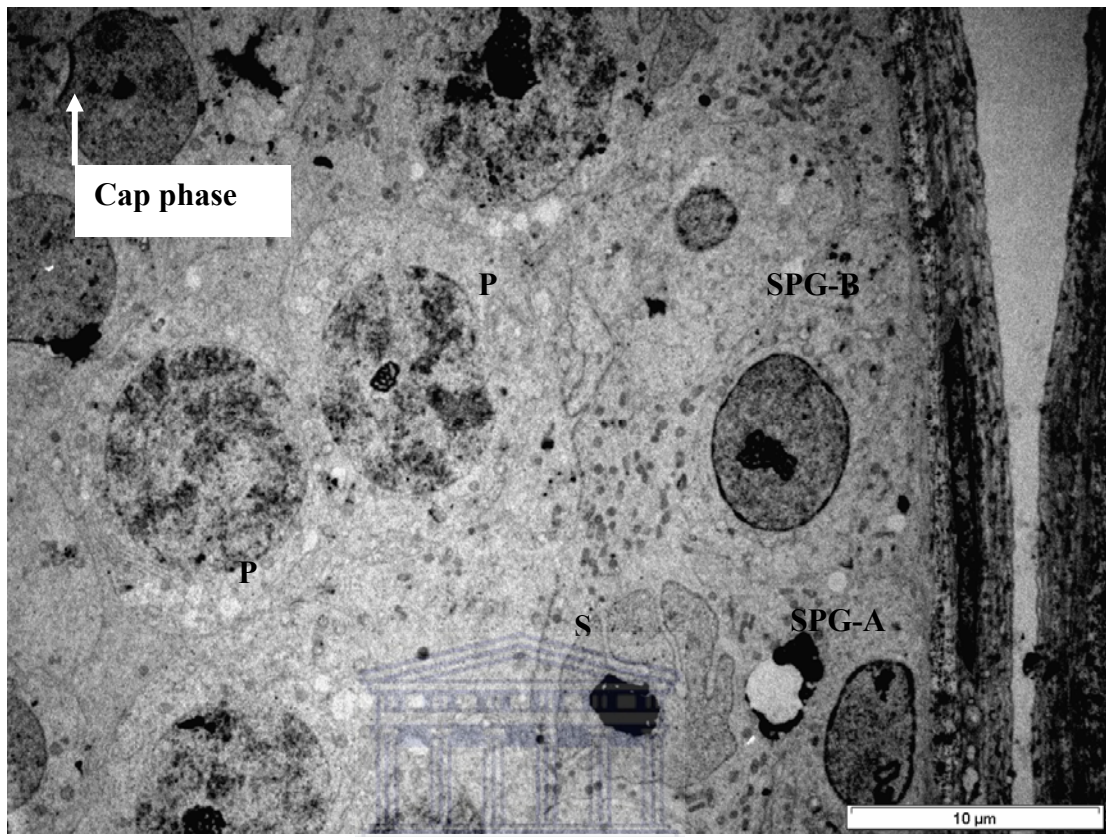


Figure 6. 33. TEM micrograph showing germ cellular associations with Sertoli cells in the seminiferous tubules of the vervet monkey, *Chlorocebus aethiops*.

Note the process of spermatogenesis (Stage II).

P – Pachytene stage, S - Sertoli cell, SPG-A - Type A Spermatogonium, SPG-B – Type B Spermatogonium.

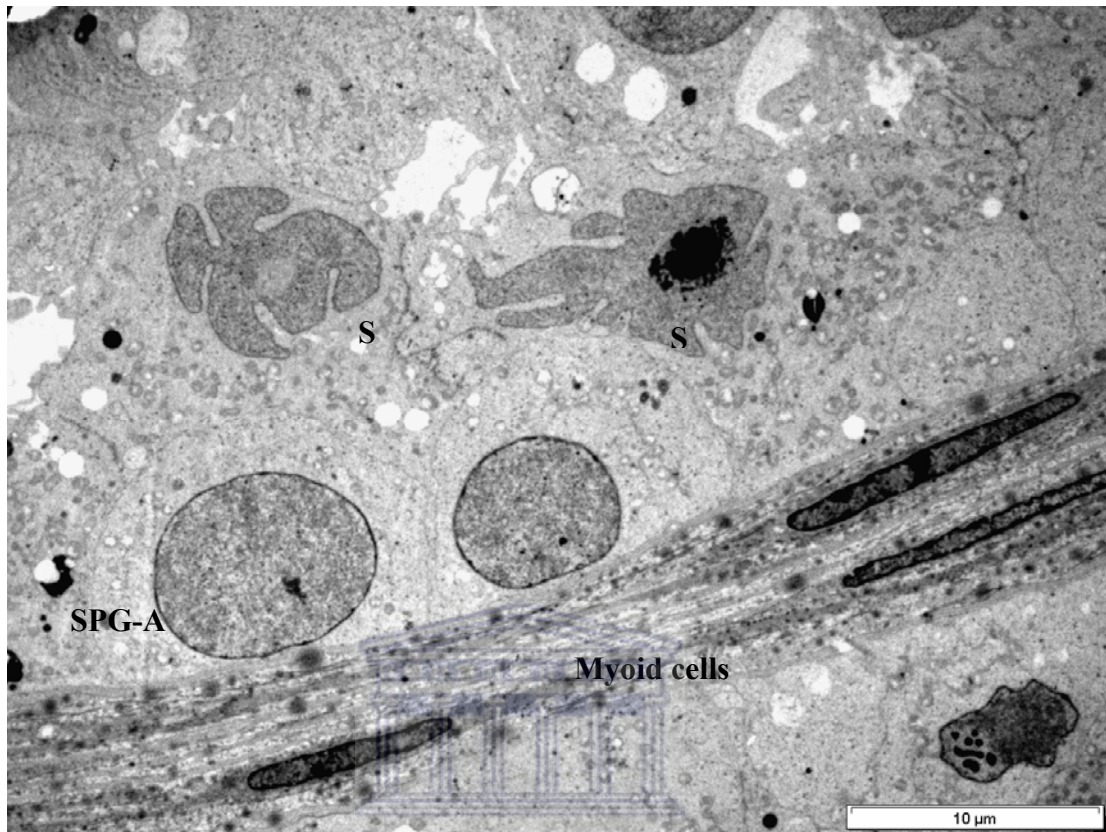


Figure 6. 34. TEM micrograph showing layers of the seminiferous tubules, two Sertoli cell nuclei, and two spermatogonia, of the vervet monkey, *Chlorocebus aethiops*.

S - Sertoli cell nucleus, SPG - A - Type A Spermatogonium.

Table 6.2 shows the cellular associations of the nine stages of the cycle of the seminiferous epithelium that could be constructed in the current study. Table 6.3 shows the germ cell and Sertoli cell distribution patterns in different regions of testicular tissue. There were no significant differences in most of the germ cells' distribution and Sertoli cell distribution, except for diplotene ($P \leq 0.01$) and round spermatids ($P \leq 0.01$).

Table 6. 2. The cellular associations of the nine stages of the cycle of the seminiferous epithelium in the vervet monkey, *Chlorocebus aethiops*.

Cells	S10	S11	S12	-	-	-	-	-	-
	S1	S2	S3	S4	S5	S6	S7	S8	S9
	P	P	P	P	P	P/D	P	P	P
	B	B	B	B/PL	PL/L	L	L	L/Z	Z
	Ap	Ap	Ap	Ap	Ap	Ap	B	B	B
	Ad	Ad	Ad	Ad	Ad	Ad	Ap	Ap	Ap
	-	-	-	-	-	-	Ad	Ad	Ad
Stages	I	II	III	IV	V	VI	VII	VIII	IX

Ad - dark type A spermatogonium

Ap – pale type A spermatogonium

B – type B spermatogonium

D - diplotene stage

L – leptotene spermatocyte

P – pachytene spermatocyte

PL – preleptotene spermatocyte

Z – zygotene spermatocyte

S1-S9- round spermatids in various stages of differentiation

S10-S12– elongated spermatids in various stages of development (Clermont, 1969).

Table 6. 3. Germ cells distribution pattern in different regions of testicular tissue of the vervet monkey, *Chlorocebus aethiops* (Mean \pm SEM).

Cell type / Cross-section	Lateral testis	Medial testis	Middle testis
Spermatogonium type A	4.67 \pm 0.79	4.67 \pm 0.36	4.89 \pm 1.11
Spermatogonium type B	8.67 \pm 1.17	8.67 \pm 1.01	8.83 \pm 0.36
Preleptotene/Leptotene	13.33 \pm 2.35	14.22 \pm 1.08	17.06 \pm 1.03
Pachytene	31.61 \pm 0.79	36.11 \pm 3.21	33.39 \pm 2.09
Round Spermatids	42.00 \pm 0.41	33.72 \pm 2.15	32.00 \pm 3.18*
Elongated spermatids	45.44 \pm 4.61	47.78 \pm 1.68	48.94 \pm 1.06
Diplotene	1.5 \pm 0.16	2.61 \pm 0.41	2.72 \pm 0.53*
Sertoli cell	10.28 \pm 0.61	9.61 \pm 0.49	8.89 \pm 0.79

* - significantly different.

$P \leq 0.01$.

6.9. DISCUSSION

The process of spermatogenesis is subdivided into three phases, that is spermatocytogenesis, meiosis, and spermiogenesis. Spermatocytogenesis involves mitotic cell division which yields stem cells and primary spermatocytes. Spermiogenesis involves the differentiation without any further division of spherical spermatids into mature spermatids which are then released from the luminal free surface of the seminiferous tubules.

There are many similarities in the process of spermiogenesis of the vervet monkey and humans. The four phases of spermiogenesis, that is Golgi, cap, acrosome, and maturation were observed in this study. Figures 6.3 to 6.12 show all the phases as outlined. It is important to note that these phases tend to overlap and it is quite convenient to label them as early, middle and late phase as described for baboons by Afzelius *et al.*, (1982).

The results showed in this study revealed that the vervet monkey has a multi-stage organization of spermatogenesis similar to that found in humans, common marmosets, chimpanzees, and other nonhuman primates. Approximately 2-3 stages can be found within a given cross section of the seminiferous tubule. This is similar to what was reported for the pattern found in the common marmoset (Holt and Moore, 1984; Millar *et al.*, 2000). The chimpanzee showed approximately, 2-4 stages or rarely 1-3 stages per cross section in a seminiferous tubule (Smithwick *et al.*, 1996). Humans showed approximately 1-5 stages per cross section in a given seminiferous tubule (Clermont, 1963). Table 6. 4 outlines the developmental steps in each of the six stages of human spermatogenic cycle as described by Hess *et al.*, (1990). Table 6.5 illustrates different mammalian species studied and the different patterns of organization of spermatogenesis in this group. These two tables further suggest that there are similarities in the spermatogenesis of vervet monkey and humans and other general mammalian species.

The results of this study again showed that the vervet monkey has two main classes of spermatogonia: type A and Type B. It was difficult to conclusively differentiate between the two A type spermatogonia i.e. type Ad and Ap. Type Ad

spermatogonium, which seemed to be quiescent at all stages of the cycle and would not normally participate in the production of spermatocytes as outlined by Clermont (1969). The type Ap spermatogonium, which appeared to be the element that periodically at each cycle of the seminiferous epithelium entered into the cell division and yielded new type Ap spermatogonia and type B spermatogonia (Clermont, 1969). Steinberger and Tjioe (1968) confirmed that for each type Ad spermatogonium, there was one type Ap spermatogonium at all stages of the cycle. In humans, two classes of type A spermatogonia were also identified, dark and pale, with morphological characteristics similar to those found in the vervet monkey. Type B spermatogonia were recognized and conclusively distinguished from the preleptotene spermatocytes and from the type A spermatogonium given their properties by previous researchers (Clermont, 1963; Clermont, 1966). Preleptotene spermatocytes were found to be smaller than the type B spermatogonia in both their cellular and nuclear diameters. The preleptotene spermatocytes are completely detached from the basement membrane as described by Cavicchia and Dym (1978) and this was also observed in this study.

Wistuba *et al.*, (2003), reported that the vervet monkey has 1.34 ± 0.08 (mean \pm SD) average number of stages per tubule and $32.5 \pm 7.65\%$ (mean \pm SD) multistage tubules. In humans, they reported 2.03 ± 0.05 (mean \pm SD) average number of stages per tubules to $79.5 \pm 3.11\%$ (mean \pm SD) multistage per tubule. Wistuba *et al.*, (2003), recorded six stages in the vervet monkey when using criteria previously described for primate spermatogenesis. However, in this study the nine- stage classification system similar to the one described by Holt and Moore (1984) was used. Holt and Moore (1984), revised Clermont's classification system by condensing the first five stages into the first three stages of spermatogenesis, *i.e.* stages I to V have been condensed in stages I to III of the described system. Stages IV to IX correspond exactly to Clermont's stages VII to XII (Holt and Moore, 1984).

The results from this study showed that the germ cell and Sertoli cell distribution in various regions of the testis are the same. There were no significant

differences in most of the germ cells' distribution and Sertoli cell distribution except for diplotene and round spermatids (Table 6.3).

Histological examination of the human seminiferous epithelium gives the impression of a very irregular pattern of germ cell development. When the topographic arrangement of germ cells was re-examined with the aid of computer modeling or ultrastructural methods, a highly ordered distribution was revealed, conforming to a helical pattern based upon the geometry of concentric spirals. Thus the human spermatogenic cycle is precisely regulated in accordance with the more familiar ordered arrangements of germ cells seen in most nonhuman primates and other mammalian species (Kerr, 1992).

6.9.1. Spermiation

Kumar and Phillips (1991), observed heads of the maturation phase spermatids to be embedded in Sertoli cells in marmoset. Some Sertoli cells displayed funnel-shaped sleeve-like processes as discussed in the previous chapter. Finger-like extensions of the Sertoli cells were also associated with late spermatids. These finger-like protuberances of the apical region of the Sertoli cells assumed different shapes and sizes. The sleeve-like processes were also observed in this study in the vervet monkey. The apparent increase in the number of very small pores in the sleeve-like processes of the spermatids may suggest a relationship with the release into the lumen of the seminiferous tubules.

Table 6. 4. Different developmental steps in each of the six stages of human spermatogenic cycle (Hess, *et al.*, 1990), unmodified.

I	II	III	IV	V	VI
Sd1	Sd2	-	-	-	-
Sa	Sa	Sb1	Sb2	Sc	Sc
P	P	P	P	P/D	M1/SS?M2
B	B/PIIm	PL	L	L/Z	Z/P
Ap	Ap	Ap	Ap	Ap	Ap/Bm
Ad	Ad	Ad	Ad	Ad	Ad

Ad - dark type A spermatogonium

Ap – pale type A spermatogonium

B – type B spermatogonium

D - diplotene stage

DI – diakinesis stage

L – leptotene spermatocyte

P – pachytene spermatocyte

PL – preleptotene spermatocyte

Z – zygotene spermatocyte

S1-S9- round spermatids in various stages of differentiation

S10-S12– elongated spermatids in various stages of development (Clermont, 1969).



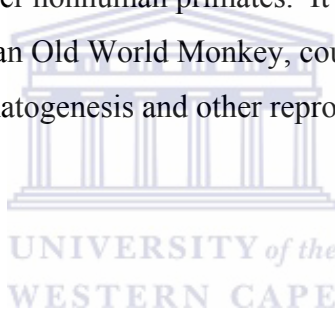
Table 6. 5. Different animal models and the number of stages that have been reported in the seminiferous tubules.

Model	Scientific Name	No. of Stages	Stages per tubular cross section	References
Rat	<i>Rattus norvegicus</i>	14	1	Hess (1990), Hess <i>et al.</i> , (1990)
Common Marmoset	<i>Callithrix jacchus</i>	9	1-5	Holt and Moore, (1984); Millar <i>et al.</i> , (2000).
Cynomologus Monkey	<i>Macaca fascicularis</i>	12	1	Fouquet and Dadone, (1986).
Stump-tailed Macaque	<i>Macaca arctoides</i>	12	-	Clermont and Antar (1973)
Rhesus Monkey	<i>Macaca mulatta</i>	12	1	de Rooij, <i>et al.</i> , (1986)
Baboon	<i>Papio anubis</i>	12	2 or more	Chowdhury and Steinberger (1976)
Chimpanzee	<i>Pan troglodytes</i>	6	2-4 rarely 1-3	Smithwick <i>et al.</i> , (1996)
Man	<i>Homo sapiens</i>	6	1-5 (average 3)	Clermont (1963)
Vervet Monkey	<i>Chlorocebus aethiops</i>	9	1-3	Current study

6. 10. CONCLUSIONS

From these results, it could be concluded that the general organization of the process of spermatogenesis is the same in all mammalian species and this can be divided into phases of development through which all germ cell pass over time. The type of organization of spermatogenesis observed in the vervet monkey has similarities to the one reported for humans. The spermatogenesis process observed in human displayed a random (helical) or spiral arrangement and the same pattern was also observed in chimpanzees. In this type of arrangement, there is more than one stage in a cross section of the seminiferous tubule.

It looks like the vervet monkey has evolved a strategy for the maturation of spermatogenic cells within the seminiferous epithelium which is almost similar to that of the humans and other nonhuman primates. It can therefore be concluded that the vervet monkey, being an Old World Monkey, could be regarded as a suitable model for studies in spermatogenesis and other reproductive studies such as toxicology and fertility.



6.11. REFERENCES

Afzelius, B. A., Johnsonbaugh, R. E., Kim, J. W., Plöen, L. and Ritzen, E. M. 1982. Spermogenesis and testicular spermatozoa of the olive baboon, (*Papio anubis*). *J. Submicrosc. Cytol.* **14**:627-639.

Behr, R., Hunt, N. Ivell, R., Wessels, J., and Weinbauer, G. F. 2000. Cloning and expression analysis of testis-specific cyclic 3', 5' - adenosine monophosphate-responsive element modulator activators in the nonhuman primate (*Macaca fascicularis*): comparison with other primate and rodent species. *Biol. Reprod.* **62**:1344-1351.

Cavicchia, J. C. and Dym, M. 1978. Ultrastructural characteristics of monkey spermatogonia and preleptotene spermatocytes. *Biol. Reprod.* **18**:219-228.

Cavicchia, J. C., Sacerdote, F. L., Morales, A. and Zhu, B. C. 1998. Sertoli cell nuclear pore number changes in some stages of the spermatogenic cycle of the rat seminiferous epithelium. *Tissue Cell.* **30**:265-273.

Chowdhury, A. K. and Steinberger, E. 1976. A study of germ cell morphology and duration of spermatogenic cycle in the baboon, *Papio anubis*. *Anat. Rec.* **185**:155-170.

Clermont, Y. 1963. The cycle of the seminiferous epithelium in man. *Am. J. Anat.* **112**:35-51.

Clermont, Y. 1966. Spermatogenesis in man. A study of the spermatogonial population. *Fertil. Steril.* **17**:705-721.

Clermont, Y. 1969. Two classes of spermatogonial stem cells in the monkey (*Cercopithecus aethiops*). *Am. J. Anat.* **126**:57-72.

Clermont, Y. 1972. Kinetics of spermatogenesis in mammals: the cycle of the seminiferous epithelium and the mode of renewal in spermatogonia. *Physiol. Rev.* **52**:198-236.

Clermont, Y. and Antar, M. 1973. Duration of the cycle of the seminiferous epithelium and the spermatogonial renewal in the monkey *Macaca arctoides*. *Am. J. Anat.* **136**:153-166.

De Rooij, D. G., van Alphen, M. M. A. and van de Kant, H. J. G. 1986. Duration of the cycle of the seminiferous epithelium and its stages in the rhesus monkey (*Macaca mulatta*). *Biol. Reprod.* **35**:587-591.

Dietrich, T., Schulze, W. and Riemer, M. 1986. Classification of the germinal epithelium in Java monkeys (*Macaca cynomolgus*) using digital image processing. *Urologe A* **25**:179-186.

Dym, M. 1983. The male reproductive system. In: Histology Cell and Tissue Biology. 5th Ed. (ed. L. Weiss). Macmillan Press. New York. pp 1000-1053.

Dym, M. and Cavicchia, C. 1978. Functional morphology of the testis. *Biol. Reprod.* **18**:1-15.

Erickson-Lawrence, M., Zabludoff, S. D. and Wright, W. W. 1991. Cyclic protein-2, a secretory product of rat Sertoli cells, is the proenzymes form of cathepsin L. *Mol. Endocrinol.* **5**:1780-1788.

Fouquet, J. P. and Dadoune, J. P. 1986. Renewal of spermatogonia in the monkey (*Macaca fascicularis*). *Biol. Reprod.* **35**:199-207.

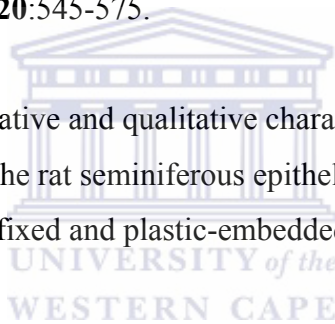
Griswold, M. D. 1993. Actions of FSH on mammalian Sertoli cell. In: The Sertoli cell (eds L. D. Russell and M. D. Griswold). Cache River Press. Clearwater, Florida. pp 439-508.

Haider, S. G., Passia, D., Treiber, A. and Milhorst, S. 1989. Description of eight phases of spermiogenesis in the marmoset testis. *Acta Anat.* **135**:180-185.

Heckert, L. L. and Griswold, M. D. 1991. Expression of follicle-stimulating hormone receptor mRNA in rat testes and Sertoli cells. *Mol. Endocrinol.* **5**:670-677.

Heller, C. G. and Clermont, Y. 1964. Kinetics of germinal epithelium in man. *Recent. Prog. Horm. Res.* **20**:545-575.

Hess, R. A. 1990. Quantitative and qualitative characteristics of the stages and the transitions in the cycle of the rat seminiferous epithelium: light microscopic observations of perfusion-fixed and plastic-embedded testes. *Biol. Reprod.* **43**:525-542.



Hess, R. A., Schaeffer, D. J., Eroschenko, V. P. and Keen, J. E. 1990. Frequency of the stages in the cycle of the seminiferous epithelium in the rat. *Biol. Reprod.* **43**:517-524.

Hess, R. A. and Chen, P. 1992. Computer tracking of germ cells in the cycle of the seminiferous epithelium and prediction of changes in cycle duration in animals commonly used in reproductive biology and toxicology. *J. Androl.* **13**:185-190.

Hess, R. A., Cooke, P. S., Bunick, D. and Kirby, J. D. 1993. Adult testicular enlargement induced by neonatal hypothyroidism is accompanied by increased Sertoli and germ cell numbers. *Endocrinol.* **132**:2607-2613.

Holt, W. V. and Moore, H. D. M. 1984. Ultrastructural aspects of spermatogenesis in the common marmoset (*Callithrix jacchus*). *J. Anat.* **138**:175-188.

Johnson, L., Charturvedi, P. K. and Williams, J. D. 1992. Missing generations of spermatocytes and spermatids in seminiferous epithelium contribute to low efficiency of spermatogenesis in humans. *Biol. Reprod.* **47**:1091-1098.

Johnson, L., Staub, C., Neaves, W. B. and Yanagimachi, R. 2001. Live human germ cells in the context of their spermatogenic stages. *Human Reprod.* **16**:1575-1582.

Kangasniemi, M., Kaipia, A., Mali, P., Toppari, J., Huhtniemi, I. and Parvinen, M. 1990. Modulation of basal and FSH-dependent cyclic AMP production in rat seminiferous tubules stages by an improved transillumination technique. *Anat. Rec.* **227**:62-76.

Kerr, J. B. 1992. Functional cytology of the human testis. *Baillière's Clin. Endocrinol. Met.* **6**:235-250.

Kluin, M., Kramer, M. F. and de Rooij, D. G. 1983. Testicular development in *Macaca irrus* after birth. *Int. J. Androl.* **6**:25-43.

Kumar, R. A. and Phillips, D. M. 1991. Spermiation and sperm maturation in the marmoset. *Anat. Rec.* **229**:315-320.

Leblond, C. P. and Cermont, Y. 1952a. Definition of the cycle of the seminiferous epithelium of the rat. *Ann. N. Y. Acad. Sci.* **55**:548-573.

Leblond, C. P. and Cermont, Y. 1952b. Spermiogenesis of the rat, mouse, hamster and guinea pig as revealed by periodic acid-sulphurous technique. *Am. J. Anat.* **90**:167-215.

McLachlan, R. I., O'Donnell, L., Stanton, P. G., Balourdos, G., Frydenberg, M., de Kretser, D and Robertson, D. M. 2002. Effects of testosterone plus medroxy progesterone acetate on semen quality, reproductive hormones and germ cell populations in normal young men. *J. Clin. Endocrinol. Metab.* **87**:546-556.

Millar, M. R., Sharpe, R. M., Weinbauer, G. F., Fraser, H. M. and Saunders P. T. K. 2000. Marmoset spermatogenesis: organizational similarities to the human. *Int. J. Androl.* **23**:266-277.

Moreno, R. D., Ramalho-Santos, J., Sutovsky, P., Chan, E. K. L. and Schatten, G. 2000. Vesicular traffic and Golgi apparatus dynamics during mammalian spermatogenesis: Implications for acrosome architecture. *Biol. Reprod.* **63**:89-98.

Ojoo, R. O., Otiang'a-Owiti, G. E., Oduor-Okelo, D. and Onyango, D. W. 2005. Frequency of stages of the seminiferous cycle in the thick-tailed bush baby (*Otolemur garnetti*), a prosimian primate: possible phylogenetic implications? *Anat. Embryol.* **209**:381-389.

Parvinen, M. 1993. Cyclic function of Sertoli cells. In: The Sertoli Cell. (eds L. D. Russell and M. D. Griswold). Cache River Press. Clearwater. Florida. pp 305-335.

Ross, M. H., Romrell, L. J. and Kaye, G. I. 1995. Histology: A Text and Atlas. 3rd Ed. Lippincott and Wilkins. Philadelphia. pp 636-665.

Russell, L. D. and Peterson, R. N. 1985. Sertoli cell functions: morphological and functional correlates. *Int. Rev. Cytol.* **94**:177-211.

Russell, L. D., Ettlin, R.A., Sinha Hikim, A. P. and Clegg, E. D. 1990. Histological and Histopathological Evaluation of the Testis. Cache River Press. Clearwater. Florida.

Sar, M., Hall, S. H., Wilson, E. H. and French, F. S. 1993. Androgen regulation of Sertoli cells. In: The Sertoli Cell. (eds. L. D. Russell and M. D. Griswold). Cache River Press. Clearwater. Florida. pp 509-516.

Sertoli, E. 1865. Dell 'esistenza di particolari cellule ramificate nei canalicoli seminiferi del testicolo umano. *Morgagni*. 7:31-39.

Shulze, W. and Rehder, U. 1984. Organization and morphogenesis of the human seminiferous epithelium. *Cell Tissue Res*. 237:395-407.

Smithwick, E. B., Young, L. G. and Gould, K. G. 1996. Duration of spermatogenesis and relative frequency of each stage in the seminiferous epithelial cycle of the chimpanzee. *Tissue Cell*. 28:357-366.

Steinberger, E. and Tjioe, D. Y. 1968. A method for quantitative analysis of human seminiferous epithelium. *Fertil. Steril*. 19:960-970.

Weinbauer, G. F., Aslam, H., Krishnamurty, H., Brinkwork, M. H., Einspanier, A. and Hodges, J. K. 2001. Quantitative analysis of spermatogenesis and apoptosis in the common marmoset (*Callithrix jacchus*) reveals high rates of spermatogonial turnover and high spermatogenic efficiency. *Biol. Reprod*. 64:120-126.

Weiss, L. 1983. The cell. In: Histology, Cell and Tissue Biology. 5th Ed. (ed. L. Weiss) Macmillan Press. New York. pp 77-84.

Wistuba, J., Schrod, A., Greve, B., Hodges, J. K., Aslam, H., Weinbauer, G. F. and Lutjens, C. M. 2003. Organization of seminiferous epithelium primates: Relationship to spermatogenic efficiency, phylogeny, and mating system. *Biol. Reprod.* **69**:582-591.



CHAPTER 7: COMPARISON OF THE MALE REPRODUCTIVE SYSTEM OF THE VERVET MONKEY AND HUMANS: A SUMMARY

7.1. INTRODUCTION

The morphology and functional features of the male reproductive system have been extensively studied in many mammalian species, including humans. The information obtained from those studies is essential in trying to solve the worldwide problem of male infertility and designing male contraceptive methods which can be reversible with minor medical complications and side effects. In this study, qualitative and quantitative data of the male reproductive system of the vervet monkey, with special reference to the process of spermatogenesis and comparisons with humans and other mammals were reported. One of the objectives of this study was to compare the macroscopic and microscopic features of the male reproductive system of the vervet monkey to those of the human. This study could be regarded as the first project to provide a clear and accurate description of the process of spermatogenesis of the vervet monkey using both light and electron microscopic techniques. This information may assist researchers in reproductive toxicology or contraceptive programs in human research. In addition, it can be suggested that this species could be useful for comparative studies involving primates particularly those studies that are related to spermatogenesis.

7.2. CONCLUDING DISCUSSION

Chapter 1 dealt with the taxonomy and ecological aspects of the vervet monkey. Chapter 2 entailed an overview of the male reproductive tract in mammals in general. In chapter 3, the gross morphology and histology of the vervet monkey was studied. There are many similarities between the gross morphology and histology of the male reproductive system of the vervet monkey and humans. The general morphology of the epididymis in the vervet monkey was found to be similar to the ones in the three macaque species (*Macaca mulatta*, *Macaca fascicularis*, and *Macaca arctoides*), studied by Ramos and Dym (1977). However, there are differences in some other aspects of reproduction such as, the number of seminiferous

layers as illustrated in Table 3.4. The number of seminiferous tubule layers in the vervet monkey testis was found to be between four and five, whereas in humans five layers have been reported. In other mammals two layers have been reported (Dym, 1972; Fawcett *et al.*, 1973). There were three to four stages per cross section found in vervet monkey and one to five stages were found in humans (Millar *et al.*, 2000).

In chapter 4, the ultrastructure of the epididymis was elucidated. The caput epididymis appeared to be well defined and bulbous whereas in humans the caput tend to be less defined and not bulbous as illustrated in Table 4.1.

The immunological role of the epididymis remains elusive. The presence of many phagocytic vesicles and lipofuscin material in the principal cells, clearly proves that the organ is not only a conduit passage for sperm cells but there are other protective roles played in reproduction. The epididymis showed a very strong phagocytic activity with the presence of numerous phagocytic vesicles. This will further support the idea that the epididymis is not just a passage of spermatozoa through to the urethra but also has some immunological functions (Chapter 4).

In Chapter 5 the ultrastructure of the testis of the vervet monkey was studied. One striking feature observed in the Sertoli cells were the funnel like structures that tend to house the elongated spermatids prior to their release in the lumen of the seminiferous tubules. These structures seemed to be well defined in the vervet monkey. Their embryological development is very important as this will elucidate their physiological roles in the normal functioning of the Sertoli cells.

Sertoli cell nuclei were found to be having four to five lobes in contrast to the three lobes found in humans. The Charcot-Böttcher crystalloid inclusion bodies were not found in this study. These bodies have been reported in humans. There are many similarities between the Leydig cells of the vervet monkey and those found in humans. The abundance of mitochondria in the basal side of the nucleus, SER, and few GER were quite evident in this study. However, there were no crystals of Reinke observed.

Chapter 6 dealt with spermiogenesis and staging of the spermatogenesis using three procedures (wax sections with PAS stain, Methacrylate resin sections, and

TEM). The phases of spermiogenesis appeared to be similar to those found in humans. Although the general organization of spermatogenesis is essentially the same in all mammals, there are some specific characteristics concerning the types and the numbers of spermatogonial generations and the morphologic aspects of germ cells present at the various stages of spermatogenesis among different species. There are clear similarities between the vervet monkey and humans in term of the association and progression of spermatogenic development. Nine stages were observed in this study which differed from the number of stages observed by previous researchers (Clermont, 1969; Wistuba *et al.*, 2003). The main factor which accounts for the difference could probably be the way in which other researchers tend to combine two or three stages together. It is a well known fact that these stages tend to overlap. Spermatogenesis studied in the vervet monkey was found to be different from other nonhuman primates in terms of the number of stages in a spermatogenic process. This was actually expected as stages vary in number and duration depending on the type of species under consideration. Therefore, it could be concluded that the distribution of spermatogenic stages in the vervet monkey resembles that of humans, with more than one stage per tubular cross-section.

The knowledge of the cycle of the seminiferous epithelium is fundamental and essential to fully understand and utilize techniques for quantifying the process of spermatogenesis. For instance, the calculation of daily spermatozoa production depends upon the rate of development of spermatogenesis (Berndtson, 1977).

7.3. FUTURE INVESTIGATIONS

Future investigations should explore structures or organs from the male reproductive system of the vervet monkey which appear to be similar to the humans. If that information is well established then one could strongly replace the human with the vervet monkey for many biomedical research programs. Secondly, future studies can focus on the molecular mechanisms involved in spermatogenic and spermiation processes in primates. This area could prove to be essential in the design of strategies to block sperm release.

The embryological origin of the sleeve-like processes of the Sertoli cells could prove to be important in understanding the process of spermiation. Sertoli cells have been in previous studies targeted as the most significant cells to understand its activity, in order to develop useful and efficient contraceptives. Further investigations on the Sertoli cell could be critical in understanding the testicular function.

This investigation shows that the vervet monkey appears to be an excellent model for many aspects related to human male reproduction.



7.4. REFERENCES

- Berndtson, W. E. 1977. Methods for quantifying mammalian spermatogenesis: A review. *J. Anim. Sci.* **44**:818-833.
- Clermont, Y. 1969. Two classes of spermatogonial stem cells in the monkey (*Cercopithecus aethiops*). *Am. J. Anat.* **126**:57-72.
- Dym, M. 1972. The fine structure of the monkey (*Macaca*) Sertoli cell and its role in maintaining the blood-testis barrier. *Anat. Rec.* **175**:639-656.
- Fawcett, D. W., Neaves, W. B. and Flores, M. N. 1973. Comparative observations on intertubular lymphatics and the organization of the interstitial tissue of the mammalian testis. *Biol. Reprod.* **9**:500-532.
- Millar, M. R., Sharpe, R. M., Weinbauer, G. F., Fraser, H. M. and Saunders P. T. K. 2000. Marmoset spermatogenesis: organizational similarities to the human. *Int. J. Androl.* **23**:266-277.
- Ramos, A. S. and Dym, M. 1977. Fine structure of the monkey epididymis. *Am. J. Anat.* **149**:501-532.
- Wistuba, J., Schrod, A., Greve, B., Hodges, J. K., Aslam, H., Weinbauer, G. F. and Lutjens, C. M. 2003. Organization of seminiferous epithelium primates: Relationship to spermatogenic efficiency, phylogeny, and mating system. *Biol. Reprod.* **69**:582-591.

CHAPTER 8: BIBLIOGRAPHY

LITERATURE CITED

Adamali, H. I. and Hermo L. 1996. Apical and narrow cells are distinct cell types differing in their structure, distribution, and functions in the adult rat epididymis. *J. Androl.* **17**:208-222.

Afzelius, B. A., Johnsonbaugh, R. E., Kim, J. W., Plöen, L. and Ritzen, E. M. 1982. Spermogenesis and testicular spermatozoa of the olive baboon, (*Papio anubis*). *J. Submicrosc. Cytol.* **14**:627-639.

Alsum, D. J. and Hunter, A. G. 1978. Regional histology and histochemistry of the ductus epididymis in the rhesus monkey (*Macaca mulatta*). *Biol. Reprod.* **19**:1063-1069.

Amann, R. P. 1987. Function of the epididymis in bulls and rams. *J. Reprod. Fertil.* (Suppl.) **34**:115-131.

André, J. 1962. Contribution á la cannaissance du chondriome; Etude de ses modifications ultrastructurales pendant la spermatogénése. *J. Ulstruct. Res.* Suppl. **3**:1-185.

Arrighi, S., Romanello, M. G. and Domeneghini, C. 1993. Ultrastructure of epididymal epithelium in *Equus caballus*. *Ann. Anat.* **175**:1-9.

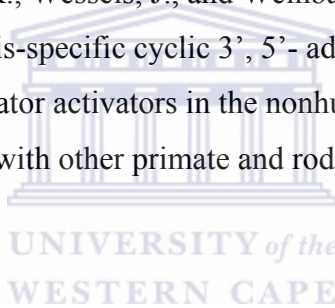
Aruldhas, M. M., Subramanian S., Sekhar, P., Vengatesh, G., Govindarajulu, P. and Akbarsha, M. A. 2006. In vivo spermatotoxic effect of chromium as reflected in the epididymal epithelial principal cells, basal cells, and intraepithelial macrophages of a nonhuman primate (*Macaca radiata* Geoffroy). *Fertil. Steril.* **86**:1097-1105.

Badia, E., Briz, M. D., Pinart, E., Sancho, S., Garcia-Gil, N, Bassols, J., Pruneda, A., Bussalleu, E., Yeste, M., Casas, I. and Bonet S. 2006. Structural and ultrastructural features of boar seminal vesicles. *Tissue Cell*. **38**:79-91.

Bajpai, V. K., Shipstone, A. C., Ratna Kumar, B. V., Qaisar, J. and Setty, B. S. 1985. Ultrastructure of the epididymal epithelium of Rhesus monkey (*Macaca mulatta*). *Acta Euro. Fert.* **61**:207-217.

Barfield, J. P., Nieschlag, E. and Cooper T. G. 2006. Fertility in wildlife: humans as a model. *Contraception* **73**:6-22.

Behr, R., Hunt, N. Ivell, R., Wessels, J., and Weinbauer, G. F. 2000. Cloning and expression analysis of testis-specific cyclic 3', 5'- adenosine monophosphate-responsive element modulator activators in the nonhuman primate (*Macaca fascicularis*): comparison with other primate and rodent species. *Biol. Reprod.* **62**:1344-1351.



Berndtson, W. E. 1977. Methods for quantifying mammalian spermatogenesis: A review. *J. Anim. Sci.* **44**:818-833.

Bloom, W. and Fawcett, D. W. 1994. A Textbook of Histology. 12th Ed. Chapman and Hall. New York. London. pp 768-813.

Booth, C. 1962. Some observations on behaviour of *Cercopithecus aethiops*. *Ann. N. Y. Acad. Sci.* **102**:477-487.

Bretschneider, L. H., 1950. Elektronenmikroskopische Untersuchungen an spermien. *Koninklijke Nederlanse Akademie van Wetenschappen proceedings.* **53**:531-543.

Brown, D. and Montesano, R. 1980. Membrane specialization in the rat epididymis. I. Rod-shaped intramembrane particles in the apical (mitochondria-rich) cell. *J Cell Sci.* **45**:187-198.

Buehr, M., Gu, S. and McLaren, A. 1992. Mesonephric contribution to testis differentiation in the fetal mouse. *Development* **117**:273-281.

Byskov, A. 1986. Differentiation of mammalian embryonic gonad. *Physiol. Rev.* **66**:77-112.

Camatini, M., Franchi, P. and Decurtis, I. 1981. Ultrastructure of the Leydig cells in the African green monkey. *J. Ultra. Res.* **76**:224-234.

Capel, B. 2000. The battle of the sexes. *Mech. Dev.* **92**:89-103.

Cavicchia, J. C. and Dym, M. 1978. Ultrastructural characteristics of monkey spermatogonia and preleptotene spermatocytes. *Biol. Reprod.* **18**:219-228.

Cavicchia, J. C., Sacerdote, F. L., Morales, A. and Zhu, B. C. 1998. Sertoli cell nuclear pore number changes in some stages of the spermatogenic cycle of the rat seminiferous epithelium. *Tissue Cell.* **30**:265-273.

Chen, I. L., and Yates, R. D. 1975. The fine structure and phosphatase cytochemistry of the Golgi complex and associated structures in the Sertoli cells of Syrian hamsters. *Cell Tissue Res.* **157**:227-238.

Chowdhury, A. K. and Steinberger, E. 1976. A study of germ cell morphology and duration of spermatogenic cycle in the baboon, *Papio anubis*. *Anat. Rec.* **185**:155-170.

Christensen, A. K. 1975. Leydig cells. In: Handbook of Physiology, Endocrinology V (eds. R. O. Greep and E. R. Asterwood). Williams and Wilkins Co. Baltimore, pp 1-19.

Clermont, Y. 1963. The cycle of the seminiferous epithelium in man. *Am.J. Anat.* **112**:35-51.

Clermont, Y. 1966. Spermatogenesis in man. A study of the spermatogonial population. *Fertil. Steril.* **17**:705-721.

Clermont, Y. 1969. Two classes of spermatogonial stem cells in the monkey (*Cercopithecus aethiops*). *Am. J. Anat.* **126**:57-72.

Clermont, Y. 1972. Kinetics of spermatogenesis in mammals: the cycle of the seminiferous epithelium and the mode of renewal in spermatogonia. *Physiol. Rev.* **52**:198-236

Clermont, Y. and Antar, M. 1973. Duration of the cycle of the seminiferous epithelium and the spermatogonial renewal in the monkey *Macaca arctoides*. *Am. J. Anat.* **136**:153-166.

Clermont, Y. and Leblond, C. P. 1959. Differentiation and renewal of spermatogonia in the monkey, *Macaca rhesus*. *Am. J. Anat.* **104**:237-274.

Conaway, C. H. and Sade, D. S. 1969. Annual testis cycle of the green monkey (*Cercopithecus aethiops*) on Kitts, West Indies. *J. Mammal.* **38**:217-219.

Connell, C. J. and Donjacour, A. 1985. A morphological study of the epididymides of control and estradiol-treated prepubertal dogs. *Biol. Reprod.* **33**:951-969.

Cooke, P. S., Kirby, J. D., Bunick, D. and Hardy, M. P. 1994. Neonatal propylthiouracil treatment as a model system for studying factors controlling testis growth and sperm production. In: *Function of Somatic Cells in the Testis*. (ed. A. Bartke) Springer Verlag. Norwel. pp 400-406.

Cooper, T. G. 1986. *The Epididymis, Sperm Maturation, and Fertilization*. Springer Verlag. New York. pp 117-230.

Cooper, T. G. 1993. The human epididymis-Is it necessary? *Int. J. Androl.* **16**:245-300.

Cooper, T. G. 1998. Epididymis. In: *Encyclopedia of Reproduction*. (ed. N. J. Knobil Ed). Academic press. San Diego. pp 1-17.

Crabo, B. 1965. Studies on the composition of epididymal content in bulls and boars. *Acta Vet. Scand.* (Suppl) **5**:1-94.

De Kretser, D. M. and Kerr, J. B. 1994. The cytology of the testis. In: *The Physiology of Reproduction*. (eds. E. Knobil and J. D. Neil.) Raven Press. New York. pp 1177-1290.

De Rooij, D. G., van Alphen, M. M. A. and van de Kant, H. J. G. 1986. Duration of the cycle of the seminiferous epithelium and its stages in the rhesus monkey (*Macaca mulatta*). *Biol. Reprod.* **35**:587-591.

De Rooij, D. G. and Russell, L. D. 2000. All you wanted to know about spermatogonia but were afraid to ask. *J. Androl.* 2000. **21**:776-798.

Despopoulos, A. and Silbernagl, S. 1986. *Color Atlas of Physiology*. 3rd Ed. Thieme Inc. New York. pp 28-29.

Dietrich, T., Schulze, W. and Riemer, M. 1986. Classification of the germinal epithelium in Java monkeys (*Macaca cynomolgus*) using digital image processing. *Urologie A* **25**:179-186.

Dixon, A. F. 1986. Plasma testosterone concentrations during postnatal development in the male common marmoset. *Folia Primatol.* **47**:166-170.

Domeniconi, R. F., Orsi, A. M., Beu, C. C. L. and Felisbino, S. L. 2007. Morphological features of the epididymal epithelium of gerbil, *Meriones unguiculatus*. *Tissue. Cell.* doi:10.1016/j.tice.2007.01.002 (in press).

Dym, M. 1972. The fine structure of the monkey (*Macaca*) Sertoli cell and its role in maintaining the blood-testis barrier. *Anat. Rec.* **175**:639-656.

Dym, M. 1983. The male reproductive system. In: Histology: Cell and Tissue Biology 5th Ed. (ed. L Weiss) Macmillan Press. New York. pp 1000-1053.

Dym, M. and Cavicchia, C. 1978. Functional morphology of the testis. *Biol. Reprod.* **18**:1-15.

Dym, M. and Romrell, L. J. 1975. Intraepithelial lymphocytes in the male reproductive tract of rats and rhesus monkeys. *J. Reprod. Fert.* **42**:1-7.

Eley, R. M. 1989. Know your monkeys: a guide to the primates of Kenya. National Museums of Kenya. pp 1-24.

Eley, R. M. 1992. Vervet reproduction. In: Occasional Papers of the National Museums of Kenya.(ed. L. A. Bennun). *Utafiti*, **4**: 1-33.

Eley, R. M., Else, J. G., Gulamhussein, N. and Lequin, R. M. 1986. Reproduction in the vervet monkey (*Cercopithecus aethiops*): Testicular volume and testosterone. *Am. J. Primatol.* **10**:229-235.

Else, J. M. 1985. Captive propagation of vervet monkeys (*Cercopithecus aethiops*) in harems. *Lab. Anim. Sci.* **35**: 373-375.

Erickson-Lawrence, M., Zabludoff, S. D. and Wright, W. W. 1991. Cyclic protein-2, a secretory product of rat Sertoli cells, is the proenzymes form of cathepsin L. *Mol. Endocrinol.* **5**: 1780-1788.

Eroschenko, V. P. 1996. Atlas of Histology with Functional Correlations. 8th Ed. Williams and Wilkins. Baltimore. pp 275.

Fairbanks, L. A. and McGuire, M. T. 1984. Determinants of fecundity and reproductive success in captive vervet monkeys. *Am. J. Primatol.* **7**: 27-38.

Fawcett, D. W. 1958. The structure of the mammalian spermatozoon. *Int. Rev. Cytol.* **7**:195-234.

Fawcett, D. W. 1970. A comparative view of sperm ultrastructure. *Biol. Reprod.* **2**:90-127.

Fawcett, D. W., Neaves, W. B. and Flores, M. N. 1973. Comparative observations on intertubular lymphatics and the organization of the interstitial tissue of the mammalian testis. *Biol. Reprod.* **9**:500-532.

Fawcett, D. W. 1975. Ultrastructural and function of the Sertoli cell. In: Handbook of Physiology. (eds. D. W. Hamilton and R. O. Greep, R. O.) Sect &, vol. **5**. Washington, D. C. American Physiology Society, pp 21-55.

Fawcett, D. W., Neaves, W. B. and Flores, M. N. 1973. Comparative observations on intertubular lymphatics and the organization of the interstitial tissue of the mammalian testis. *Biol. Reprod.* **9**:500-532.

Flechon, J. E., Bustos-Obregon, E., Steger, R. W. and Hafez, E. S. 1976. Ultrastructure of the testes and excurrent ducts in the bonnet monkey (*Macaca radiata*). *J. Med. Primatol.* **5**: 321-335.

Flickinger, C. J., Bush, L. A., Howards, S. S. and Herr, J. C. 1997. Distribution of leukocytes in the epithelium and interstitium of four regions of the Lewis rat epididymis. *Anat. Rec.* **248**:380-390.

Fouquet, J. P., Meusy-Dessole, N. and Dang, D. C. 1984. Relationships between Leydig cells morphometry and plasma testosterone during postnatal development of the monkey, *Macaca fascicularis*. *Reprod. Nutri. Dev.* **24**:281-296.

Fouquet, J. P. and Dadoune, J. P. 1986. Renewal of spermatogonia in the monkey (*Macaca fascicularis*). *Biol. Reprod.* **35**:199-207.

Franca, L. R., Hess, R.A., Cooke, P. S. and Russell, L. D. 1995. Neonatal hypothyroidism causes delayed Sertoli cell maturation in rats treated with propylthiouracil: evidence that the Sertoli cell controls testis growth. *Anat Rec.* **242**:57-69.

Galdieri, M. Monaco, L. and Stefanini, M. 1977. Secretion of androgen binding protein by Sertoli cells is influenced by contact with germ cells. *J. Androl.* **5**:409-415.

Goodwin, W. J. 1970. Current use of nonhuman primate in biomedical research. *Lab. Anim. Care.* **20**:329-332.

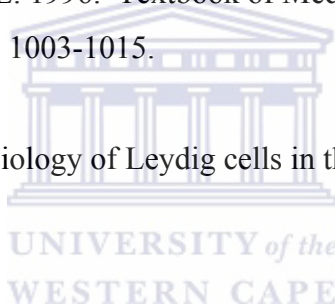
Gould, K. G. 1980. Scanning electron microscopy of the primate sperm. *Int. Rev. Cyt.* **63**:323-355.

Gould, K. G., Young, L. G., Smithwick, E. B. and Python, S. R. 1993. Semen characteristics of the adult male chimpanzee (*Pan troglodytes*). *Am. J. Primatol.* **29**:221-232.

Griswold, M. D. 1993. Actions of FSH on mammalian Sertoli cell. In: The Sertoli cell (eds. L. D. Russell and M. D. Griswold). Cache River Press. Clearwater, Florida. pp 439-508.

Guyton, A. C. and Hall, J.E. 1996. Textbook of Medical Physiology. 9th Ed. W.B Saunders. Philadelphia. pp 1003-1015.

Haider, S. G. 2004. Cell biology of Leydig cells in the testis. *Int. Rev. Cyt.* **233**:181-241.



Haider, S. G., Passia, D., Treiber, A. and Milhorst, S. 1989. Description of eight phases of spermiogenesis in the marmoset testis. *Acta Anat.* **135**:180-185.

Hamilton, D. W. 1972. The mammalian epididymis. In: Reproductive Biology. (eds. H. Balin and S. Glasner) Excerpta Medica. Amsterdam. pp 268-337.

Hamilton, D. W. 1975. Structure and function of the epithelium lining the ductuli efferentes, ductus epididymidis, and ductus deferens in the rat. In: Handbook of Physiology. (eds. R. O. Greep and E. B. Astwood) Sect. 7. Endocrinology, Male Reproductive System. American Physiology Society. **5**:259-301.

Hammerstedt, R. H. and Rowan, J. E. 1982. Phosphaditylcholine of blood lipoproteins is the precursor of glycerylphosphorylcholine found in seminal plasma. *Biochim. Biophys. Acta.* **710**:370-406.

Harcourt, A. H., Harvey, P. H., Lawson, S. G., and Short, R. V. 1981. Testis weight, body weight and breeding systems in primates. *Nature* **293**:55-57.

Hardy, M. P., Zirkin, B. R. and Ewing, L. L. 1989. Kinetics studies on the development of the adult population of Leydig cells testes of the pubertal rat. *Endocrinol.* **124**:762-770.

Harris, R. S. 1970. Feeding and nutrition of nonhuman primates. Academic Press, New York.

Hayat, M.A. 1986. Basic Techniques for Transmission Electron Microscopy. Academic Press Inc., New York, pp 208.

Hayat, M.A. 2000. Principles and techniques of electron microscopy: Biological Applications. Cambridge University Press, pp 543.

Heckert, L. L. and Griswold, M. D. 1991. Expression of follicle-stimulating hormone receptor mRNA in rat testes and Sertoli cells. *Mol. Endocrinol.* **5**:670-677.

Heckert, L. L. and Griswold, M. D. 2002. The expression of the follicle-stimulating hormone receptor in spermatogenesis. *Recent. Prog. Horm. Res.* **57**:129-148.

Heller, C. G. and Clermont, Y. 1964. Kinetics of germinal epithelium in man. *Recent. Prog. Horm. Res.* **20**:545-575.

Hermo, R., Oko, R. and Morales, C. R. 1994. Secretion and endocytosis in the male reproductive tract: a role in sperm maturation. *Int. Rev. Cytol.* **154**:106-189.

Hess, R. A. 1990. Quantitative and qualitative characteristics of the stages and the transitions in the cycle of the rat seminiferous epithelium: light microscopic observations of perfusion-fixed and plastic-embedded testes. *Biol. Reprod.* **43**:525-542.

Hess, R. A., Schaeffer, D. J., Eroschenko, V. P. and Keen, J. E. 1990. Frequency of the stages in the cycle of the seminiferous epithelium in the rat. *Biol. Reprod.* **43**:517-524.

Hess, D. L., Hendricks, A. G. and Stabenfeldt, G. H. 1979. Reproductive and hormonal patterns in the African green monkey (*Cercopithecus aethiops*). *J. Med. Primatol.* **8**:273-281.

Hess, R. A. and Chen, P. 1992. Computer tracking of germ cells in the cycle of the seminiferous epithelium and prediction of changes in cycle duration in animals commonly used in reproductive biology and toxicology. *J. Androl.* **13**:185-190.

Hess, R. A., Cooke, P. S., Bunick, D. and Kirby, J. D. 1993. Adult testicular enlargement induced by neonatal hypothyroidism is accompanied by increased Sertoli and germ cell numbers. *Endocrinol.* **132**:2607-2613.

Hoffer, A. P. 1976. The ultrastructure of the ductus deferens in man. *Biol. Reprod.* **14**:425-443.

Holschbach, C. and Cooper, T. G. 2002. A possible extratubular origin of epididymal basal cells in mice. *Reproduction* **123**:517-525.

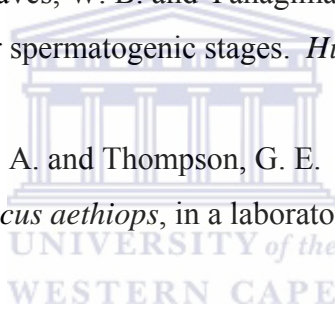
Holt, W. V. and Moore, H. D. M. 1984. Ultrastructural aspects of spermatogenesis in the common marmoset (*Callithrix jacchus*). *J. Anat.* **138**:175-188.

Ichihara, I., Kawamura, H., Nakano, T. and Pelliniemi, L. J. 2001. Ultrastructural, morphometric, and hormonal analysis of the effects of testosterone treatment on Leydig cells and other interstitial cells in young adults rats. *Ann. Anat.* **183**:413-426.

Johnson, L., Charturvedi, P. K. and Williams, J. D. 1992. Missing generations of spermatocytes and spermatids in seminiferous epithelium contribute to low efficiency of spermatogenesis in humans. *Biol. Reprod.* **47**:1091-1098.

Johnson, L., Staub, C., Neaves, W. B. and Yanagimachi, R. 2001. Live human germ cells in the context of their spermatogenic stages. *Human Reprod.* **16**:1575-1582.

Johnson, P. T., Valerio, D. A. and Thompson, G. E. 1973. Breeding the African green monkey, *Cercopithecus aethiops*, in a laboratory environment. *J. Anim. Sci.* **23**: 355-359.



Joyce, K. L., Porcelli, J. and Cooke, P. S. 1993. Neonatal goitrogen treatment increases adult testis size and sperm production in the mouse. *J. Androl.* **14**:448-455.

Junqueira, L. C., Carneiro, J. and Contopoulos, A. N. 1983. Basic Histology. 4th Ed. Lange Medical Publications. California. pp 451-467.

Junqueira, L. C. and Carneiro, J. 2003. Basic Histology: Text and Atlas, 10th Ed. Lange Medical Books McGraw-Hill. New York. pp 443-444.

Kangasniemi, M., Kaipia, A., Mali, P., Toppari, J., Huhtniemi, I. and Parvinen, M. 1990. Modulation of basal and FSH-dependent cyclic AMP production in rat

seminiferous tubules stages by an improved transillumination technique. *Anat. Rec.* **227**:62-76.

Karl, J. and Capel, B. 1998. Sertoli cells of the mouse testis originate from the coelomic epithelium. *Dev. Biol.* **203**:323-333.

Kelly, D. E., Wood, R. L. and Enders, A. C. 1984. Bailey's Textbook of Microscopic Anatomy. 18th Ed. Williams and Wilkins. Philadelphia. pp 687-722.

Kerr, J. B. 1988. An ultrastructural and morphometric analysis of the Sertoli cell during the spermatogenic cycle in the rat. *Anat. Embryol.* **179**:191-203.

Kerr, J. B. 1992. Functional cytology of the human testis. Baillière's *Clin. Endocrinol. Met.* **6**:235-250.

Kluin, M, Kramer, M. F. and de Rooij, D. G. 1983. Testicular development in *Macaca irrus* after birth. *Int. J. Androl.* **6**: 25-43.

Krause, W. J. and Cutts, J. H. 1986. Concise text of histology. 2nd Ed. Lippincott Williams and Wilkins. Baltimore. pp 409-439.

Kumar, R. A. and Phillips D. M. 1991. Spermiation and sperm maturation in the marmoset. *Anat. Rec.* **229**:315-320.

Kuopio, T., Tapanainen, J., Pelliniemi, L. J. and Huhtaniemi, I. 1989. Developmental stages of fetal-type Leydig cells in pubertal rats. *Development.* **107**:213-220.

- Kushner, H., Kraft-Schreyer, N., Angelakos, E. T. and Wudarski, E. M. 1982. Analysis of reproductive data in a breeding colony of African green monkeys. *J. Med. Primatol.* **11**:77-84.
- Leblond, C. P. and Cermont, Y. 1952a. Definition of the cycle of the seminiferous epithelium of the rat. *Ann. N. Y. Acad. Sci.* **55**:548-573.
- Leblond, C. P. and Cermont, Y. 1952b. Spermiogenesis of the rat, mouse, hamster and guinea pig as revealed by periodic acid-sulphurous technique. *Am. J. Anat.* **90**:167-215.
- Leeson, C. R., Leeson, T. S. and Paparo, A. A. 1985. Textbook of Histology. W. B. Saunders Co. Philadelphia. pp 492-517.
- Leong, S. K. and Singh, G. 1990. Ultrastructure of the monkey vas deferens. *J. Anat.* **171**:85-92.
- Leung, G. P. H., Cheung, K. H., Leung, C. T., Tsang, M. W. and Wong, P. Y. D. 2004. Regulation of epididymal principal cell functions by basal cells: Role of transient receptor potential (Trp) proteins and cyclooxygenase-1 (COX-1). *Mol. Cell. Endocrinol* **216**:5-13.
- Leydig, F. 1850. Zur Anatomie der Mannlichen Geschlechtsorgane and Analdrüsen der Säugethiere. *Z. Wissenschaftliche Zool.* **2**:1-57.
- Luft, J.H. 1961. Improvements in epoxy resin embedding methods. *J. Biophys. Biochem. Cytol.* **9**:409-414.
- Lunn, S. F., Recio, R., Morris, K. and Fraser, H. M. 1994. Blockade of the neonatal rise in testosterone by a gonadotrophin-releasing hormone antagonist: Effects on

timing of puberty and sexual behaviour in the male marmoset monkey. *J. Endocrinol.* **141**:439-447.

Majumdar, S. S., Winters, S. J. and Plant, T. M. 1998. Procedures for the isolation and culture of Sertoli cells from the testes of infant, juvenile, and adult rhesus monkeys (*Macaca mulatta*). *Biol. Reprod.* **58**:633-640.

Marengo, S. R. and Amann, R. P. 1990. Morphological features of principal cells in the ovine epididymis: a quantitative and qualitative study. *Biol. Reprod.* **42**:167-179.

Marquis, N. R., and Fritz, I. B. 1965. Effects of testosterone on the distribution of carnitine, acetylcarnitine and carnitine acetyltransferase in tissue of the reproductive system of the male rat. *J. Biol. Chem.* **240**:2197-2200.

Martin, C. W., Anderson, R. A., Cheng, L., Ho, P. C., van der Spuy, Z., Smith K. B., Glasier, A. F., Everington, D. E. and Baird D. T. 2000. Potential impact of hormonal male contraception: cross-cultural implications for development of novel preparations. *Human Reprod.* **15**:637-645.

McLachlan, R. I., O'Donnell, L., Stanton, P. G., Balourdos, G., Frydenberg, M., de Kretser, D and Robertson, D. M. 2002. Effects of testosterone plus medroxy progesterone acetate on semen quality, reproductive hormones and germ cell populations in normal young men. *J. Clin. Endocrinol. Metab.* **87**: 546-556.

Merchant-Larios, H., Moreno-Mendoza, N. and Buehr, M. 1993. The role of the mesonephros in cell differentiation and morphogenesis of the mouse fetal testis. *Int.J. Dev.Biol.* **37**:407-417.

Millar, M. R., Sharpe, R. M., Weinbauer, G. F., Fraser, H. M. and Saunders P. T. K. 2000. Marmoset spermatogenesis: organizational similarities to the human. *Int. J. Androl.* **23**:266-277.

Morales, C. and Clermont, Y. 1982. Evolution of Sertoli cells processes invading the cytoplasm of rat spermatids. *Anat. Rec.* **203**:233-244.

Moreno, R. D., Ramalho-Santos, J., Sutovsky, P., Chan, E. K. L. and Schatten, G. 2000. Vesicular traffic and Golgi apparatus dynamics during mammalian spermatogenesis: Implications for acrosome architecture. *Biol. Reprod.* **63**:89-98.

Murakami, M., Sugita, A. and Hamasaki, M. 1982. Scanning electron microscopic observations of the vas deferens in man and monkey with special reference to spermiphagy in its ampullary region. *Scan. Electr. Micro.* **111**:1333-1339.

Nishino, K., Yamanouchi, K., Naito, K. and Tojo, H. 2001. Characterization of mesonephric cells that migrate into the XY gonad during testis differentiation. *Exp. Cell. Res.* **267**:225-232.

Nistal, M., Panigua, R., Regadera, J., Santamaria, L. and Amat, P. 1986. A quantitative morphological study of human Leydig cells from birth to adulthood. *Cell Tissue Res.* **246**:229-236.

Ojoo, R. O., Otiang'a-Owiti, G. E., Oduor-Okelo, D. and Onyango, D. W. 2005. Frequency of stages of the seminiferous cycle in the thick-tailed bush baby (*Otolemur garnetti*), a prosimian primate: possible phylogenetic implications? *Anat. Embryol.* **209**:381-389.

Orth, J. M. 1993. Cell biology of testicular development in fetus and neonate. In: Cell Biology and Molecular Biology of the Testis. (eds. C. Desjardins and L.L. Ewing) Oxford University Press. New York. pp 3-42.

Parks, J. E. and Hammerstedt, R. H. 1985. Developmental changes occurring in the lipids of ram epididymal spermatozoa plasma membrane. *Biol. Reprod.* **32**:653-668.

Parvinen, M. 1982. Regulation of the seminiferous epithelium. *Endocrinol. Rev.* **3**:404-417.

Parvinen, M. 1993. Cyclic function of Sertoli cells. In: The Sertoli Cell. (eds: L. D. Russell and M. D. Griswold). Cache River Press. Clearwater. Florida. pp 305-335.

Pelliniemi, L. J. 1975. Ultrastructure of the early ovary and testis in pig embryos. *Am. J. Anat.* **144**:89-111.

Pelliniemi, L. J., Frojzman, K. and Paranko, J. 1993. Embryological and prenatal development and function of Sertoli cells. In: The Sertoli Cell. (eds. L.D. Russell and M. D. Griswold) Clearwater, Cache River Press. Florida. pp 87-114.

Pesch, S. and Bergmann, M. 2006. Structure of mammalian spermatozoa in respect to viability, fertility and cryopreservation. *Micron* **37**:597-612.

Plant, T. M. 1981. Time courses of concentrations of circulating gonadotropin, prolactin, testosterone and cortisol concentrations in adult male rhesus monkeys (*Macaca mulatta*) throughout the 24h light-dark cycle. *Biol. Reprod.* **25**:244-251.

Potts, M. 1996. The myth of a male pill. *Nature Med.* **2**:38-399

Prince, F. P. 1999. A Reinke-like inclusion within the Leydig cells of the marmoset monkey (*Callithrix jacchus*). *J. Anat.* **195**:311-313.

Prince, F. P. 2001. The triphasic nature of Leydig cell development in humans, and comments on nomenclature. *J. Endocrinol.* **168**:213-216.

Ramesh, V., Ramachandra, S. G., Krishnamurthy, H. N. and Rao, A. J. 1998. Electroejaculation and seminal parameters in bonnet monkeys (*Macaca radiata*). *Andrologia* **30**:97-100.

Ramos, A. S. and Dym, M. 1977a. Ultrastructure of the ductuli efferentes in monkeys. *Biol. Reprod.* **17**:339-349.

Ramos, A. S. and Dym, M. 1977b. Fine structure of the monkey epididymis. *Am. J. Anat.* **149**:501-532.

Ramos, A. S. and Dym, M. 1979. Ultrastructural differentiation of rat Sertoli cells. *Biol. Reprod.* **21**:909-922.

Ramos, A. S. 1979. Morphologic variations along the length of the monkey vas deferens. *Arch. Androl.* **3**:187-196.

Rana, B. K. and Bilaspuri, G. S. 2000. Changes in interstitial cells during development of buffalo testis. *Vet. J.* **159**:179-185.

Rey, R. A. Nagle, C. A. and Chemes, H. 1996. Morphometric study of the testicular interstitial tissue of the monkey *Cebus apella* during postnatal development. *Tissue Cell.* **28**:31-42.

Reynolds, E. 1963. The use of lead citrate at high pH as an electron opaque stain in electron microscopy. *J. Cell Biol.* **17**: 208-212.

Robaire, B. and Hermo, L. 1988. Efferent ducts, epididymis and vas deferens: Structure, functions, and their regulation. In: *The Physiology of Reproduction* (eds. E. Knobil and J. Neill). Raven Press. New York. pp 999-1080.

Rosen, S. I. 1974. *Introduction to Primates – Living and Fossils*. Prentice – Hall Inc. New Jersey.

Ross, M. H., Romrell, L. J. and Kaye, G. I. 1995. *Histology: A Text and Atlas*. 3rd Ed. Lippincott Williams and Wilkins. Philadelphia. pp 636-665.

Rowell, T. E. 1970. Reproductive cycles of *Cercopithecus* monkeys. *J. Reprod. Fertil.* **22**:321-338.

Russell, L. D. and Peterson, R. N. 1985. Sertoli cell functions: morphological and functional correlates. *Int. Rev. Cytol.* **94**:177-211.

Russell, L. D., Ettlin, R.A., Sinha Hikim, A. P. and Clegg, E. D. 1990. *Histological and Histopathological Evaluation of the Testis*. Cache River Press. Clearwater. Florida.

Sakai, Y., Nakamoto, T. and Yamashina, S. 1988. Dynamic changes in Sertoli cell Processes invading spermatid cytoplasm during mouse spermiogenesis. *Anat. Rec.* **220**:51-57.

Sapsford, C. S. and Rae, C. A. 1969. Ultrastructural studies on Sertoli cells and spermatids in the bandicoot and ram during the movement of mature spermatids into the lumen of the seminiferous tubule. *Aust. J. Zool.* **17**:415-445.

Sar, M., Hall, S. H., Wilson, E. H. and French, F. S. 1993. Androgen regulation of Sertoli cells. In: The Sertoli Cell. (eds. L. D. Russell and M. D. Griswold). Cache River Press. Clearwater. Florida. pp 509-516.

Schnoor, B. 1996. Embryology of domestic animals Enke. *Stuttgart* 10-13.

Seier, J. V. 1986. Breeding vervet monkeys in a closed environment. *J. Med. Primatol.* **15**:339-349.

Seier, J. V. 2005. Vervet monkey breeding. In: The Handbook of Experimental Animals. The Laboratory Primate. (ed. S. Wolfe-Coote). Chapter 12, Elsevier Academic Press. Amsterdam. pp 175-179.

Seiler, P., Cooper, T. G. and Nieschlag, E. 2000. Sperm number and condition affect the number of basal cells and their expression of macrophage antigen in the murine epididymis. *Int. J. Androl.* **23**:65-76.

Seiler, P., Wenzel, I., Wagenfeld, A., Yeung, C. H. and Nieschlag, E. 1998. The appearance of basal cells in the developing murine epididymis and their temporal expression of macrophage antigens. *Int. J. Androl.* **21**:217-226.

Sertoli, E. 1865. Dell 'esistenza di particolari cellule ramificate nei canalicoli seminiferi del testicolo umano. *Morgagni.* **7**:31-39.

Sharpe, R. M., McKinnell, C., Kivlin, C. and Fischer, J. S. 2003. Proliferation and functional maturation of Sertoli cells, and their relevance to disorders of testis function in adulthood. *Reproduction* **125**:769-784.

Sherwood, L. 2004 Human Physiolog: From Cells to Systems. 5th Ed. Brooks/Cole. USA. pp 751-755.

Shulze, W. and Rehder, U. 1984. Organization and morphogenesis of the human seminiferous epithelium. *Cell Tissue Res.* **237**:395-407.

Shupnik, M. A. and Schreihofe, D. A. 1997. Molecular aspects of steroid hormone action in the male reproductive axis. *J. Androl.* **18**:341-344.

Skinner, J. D., and Smithers, R. H. N. 1990. The Mammals of the Southern African Subregion. University of Pretoria Press. Pretoria. pp 159-164.

Skinner, M. K. 1991. Cell-cell interactions in the testis. *Endocrinol. Rev.* **12**:45-77.

Smithwick, E. B. and Young, L. G. 2001. Histological effects of androgen deprivation on the adult chimpanzee epididymis. *Tissue Cell.* **33**:450-461.

Smithwick, E. B., Young, L. G. and Gould, K. G. 1996. Duration of spermatogenesis and relative frequency of each stage in the seminiferous epithelial cycle of the chimpanzee. *Tissue Cell.* **28**:357-366.

Sprando, R. L., Collins, T. F. X., Black, T. N., Olejnik, N., Rorie, J. I., West, L. J., Bower, J. O., Sass, N. and Robl, N. 1999. Light microscopic observation on the reproductive tract of the male sand rat, *Psammomys obesus*. *Tissue Cell.* **31**:99-115.

Steinberger, E. and Tjioe, D. Y. 1968. A method for quantitative analysis of human seminiferous epithelium. *Fertil. Steril.* **19**:960-970.

Steiner, R. A. and Bremner, W. J. 1981. Endocrine correlates of sexual development in the male monkey, *Macaca fascicularis*. *Endocrinol.* **109**:914-919.

Sullivan, R., Saez, F., Girouard, J. and Frenette, G. 2005. Role of exosomes in sperm maturation during the transit along the male reproductive tract. *Blood Cells. Mol. Dis* **35**:1-10.

Sutovsky, P., Moreno, R., Ramalho-Santos, J., Dominco, T., Thompson, W. E. and Schatten, G. 2001. A putative, ubiquitin-dependent mechanism for the recognition and elimination of defective spermatozoa in the mammalian epididymis. *J. Cell. Sci.* **114**:1665-1675.

Tarantal, A. F., Vandevort, C. A. and Overstreet, J. W. 1990. Intrauterine insemination with ultrasound guidance in the long-tailed macaque (*Macaca fascicularis*). *J. Med. Primatol.* **19**: 447-453.

Turner, M. L. 2003. The micromorphology of the blesbuck louse *Damalinia (Damalinia) crenelata* as observed under the scanning electron microscope. *Koedoe* **46**(1): 65-71.

Turner, T. R., Whitten, P. L., Jolly, C. J. and Else, J. G. 1987. Pregnancy outcome in free ranging vervet monkeys (*Cercopithecus aethiops*). *Am. J. Primatol.* **12**:197-200.

Ueno, H. and Mori, H. 1990. Morphometrical analysis of Sertoli cell ultrastructure during the seminiferous epithelial cycle in rats. *Biol. Reprod.* **43**:769-776.

United Nations. 1994. World Contraceptive use. UN Department for Economic and Social Information and Policy Analysis, Population Division. New York (ST/ESA/SER.A/143).

Van der Horst, G. 1995. Computer aided sperm motility analysis of selected mammalian species. Unpublished PhD Thesis. University of Stellenbosch. pp 278.

Van der Horst, G. 2005. Reproduction. In: The Handbook of Experimental Animals. The Laboratory Primate.(ed. S. Wolfe-Coote). Chapter 31, Elsevier Academic Press Amsterdam. pp 527-536.

Van der Horst, G., Seier, J. V., Spinks, A. C. and Hendricks, S. 1999. The maturation of sperm motility in the epididymis and vas deferens of the vervet monkey, *Cercopithecus aethiops*. *Int. J. Androl.* **22**:197-207.

Vergouwen, R. P., Jacobs, S. G., Huiskamp, R., Davids, J. A. and De Rooij, D. G. 1991. Proliferative activity of gonocytes, Sertoli cells and interstitial cells during testicular development in mice. *J. Reprod. Fertil.* **93**:233-243.

Vihko, K. K., Souminen, J. J. O. and Parvinen, M. 1984. Cellular regulation of plasminogen activator secretion during spermatogenesis. *Biol. Reprod.* **31**: 383-389.

Wagley, L. M., Vershuis, T. D. Brown, D. V. and Amann, R. P. 1984. Culture of principal cells from the ram epididymis: a comparison of the morphology of principal cell in culture and insitu. *J. Androl.* **5**:389-408.

Wang, Y. F. and Holstein, A. F. 1983. Intraepithelial lymphocytes and macrophages in the human epididymis. *Cell Tissue Res.* **233**:517-521.

Wartenberg, H., Kinsky, I., Viebahn, C. and Schmolke, C. 1991. Fine structural characteristics of testicular cord formation in the developing rabbit gonad. *J. Electron Microsc. Tech.* **19**:133-157.

Weinbauer, G. F., Aslam, H., Krishnamurty, H., Brinkwork, M. H., Einspanier, A. and Hodges, J. K. 2001. Quantitative analysis of spermatogenesis and apoptosis

the common marmoset (*Callithrix jacchus*) reveals high rates of spermatogonial turnover and high spermatogenic efficiency. *Biol. Reprod.* **64**:120-126.

Weiss, L. 1983. The cell. In: Histology: Cell and Tissue Biology. 5th Ed. (ed. L. Weiss) pp 77-84.

Winter, J. S. D., Hughes, I. A., Reyes, F. I. and Faiman, C. 1976. Pituitary gonadal relations in infancy. 2. Patterns of serum gonadal steroid concentrations in man from birth to two years of age. *J. Clin. Endocrinol. Metabol.* **42**:679-686.

Wistuba, J., Schrod, A., Greve, B., Hodges, J. K., Aslam, H., Weinbauer, G. F. and Lutjens, C. M. 2003. Organization of seminiferous epithelium primates: Relationship to spermatogenic efficiency, phylogeny, and mating system. *Biol. Reprod.* **69**:582-591.

Wong, V. and Russell, L. D. 1983. Three-dimensional reconstruction of a rat stage V Sertoli cell: I. Methods, basic configuration, and dimensions. *Am. J. Anat.* **167**:143-161.

Yeung, C. H., Cooper, T. G., Bergmann, M. and Schulze, H. 1991. Organization of tubules in the human caput epididymis and the ultrastructure of their epithelia. *Am. J. Anat.* **191**:261-279.

Yeung, C. H., Nashan, D., C. Sorg, F. Oberpenning., H. Schulze., Nieschlag, E. and Cooper, T. G. 1994. Basal cells of the human epididymis –antigenic and ultrastructural similarities to tissue-fixed macrophages. *Biol. Reprod.* **50**: 917-926.

Zatuchni, B., Hahn, D. W. and Zaneveld, L. J. 1981. Postcoital, vaginal, spermicidal potency of formulations: *Macaca arctoides* (stumptailed macaque) as animal model. *Fertil. Steril.* **35**: 683-690.

CHAPTER 9: APPENDICES

Transmission Electron Microscopy (TEM)

1. Specimens collected from the specified muscles were fixed in 2,5% Glutaraldehyde in 0.1M phosphate buffer (pH 7.4, at 4°C) .
2. Specimens were rinsed in phosphate buffer for 15 minutes
3. Contrasting was performed using 1% OsO₄ for 60 minutes
4. *En bloc* staining was preceded by a thorough rinse of the specimens in distilled water to remove phosphate buffer, which is precipitated by uranyl salts (Hayat, 1986).
5. Fixed specimen blocks were immersed in 2% aqueous uranyl acetate (pH 3.9) for 60 min (time adapted from 30min by Hayat, 1986)) of *en bloc* staining before dehydration.
6. Specimens were thereafter routinely processed by dehydration through graded ethanol (50%-100%), placed in propylene oxide (Luft, 1961), infiltrated and embedded in a water-immiscible embedding medium (Embed-812[®], Electron Microscopy Sciences U.K.).
7. Ultramicrotomy of sections was performed by means of an Ultracut E (Reichert Jung, Germany) ultramicrotome using a diamond knife (Diatome Ltd., Switzerland) with a 2mm cutting edge.
8. Semi-thin sections (1µm) were dried onto glass slides, stained with toluidene blue (Appendix) for orientation, viewed and photographed (Olympus, Tokyo) by means of light microscopy.
9. Gold sections (70nm) were lifted onto copper grids (#200, Electron Microscopy Sciences, U.K.) and subsequently stained with uranyl acetate (Watson, 1958) and lead citrate (Reynolds, 1963).
10. Grids were viewed by means of a Jeol JEM1010 (Jeol Inc., Tokyo) transmission electron microscope (TEM) at 100 kV.
11. Digital micrographs were captured using a Megaview III[™] digital camera and SiS Image Analysis Software[®] (Soft Imaging System Ltd.).

Scanning Electron Microscopy (SEM)

1. The specimens were fixed in 2,5% Glutaraldehyde in 0.1M phosphate buffer (pH 7.4, at 4°C) to preserve ultrastructure of the tissue.
2. Specimens were then washed in three changes of distilled water for 10 min each.
3. Tissues were dehydrated through a graded ethanol series, critically point dried from liquid CO₂ by means of a Polaron[®] (Polaron, U.K.) critical point drying apparatus and there after mounted on pin-type aluminium stubs.
4. Specimens were sputter coated with carbon and gold, and viewed in a Leica Stereoscan 420[®] (Leica, Cambridge) SEM at 5-10kV.

HAYAT, M.A. 1986. Basic Techniques for Transmission Electron Microscopy. Academic Press Inc., New York, pp 208.

HAYAT, M.A. 2000. Principles and techniques of electron microscopy: Biological Applications. Cambridge University Press, pp 543.

LUFT, J.H. 1961. Improvements in epoxy resin embedding methods. *J. Biophysic and Biochem. Cytol.* **9**: 409-414.

REYNOLDS, E. 1963. The use of lead citrate at high pH as an electron opaque stain in electron microscopy. *J. Cell Biol.* **17**: 208-212.

(a) 0.1M Phosphate buffer (Sørensen) according to Hayat (2000)-

Solution A: Sodium phosphate, dibasic (Na₂HPO₄. 2H₂O)11.876g
Distilled water to make 1000 ml

Solution B: Potassium phosphate monobasic (KH₂PO₄) 9.08g
Distilled water to make 1000 ml

The desired pH of 7.4 can be obtained by adding 81.8ml of solution A to 19.2ml of solution B, to make a total volume of 100ml.

(b) Toluidene blue stain

Staining Solution:

Toluidene blue	1g
Borax	1g
Distilled water	100ml
BORAX= Sodium tetraborate ($\text{Na}_2\text{B}_4\text{O}_7 \cdot 10\text{H}_2\text{O}$) + Boric acid (H_3BO_3)	

1. Dissolve the borax in water and add dye with constant agitation.
2. When dissolved, filter solution and store in an amber container.
3. Cover dried sections on a slide with a large droplet of stain, and heat slide at 60°C until golden-coloured rim appears around the stain edges.
4. Wash off excess stain and mount the sections with Entellan® and a coverslip for light microscopy.